Protein Folding and Disease

The Mitochondrial Protein Frataxin

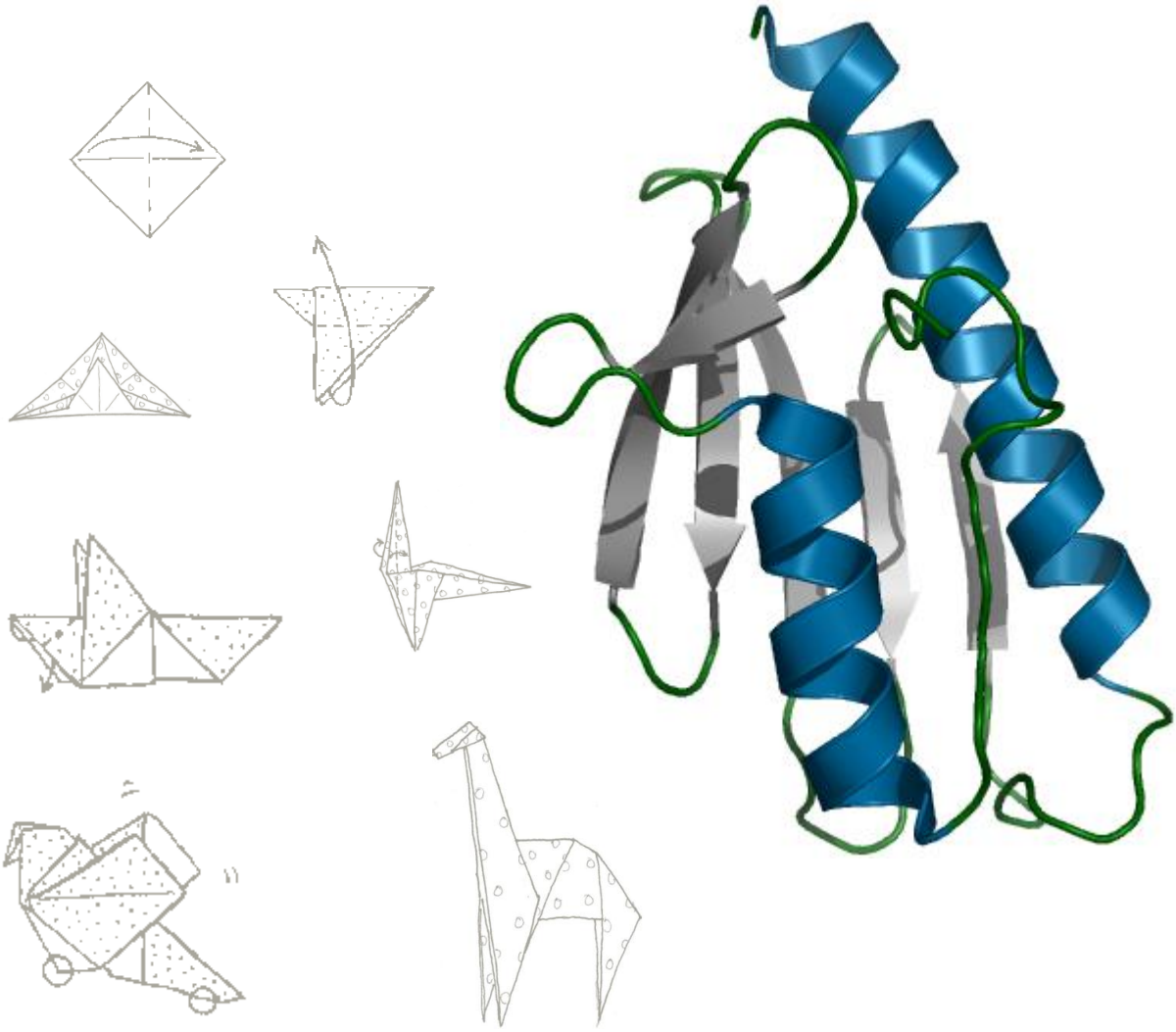

Ana R. Correia

Dissertation presented to obtain a Ph.D. degree in Biochemistry
at Instituto de Tecnologia Química e Biológica,
Universidade Nova de Lisboa
Oeiras, February 2010

PROTEIN FOLDING AND DISEASE

THE MITOCHONDRIAL PROTEIN FRATAXIN

Ana Raquel Viegas Correia

Dissertation presented to obtain a PhD degree in Biochemistry
at Instituto de Tecnologia Química e Biológica,
Universidade Nova de Lisboa

Supervisor

Cláudio Emanuel Moreira Gomes

Opponents

Mark M. Fisher & Ana Margarida Damas

Instituto de Tecnologia Química e Biológica,
Universidade Nova de Lisboa

Oeiras, February 2010

Second Edition, February 2010

ITQB - Protein Biochemistry Folding and Stability group

Instituto de Tecnologia Química e Biológica,

Universidade Nova de Lisboa

Av. da República (EAN), 2785-572 Oeiras, Portugal

http://www.itqb.unl.pt/pbfs

FOREWORD

This dissertation describes the work performed under the supervision of Dr. Cláudio Gomes, at the Protein Biochemistry Folding and Stability Laboratory, at the Instituto de Tecnologia Química e Biológica, from January 2006 to August 2009.

The studies presented here aim to contribute to a better understanding of frataxin conformational and functional properties and, at the same time, also intend to shed some light into the pathological process associated to Friedreich's ataxia (FRDA). Initially, the impact of FRDA-related mutations in human frataxin (FXN) was studied and their potential rescue by chemical chaperones addressed. Still focusing on the mechanisms underlying FRDA pathogenesis the susceptibility and possible role of oxidative stress relations on human frataxin were investigated. Further, the yeast frataxin orthologue (Yfh1) was used to explore the conformational and functional properties of frataxin.

This thesis is organised in three parts. The first is an introduction comprising two chapters: the first one presenting an overview on the protein folding problem and on how protein misfolding is associated to disease; the second chapter focuses on the state of the art on frataxin, its function and association with Friedreich's ataxia (FRDA). The second part of the thesis is organised in six chapters describing the experimental results obtained. The third and last part consists of a single chapter where a general discussion integrating the results is presented.

ACKNOWLEDGEMENTS

I would like to express my sincere gratitude to the following people:

My supervisor, Cláudio M. Gomes, to whom I am deeply grateful for the opportunity to learn and to grow to be a scientist in an amazing environment. His passion for science, dedication, critical sense, persistence and broad awareness are a source of inspiration. I am thankful for his support, for the freedom to explore different paths and for the opportunities to visit other laboratories.

Annalisa Pastore from the National Institute for Medical research (UK), for accepting me as a visiting student at her laboratory and for scientific training in molecular biology techniques and NMR.

Salvatore Adinolfi and John McCormick for teaching me molecular biology techniques. Chiara Pastore, Veronica Esposito and Goeff Kelly for the NMR experiments.

Paula Chicau and Ana Coelho for the HPLC separations and MS analysis of the peptides from the limited proteolysis experiments.

Peter Bross from the University of Aarhus (DK), for useful discussions and for sharing Lon and ClpXP plasmids.

Mark Fisher and Subhashchandra Naik from the University of Kansas Medical Center (US) for support, sharing of immobilized GroEL beads and for optimizing the conditions for the GroEL-Frataxin system.

Philip C. Wright and Saw Y. Ow from the University of Sheffield (UK), for performing the MS analysis of modified frataxin.

Elizabeth E. Craig and Tao Wang from the University of Wisconsin (US) for useful discussions, sharing of plasmids and for their functional studies on FRDA yeast model.

Miguel Teixeira from ITQB for useful discussions, support and for performing the EPR measurements.

Joan Valentine, from UCLA (US), is gratefully acknowledged for sharing SOD1 and Apo-SOD1 proteins.

My colleagues and friends at the Protein Biochemistry, Folding and Stability group for the friendly and positive environment, constant support and helpful discussions: Sónia Leal, Hugo Botelho, João Rodrigues, Ema Alves, Vesna Prosinecki and Patrícia Faísca.

Bárbara Henriques, for always being there, for being an amazing listener, for the helpful discussions and for the laughs we shared in and out of the lab.

All my friends, especially Sofia, Ana Paula, Patrícia, Lígia and Vera, with whom I've shared the excitement and also the down moments of these last 4 years.

All my family for the constant support and love, especially my grandfather Viegas who has always listened with unbelievable attention what was going on in the lab in spite of not having the faintest idea of what I was talking about.

João for his love, patience, encouragement and support.

Fundação para a Ciência e Tecnologia is acknowledged for financial support, by awarding a PhD fellowship (SFRH/BD/24949/2005)

This work was supported by the National Ataxia Foundation Grant (to CMG) and by a collaborative grant from the Conselho Reitores das Universidades Portuguesas (CRUP, Portugal to C.M.G.).

THESIS PUBLICATIONS

1. **Correia, A. R.**, Adinolfi, S., Pastore, A., Gomes, C. M. "Conformational stability of human frataxin and effect of Friedreich's ataxia-related mutations on protein folding"
Biochem. J. **398**, 605-611 (2006).

2. **Correia, A. R.** [*], Pastore, C. [*], Adinolfi, S., Pastore, A., Gomes, C. M. "Dynamics, stability and iron-binding activity of frataxin clinical mutants"
FEBS J. **275**, 3680-3690 (2008).

3. **Correia, A. R.**, Ow, S. Y., Wright, P. C., Gomes, C. M. "The conserved Trp-155 in human frataxin as a hotspot for oxidative stress related chemical modifications"
BBRC - Biochemical and Biophysical Research communication, **390**(3):1007-11 (2009).

4. **Correia, A. R.**, Wang, T. Craig, E. A., Gomes, C. M. "Iron binding activity in yeast frataxin entails a trade off with stability in the $\alpha 1/\beta 1$ acidic ridge region"
Biochem J. **426**(2):197-203 (2010).

Other publications not included in this thesis
5. Amaral. J. D.[*], **Correia, A. R**. [*], Steer, C. J., Gomes, C. M., Rodrigues, C. M. P. "No evidence of direct binding between ursodeoxycholic acid and the p53 DNA-binding domain"
Bioscience Reports, in press.

[*] Equally contributing authors.

x

DISSERTATION ABSTRACT

This dissertation focuses on the study of frataxin, a small mitochondrial protein whose deficiency is associated with the neurodegenerative disease Friedreich's ataxia (FRDA). Aiming at a better understanding of frataxin conformational and functional properties, two lines of research were followed: first, the effect of FRDA-related mutations in human frataxin (FXN) were studied and the role of oxidative stress related modification addressed; second, yeast frataxin (Yfh1) orthologue was used to explore the conformational and functional properties of the protein.

FRDA is the most common recessive ataxia among the Caucasian population with an estimate prevalence of 1-2 cases per 40,000 individuals in Europe. Most patients are homozygous for a GAA triplet expansion in a non-coding region that reduces the transcription of the gene encoding for frataxin, leading to reduced protein levels (5-30% of the normal levels). However, some patients (~4%) are compound heterozygous patients, meaning that they have the expansion in one allele and a deleterious point mutation on the other. The currently known mutations include missense, non-sense and splice mutations. Here we focused on the study and characterisation of four of the indentified missense mutations. Deletion of frataxin gene in eukaryotes is lethal, hence, even if in residual levels, all FRDA patients must express the protein.

The first part of the work was focused on the study of the following FRDA-related mutations: D122Y, G130V, I154F and W155R. While the first two mutations are associated to mild presentations of the disease the other two are associated to a severe phenotype identical to the

observed for homozygous patients. None of the studied mutations compromised the protein fold; nevertheless, they decreased the protein's intrinsic stability (ΔTm varying between approximately -5ºC and -23ºC). Opposite to what might have been expected, the mutants associated to milder phenotypes were more destabilised ($\Delta(\Delta G)$=2.11-2.86 kcal.mol^{-1}) than the mutants associated to severe phenotypes ($\Delta(\Delta G)$=1.35-1.66 kcal.mol^{-1}), suggesting that the pathological process in heterozygous patients is not exclusively related to the decreased stability of the mutants. The foldability and conformational flexibility of the clinical variants were also shown to be altered. Variants associated with severe phenotypes presented a higher tendency towards aggregation and exhibited increased conformational flexibility, as shown by NMR and limited proteolysis experiments. Iron binding, essential for frataxin cellular functional, was shown to be differently affected by the clinical mutations. Under controlled pH conditions and at 25ºC, we have observed that the FXN-D122Y and FXN-G130V appear to have their iron binding capacity partially compromised, binding only 4 irons per frataxin instead of the 6/7 observed for the wild type. The other two mutants, FXN-W155R and FXN-I154F, precipitated above the threshold of 2 irons per frataxin. Thus, mutations seem to compromise frataxin ability to bind iron but do not abolish it. Altogether, the data here presented suggests that the clinical effects in heterozygous FRDA patients are likely to result from a combination of effects, such as a reduced efficiency of protein folding, an accelerated degradation *in vivo* and misfolding and conformational destabilisation, which altogether contribute to a decrease in the levels of functional frataxin. In this scenario, FRDA in heterozygous patients carrying frataxin single point mutations could be considered a type of protein misfolding disorder.

Small compounds, such as sugars and polyols, are often called chemical chaperones due to their ability to stabilise proteins and to correct their misfolding or folding defects. Thus, the presence of these compounds is particularly relevant in the context of a genetic modification, such as a clinical point mutation, or in adverse environment conditions. The therapeutic potential of these compounds has been explored for many misfolding diseases like Gaucher's or cystic fibrosis and here we have evaluated the potential chaperone-like behaviour of four small compounds on two frataxin FRDA-related variants: FXN-D122Y and FXN-I154F. The wild type was used as a control and 4-phenyl butyrate (small fatty acid), trehalose (sugar), trimethylamine-N-oxide (methylamine) and glycerol (polyol) were tested for their potential chaperone-like effect on frataxin clinical variants.

First, the effect of small compounds on early folding events was tested. Using the *E. coli* expression system, the mutants were expressed in the presence of different concentrations of the small compounds and the ratio between expressed soluble and insoluble protein allowed to assess the impact of the compounds on the proteins' folding efficiency. Intriguingly, the effect of the different compounds was mutant dependent. While the FXN-D122Y folding efficiency was only modestly improved, the FXN-I154F folding efficiency improved significantly with the amount of expressed soluble protein increasing up to ~3fold in the presence of glycerol.

Furthermore, we have also evaluated the impact of the small compounds on the folded native-like variants, namely the compounds' effect on the proteins conformation and stability was addressed. FXN-D122Y is more positively affected. The presence of trehalose and trimethylamine-N-oxide (TMAO) improved FXN-D122Y thermal stability to values close to the determined for the wild type in the absence of the compounds, as shown by the melting temperatures obtained by

differential scanning fluorimetry (ΔT_m of up to ~7.8ºC). Three of the compounds, 4PBA, trehalose and glycerol, showed a positive impact on the FXN-D122Y conformational defects, as evaluated through the GroEL sink assay (GroEL specifically binds exposed hydrophobic regions, thus when conformational defects are present the proteins patition onto GroEL). The effects on the folded FXN-I154F were moderate; stability was only increased up to a ΔT_m of ~2.5ºC. However, the addition of TMAO (500mM) positively affected this mutant's conformation, preventing its partitioning onto the molecular chaperone GroEL.

Our results show that the effects induced during the early folding events are distinct from those observed on the folded protein and also, different point mutations are modulated by the same chemical chaperone in a different manner. These differences are likely to result from the conformational variations introduced by each mutation. The results presented here suggest that FXN-D122Y conformational variation might be overcome by the presence of chemical chaperones and *in vivo* increased concentrations of different chemical chaperones may rescue the pathological phenotype associated to this mutant. On the other hand, the FXN-I154F mutant should only be partially rescued, but the presence of small compounds may attenuate the phenotype observed.

One other aspect that was investigated concerns the impact of oxidative stress related modification on frataxin. A priori, frataxin is a potential target for oxidative stress modifications, not only due to its location in the mitochondria, where oxygen and nitric oxide are available in a reducing environment, but also as a result of its iron-binding properties. Thus, wild type frataxin was subjected to conditions mimicking increased oxidative stress inside the mitochondria (H_2O_2 +

Fe(II) and $ONOO^-$) and then analysed by mass spectrometry for the presence of oxidative stress related modifications. The protein is susceptible to carbonylation and nitration modifications in residues from the β-sheet surface (Tyr143, Tyr174, Tyr205 and Trp155). Frataxin functions are not significantly affected: frataxin-mediated protection against ROS is still observed, as well as iron-binding necessary for the metallochaperone activity. However, the protein is up to 1.0 $kcal.mol^{-1}$ destabilised, with conformational opening, as shown by the thermal unfolding reactions and the limited proteolysis experiments. Interestingly, the strictly conserved Trp155, whose mutation leads to FRDA, is both susceptible to carbonylation and nitration modifications, suggesting that this residue may be a functional hotspot in frataxin.

The human and yeast frataxin orthologues have a high degree of amino acid and structural identity. In addition, the phenotype caused by frataxin depletion is very similar in human and yeast cells, thus the yeast model system has been proven to be a very useful model to study frataxin function. Here, when addressing frataxin functional and conformational properties we have used the yeast frataxin orthologue (Yfh1). Aiming at a better functional understanding of frataxin structure, we have characterised eight variants involving mutations on two putative functional regions – the α1/β1 acidic ridge and the conserved β-sheet surface. Frataxin's iron binding capacity was shown to be quite robust: even when five of the most conserved residues from the putative iron binding region are mutated, the protein still binds iron (~2 iron atoms per monomer), although with decreased affinity. Furthermore, it is observed that the negative charges comprising the iron binding region also have structural and conformational implications. Removing five of those charges results in a thermal stabilisation of ~24ºC and reduces the inherent conformational plasticity. This

illustrates a rather interesting tradeoff between activity and stability in this region. In addition, our study suggests that residues Asp101 and Glu103 are involved in the iron-mediated interaction between Isu and Yfh1, but their alteration does not abrogate the interaction, as evidenced by the rescue of the *Δyfh1* phenotype.

Mutations on the conserved β-sheet residues had been shown to severely compromise frataxin function; here we show that these mutations only have a modest impact on the protein stability (ΔT_m ~0-4ºC), which highlights the functional importance of residues 122-124.

Frataxin has been shown to be stabilised by different metal ions and, in addition, nickel has been shown to be able to rescue, at least partially, FRDA-mutants cellular deficiencies. Therefore, we have explored the frataxin's ability to bind other metals ions besides iron. Among the tested metals - calcium, copper, sodium, magnesium, nickel, manganese and zinc - only copper was shown to cause Yfh1 Trp fluorescence emission quenching, suggesting that the protein only binds this metal ion. Frataxin was shown to be able to bind Cu(I) (3Cu(I):Yfh1) and Cu(II) (4Cu(II):Yfh1), but its affinity for Cu(I) is higher. The binding of Cu(II) to the protein was further confirmed by EPR, these experiments confirmed the copper binding behaviour and also suggested the existence of different binding sites. Considering Yfh1 mitochondrial localisation and the high levels of copper in the matrix it may be suggested that frataxin contributes to the balance of the mitochondrial copper homeostasis by preventing copper Fenton reactions. Iron binding induces frataxin oligomerisation, maximising its protective role against free iron. However, DLS experiments have shown that Yfh1 oligomerisation is not induced by copper and, as a result, if Yfh1 has a protective role against copper toxicity it does not involve its oligomerisation. Frataxin affinities to copper and to iron are

identical which may suggest another hypothesis as to the role of Yfh1 copper binding ability. Copper may regulate frataxin iron-chaperone function, and, as shown by copper/iron competition assays, this might be occurring at least to some extent. The presence of copper was shown to be able to reduce Yfh1 affinity to Isu however, even the excess of copper does not abrogate this interaction. Alternatively, it may be suggested that, in addition to its already described iron-chaperone function, frataxin may also act as a copper-chaperone, directing the copper present in the matrix to the appropriate copper-chaperones within the IMM. Thus, we have evaluated frataxin copper-chaperone ability and we have found that frataxin improves SOD1 reconstitution, meaning that this protein may act as a copper chaperone. Frataxin copper binding ability must be further explored: first it has to be assessed whether this feature is also occurring *in vivo* and if does what is its biological meaning; in addition, a more chemical approach must be followed in order to characterise in detail the binding of copper to this protein.

The results here presented aim to contribute to a better understanding of FRDA pathological process. The studies on frataxin's yeast orthologue contributed to the characterisation of frataxin's functional regions and also revealed a new functional feature of the protein.

RESUMO DA DISSERTAÇÃO

A presente tese foca-se no estudo da frataxina, uma proteína mitocondrial cuja deficiência está associada à doença neurodegenerativa atáxia de Friedreich (FRDA). Com o objectivo de contribuir para uma melhor compreensão das propriedades conformacionais e funcionais da frataxina, foram seguidas duas linhas de investigação: a primeira envolveu o estudo de mutantes clínicos da frataxina humana e também a avaliação do efeito das modificações associadas a condições de stress oxidativo; a segunda focou-se na investigação das propriedades funcionais e conformacionais da proteína, tendo os estudos sido realizados com a frataxina de levedura (Yfh1).

A atáxia de Friedreich é a atáxia recessiva mais comum na população caucasiana, sendo a sua prevalência na Europa de cerca de 1-2 casos por cada 40,000 indivíduos. A maioria dos pacientes são homozigóticos para uma expansão do tripleto GAA numa região não codificante, a qual causa uma redução da transcrição do gene que codifica a frataxina e que resulta em reduzidos níveis celulares de frataxina (5-30% dos níveis normais). No entanto, alguns pacientes são heterozigóticos (~4%), o que significa que apresentam a expansão num dos alelos e uma mutação nociva no outro. As mutações conhecidas até a data incluem mutações *missense*, *non-sense* e mutações que alteram o *splicing.* O estudo focou-se na caracterização de quatro mutações *missense* identificadas em pacientes com FRDA. Nos organismos Eucariotas, a supressão do gene que codifica a

frataxina é letal, pelo que, ainda que com níveis reduzidos, todos os pacientes expressam frataxina.

A primeira parte do trabalho aqui apresentado centrou-se no estudo do impacto das seguintes mutações clínicas: D122Y, G130V, I154F e W155R. Enquanto as duas primeiras mutações estão associadas a um fenótipo moderado da doença, as duas outras estão associadas a um fenótipo severo e idêntico ao observado em pacientes homozigóticos. Nenhuma das mutações aqui estudadas impede o enrolamento da proteína, no entanto, causam uma diminuição da sua estabilidade intrínseca (o ΔTm varia aproximadamente entre -5ºC e -23ºC). Contrariamente ao que seria esperado, os mutantes associados a fenótipos moderados são aqueles que causam uma maior destabilização da proteína ($\Delta(\Delta G)$=2.11-2.86 kcal.mol^{-1}), o que sugere que o processo patológico associado aos pacientes heterozigóticos não resulta exclusivamente de uma menor estabilidade apresentada pelos mutantes. A capacidade de enrolamento e a flexibilidade conformacionais também são alteradas pela inserção das mutações. Mutantes associados a fenótipos severos apresentam uma maior susceptibilidade para agregarem e simultaneamente apresentam uma maior flexibilidade conformacional, como é observado através das experiências de NMR e proteólise limitada. A capacidade de ligar ferro, essencial para a função celular da frataxina, também é alterada pelas mutações. Em condições controladas de pH e temperatura, verifica-se que a capacidade dos mutantes FXN-D122Y e FXN-G130V ligarem ferro é afectada pelas mutações e que estes passam a ligar apenas 4 ferros em vez de 6/7 como é observado para a proteína selvagem. Os outros dois mutantes, FXN-W155R e FXN-I154F, precipitam quando a estequiometria ferro:proteína é maior que 2. Assim, os resultados demonstram que embora as mutações estudadas afectem a

capacidade de a proteína ligar ferro não a comprometem por completo. Em suma, os resultados aqui apresentados sugerem que os efeitos clínicos observados para os pacientes heterozigóticos resultam provavelmente da combinação de várias factores, tais como a redução da capacidade de enrolamento, o aumento da degradação *in vivo*, o mau enrolamento e a destabilização conformacional, que, em conjunto, contribuem para uma redução dos níveis funcionais de frataxina. Considerando este cenário, a atáxia de Friedreich em pacientes heterozigóticos pode ser considerada uma doença conformacional (*misfolding disorder*).

Compostos pequenos, como os açúcares e os polióis, são frequentemente designados chaperões químicos uma vez que estabilizam e corrigem alguns defeitos de enrolamento das proteínas. Assim, estes compostos são particularmente relevantes num contexto biológico, quando ocorre uma modificação genética ou em condições adversas como um aumento da temperatura. O potencial terapêutico destes compostos tem sido explorado para muitas patologias conformacionais, como sendo a doença de Gaucher ou a fibrose quística. Assim, avaliámos aqui a potencial utilização de quatro compostos como chaperões químicos de dois mutantes clínicos da frataxina: FXN-D122Y e FXN-I154F. A proteína selvagem foi utilizada como controlo e o 4-phenilbutirato (ácido gordo), a trealose (açúcar), a trimetilamina-N-oxide (metilamina) e o glicerol (poliol) foram testados no sentido de avaliar as suas capacidades como chaperões químicos dos mutantes estudados.

Primeiro, o efeito dos compostos na capacidade de enrolamento foi testado. Recorrendo ao sistema de expressão em *E. coli*, os mutantes foram expressos na presença de diferentes concentrações dos compostos e a razão entre proteína solúvel e insolúvel determinada de

forma a permitir uma quantificação do efeito dos compostos na eficiência do processo de enrolamento proteico. Curiosamente, o efeito dos compostos depende do mutante considerado. Enquanto a eficiência de enrolamento do mutante FXN-D122Y foi apenas marginalmente alterada, a do mutante FXN-I154F aumentou significativamente com a presença dos vários compostos, nomeadamente a adição de glicerol triplicou a quantidade de FXN-I154F solúvel. Posteriormente, o efeito dos compostos na proteína enrolada, mais especificamente o efeito na conformação e estabilidade, foi também avaliado. Considerando a proteína já enrolada, os efeitos no mutante FXN-D122Y são mais significativos. A presença de TMAO resulta num aumento da estabilidade térmica do mutante FXN-D122Y para valores idênticos aos determinados para a proteína selvagem na ausência dos compostos (o aumento máximo do T_m de ~7.8ºC). Os estudos com a GroEL (*GroEL sink assay*) permitiram ainda avaliar os defeitos conformacionais dos mutantes e a potencial correcção desses defeitos em consequência da presença dos chaperões químicos. Três dos compostos testados (4PBA, trealose e glicerol) permitiram corrigir pelo menos parte dos defeitos conformacionais associados a mutação D122Y, resultando num atenuamento da ligação da proteína mutante à GroEL. Os efeitos destes compostos no mutante FXN-I154F enrolado são, no entanto, mais modestos: em termos de estabilização da proteína os compostos conseguem apenas induzir pequenas variações (máx. ΔT_m de ~2.5ºC); considerando a conformação deste mutante, o ensaio com a GroEL revelou que apenas o TMAO (500mM) consegue reverter os defeitos conformacionais associados a este mutante, retardando a sua interacção com o GroEL.

Este estudo revelou que os efeitos induzidos pelos potencias chaperões químicos durante o enrolamento são distintos dos observados na proteína enrolada. Verificou-se ainda que diferentes

mutantes são modulados de forma distinta pelo mesmo composto. Provavelmente estas diferenças resultam das variações conformacionais causadas por cada mutação. Os resultados aqui apresentados sugerem que provavelmente a variação conformacional inerente ao mutante FXN-D122Y pode ser ultrapassada, ou parcialmente revertida, pela presença de chaperões químicos, e, *in vivo*, a presença de chaperões químicos deverá presumivelmente evitar o fenótipo patológico associado à expressão deste mutante. Por outro lado, a presença de chaperões químicos *in vivo* deve apenas atenuar o fenótipo patológico associado à mutação I154F.

O estudo aqui apresentado abordou ainda o impacto de modificações associadas ao s*tress* oxidativo na frataxina humana. *A priori*, a frataxina é um potencial alvo de modificações associadas a este tipo de stress, não só devido a sua localização na mitocôndria, em que oxigénio e óxido nítrico estão disponíveis num ambiente redutor, mas também devido a sua função de chaperão de ferro. Assim, a frataxina humana selvagem foi submetida a condições que simulam o aumento de stress oxidativo dentro da mitocondria (H_2O_2 + Fe(II) ou alternativamente $ONOO^-$), e posteriormente a proteína foi analisada por espectrometria de massa de forma a identificar possíveis modificações. Verificou-se que os resíduos na superfície da folha β são susceptíveis a carbonilações e nitrações (Tyr143, Tyr174, Tyr205 e Trp155). No entanto, estas modificações não alteram significativamente as propriedades funcionais da frataxina: a proteína modificada retém a sua capacidade de evitar a formação de espécies reactivas de oxigénio bem como a sua capacidade de ligar ferros essencial às suas funções como chaperão de ferro. Contudo, as modificações destabilizam a proteína (1.0 $kcal.mol^{-1}$) e induzem uma abertura da conformação, como é evidenciado pelas desnaturações térmicas e pelas reacções de

proteólise limitada. Curiosamente, o Trp155, que é estritamente conservado e cuja mutação resulta em FRDA, é susceptível aos dois tipos de modificação identificadas, o que sugere que este resíduo talvez seja um *hotspot* funcional.

A frataxina humana e de levedura têm um elevado grau de identidade estrutural também em termos da sua sequência de amino ácidos. Adicionalmente, o fenótipo inerente à ausência de frataxina é idêntico em células humanas e de levedura. Assim, o sistema modelo de levedura tem-se revelado extremamente útil no estudo da função da frataxina. Os estudos de seguida apresentados, em que as propriedades conformacionais e funcionais da frataxina são avaliadas, realizaram-se com o ortólogo de levedura (Yfh1). Com vista a uma melhor compreensão das propriedades funcionais e estruturais da frataxina, caracterizámos oito variantes envolvendo mutações nas duas regiões funcionais da proteína: a região entre a hélice α1 e a fita β1 e a superfície conservada da folha β. A capacidade da frataxina ligar ferros revelou-se bastante robusta, alterando cinco dos resíduos mais conservados da região envolvida na ligação do ferro. Não foi, contudo, suficiente para inibir a ligação de ferros. Assim, embora com uma menor afinidade, este mutante quíntuplo retém a capacidade de ligar ferro (2 Fe(II) por monómero). Os resultados aqui apresentados revelam ainda que estas cargas negativas, que estão associadas à capacidade da frataxina ligar ferro, têm também um papel estrutural e conformacional. A neutralização de cinco dessas cargas induz uma estabilização térmica de cerca de 24ºC e, simultaneamente, reduz a plasticidade conformacional da proteína. Estas observações, ilustram um interessante compromisso entre actividade e estabilidade associado a esta região da proteína. Adicionalmente, os resultados sugerem que os resíduos Asp101 e Glu103 estão também envolvidos

na interacção entre a Yfh1 e a Isu, mas que no entanto a sua alteração não é suficiente para abolir a referida interacção, como é evidenciado pela recuperação do fenótipo causado pela *Δyfh1.*

É também aqui demonstrado que os resíduos 122-124, cuja mutação compromete de forma drástica a função da frataxina, têm apenas um impacto modesto em termos da estabilidade da proteína (ΔT_m ~0-4ºC) o que evidencia a importância destes resíduos na interacção com a Isu.

A frataxina é estabilizada por diferentes iões metálicos; posteriormente foi também descrito que o níquel pode recuperar, pelo menos parcialmente, as deficiências celulares associadas aos mutantes clínicos. Assim, pretendeu-se explorar a hipótese de a frataxina ligar outros metais, além do ferro. De entre os metais estudados - cálcio, cobre, sódio, magnésio, níquel, manganês e zinco - apenas o cobre causa o *quenching* da fluorescência emitida pelos Trp da Yfh1, sugerindo que este metal se liga à frataxina. A frataxina liga Cu (I) (3Cu(I):Yfh1) e Cu(II) (4Cu(II):Yfh1), sendo a sua afinidade para Cu (I) maior. A ligação do Cu(II) à proteína foi posteriormente avaliada por EPR. Estas experiências permitiram confirmar que o cobre se liga especificamente à frataxina e também sugeriram a existência de diferentes locais de ligação. Uma vez que a frataxina se localiza na matriz mitocondrial e este compartimento apresenta uma elevada concentração de Cu(I), é talvez possível que a frataxina contribua para o equilíbrio da homeostase mitocondrial de cobre: ao ligar-se ao cobre, a frataxina poderá evitar a formação de espécies reactivas de oxigénio em consequência da oxidação do cobre. O ferro, ao ligar-se à frataxina, induz a sua oligomerização, maximizando a função protectora da frataxina. Contudo, as medições por DLS revelaram que a ligação de cobre à frataxina não induz a sua oligomerização. Assim, se de facto a

frataxina está envolvida na protecção contra a toxicidade do cobre, esta hipotética função não está associada à oligomerização da proteína. A afinidade para o cobre e para o ferro são idênticas, o que pode sugerir uma função alternativa para a capacidade desta proteína ligar cobre. Este metal pode potencialmente regular a função da frataxina como chaperão de ferro e, de acordo com os ensaios de competição cobre/ferro, isto pode ocorrer parcialmente. A presença de cobre em solução reduz a afinidade da Yfh1 para a Isu, no entanto, mesmo em excesso, a presença de cobre não impede esta interacção. Alternativamente, além de uma função com chaperão de ferro, a frataxina poderá também funcionar como um chaperão de cobre, direccionando o cobre presente na matriz para os chaperões de cobre presentes na membrana interna da mitocôndria. Assim, a potencial capacidade de a frataxina funcionar como um chaperão de cobre foi avaliada através da reconstituição da Apo-SOD1 *in vitro*. Os resultados aqui apresentados revelam que a presença de frataxina facilita a reconstituição da apo-SOD1, o que sugere que esta proteína poderá efectivamente funcionar como um chaperão de cobre.

A capacidade de a frataxina ligar cobre tem que ser mais explorada: primeiro é necessário estabelecer se, *in vivo*, a frataxina é também capaz de ligar cobre e, caso isto se verifique, mais estudos serão necessários no sentido de clarificar o significado biológico de a frataxina ligar cobre. Adicionalmente, um estudo mais químico visando a caracterização da ligação do cobre à frataxina terá que ser realizado.

Os resultados aqui apresentados pretendem contribuir para uma melhor compreensão do processo patológico da ataxia de Friedreich. Os estudos realizados com o ortológo de levedura permitiram contribuir para a caracterização das regiões funcionais da frataxina e revelaram ainda uma nova propriedade destas proteínas.

ABBREVIATIONS

4PBA	4-Phenylbutyrate	K_{sv}	Stern-Volmer constant
ATP	Adenosine triphosphate nucleotide	mtDNA	Mitochondrial DNA
CcO	Cytochrome c oxidase	mFXN	Murine frataxin orthologue
CuL	Copper - non-proteinaceous ligand complex	N	Native state
CyaY	*Escherichia coli* frataxin orthologue	NOE	Nuclear Overhauser Enhancement
D	Denatured state	OXPHOS	Oxidative phosphorylation
$[D]_{1/2}$	Midpoint of the chemical denaturation curve	PD	Parkinson's disease
Dfh1	Drosophila melanogaster frataxin orthologue	QC	Quality control
DLS	Dynamic light scattering	ROS	Reactive oxigen species
DMS	methylsulfonium solutes	SOD	Superoxide dismutase
Dox	doxycycline	T_1	Longitudinal relaxation rates
DSF	Differential scanning fluorimetry	T_2	Transverse relaxation rates
ETF	Electron transfer flavoprotein	$(TBA)_2$-MDA	Tiobarbituric acid-melondialdehyde complex
F	Fold	TFA	Trifluoroacetic acid
FeS	Iron-sulphur	T_m	Midpoint of the thermal unfolding curve
FRDA	Friedreich's Ataxia	TMAO	Trimethylamine N-oxide
FXN	Human frataxin orthologue	TS	Transition state
GdmCl	Guanidinium chloride	U	Unfolded state
GST	Gluthathione-Stransferase	UPS	ubiquitin-proteasome system
GuSCN	Guanidine thiocyanate	Yfh1	Yeast frataxin orthologue
HD	Huntington's disease	ΔG_{H2O}	Unfolding Gibbs free energy change in water
Hsp	Heat shock protein	ΔH_m	Enthalphy change for unfolding at Tm
HSQC	Heteronuclear single quantum coherence	$\Delta(\Delta G)$	Difference in unfolding Gibbs free energy change
HTT	Huntingtin	$\Delta\psi_m$	Mitochondrial membrane potential
I	Intermediate state	τ_c	Correlation time
K_d	Dissociation constant		

TABLE OF CONTENTS

CHAPTER 1 PROTEIN MISFOLDING AND DISEASE

CHAPTER 2 FRATAXIN AND FRIEDREICH'S ATAXIA

CHAPTER

5 SMALL MOLECULES AS MODULATORS OF FRDA FRATAXIN VARIANTS

CHAPTER 6 THE CONSERVED TRP-155 IN HUMAN FRATAXIN AS A HOTSPOT FOR OXIDATIVE RELATED CHEMICAL MODIFICATIONS

CHAPTER 9 DISCUSSION

FIGURES

TABLES

CHAPTER

1 PROTEIN MISFOLDING AND DISEASE

1.1. The Importance of Folding

Proteins are remarkable and mysterious molecules. Not only they are the most abundant molecules in biology (besides water) but they are also responsible for every chemical process that makes the existence of living systems possible. Proteins are synthesised as polymeric sequences of amino acid residues but, in order to be functional, most proteins need to acquire a specific three-dimensional structure. The folding process is usually extremely efficient, leading to the formation of highly specific structures that grant proteins selective and diverse functions. However, the folding process is not fail proof and indeed a percentage of all proteins produced in the cell fail to fold correctly. Misfolded proteins are not only a product of inefficient folding but can also be formed as a consequence of stress conditions. Changes in the cellular environment due to ageing or temperature fluctuations, as well as genetic mutations, are known to cause protein misfolding or unfolding. To cope with misfolding and unfolding of proteins, cells have developed a protein quality control system, which comprises both chaperones and proteases and is responsible for limiting this burden. Unfortunately, the capacity of the protein quality control is limited and protein aggregation and misfolding are now recognised as the cause of a large and diverse group of diseases called protein conformational diseases or misfolding diseases.

This chapter describes the mechanisms proposed to explain the protein folding problem to then focus on the complexities inherent to protein folding in the crowded cellular environment and further the consequences of overloading the protein quality control system are addressed.

1.1.1. The Protein Folding Mystery

How a protein folds to its functional native state is a fundamental process that has occupied the mind of scientists for almost 50 years. The protein folding process can be divided in two major problems. The first was introduced through the pioneering work of Anfinsen and his co-workers on the folding/refolding of ribonuclease A [1-2]. They have shown that a polypeptide chain can spontaneously fold downhill to its lowest free-energy conformation (predetermined functional native state) without the help of any other biological machinery. This observation encompasses one of the key concepts in protein science, which is that all the information necessary for a protein to fold is encoded in its own amino acid sequence.

The second problem focuses on the kinetics and dynamics of folding, and it was introduced by Levinthal in 1968 [3-4]. He has demonstrated that the folding process could not consist of a systematic search of all the conformational space otherwise it would take an enormous amount of time for a protein to acquire the native state, approx. 10^{52} sec for a protein with ~100 amino acid residues - Levinthal Paradox.

The solution to the second problem would automatically solve the first one, however, in spite of the numerous folding studies, both theoretical and experimental, that have focused on the folding kinetics and dynamics, this is still an open field and many questions and uncertainties remain. Methods such as threading [5] and homology modelling [6-7] will probably allow for the prediction of the native structure, thus solving the first problem without going over a complete description of how a polypeptide acquires its structure in a short amount of time.

1.1.2. The Search for a Protein Folding Mechanism

During the folding process, amino acid residues are not independent pieces: they interact with each other and these interactions are not limited to consecutive residues. Long-range interactions are also involved in the folding process and if on one hand these interactions allow the folding process to be cooperative, they also increase the complexity of describing the folding process of any given protein [8-9]. In addition, folding kinetics are also puzzling, as folding is generally accomplished in a timescale in the order of milliseconds to seconds. Levinthal postulated the first protein folding model, proposing that the folding pathway occurs through a well defined and sequential path (sequential model) [10]. Since then other models have been postulated aiming at describing the folding process. Here, an overview of those models is presented.

In 1973, Wetlaufer has proposed the classical nucleation model [11]. This model suggests that the folding process is initiated by the formation of native secondary structure through the interaction of consecutive/neighbouring residues. The first elements of secondary structure will then act as seeds for the folding process, which occurs in a stepwise way without the formation of intermediates. During the 1970s and the 1980s, scientists have focused on the study of folding intermediates [12] and the classical nucleation model was discredited.

In 1976, and based on Afinsen experiments [2] and on the Ptitsyn and Rashin model [13-14], Karplus and Weaver postulated the diffusion-collision model (**Fig. 1.1**) [15-16]. This model relies on the existence of small elements of secondary structure, microdomains, which can assemble and disassemble transiently. Microdomains diffuse and their collision and coalescence lead to the formation of long-range interaction - tertiary structure. The model contemplated the existence of multiple folding pathways as coalescence can proceed

through a unique path or by parallel paths. Folding process dynamics are reduced as they rely on the global properties of each microdomain and its interactions. A few years later, in 1982, and based on experimental evidence, Kim and Baldwin proposed the framework model [12] whose description did not differ significantly from the diffusion-collision.

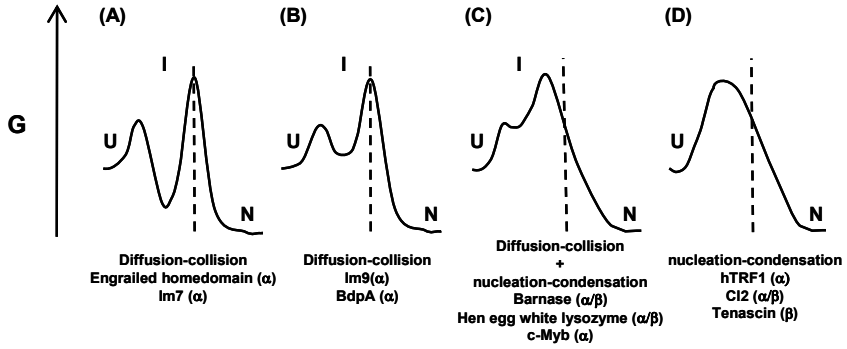

Figure 1.1: Simplified energy diagrams for folding of small single-domain proteins describing the differences between diffusion-collision and nucleation-condensation models. (A) Pure diffusion-collision: first secondary structure is formed leading to the formation of a low energy intermediate and then through diffusion and collision of secondary structure elements the tertiary structure is formed; (B) pure diffusion-collision as in (A) but a high energy intermediate is formed; (C) mixed diffusion-collision/nucleation-condensation: the formation of a high energy intermediate containing secondary and tertiary structure; (D) pure nucleation-diffusion: no intermediate is formed and at the transition state both secondary and tertiary structures are formed concurrently. As the propensity to form secondary structure increases, the folding mechanism shifts from the nucleation-condensation to the diffusion-collision. Adapted from [17].

The jigsaw-puzzle model was proposed by Harrison and Durbin in 1985 and suggests that folding occurs through different, parallel pathways rather than through a single path [18]. The existence of multiple paths makes folding more robust (kinetically) to mutations that do not disrupt the native structure. According to this model, the selection of the pathways follows the search for structures with increasing stability. Several unfolded states can be considered and the paths are enumerable, meaning that if intermediates do exist they

should comprise a random assortment of substructures of the native protein. Pulsed hydrogen exchange studies have demonstrated that the folding intermediates formed along the folding pathway are specific. These observations contradict what was proposed by the jigsaw-puzzle model and thus the model was abandoned.

The hydrophobic collapse model [19-21], suggests the existence of an initial hydrophobic collapse that restricts and consequently guides the subsequence folding steps, since folding/conformations are only allowed within the confined volume defined by the initial collapse.

Later, folding studies on CI2 [22-23] have demonstrated that folding does not rely on the accumulation of intermediates and that, in fact, folding can occur via a simple two state kinetics. These results, together with the CI2 Φ-value analysis, lead to the formulation of a new folding model: the nucleation-condensation model [24-25]. Φ-value analysis is the only experimental method allowing the evaluation and characterisation of the transition state (**Fig. 1.2**) [26-29]. It consists on the systematic study of the energetic consequences of introducing mutations throughout the protein. The effect of mutations is measured in both kinetic and equilibrium studies yielding information on the transition states of the folding-unfolding reaction. Mutations can be regarded as structural probes of each residue and the Φ-value is defined by the following equation:

$$\Delta\Delta\Phi = \frac{(\Delta G_{TS-D} - \Delta G'_{TS-D})}{(\Delta G_{N-D} - \Delta G'_{N-D})} = \frac{\Delta\Delta G_{TS-D}}{\Delta\Delta G_{TS}} \quad \text{(equation 1)}$$

$\Delta G_{TS\text{-}D}$ and $\Delta G_{N\text{-}D}$ are the free energies of the transition state/intermediate and the native state, respectively, relative to the denatured state for the wild type protein.

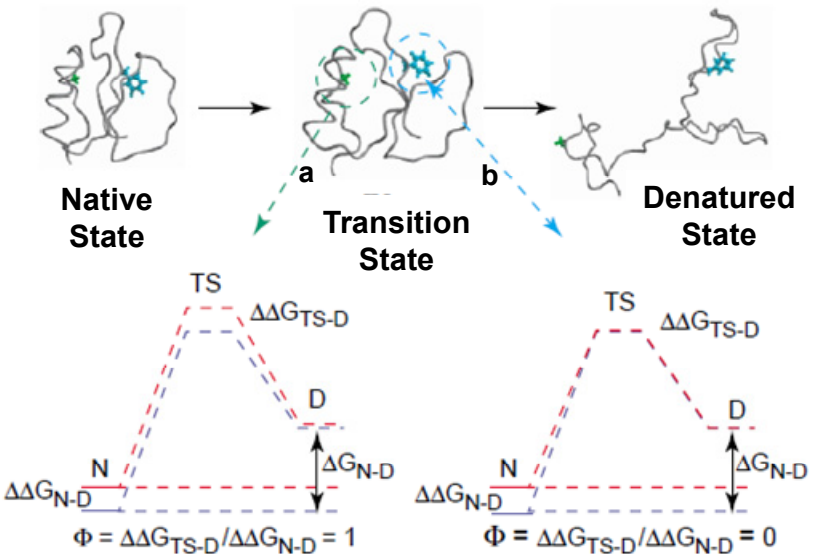

Figure 1.2: Information redrawn from the Φ-value analysis. After introducing a mutation, if the transition state energetics is the same as in the native state, the protein is immune to that mutation until after the transition state is reached, meaning that both the transition and the native states are equally affected by the mutation ($\Delta G_{TS-D} = \Delta G_{N-D}$), $\Phi = 1$ (residue a). On the contrary, $\Phi = 0$ means that the structure of the transition state at the site of the mutation is the same as in the denatured stated (residue b). $0 < \Phi < 1$, correspond to structures that are partially folded at the transition state. From [30].

The nucleation-condensation model conciliates the concepts from the framework and the hydrophobic-collapse models. It postulates the existence of a nucleus that constitutes the transition state; if a mutation occurs within the residues of the nucleus, this will not abolish the folding process but it will slow it down. The folding process is guided by an initial collapse around the protein hydrophobic side chains (generating the nucleus), after which the structure rearranges from the restricted conformational space occupied by the intermediate until it acquires the native like structure. According to this model the secondary structure formation is guided by the native-like tertiary interactions formed during the initial collapse (**Fig. 1.1**).

1.1.3. Energy Landscapes

With the exception of the diffusion-collision model, that correlates the folding time with some of the system parameters, the models presented above describe the phenomenological aspects of the folding process without addressing the kinetic problem. In 1994, Sali, Shakhnovich and Karplus postulated a model that solves Levinthal's paradox [31-32]. They have used a lattice Monte Carlo model to simulate the folding reaction. In this model, the allowed interactions within the polypeptide chain are expressed by a potential function. The protein is described as a string/chain of self-avoiding beads positioned at determined sites on a cubic lattice: Due to steric constraints for a given conformation, each site can at most be occupied by one bead. The beads interact with each other by pair wise contact potentials that represent the residue-residue interactions [33-34]. Changes in the chain conformation are made repeatedly and accepted or rejected according to the energy change they induce. The algorithm is designed to favour conformational changes that lead to a decrease in energy, which is in agreement with the folding search of a real protein where native-like interactions are on average more stabilised (have lower energy) than non-native ones. The successive conformational changes are described by a potential energy function and constitute the folding trajectory. This new model allows for the exact determination of the native state, for the calculation of the thermodynamic properties of the system as a function of the folding coordinate (amount of native contacts formed) and for the calculation of the free-energy surface for the folding reaction. The free-energy surface is a schematic three-dimensional representation of the folding progress coordinates where the free energy of each conformation is represented as a function of the total number of contacts, native and non-native, between non-consecutive residues and the number of

native contacts. The Monte Carlo simulations performed by Karplus and his co-workers on a simplified protein model, a 27-bead self avoiding chain on a cubic lattice, lead to the establishment of a three-stage folding model (**Fig. 1.3**).

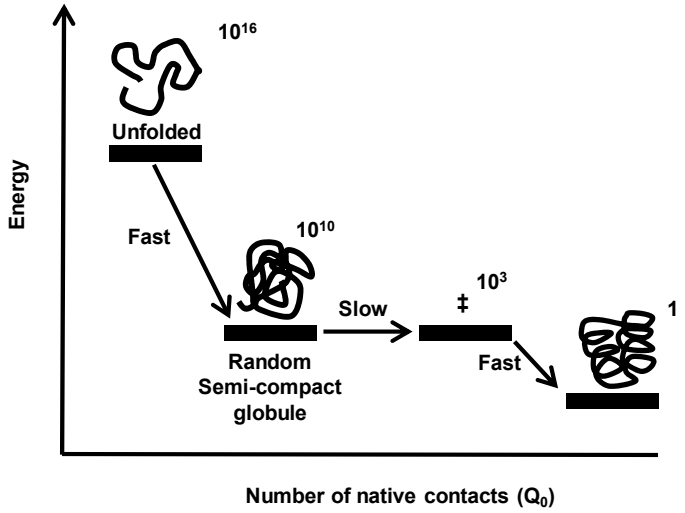

Figure 1.3: Three-stage mechanism of folding proposed by Karplus and co-workers (Lattice model). The number of states was calculated considering a 27-mer.Adapted from [31].

The first step involves a rapid collapse to a semi-compact random globule (with ~60% of the total number of possible contacts), this step reduces the amount of possible conformation from ~10^{16} to ~10^{10} [32]. The second step is the rate limiting step and involves the search for the transition states that will successfully and rapidly lead to the native state. The transition states are similar to the native state and comprise 80-95% of the native contacts. In the last step, the native state is rapidly obtained from any of the transition states. As folding proceeds along the three stages, the number of available conformations decreases and this loss of entropy between stages is determinant for the shape of the free-energy surface. If the contribution to the free-

energy of the conformational entropy decreases faster than the average energies, a barrier is formed on the free-energy surface, corresponding to the transition states [35]. Also, this decrease in the available conformations as the sequence approaches the native fold leads to the introduction of an important concept in protein folding – the folding funnel [36].

Although all the phenomenological models previously described already contain energetic concepts, the lattice simulation imposed a need to describe the energetic factor biasing the folding process. Also, the Monte Carlo simulations highlighted the fact that a sequence can undergo several folding trajectories at the same time, leading to an ensemble of high energy intermediate states close in structure to the native state that corresponds to the unique transition state described by experimentalists. The pathway view is replaced by the energy landscape description, and the folding process is viewed as an ensemble of conformations sliding down through a unique energy funnel leading to the most energetically stable conformation - the native state. As proteins increase in size, the folding process becomes more complex and barriers to the organisation on the collapse-state are likely to be larger, leading to rougher landscapes and multiple "pathways" [37]. Experiments on lysozyme (129 aa) showed that the folding kinetics of this protein are quite complex and heterogeneous [38-40]. Nonetheless, they can be explained, qualitatively, through a free-energy surface (**Fig. 1.4**). At least two folding trajectories/scenarios can be put forward, a fast trajectory involving a rate constant of less than 100 ms (yellow) [41] and a slower one that although significantly more populated (~70%) has a rate constant of ~400 ms (red) [40].

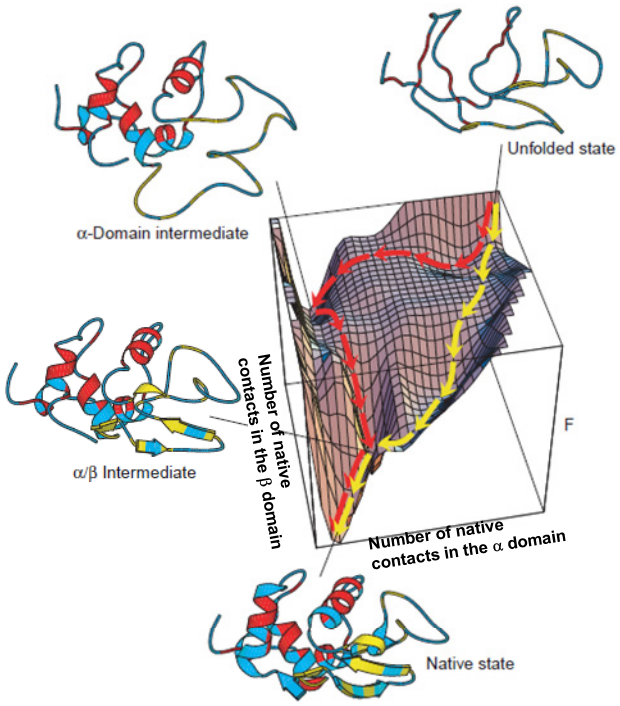

Figure 1.4: Schematic free-energy (F) surface representing features of the folding of hen lysozyme (a protein comprising an α and a β domain with 129 amino acid residues). Through the yellow trajectory (*fast track*) the α and the β domains are formed concurrently populating the intermediate only briefly. Through the red trajectory (*slow track*) the polypeptide chain is trapped in a long-lived intermediate with persistent structure involving only the α-domain. Further folding from this intermediate involves either a transition over a higher barrier or partially unfolding. Adapted from [35].

When the unfolded state proceeds through the yellow trajectory, both α and β lysozyme domains are simultaneously formed and the transition state is very close to the native state. However, when folding follows the red trajectory, the formation of the two domains is not simultaneous. First, the α domain is formed, leading to an intermediate that traps the folding process, a free-energy minimum. For the β-domain to be formed, it is not clear whether the α domain has to be partially unfolded or go over a higher barrier. The last step of the two

trajectories seems to be identical and comprises the docking of the two domains [40]. The similarity between the folding landscape obtained experimentally for lysozyme and the one obtained when simulating the folding of a 125-mer with a 5x5x5 cubic native state is remarkable. Therefore, energy landscapes constitute a conceptual framework for understanding both two-state and multi-state folding kinetics [35, 42]. Since the folding time will increase exponentially with the chain length, due to the fact that the number of semi-compact states increases faster than the number of transition states, the three-stage model will not be able to give reasonable folding times for long chains.

The traditional models can, in particular cases, be better phenomenological descriptions of the folding process, but this 'new view' of folding provides a unifying mechanistic description for the different proteins regardless of their folding complexity. More importantly, it provides a framework for the interpretation of experimental observations.

1.1.4. Protein Folding in the Cell

Partially folded proteins expose regions that in the native state are buried and this promotes inappropriate intramolecular interactions that may lead to aggregation. To overcome this problem, biological systems have developed the molecular chaperone machinery that prevent and guarantee efficient folding within the cellular environment. Molecular chaperones stabilise and guide folding without altering the predetermined native fold. It has been shown that a large portion of the proteins that are synthesised require further assistance in order to fold correctly in a biologically relevant amount of time. The physical principles guiding folding *in vitro* and *in vivo* are the same but *in vivo*

additional factors will affect the success of folding. The first obvious difference between the test tube and cellular environment is the concentrations of macromolecules. While polypeptide chains *in vitro* refold in very diluted solutions (<1 mg/ml), the cellular environment is extremely crowded (300-400 mg/ml of proteins and other macromolecules [43]) which significantly increases the affinity between the different species present such as folding intermediates and could lead to aggregation [44]. The crowding effect can indeed increase the association constants between macromolecules, favouring aggregation, but this effect is more significant for small proteins, as larger ones will have a reduced diffusion which limits the encounter rate with other macromolecules. Nevertheless, crowding may also have a positive impact on the folding propensity [45-46]. It promotes the exclusion volume, stabilising the native and compact states. In addition, it may increase molecular chaperones function by promoting their encounter with partially unfolded proteins, facilitating chaperones successive reaction cycles with non-native proteins [44, 47].

In the cell folding can be co-translational and, while on a first approach this could be regarded as a mechanism to avoid the harmful interaction between polypeptide chains and to guide proper folding, it can also have a negative impact. As chains elongate, the polypeptide chains move along the ribosome tunnel until they are released to the cytosol. However, this tunnel is quite long and not very wide [48] (only after the addition of 20-40 amino acids the chain starts to emerge from the ribosome [49]), which represents constraints to the conformational space available to the nascent chain [50-51]. This conformational constraint can guide the folding process and avoid harmful interactions but, at the same time, also avoid native–like interactions or promote non-native ones leading to folding traps. The conformational constraints imposed by the ribosome tunnel can be particularly harmful

for the assembly of parallel β-sheets and complex antiparallel β-sheet topologies since these structure elements involve interactions between residues that are distant in sequence. In addition, translation is relatively slow (~15-75s for a 300 amino-acid protein [52]) leading to the exposure of partially folded nascent chains to cellular environment for a long period of time which represents another challenge for the *de novo* folding. Individual ribosomes are grouped in polysomes during active protein synthesis.

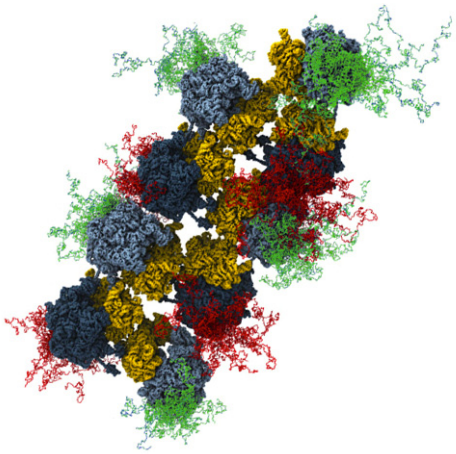

Figure 1.5: Model of nascent chain configurations in a representative polysome. From [53].

The 3D organisation of the polysomes revealed that ribosomes are organised along the mRNA through a pseudohelical orientation. The transcript is sequestered inside, while the tRNA entrance sites as well as the polypeptide exit sites face the cytosol (**Fig. 1.5**). This orientation allows for the maximisation of the distance between nascent chains on adjacent ribosomes, thus also contributing for decreasing the probability of intermolecular interactions that would lead to aggregation.

Considering the complexity inherent to the folding process within the cell, a new schematic energy landscape had to be re-drawn to describe protein folding and the aggregation process under physiological conditions [54].

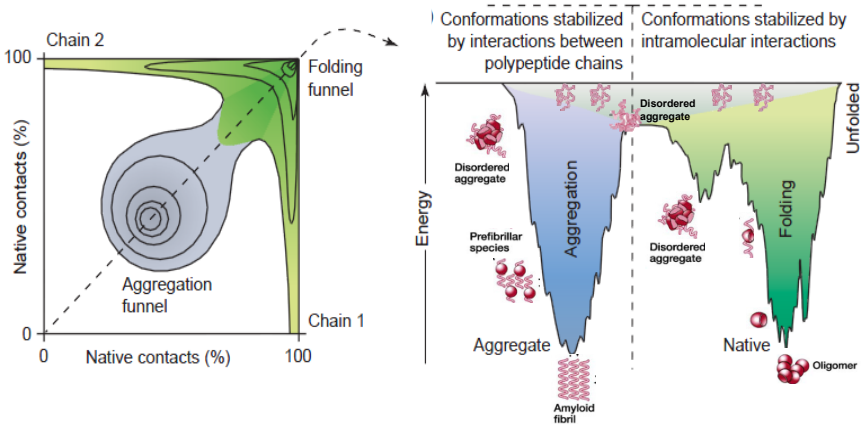

Figure 1.6: Folding funnels designed to describe the competition between productive/efficient folding and aggregation. **Left.** A higher-dimensional energy landscape contour plot that includes stabilising interactions between two polypeptide chains. In this simplified example, the stable aggregate is formed via intermolecular stabilising interactions that develop between two partially folded conformations with about 50% of the contacts present in the native state. Darker colours represent lower energy conformations. **Right.** A double funnel depicting the competition between folding and aggregation. The surface shows the ensemble of unfolded conformations funnelling towards the native state via intramolecular contacts formation or towards the formation of aggregated states via intermolecular contacts. The relative population of the different states depend on the kinetics and thermodynamics of the various equilibrium states. The lowest energy state for the aggregate might or might not represent the true global energy minimum regardless of this it is sufficiently kinetically trapped from the native conformation and in living systems, the fate of a given protein molecule is closely related by the protein quality control. Adapted from [54-56].

This new energy landscape formulation was extended to contemplate different scenarios like aggregation, fibril formation and co-translational folding, as well as the action of molecular chaperones and other cellular factors (**Fig. 1.6**) [57-59]. The surface shows the diversity of the unfolded state as previous descriptions. On the left side of the funnel, intermolecular contacts lead to the formation of non-native structures such as aggregates and amyloid fibrils that are likely to occur due to misfolding and exposure of hydrophobic regions. Intermolecular contacts lead to the deepest minima (more stable), thus the native state is not necessarily the most stable structure. On the

funnel right hand side, intramolecular interactions are dominant, and the native state is formed, however, intermediates that might need some refolding to evolve towards the native state are also present.

1.1.5. Protein Evolution

The concept of a funnelled energy landscape has its biological consequences, the first immediate one being that proteins are structurally robust [60]. A mutation may not disrupt the balance between the entropy of the unfolded state and the free energy of the folded state; if this occurs, the funnel landscape model allows for the new native state to be identical in terms of structure and stability to the primordial protein and likely function is also retained [61-62].

Structural studies on proteins have shown that different unrelated sequences (no homology) can assume the same fold, which means that the space of possible sequences exceeds by far the space of allowed structures. Also, proteins with the same fold may not have the same ancestor, which constitutes evidence of a convergent evolution [63]. Proteins that are structurally homologous usually show an identical folding funnel since their folding mechanism is expected to be conserved. Transition state conformations among homologous proteins are likely to be identical and thus the differences in terms of folding rate are a direct consequence of different native state stabilities [61]. The enzymes' ability to process chemicals that have only recently appeared on this planet and the emergence of drug resistance highlights the proteins' tremendous capacity to acquire new functions and structures. Evolution of function within the same fold is largely accepted [64], however, the mechanisms underlining structural evolution are still controversial. Tawfik and co-workers suggested that protein evolution relies on protein functional promiscuity and

conformational diversity [65-66]. Natively unfolded proteins constitute the most extreme, yet remarkable, example of protein conformational diversity. These proteins can have two distinct structures: unfolded and folded once they bind to their ligands or proteins partners [67]. The analysis of several proteomes has shown that natively unfolded proteins are not rare events, and in fact eukaryotes have a percentage of natively unfolded proteins between 31-51% [68]. Eukaryote organisms have the higher percentage of natively unfolded proteins which may result from the fact that these organisms have a greater need for protein mediated signalling, regulation and control, functions that are common among natively unfolded proteins. The identification of intrinsically unfolded/disorder proteins has imposed a review of the structure-function paradigm, a defined structure is no longer a prerequisite for function or at least not for all proteins.

Fold is likely to have co-evolved with function and accordingly, structural plasticity (the ability to adapt to mutations) enables a parallel and smooth evolutionary transformation of structure and function via intermediates containing a structural ensemble [65, 69]. Two different folds may not be totally separated in sequence space and the marginal stability of native folds ensures that novel folds are evolvable upon a few mutations via intermediate bridge sequences called evolutionary bridges (**Fig. 1.7**, [70]). The existence of these bridges allows proteins to explore new structures and new functions but at the same time retain the original ones. The sequence of these bridges impairs the exclusive selection of one of the possible folds and crossing this state will depend on the functionality of both folds. However, these bridges can also result in evolutionary discontinuity. They can be regarded as evolutionary dead ends when leading to constrains to allosteric systems or protein misfolding.

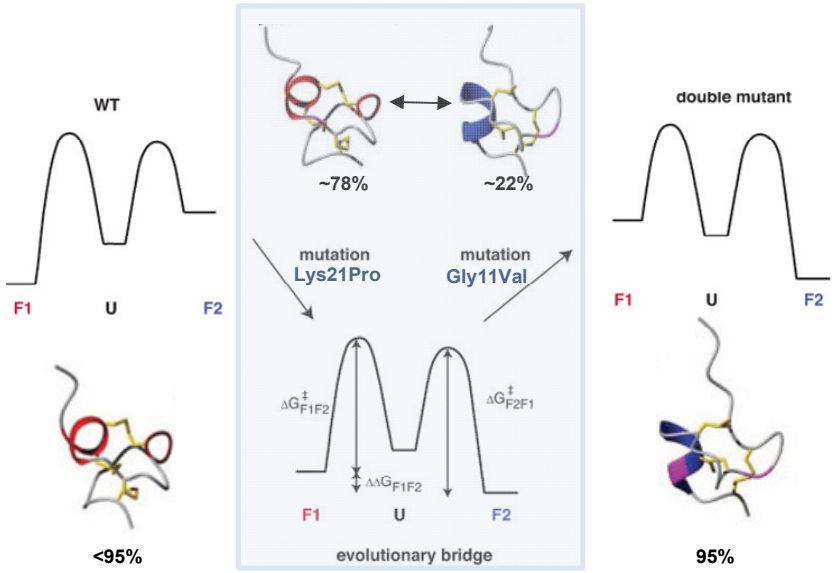

Figure 1.7: Transition folds through an evolutionary bridge. Two different topologies (mediated by three different disulfide bridges) are found in two naturally occurring cysteine-rich domains (NW1 and Mcol1C) that show almost no sequence identity beyond the conserved cysteines. Conversion between these topologies was demonstrated via one mutation Lys21 → Pro21 (K21P). This mutation leads to an intermediate that equilibrates between the two topologies (evolutionary bridge). A second mutation Gly11→Val11 (G11V) completes the transition [71]. Adapted from [70] .

Protein folds are robust not only as a result of sequence selection, but also due to the presence of chaperones and to the stability thresholds associated to each fold that may lead to the accumulation of damaging mutations [72-74]. By stabilising proteins against misfolding chaperones, they act like buffers preventing the formation of non-native structures extending the neutral networks (no effect results from the introduction of mutations). Due to the chaperones sensitivity and response to environmental stress, they are likely to act like evolutionary aiders.

Considering this scenario of co-evolution of fold and function, and the existence of proteins with structural plasticity, it may be suggested

that the early folds evolved from functional but yet intrinsically unfolded proteins [75].

1.2. When the Folding Process Goes Wrong: Misfolding and Aggregation

Life depends enormously on the ability of proteins to be functional, which for most relies on their ability to fold into their correct native-like three dimensional structures. However, the folding process is not perfect and proteins may not fold correctly. In fact, ~20% of newly synthesised proteins are unable to attain the correct fold, even with the help of molecular chaperones, and are degraded by proteases [76]. In a concerted way, molecular chaperones and proteases supervise and regulate the folding process (protein quality control). Only when these fail or become overloaded pathological behaviours associated with protein misfolding start to be observed. Changes in the cellular environment, such as temperature fluctuations, increased oxidative stress and ageing, as well as changes at the protein level, such as the insertion of mutations, culminate in an increase of the burden of misfolded proteins, leading to the failure of the protein quality control. Protein misfolding and aggregation can result in a large and diverse group of diseases described as 'protein misfolding' or 'protein conformational' diseases [77]. These pathologies may result either from a 'loss-of-function' or a 'gain-of-function'. Typically, pathologies associated to 'loss-of-function', such as Cystic Fibrosis, result from a high proteolytic degradation of a given protein. If a protein misfolds to a greater extent and is unable to refold, it is degraded by the protelytic system which results in reduced functional levels of that protein. Alternatively, misfolding can lead to a 'gain-of-function' if it confers cytotoxicity to the 'diseases protein', promoting inappropriate

interactions that lead to protein aggregation. Amyloid diseases and Huntington's are examples of diseases associated to a 'gain-of-function' [78]. Mutations increasing the protein's hydrophobicity or decreasing its charge favour intramolecular interactions and hence aggregation. Also, alterations to proteins that lead to a deficient processing may result in the accumulation of protein fragments that can act as seeds of the aggregation process [55, 79-80].

1.2.1. Molecular Chaperones

Molecular chaperones are involved in a wide range of cellular processes including *de novo* folding, refolding of stress-denatured proteins, oligomeric assembly, intracellular protein transport and assistance in proteolytic degradation (**Table 1.1**) [52]. Chaperones interact, stabilise and guide non-native proteins to fold into the native-state, but do not determine the native fold nor are present in the final functional structure.

Chaperones are expressed in multiple cellular compartments. Although not much is known about their cellular concentration or whether they are freely available in the cell to cope with sudden folding requirements, they should constitute a considerable fraction of the cellular machinery [81-83]. These folding 'helpers' are growth-regulated and stress-responsive bridging stress signalling processes with protein homeostasis. The key regulator of molecular chaperones in eukaryotes is the heat-shock factor-1 (HSF1) which is highly conserved and ubiquitously expressed. Its DNA-binding and transcriptional activities are inhibited and regulated by the molecular chaperones themselves that remain weakly bound to HSF1 in the absence of stress [83].

Table 1.1: Major chaperone and proteases families.

Family	E.Coli	Interacting partner (co-chaperone)	Eukaryotic Homolog (localization)[a]	Activity[b]	Phenotype (null mutants)	Ref.[d]
AAA+ (Hsp100/ Clp)	Clp A	Clp P	Clp P (m)	AP	No Phenotype	[76, 84]
	Clp B		Hsp104 (c), Hsp 78 (m)	AD of aggregates	Impaired Thermo-tolerance	[85-89]
	Clp X	Clp P	Clp X (Humans - m; plants - ch)	AP	No phenotype	[90-94]
	Clp Y (HslU)	Clp Q (HslV)		AP	No phenotype	[95-97]
	FtSH		Agf3, Rcalp (m)	AP	Lethal	[98-101]
	Lon		PIM1 (m)	AP	Mucoid Growth	[102-107]
Hsp 90	Htp G		Hsp 82	AC	Reduced growth rate at 44ºC	[108]
Hsp 70	DnaK	DnaJ, CbpA, DjlA	Hsp70, Hsp72, Bip, etc	AC	Temperature sensitive growth (39ºC)	[108]
	Hsc A	Hsc B	Ssq1p	AC[c]	Slow Growth	[109]
	Hsc 62	(YbeS, YbeY)		AC	No phenotype	[110-111]
Hsp 60	GroEL	GroES	CCT, TriC	AC	Lethal	[109]
sHSP	IbpA, IbpB		Hsp 25, etc	AC	No phenotype	[109]
Hsp 33	Hsp33			Redox-regulated AiC	Slightly sensitive towards High temperature and H2O2	[109]
TF	Trigger factor			PPIase, AiC	No phenotype	[109]

[a] (m) – mitochondria, (c) – cytosol and (ch) – chloroplasts;
[b] AP – ATP-dependent proteolysis; AD – ATP-dependent disaggregation; AC – ATP-dependent chaperone; ATP-independent chaperone;
[c] ATP-dependent chaperone involved in Fe-S cluster formation and protein maturation
[d] References are not all-inclusive. Emphasis on review articles and papers demonstrating the chaperon/protease activity.

Molecular chaperones selectively bind to hydrophobic residues and/or unstructured backbone regions, features that are normally exposed in non-native states but are shielded in the native state [112-113]. When binding to non-native conformations, chaperones 'hold' the proteins in an 'on-pathway' conformation avoiding harmful interactions

that could lead either to aggregation, or to conformational trapping (e.g. Hsp104 and sHSPs). In addition to being able to block deleterious interaction, some chaperones are also able to promote the correct folding (Hsp70 system) [112, 114]. Apart from these two remarkable features, the Hsp60/CCT/Clp/Hsp104 chaperone machinery can also reverse intra-molecular misfolding, by unfolding and disrupting small aggregates [115]. For a growing number of proteins the chaperone activity has to be combined with isomerase activity (PDIs and PPIases) in order for the correct fold to be guaranteed [116].

Two molecular chaperone systems are involved in the protection against the proteotoxic effect inherent to misfolding diseases: the Hsp 70 and the chaperonins. The members of the Hsp70 family exist in the cytosol of eukaryotes as well as in their organelles such as endoplasmatic reticulum and mitochondria [117]. Comprising a wide range of functions such as assisting *de novo* folding, assembling of newly synthesised proteins into macromolecular complexes, avoiding aggregation, dissolving and refolding aggregated proteins, protein trafficking and assistance in the proteolytic degradations of terminally misfolded proteins, this family of molecular chaperones is not only constitutively expressed but their expression is also induced/increased under stress conditions [117-119]. Hsp70's have two domains, an N-terminal ATP-binding domain (NBD) and a C-terminal substrate binding domain (SBD) and both are essential for its chaperone activity. The binding of ATP to the NBD domain induces an "open" conformation that allows for the substrate to be recognised. When a substrate binds to the SBD domain, ATP is hydrolysed and the SDB domain conformation "closes", stabilising the chaperone-substrate complex. ADP is then released and the binding of another ATP molecule to the NBD will induce the opening of the SBD domain and consequently the substrate will be released. This cycle of binding and

release of the substrate promotes folding and at the same time prevents aggregation [114, 120]. The molecular process by which Hsp70's induce conformational changes is still not clear, but a mechanism involving entropic pulling is hypothesised [121]. According to this mechanism, when Hsp70 binds to the substrate it locally stabilises it in the unfolded state. Disaggregation is favoured and, once the substrate is released, it can fold into the native state. Co-factors (NEF) and co-chaperones (Hsp40/DnaJ) participate and regulate Hsp70 chaperone activities. While co-factors control the Hsp70 cycles by facilitating the ADP release and rebinding of ATP, co-chaperones control the specificity of Hsp70's by targeting the substrates to the chaperone [52, 81]. Bag-1, a co-chaperone of this system, binds to the proteosome directing proteins for degradation, and thus has a crucial and regulatory role in protein degradation [122].

The Hsp70 machinery has been implicated in the pathogenesis of misfolding and age-related diseases [123]. Hsp 70, as well as other chaperones and components of the ubiquitin-proteosome system, have been found in inclusion bodies/plaques characteristic of neurodegenerative diseases associated to protein misfolding [124]. In addition, although Hsp70 machinery is active in polyglutamine cell models it is unable to prevent protein aggregation. Together, these observations suggest that Hsp70 machinery is indeed activated during misfolding pathologies, however its capacity is likely to be exceeded. [125-127]. Ageing cells show a decreased transcription of the Hsp70 machinery and a decreased DNA binding activity of the transcription factor HSF-1 (the regulator of Hsp expression), thus these cells are more prone to the accumulation of toxic misfolded proteins [128-131]. In agreement, the most severely affected neurons in Huntington's disease, a pathology associated to protein misfolding and aggregation, show reduced Hsp70 expression levels [132-133], highlighting the

importance of this chaperone system in the regulation of neuronal susceptibility towards degeneration.

Chaperonins are large (~800kDa), doubled ring complexes enclosing a central cavity (**Fig. 1.8**). Conserved throughout evolution, chaperonins are divided in 2 subgroups [52, 117]. Group I (Hsp60's) occurs in bacteria (GroEL), mitochondria and chloroplasts. GroES (bacteria) or Hsp10 family cooperate with this group by acting as a lid of the ring complex. Chaperonins have a crucial role in the regulation of protein homeostasis and a single point mutation (V98I) on mitochondrial Hsp60 severely impairs its regulatory function in some cell types leading to the development of hereditary spastic paraplesgia (**Table 2**) [134-135]. Group II is present in archea and eukaryotic cytosol (TRiC/CCT), and, is GroES independent since their lid function is embedded into the chaperonin ring in the form of specialised α-helical extensions. TRiC promotes the folding of newly synthesised peptides (that may be presented by the Hsp70 and/or the co-chaperone prefoldin), its expression is transcriptionally and functionally linked to protein synthesis and is not stress induced [136-137]. The group II has been extensively implicated in the development of neurodegenerative diseases, especially in Huntington's disease. Several experimental evidences suggest that TRiC modulates huntingtin aggregation [123, 138]. The TRiC polypeptide binding region has diverged during evolution to create substrate binding specificity. Its substrates tend to be large hydrophobic proteins with β-strands and high aggregation propensity, which are characteristics present in polyQ- expanded huntingtin as well as other amyloidogenic proteins [139-141]. The concerted action with Hsp70 optimises TRiC neuroprotective properties [142].

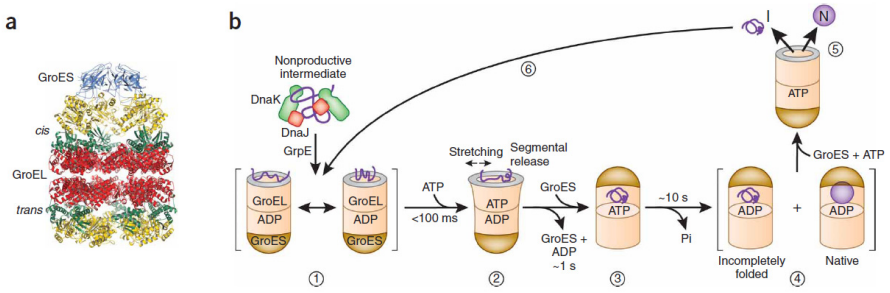

Figure 1.8: The GroEL-ES chaperonin. A) Crystal structure of the aymetric GroEL-ES complex (PBD 1AON). B) Working model summarising the conformational changes in a substrate protein upon transfer from Hsp70 system (DnaK, DnaJ and GrpE) to GroEL and during GroEL-GroES-mediated folding (ATP dependent cycles). (1) Substrate protein may be delivered to the GroEl by the Hsp70 system in a non-aggregated but kinetically trapped state. Upon binding to GroELit undergoes local unfolding to an ensemble of expanded and more compact conformations. (2) ATP-dependent domain movement of the apical GroEL domains results in stretching of tightly bound regions of substrate and in release and partial compaction of less stably bond regions. (3) Compaction is completed upon substrate encapsulation by GroES. (4) Folding in the chaperonin cage. (5) Substrate release upon GroES dissociation. (6) Rebinding of incompletely folded states. N, Native state and I, folding intermediate. From [52].

The mechanism of action of chaperonins is to some extent identical to the observed for the Hsp70 family. Similarly, it depends on ATP hydrolysis and folding is promoted by substrate binding/releasing cycles. However, chaperonins promote folding through cycles of global protein encapsulation that may involve mechanical stress and this constitutes the main difference in terms of the mechanism of action of these two chaperone systems. Non-native substrates bind, through hydrophobic interactions, to apical domains of the unoccupied ring; the co-chaperone and ATP then bind to the ring and the substrate is encapsulated inside. The binding of a co-chaperone induces conformational changes on the GroEL ring, which result in strong upward and outward motions of the ring, causing a significant expansion of the distance between the encapsulated polypeptide binding regions [52]. Thus, the substrate is subject to stretching forces

that can induce unfolding as it was observed for lysozyme and rhodanese [143-145]. The mechanism of action and the nature of group II binding sites are not yet understood.

1.2.2. Rescuing of Misfolding Defects by Small Molecules- Chemical Chaperoning

An increasing number of studies describe the use of low molecular weight compounds to overcome folding defects in proteins involved in conformational disorders (**Table 1.2**). These small molecules, often also called chemical chaperones, can have a direct impact on the protein stability and solubility and can also regulate or substitute the folding activities of molecular chaperones [146]. The effect of these molecules can be particularly relevant in the context of misfolding/conformational diseases, namely when partial rescuing of the perturbed protein is enough to obtain the minimal activity required or at least to partially attenuate the observed defects [147-150]. In some particular cases, chemical chaperoning is likely to lead to a concrete pharmacological use especially in lysosomal storage disorders such as Gaucher's disease [151-152]. Many of these small compounds are known to serve as organic osmolytes and other compatible solutes, synthesised or uptaken by living organisms from micro-organisms to plants and animals, to minimise protein denaturation, allowing the adaptation to harsh environments or stress [153-155]. These molecules fall into six major categories: small carbohydrates including sugars (e.g. trehalose), polyols and derivatives (e.g. glycerol, inositol, sorbitol, and o-methyl-inositol), amino acids and derivatives (e.g. glycine proline taurine and ectoine), methylamines (TMAO and glycine betaine), methylsulfonium solutes (DMS) and hydrophobic compound (4PBA) [156-157]. The mechanism

by which osmolytes promote protein folding and increase thermodynamic stability has been extensively studied. These chemical compounds do not bind directly to proteins, their mode of action is not specific and it can be described by the “solvophobic” effect. The interactions of the osmolyte with the peptide backbone are unfavourable causing a preferential exclusion of osmolytes from the water-protein interface leading to a preferential hydration of the protein surface. The presence of osmolytes also results in an increased solvent density that restrains the proteins’ free movements, increasing its compactness [158-161]. This non-specific mechanism of the chemical chaperones action allows them to intervene in different stages of the folding process [162-164]. Chemical chaperones can stabilise the native state, preventing aggregation or degradation, direct the folding pathway or promote refolding of misfolded/destabilised proteins [165]. It should be noted that, since their mechanism of action is not specific, the same compound may have different effects if present in different stages of folding process or opposite effects for two different proteins. Both cytosolic and endoplasmic reticulum (ER) folding can be modulated by chemical chaperones. Their actions allow restoring a protein function by stabilising the protein conformation or by correcting trafficking defects [152, 166-167]. Also, these compounds have been shown to be able to promote the assembly of complexes through the stabilisation of intermediates states, to stabilise aggregation prone proteins and to induce structure in intrinsically unstructured proteins, thus regulating biochemical processes [147, 168-169]. Apart from this direct action on the folding reaction, certain chemical chaperones can also regulate molecular chaperones and the unfolded protein response system [146, 170]. A subgroup of chemical chaperones, the pharmacological chaperones, is often distinguished. Opposite to the above described general and unspecific effect of

chemical chaperones, these compounds have a specific action on a given target protein. This subgroup comprises competitive inhibitors, ligands, agonists/antagonists and protein's co-factors such as metals and flavins. Copper may be regarded as a pharmacological chaperone: its use may prevent the trafficking impairments associated to Menkes' disease. Mutations in the copper transporter P-type ATPase (MNK) leads to its ER retention and the development of Menkes disease. MNK disease-related mutant, G1019D, accumulates in the ER, but if the cells expressing this mutant are supplemented with copper, the protein is efficiently processed in the Golgi and reaches the plasma membrane. Thus, copper, MNK ligand, may act as a pharmacological chaperone by promoting its proper trafficking [171].

1.2.3. Protein Quality Control and Disease Prevention

The concerted action of molecular chaperones and protein degradation systems constitutes the cellular protein quality control (**Fig.1.9**). In Eukaryotes, two different degradations systems are present. While cytosolic proteins are degraded by the ubiquitin-proteasome system (UPS) [172-173], mitochondrial proteins are degraded by ATP-dependent proteases [174]. Degradation of proteins is an essential endpoint that contributes to protein homeostasis. Chaperones and proteases/proteasome actions have to be concerted in order to prevent early degradation and, at the same time, to guarantee that extensively damaged proteins are efficiently degraded before aggregation. Two other pathways are also involved in protein degradation and proteostasis: the lysomal and the autophagic trafficking pathways (reviewed in [175]).

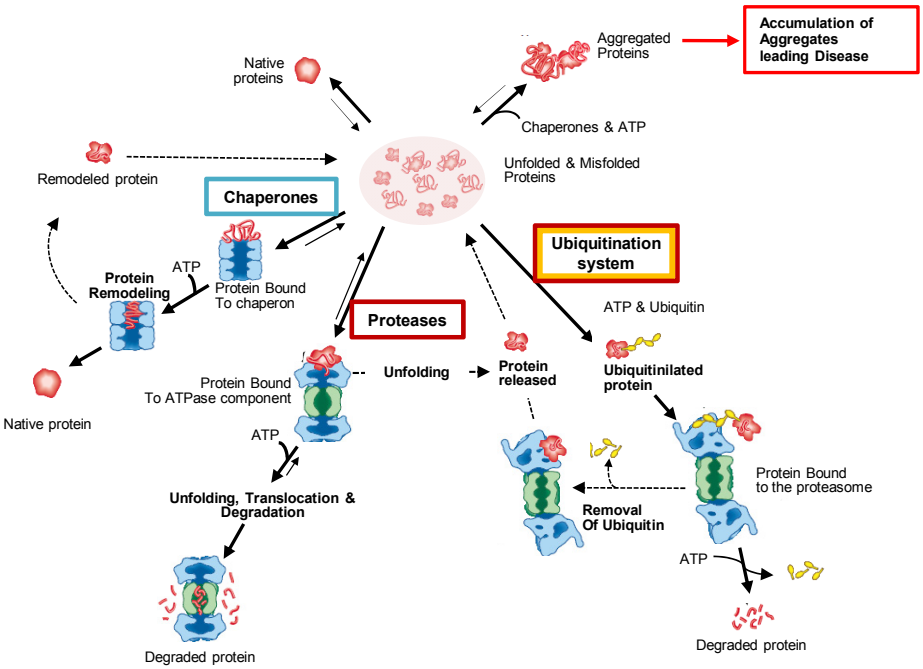

Figure 1.9: Protein Quality control. Cells have a pool of misfolded or unfolded proteins. These non-native states result from the biosynthesis of normal (but unable to fold without the assistance of molecular chaperones) or aberrant proteins (mutated), the chaperones cycles and as the result of stress conditions (such as thermal fluctuations and increased oxidative stress). Non-native proteins are recognised by the cell's protein quality control. Exposed hydrophobic regions are recognised by chaperones (all families) and by ATP-dependent proteases. **Chaperone** binding and release of folding intermediates may allow proteins to reach the native state or they may return to the non-native proteins pool where they can rebind to chaperones or bind to proteases. **Protease** binding followed by the ATP-dependent unfolding and subsequent degradation removes the protein from the non-native proteins pool. After being unfolded by the protease, if the protein is repaired it will be released prior to degradation. In eukaryotes the degradation pathway in the cytosol involves the **ubiquitination system**. Non-native proteins are recognised and ubiquitinilated and targeted to the proteasome where they are degraded. Similar to what is observed for the proteases after unfolding reaction inside the chambers of the proteasome the protein may be deubiquitilated and return to the pool of free cytosolic proteins avoiding degradation. Chaperones main action is to avoid aggregations, however, some chaperones can also promote disaggregation. Protein aggregates are relatively resistant to proteolysis so, in order to be degraded, aggregates have to be dissolved first. Misfolded or partially folded proteins can aggregate and if the protein quality control fails aggregated proteins accumulate leading to disease. Adapted from [76].

The main difference between the action of proteases and proteasomes relies on their mechanisms of substrate recognition. In mitochondria, ATP-dependent proteases selectively bind to non-native proteins by recognising, like chaperones, exposed hydrophobic regions and/or unstructured regions. In the cytosol, proteins are marked for proteolysis by the covalent attachment of polyglubiquitin chain(s) which are recognised by the 26S proteasome [176-177]. Ubiquitination is a multistep process involving three enzymes that select the targets for degradation and facilitate ubiquitination. Modulator proteins, such as E3 ligases and chaperone co-factors (CHIP and Bag1) link chaperones to the UPS which supports the idea of direct communication between folding and degradations systems [122].

In the mitochondria, the fact that chaperones and proteases bind to the same substrates could result in competition, but since chaperones are more abundant, probabilistically non-native proteins will bind to the latter before interacting with proteases [178]. After being released from chaperones, non-native proteins can either acquire the native fold (that is not recognised by the protein quality control elements) or remain in a non native state and then interact again with a chaperone or a protease [179]. When encountering a protease, the most likely scenario is protein degradation. However, a fraction of the proteins that are unfolded by the chaperone component of the proteolitic complex may be in fact released [180].

Mitochondrial ATP-dependent proteases derive from the bacterial proteases and are highly conserved in Eukaryotes [181]. These proteases degrade misfolded or non-assembled proteins to peptides which are either exported or further degraded by oligopeptidases. The AAA proteases are localised in the inner membrane, while Lon and

ClpXP are present in the matrix [182-185]. AAA proteases are integrated in the mitochondrial inner membrane; m-AAA catalytic domain is turned to the matrix while i-AAA catalytic domain is in the intermembrane region. These proteases overlap in substrate specificity and the fact that they are inversely inserted into the membrane allows for the efficient degradation of damaged membrane proteins independently of their topology. AAA proteases also dislocate the substrate proteins allowing their degradation in a hydrophilic environment through an ATP-dependent process [186]. Matrix proteases have a chaperone domain preceding the proteases domain. ClpXP has a barrel like structure with the two heptameric rings of ClpP (the proteolitic core) flanked on both sides by the hexameric rings of ClpX. The barrel has a series of aqueous chambers connected by an axial chamber, thus, the proteolytic domain on ClpP is isolated and inaccessible to other proteins (this isolation of the proteolytic site is identical to the observed in the proteasome). The ClpX has ATPase and chaperone activities and their aqueous chamber may function analogously to what is described for the GroEL family: in addition to preventing aggregation it can also promote disaggregation [92-94]. Lon functional organisation is still unknown; *in vivo* it was shown that proteolytic inactive Lon can protect substrates from other proteases, which suggests the existence of binding sites or chambers that sequester the substrate proteins from the surrounding medium [187]. Also, proteolytic inactive yeast Lon was shown to be able to promote the assembly of inner membrane complexes but its chaperone activity is ATP-dependent [187]. Lon degrades misfolded proteins in the matrix, including thermally denatured proteins and oxidatively damaged proteins such as aconitase [182-183, 185]. Although the mitochondrial protein quality control is quite robust, it has limited capacity and oxidatively modified proteins and aggregated aconitase

accumulate in the mitochondrial matrix of aged cells which may contribute to the age-related mitochondrial decline [83, 127].

The degradation and the chaperone machineries are responsible for repairing and removing most forms of aberrant proteins, avoiding protein aggregation. Both systems are induced by stress conditions such as temperature and their expression levels increase in parallel, guaranteeing the balance between them. Mutations on either proteases or chaperones result in an imbalance of protein homeostasis, accumulation of insoluble proteins (inclusion bodies) and increased cellular sensitivity to stress [178, 188]. These observations highlight the importance of chaperones and proteases on protein homeostasis.

If these two systems fail, proteins aggregate, triggering deleterious biological processes that compromise the cell homeostasis. Protein aggregation has been linked to many diseases including diabetes II, Alzheimer's and Creutzfeldt-Jakob's diseases [55, 189]. Aggregates may form structures that can disrupt some cellular functions (such as pores in membranes reducing the potential across the membrane [190]), serve as seeds for the aggregation of other unrelated proteins or engaged and block molecular chaperones and proteases, decreasing their availability to other substrates. Protein aggregation is a progressive process that starts with non-specific interaction leading to the formation of oligomeric species. Small oligomers can evolve to more organised structures such as 'protofilaments' and ultimately well-defined fibbers (amyloid fibbers) are formed [191-192].

1.2.4. Mitochondrial Dysfunction and Neurodegeneration

Mitochondria are essential and extremely specialised organelles, with a plethora of function including energy production and cellular

homeostasis [193]. Mitochondrial dysfunction has severe cellular consequences and is associated with several neurodegenerative diseases **(Table 1.2)**. Mitochondria harbour the respiratory chain, whose efficient function constitutes the cell's main driving force (it produces more than 15 times the ATP generated by anaerobic glycolysis). In addition, these intricate organelles are also involved in fatty acid oxidation, steroid metabolism, intermediate metabolic pathways, calcium homeostasis and free radical scavenging. Although most mitochondrial proteins are encoded by the nuclear genome, mitochondria also have their own genome (mtDNA). The mtDNA encodes 13 polypeptide components of the respiratory chain as well as all the components necessary to ensure intramitochondrial protein synthesis [194]. Mitochondrial morphology is complex and plastic, mediated by conserved cellular machineries mitochondria undergoes constant fusion and fission events that constitute a reticulated mitochondrial network and allow the adaptation of these organelles to different physiological demands. Mitochondria change shape, size and location and this dynamic behaviour, together with their plastic morphology, contribute to their functional optimisation, which ensures an accurate response to their changing intracellular needs [195]. Despite all the functions described so far that contribute to maintain and improve cellular metabolism and viability, mitochondria are also involved in cell death. The intermembrane space contains pro-apoptotic factors (cytocrome c, Smac/DIABLO and endonuclease G) and insults to the mitochondria may cause the release of those factors to the cytosol and consequently promote apoptosis. For instance, if cytochrome *c* is released to the cytosol, it will bind to Apaf1 and co-caspase 9 to form the apoptosome initiating a downstream cascade that results in cell death [196].

Table 1.2: Proteins associated to neurodegenerative diseases that involve mitochondrial dysfunction/decline.

Protein	Function	Disease	Clinical Features
APP	Unknown. Precursor of Aβ peptide the primary component of senile plaques	Alzheimer's disease	Most common dementia. Confusion, language breakdown and social withdrawal.
Presenilins 1 and 2	Component of γ-secretase which cleaves APP to yield Aβ		
α-Synuclein	Unknown, but interacts with tubulin. Primary component of Lewy bodies	Parkinson's Disease	Progressive rigidity, bradykinesia and tremor.
Parkin	Ubiquitin E3 ligase		
PINK1	Mitochondrial kinases, although the function is unknown seems t protect against cell death		
LRRK2	Kinase. Function unknown		
DJ-1	Protects the cell against oxidant-induced cell death		
HtrA2	Serine protease in the mitochondrial intermembrane space. Degrades denatured proteins within mitochondria. Degrades the inhibitor of apoptosis proteins and if released to the cytosol promotes apoptosis		
SOD1	Converts superoxide to hydrogen peroxide	Amyotrophic lateral sclerosis	Progressive weakness, atrophy and spasticity of muscle tissue
Huntingtin	Unknown. Maybe involved in vesicular transport regulation during neurotransmitter release	Huntingtons's Disease	Uncoordinated body movements, decline in cognitive abilities and reduction in life-spam
Frataxin	Mitochondrial iron chaperone that promotes biogenesis and repair of Fe-S clusters. Also involved in Heme biosynthesis and iron detoxification.	Friedreich's Ataxia	Ataxia and neuropathy due to degeneration of spinocerebellar tracts and dorsal-root ganglia; diabetes and cardiomyopathy
Paraplegin	Subunit of hetero-oligomeric m-AAA protease in mitochondrial inner membrane	Hereditary spastic paraplegia (HSP)	Slowly progressive weakness and spasticity of the legs
Hsp 60	Mitochondrial matrix chaperonin		
Opa1	Mitochondrial dynamin-like GTPase required for inner membrane fusion and cristae morphology	Autosomal dominant optic atrophy (DOA)	Optic neuropathy causing progressive visual loss
MFN2 (subtype 2A)	Mitochondrial outer membrane Dynamin-like GTPase that mediates fusion	Charcot-Marie-Tooth disease	Neuropathy of motor and sensory nerves. Weakness of the foot and lower leg muscles.
GDAP1 (Subtype 4A)	Mitochondrial outer membrane protein that promotes fusion		
Pantothene kinase 2	Mitochondrial, catalysis the 1st step in coenzyme A synthesis.	Neurodegeneration with brain ion accumulation (NBIA)	Progressive dementia, rigidity, involuntary movements, spasticity and retinal degeneration

Mitochondria have developed an elaborate protective mechanism, composed by 3 systems that enable them to overcome the diverse challenges threatening their function and integrity. The first comprises a highly conserved intra-organellar proteolysis system: the mitochondrial protein quality control; molecular chaperones and energy-dependent proteases evaluate the folding and assembly of mitochondrial proteins and remove excess and damaged proteins from the mitochondria [181, 184]. The second relies on the dynamic nature of the mitochondrial population: damaged mitochondria can be repaired/restored by fusing with healthy neighbouring mitochondria [195, 197]. The last defence system consists on the removal of damaged mitochondria which enables the survival of the cell. Once the damage to the mitochondria is too extensive, fusion no longer occurs; instead, mitochondria are fragmented and selectively removed from the cell through an autophagyc process named mitophagy [198-199]. This is a cytoprotective system since it eliminates mitochondria without the release of the pro-apototic factors that would destroy the cell.

In spite of these protective mechanisms, mitochondria dysfunction still occurs and is associated with ageing and neurodegenerative diseases [200-203]. Ageing is the greatest risk factor in many neurodegenerative diseases such as Alzheimer’s disease, Parkinson’s disease or amyotrophic lateral sclerosis. Also, many of the specific proteins implicated in neurodegenerative diseases interact with mitochondria.

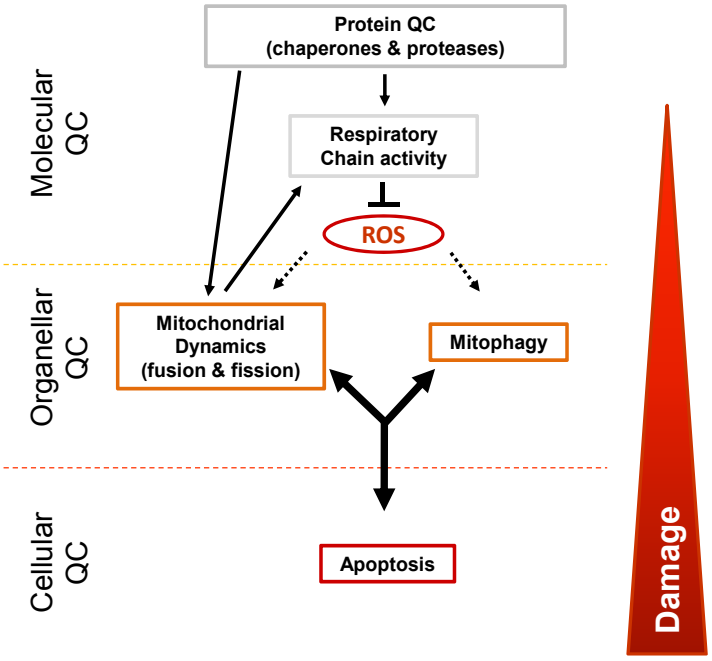

Figure 1.10: Mitochondrial quality control (QC) mechanisms. Intraorganellar protein quality control ensures the correct folding and assembly of mitochondrial proteins and the degradation of excess or damaged proteins. If the protein quality control fails, mitochondrial function can be restored by fusion and fission processes. Ultimately, if the mitochondrial damage is too extensive, mitochondria are fragmented and removed through mitophagy preventing the release of pro-apoptotic proteins. If these 3 systems fail, pro-apoptotic proteins (e.g. cytochrome C) are released leading to apoptosis. Adapted from [181].

Aging leads to the accumulation of mitochondrial DNA mutations, especially large-scale deletions and point mutations, and also to an increase in oxidative stress [204-205]. Proofreading-deficient POLG mice present a marked increase in mtDNA mutations, much like in ageing cells, and consequently exibit decreased ATP production and decreased activity of respiratory enzymes. At 25 weeks of age, these mice began to present pathologies frequent in ageing humans and their lifespan is significantly reduced. In functional mitochondria the amount of reactive oxygen species (ROS) produced through the multiple electron carriers is balanced by the extensive mitochondrial

network of the anti-oxidant defences. However, once mitochondria are damaged, which is believed to occur with ageing, the balance is lost and more ROS is produced, leading to further mitochondrial disfunction [194]. Overexpressing superoxide dismutase, methionine sulphoxide reductase or catalase (three antioxidant enzymes) in *Drosophila* has been shown to prolong flies' lifespan, highlighting the role of ROS in ageing-related mitochondria disfunction [206]. A study performed in human ageing brains, suggests that mitochondrial disfunction is associated to the down-regulation of genes involved in synaptic transmission, vesicular transport and mitochondrial function. In addition, the promoter region of these genes has also shown an increased sensitivity towards oxidative stress, either to their G/C-rich sequences or their inability to undergo transcription-coupled repair [128].

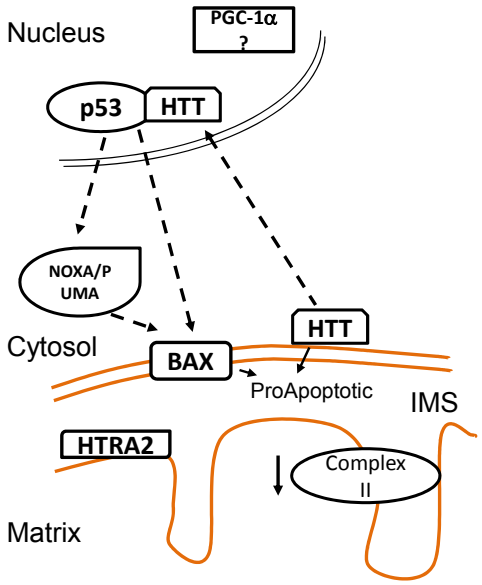

Figure 1.11: Molecular mechanism associated to the development of Huntington disease. Complex II activity is decreases in HD brains. Mutated HTT (with gluthamine expansions) associated to the outer mitochondrial membrane increases the sensitivity towards Calcium-induced cytochrome C release (apoptosis). Mutant HTT also translocates to the nucleus where it binds and induces p53 expression (Apoptotic pathway involving BAX or NOXA/PUMA from the Bcl-2 family). Deletion of PGC-1α or missense mutations on Htr2 are also associated to a HD phenotype [200].

For example, Huntington's disease (HD) involves the loss of long projection neurons in the cortex and stradium. This disorder is associated with a plygluthamine extension on huntingtin protein. The gene coding for this protein normally has less than 36 CAG

trinucleotide repeats but disease related genes show an extension of over 40 repeats [200]. Several evidence, namely increased levels of lactate in patient's cortex and basal ganglia and decreased activities of complexes II and III in human HD brains, suggest that the pathological process may result from mitochondrial dysfunction [207]. Different mechanisms could explain how mutant huntingtin (HTT) results in mitochondrial disfunction and thus the pathological process is still unclear. *In vivo* experiments with HD mouse models, have suggested that HTT may interact directly with the mitochondria. The presence of the polyglutamine expansion results in lower mitochondrial membrane potentials that depolarise at low calcium loads [208-209]. Alternatively, HTT may not interact directly with the mitochondria, but it may alter transcription of several proteins involved in mitochondrial homeostasis [210]. It is known that HTT interacts with p53, CREB-binding protein and SP1. For instance, binding of HTT to p53 increases its levels leading to the up-regulation of downstream targets, BAX and PUMA, and ultimately to mitochondrial depolarisation [211].

Parkinson's disease (PD), another age-related neurodegenerative disease, is also associated to mitochondrial dysfunction. However, the aetiology of this disease is far more heterogeneous and the mutation of several genes has been associated to PD [212]. Independently of the mutated gene, complex I inhibition and increased oxidative stress are prevalent, highlighting the role of mitochondrial dysfunction in PD pathogenesis. At the molecular level, this disorder is characterised by the selective loss of dopamine-secreting neurons in the substantia nigra and the accumulation of cytoplasmatic inclusions - Lewy Bodies. α-synuclein is the major component of Lewy Bodies, but ubiquitin is also present [200]. Among the nuclear genes so far associated to PD, six are involved in mitochondrial functions: α-synuclein, parkin, DJ-1, phosphatase and tensin homologue (PTEN)-induced kinase 1 (PNK1),

leucine-ric-repeat kinase 2 (LRRK 2) and HTRA 2. α-synuclein overexpression impairs mitochondria function and increases oxidative stress and the sensitivity towards MPTP (a complex I inhibitor) [213]. Parkin migrates to the outer mitochondrial membrane, avoids the release of cytochrome *c*, and may also enhance mitochondrial biogenesis by interacting with the mitochondrial transcription factor A [214-215].

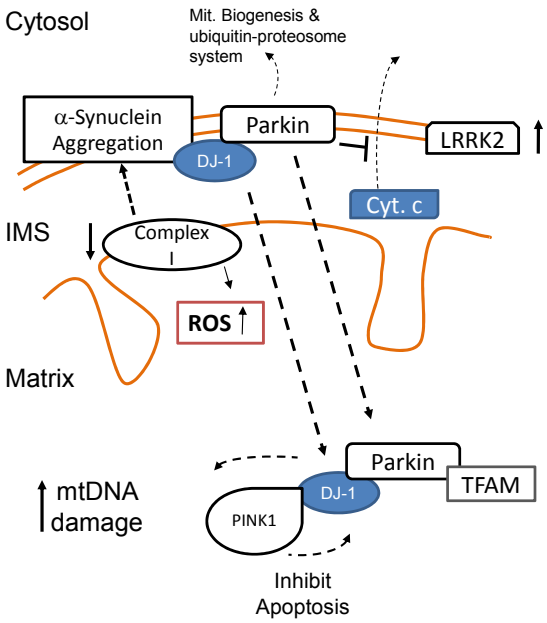

Figure 1.12: Molecular mechanisms associated to the development of Parkinson's disease (PD). Many of the genes associated to the development of this disease are associated to the mitochondria. Complex I activity is decreased which increases the amount of ROS and decreases the mitochondrial ATP production. mtDNA mutations are increased and some patients have mutations on the mtDNA polymerase γ gene which results in multiple mtDNA mutations. Mutation on α-synuclein and parkin are also associated to PD. While α-synuclein mutations lead to its aggregation causing citotoxicity, a 'gain-of-function', mutations on parkin are deleterious by causing a 'loss-of-function' since this protein encodes an ubiquiting E3 ligase and has an anti-apoptotic activity. Dj-1 interacts with α-synuclein, parkin and Pink1, and acts as a redox sensor preventing cells death. Pink1 is also believed to prevent cell death. Mutations on LRRK2 are associated to familial late-onset PD. HTR2 is a putative quality control agent within the mitochondria and pro-apoptotic factor when released into the cytosol, mutations on its gene have been associated to PD. Adapted from **[200].**

DJ-1 when oxidised down-regulates the PTEN-tumor suppressor protecting cells from oxidative-stress-induced cell death [216]. The mitochondrial kinase PINK1 also has an anti-apoptotic role and which is reduced by PD-related mutations [217-218]. Genetic evidence suggest that DJ-1, PINK 1 and parkin function in a sequential way on the same pathway supporting this hypothesis; the physical associations between Dj-1 and α-synuclein, Dj-1 and parkin, and Dj-1 and PINK 1 have been reported. Mutations in the LRRK2 are the most common known cause of familial late-onset PD and, in addition, are also responsible for 1-2% of sporadic cases [219]. HTRA2 was most recently associated with PD: HtrA2 is believed to be one of the proteins involved in mitochondrial protein quality control system; however, when this protein is released to the cytosol, it acts like a pro-apoptotic factor [220-221].

1.3. References

1. Anfinsen, C.B., et al., *The kinetics of formation of native ribonuclease during oxidation of the reduced polypeptide chain.* Proc Natl Acad Sci U S A, 1961. **47**: p. 1309-14.
2. Anfinsen, C.B., *Principles that govern the folding of protein chains.* Science, 1973. **181**(96): p. 223-30.
3. Levinthal, C., *How to fold graciously.* In Mossbauer Spectroscopy in Biological systems. Proceedings 1969. **67**: p. 22-24.
4. Levinthal, C., *Molecular model-building by computer.* Sci Am, 1966. **214**(6): p. 42-52.
5. Elofsson, A., et al., *A study of combined structure/sequence profiles.* Fold Des, 1996. **1**(6): p. 451-61.
6. Moult, J., et al., *A large-scale experiment to assess protein structure prediction methods.* Proteins, 1995. **23**(3): p. ii-v.
7. Sali, A., *Modeling mutations and homologous proteins.* Curr Opin Biotechnol, 1995. **6**(4): p. 437-51.
8. Privalov, P.L., *Thermodynamic problems of protein structure.* Annu Rev Biophys Biophys Chem, 1989. **18**: p. 47-69.
9. Shakhnovich, E.I. and A.V. Finkelstein, *Theory of cooperative transitions in protein molecules. I. Why denaturation of globular protein is a first-order phase transition.* Biopolymers, 1989. **28**(10): p. 1667-80.
10. Levinthal, C., *Are there pathways for protein folding?* J. Chim. Physique, 1968.
11. Wetlaufer, D.B., *Nucleation, rapid folding, and globular intrachain regions in proteins.* Proc Natl Acad Sci U S A, 1973. **70**(3): p. 697-701.

12. Kim, P.S. and R.L. Baldwin, *Specific intermediates in the folding reactions of small proteins and the mechanism of protein folding.* Annu Rev Biochem, 1982. **51**: p. 459-89.
13. Ptitsyn, O.B., *[Stages in the mechanism of self-organization of protein molecules].* Dokl Akad Nauk SSSR, 1973. **210**(5): p. 1213-5.
14. Ptitsyn, O.B. and A.A. Rashin, *A model of myoglobin self-organization.* Biophys Chem, 1975. **3**(1): p. 1-20.
15. Karplus, M. and D.L. Weaver, *Protein-folding dynamics.* Nature, 1976. **260**(5550): p. 404-6.
16. Karplus, M. and D.L. Weaver, *Protein folding dynamics: the diffusion-collision model and experimental data.* Protein Sci, 1994. **3**(4): p. 650-68.
17. Gianni, S., et al., *Unifying features in protein-folding mechanisms.* Proc Natl Acad Sci U S A, 2003. **100**(23): p. 13286-91.
18. Harrison, S.C. and R. Durbin, *Is there a single pathway for the folding of a polypeptide chain?* Proc Natl Acad Sci U S A, 1985. **82**(12): p. 4028-30.
19. Baldwin, R.L., *How does protein folding get started?* Trends Biochem Sci, 1989. **14**(7): p. 291-4.
20. Kauzmann, W., *Some factors in the interpretation of protein denaturation.* Adv Protein Chem, 1959. **14**: p. 1-63.
21. Tanford, C., et al., *Effect of ethylene glycol on the conformation of gama-globulin and beta-lactoglobulin.* J Biol Chem, 1962. **237**: p. 1168-71.
22. Itzhaki, L.S., D.E. Otzen, and A.R. Fersht, *The structure of the transition state for folding of chymotrypsin inhibitor 2 analysed by protein engineering methods: evidence for a nucleation-condensation mechanism for protein folding.* J Mol Biol, 1995. **254**(2): p. 260-88.
23. Otzen, D.E., et al., *Structure of the transition state for the folding/unfolding of the barley chymotrypsin inhibitor 2 and its implications for mechanisms of protein folding.* Proc Natl Acad Sci U S A, 1994. **91**(22): p. 10422-5.
24. Fersht, A.R., *Optimization of rates of protein folding: the nucleation-condensation mechanism and its implications.* Proc Natl Acad Sci U S A, 1995. **92**(24): p. 10869-73.
25. Fersht, A.R., *Nucleation mechanisms in protein folding.* Curr Opin Struct Biol, 1997. **7**(1): p. 3-9.
26. Fersht, A.R., *Linear free energy relationships are valid!* Protein Eng, 1987. **1**(6): p. 442-5.
27. Fersht, A.R., *Characterizing transition states in protein folding: an essential step in the puzzle.* Curr Opin Struct Biol, 1995. **5**(1): p. 79-84.
28. Fersht, A.R., A. Matouschek, and L. Serrano, *The folding of an enzyme. I. Theory of protein engineering analysis of stability and pathway of protein folding.* J Mol Biol, 1992. **224**(3): p. 771-82.
29. Leatherbarrow, R.J., A.R. Fersht, and G. Winter, *Transition-state stabilization in the mechanism of tyrosyl-tRNA synthetase revealed by protein engineering.* Proc Natl Acad Sci U S A, 1985. **82**(23): p. 7840-4.
30. Daggett, V., *Molecular dynamics simulations of the protein unfolding/folding reaction.* Acc Chem Res, 2002. **35**(6): p. 422-9.
31. Sali, A., E. Shakhnovich, and M. Karplus, *How does a protein fold?* Nature, 1994. **369**(6477): p. 248-51.
32. Sali, A., E. Shakhnovich, and M. Karplus, *Kinetics of protein folding. A lattice model study of the requirements for folding to the native state.* J Mol Biol, 1994. **235**(5): p. 1614-36.
33. Bryngelson, J.D., et al., *Funnels, pathways, and the energy landscape of protein folding: a synthesis.* Proteins, 1995. **21**(3): p. 167-95.
34. Dill, K.A. and H.S. Chan, *From Levinthal to pathways to funnels.* Nat Struct Biol, 1997. **4**(1): p. 10-9.

35. Dinner, A.R., et al., *Understanding protein folding via free-energy surfaces from theory and experiment.* Trends Biochem Sci, 2000. **25**(7): p. 331-9.
36. Wolynes, P.G., J.N. Onuchic, and D. Thirumalai, *Navigating the folding routes.* Science, 1995. **267**(5204): p. 1619-20.
37. Kim, P.S. and R.L. Baldwin, *Intermediates in the folding reactions of small proteins.* Annu Rev Biochem, 1990. **59**: p. 631-60.
38. Kiefhaber, T., *Kinetic traps in lysozyme folding.* Proc Natl Acad Sci U S A, 1995. **92**(20): p. 9029-33.
39. Matagne, A., S.E. Radford, and C.M. Dobson, *Fast and slow tracks in lysozyme folding: insight into the role of domains in the folding process.* J Mol Biol, 1997. **267**(5): p. 1068-74.
40. Radford, S.E., C.M. Dobson, and P.A. Evans, *The folding of hen lysozyme involves partially structured intermediates and multiple pathways.* Nature, 1992. **358**(6384): p. 302-7.
41. Kulkarni, S.K., et al., *A near-native state on the slow refolding pathway of hen lysozyme.* Protein Sci, 1999. **8**(1): p. 35-44.
42. Dinner, A.R., A. Sali, and M. Karplus, *The folding mechanism of larger model proteins: role of native structure.* Proc Natl Acad Sci U S A, 1996. **93**(16): p. 8356-61.
43. Zimmerman, S.B. and S.O. Trach, *Estimation of macromolecule concentrations and excluded volume effects for the cytoplasm of Escherichia coli.* J Mol Biol, 1991. **222**(3): p. 599-620.
44. Ellis, R.J., *Macromolecular crowding: obvious but underappreciated.* Trends Biochem Sci, 2001. **26**(10): p. 597-604.
45. van den Berg, B., R.J. Ellis, and C.M. Dobson, *Effects of macromolecular crowding on protein folding and aggregation.* EMBO J, 1999. **18**(24): p. 6927-33.
46. van den Berg, B., et al., *Macromolecular crowding perturbs protein refolding kinetics: implications for folding inside the cell.* EMBO J, 2000. **19**(15): p. 3870-5.
47. Martin, J. and F.U. Hartl, *The effect of macromolecular crowding on chaperonin-mediated protein folding.* Proc Natl Acad Sci U S A, 1997. **94**(4): p. 1107-12.
48. Ban, N., et al., *The complete atomic structure of the large ribosomal subunit at 2.4 A resolution.* Science, 2000. **289**(5481): p. 905-20.
49. Malkin, L.I. and A. Rich, *Partial resistance of nascent polypeptide chains to proteolytic digestion due to ribosomal shielding.* J Mol Biol, 1967. **26**(2): p. 329-46.
50. Lu, J. and C. Deutsch, *Folding zones inside the ribosomal exit tunnel.* Nat Struct Mol Biol, 2005. **12**(12): p. 1123-9.
51. Woolhead, C.A., P.J. McCormick, and A.E. Johnson, *Nascent membrane and secretory proteins differ in FRET-detected folding far inside the ribosome and in their exposure to ribosomal proteins.* Cell, 2004. **116**(5): p. 725-36.
52. Hartl, F.U. and M. Hayer-Hartl, *Converging concepts of protein folding in vitro and in vivo.* Nat Struct Mol Biol, 2009. **16**(6): p. 574-81.
53. Brandt, F., et al., *The native 3D organization of bacterial polysomes.* Cell, 2009. **136**(2): p. 261-71.
54. Clark, P.L., *Protein folding in the cell: reshaping the folding funnel.* Trends Biochem Sci, 2004. **29**(10): p. 527-34.
55. Dobson, C.M., *Principles of protein folding, misfolding and aggregation.* Semin Cell Dev Biol, 2004. **15**(1): p. 3-16.
56. Jahn, T.R. and S.E. Radford, *The Yin and Yang of protein folding.* FEBS J, 2005. **272**(23): p. 5962-70.
57. Lashuel, H.A., et al., *Alpha-synuclein, especially the Parkinson's disease-associated mutants, forms pore-like annular and tubular protofibrils.* J Mol Biol, 2002. **322**(5): p. 1089-102.
58. Locker, C.R. and R. Hernandez, *A minimalist model protein with multiple folding funnels.* Proc Natl Acad Sci U S A, 2001. **98**(16): p. 9074-9.

59. Wetzel, R., *For protein misassembly, it's the "I" decade.* Cell, 1996. **86**(5): p. 699-702.
60. Nelson, E.D. and J.N. Onuchic, *Proposed mechanism for stability of proteins to evolutionary mutations.* Proc Natl Acad Sci U S A, 1998. **95**(18): p. 10682-6.
61. Gunasekaran, K., et al., *Keeping it in the family: folding studies of related proteins.* Curr Opin Struct Biol, 2001. **11**(1): p. 83-93.
62. Onuchic, J.N. and P.G. Wolynes, *Theory of protein folding.* Curr Opin Struct Biol, 2004. **14**(1): p. 70-5.
63. Chothia, C. and A.M. Lesk, *The relation between the divergence of sequence and structure in proteins.* EMBO J, 1986. **5**(4): p. 823-6.
64. Anantharaman, V., L. Aravind, and E.V. Koonin, *Emergence of diverse biochemical activities in evolutionarily conserved structural scaffolds of proteins.* Curr Opin Chem Biol, 2003. **7**(1): p. 12-20.
65. James, L.C. and D.S. Tawfik, *Conformational diversity and protein evolution--a 60-year-old hypothesis revisited.* Trends Biochem Sci, 2003. **28**(7): p. 361-8.
66. Tokuriki, N. and D.S. Tawfik, *Protein dynamism and evolvability.* Science, 2009. **324**(5924): p. 203-7.
67. Dunker, A.K., et al., *Intrinsic disorder and protein function.* Biochemistry, 2002. **41**(21): p. 6573-82.
68. Dunker, A.K., et al., *Intrinsic protein disorder in complete genomes.* Genome Inform Ser Workshop Genome Inform, 2000. **11**: p. 161-71.
69. Smith, J.M., *Natural selection and the concept of a protein space.* Nature, 1970. **225**(5232): p. 563-4.
70. Meier, S. and S. Ozbek, *A biological cosmos of parallel universes: does protein structural plasticity facilitate evolution?* Bioessays, 2007. **29**(11): p. 1095-104.
71. Meier, S., et al., *Continuous molecular evolution of protein-domain structures by single amino acid changes.* Curr Biol, 2007. **17**(2): p. 173-8.
72. Bergman, A. and M.L. Siegal, *Evolutionary capacitance as a general feature of complex gene networks.* Nature, 2003. **424**(6948): p. 549-52.
73. Queitsch, C., T.A. Sangster, and S. Lindquist, *Hsp90 as a capacitor of phenotypic variation.* Nature, 2002. **417**(6889): p. 618-24.
74. Rutherford, S.L. and S. Lindquist, *Hsp90 as a capacitor for morphological evolution.* Nature, 1998. **396**(6709): p. 336-42.
75. James, L.C., P. Roversi, and D.S. Tawfik, *Antibody multispecificity mediated by conformational diversity.* Science, 2003. **299**(5611): p. 1362-7.
76. Wickner, S., et al., *A molecular chaperone, ClpA, functions like DnaK and DnaJ.* Proc Natl Acad Sci U S A, 1994. **91**(25): p. 12218-22.
77. Chiti, F. and C.M. Dobson, *Protein misfolding, functional amyloid, and human disease.* Annu Rev Biochem, 2006. **75**: p. 333-66.
78. Lim, J., et al., *Opposing effects of polyglutamine expansion on native protein complexes contribute to SCA1.* Nature, 2008. **452**(7188): p. 713-8.
79. Dobson, C.M., *Protein folding and disease: a view from the first Horizon Symposium.* Nat Rev Drug Discov, 2003. **2**(2): p. 154-60.
80. Dobson, C.M., *Protein folding and misfolding.* Nature, 2003. **426**(6968): p. 884-90.
81. Bukau, B., J. Weissman, and A. Horwich, *Molecular chaperones and protein quality control.* Cell, 2006. **125**(3): p. 443-51.
82. Ron, D. and P. Walter, *Signal integration in the endoplasmic reticulum unfolded protein response.* Nat Rev Mol Cell Biol, 2007. **8**(7): p. 519-29.
83. Morimoto, R.I., *Proteotoxic stress and inducible chaperone networks in neurodegenerative disease and aging.* Genes Dev, 2008. **22**(11): p. 1427-38.
84. Kessel, M., et al., *Homology in structural organization between E. coli ClpAP protease and the eukaryotic 26 S proteasome.* J Mol Biol, 1995. **250**(5): p. 587-94.

85. Chernoff, Y.O., et al., *Role of the chaperone protein Hsp104 in propagation of the yeast prion-like factor [psi+].* Science, 1995. **268**(5212): p. 880-4.
86. Moczko, M., et al., *The mitochondrial ClpB homolog Hsp78 cooperates with matrix Hsp70 in maintenance of mitochondrial function.* J Mol Biol, 1995. **254**(4): p. 538-43.
87. Parsell, D.A., A.S. Kowal, and S. Lindquist, *Saccharomyces cerevisiae Hsp104 protein. Purification and characterization of ATP-induced structural changes.* J Biol Chem, 1994. **269**(6): p. 4480-7.
88. Schirmer, E.C., et al., *HSP100/Clp proteins: a common mechanism explains diverse functions.* Trends Biochem Sci, 1996. **21**(8): p. 289-96.
89. Vogel, J.L., D.A. Parsell, and S. Lindquist, *Heat-shock proteins Hsp104 and Hsp70 reactivate mRNA splicing after heat inactivation.* Curr Biol, 1995. **5**(3): p. 306-17.
90. Horwich, A.L., *Molecular chaperones. Resurrection or destruction?* Curr Biol, 1995. **5**(5): p. 455-8.
91. Kruklitis, R., D.J. Welty, and H. Nakai, *ClpX protein of Escherichia coli activates bacteriophage Mu transposase in the strand transfer complex for initiation of Mu DNA synthesis.* EMBO J, 1996. **15**(4): p. 935-44.
92. Levchenko, I., L. Luo, and T.A. Baker, *Disassembly of the Mu transposase tetramer by the ClpX chaperone.* Genes Dev, 1995. **9**(19): p. 2399-408.
93. Wawrzynow, A., B. Banecki, and M. Zylicz, *The Clp ATPases define a novel class of molecular chaperones.* Mol Microbiol, 1996. **21**(5): p. 895-9.
94. Wawrzynow, A., et al., *The ClpX heat-shock protein of Escherichia coli, the ATP-dependent substrate specificity component of the ClpP-ClpX protease, is a novel molecular chaperone.* EMBO J, 1995. **14**(9): p. 1867-77.
95. Kessel, M., et al., *Six-fold rotational symmetry of ClpQ, the E. coli homolog of the 20S proteasome, and its ATP-dependent activator, ClpY.* FEBS Lett, 1996. **398**(2-3): p. 274-8.
96. Missiakas, D., et al., *Identification and characterization of HsIV HsIU (ClpQ ClpY) proteins involved in overall proteolysis of misfolded proteins in Escherichia coli.* EMBO J, 1996. **15**(24): p. 6899-909.
97. Rohrwild, M., et al., *HslV-HslU: A novel ATP-dependent protease complex in Escherichia coli related to the eukaryotic proteasome.* Proc Natl Acad Sci U S A, 1996. **93**(12): p. 5808-13.
98. Herman, C., et al., *Cell growth and lambda phage development controlled by the same essential Escherichia coli gene, ftsH/hflB.* Proc Natl Acad Sci U S A, 1993. **90**(22): p. 10861-5.
99. Tomoyasu, T., et al., *Escherichia coli FtsH is a membrane-bound, ATP-dependent protease which degrades the heat-shock transcription factor sigma 32.* EMBO J, 1995. **14**(11): p. 2551-60.
100. Tomoyasu, T., et al., *Topology and subcellular localization of FtsH protein in Escherichia coli.* J Bacteriol, 1993. **175**(5): p. 1352-7.
101. Tomoyasu, T., et al., *The Escherichia coli FtsH protein is a prokaryotic member of a protein family of putative ATPases involved in membrane functions, cell cycle control, and gene expression.* J Bacteriol, 1993. **175**(5): p. 1344-51.
102. Goldberg, A.L., et al., *ATP-dependent protease La (lon) from Escherichia coli.* Methods Enzymol, 1994. **244**: p. 350-75.
103. Gottesman, S., *Proteases and their targets in Escherichia coli.* Annu Rev Genet, 1996. **30**: p. 465-506.
104. Maurizi, M.R., *Proteases and protein degradation in Escherichia coli.* Experientia, 1992. **48**(2): p. 178-201.
105. Rep, M., et al., *Promotion of mitochondrial membrane complex assembly by a proteolytically inactive yeast Lon.* Science, 1996. **274**(5284): p. 103-6.
106. Suzuki, C.K., et al., *Requirement for the yeast gene LON in intramitochondrial proteolysis and maintenance of respiration.* Science, 1994. **264**(5161): p. 891.

107. Wagner, I., et al., *Molecular chaperones cooperate with PIM1 protease in the degradation of misfolded proteins in mitochondria.* EMBO J, 1994. **13**(21): p. 5135-45.
108. Chang, H.C., et al., *SnapShot: molecular chaperones, Part I.* Cell, 2007. **128**(1): p. 212.
109. Tang, Y.C., et al., *SnapShot: molecular chaperones, Part II.* Cell, 2007. **128**(2): p. 412.
110. Yoshimune, K., T. Yoshimura, and N. Esaki, *Hsc62, a new DnaK homologue of Escherichia coli.* Biochem Biophys Res Commun, 1998. **250**(1): p. 115-8.
111. Yoshimune, K., et al., *Hsc62, Hsc56, and GrpE, the third Hsp70 chaperone system of Escherichia coli.* Biochem Biophys Res Commun, 2002. **293**(5): p. 1389-95.
112. Bukau, B. and A.L. Horwich, *The Hsp70 and Hsp60 chaperone machines.* Cell, 1998. **92**(3): p. 351-66.
113. Smith, C.K., T.A. Baker, and R.T. Sauer, *Lon and Clp family proteases and chaperones share homologous substrate-recognition domains.* Proc Natl Acad Sci U S A, 1999. **96**(12): p. 6678-82.
114. Mayer, M.P. and B. Bukau, *Hsp70 chaperones: cellular functions and molecular mechanism.* Cell Mol Life Sci, 2005. **62**(6): p. 670-84.
115. Horwich, A.L., et al., *Two families of chaperonin: physiology and mechanism.* Annu Rev Cell Dev Biol, 2007. **23**: p. 115-45.
116. Schiene, C. and G. Fischer, *Enzymes that catalyse the restructuring of proteins.* Curr Opin Struct Biol, 2000. **10**(1): p. 40-5.
117. Hartl, F.U. and M. Hayer-Hartl, *Molecular chaperones in the cytosol: from nascent chain to folded protein.* Science, 2002. **295**(5561): p. 1852-8.
118. Freeman, B.C. and R.I. Morimoto, *The human cytosolic molecular chaperones hsp90, hsp70 (hsc70) and hdj-1 have distinct roles in recognition of a non-native protein and protein refolding.* EMBO J, 1996. **15**(12): p. 2969-79.
119. Langer, T., et al., *Successive action of DnaK, DnaJ and GroEL along the pathway of chaperone-mediated protein folding.* Nature, 1992. **356**(6371): p. 683-9.
120. McCarty, J.S., et al., *The role of ATP in the functional cycle of the DnaK chaperone system.* J Mol Biol, 1995. **249**(1): p. 126-37.
121. Goloubinoff, P. and P. De Los Rios, *The mechanism of Hsp70 chaperones: (entropic) pulling the models together.* Trends Biochem Sci, 2007. **32**(8): p. 372-80.
122. Esser, C., S. Alberti, and J. Hohfeld, *Cooperation of molecular chaperones with the ubiquitin/proteasome system.* Biochim Biophys Acta, 2004. **1695**(1-3): p. 171-88.
123. Broadley, S.A. and F.U. Hartl, *The role of molecular chaperones in human misfolding diseases.* FEBS Lett, 2009. **583**(16): p. 2647-53.
124. Barral, J.M., et al., *Roles of molecular chaperones in protein misfolding diseases.* Semin Cell Dev Biol, 2004. **15**(1): p. 17-29.
125. Gidalevitz, T., et al., *Progressive disruption of cellular protein folding in models of polyglutamine diseases.* Science, 2006. **311**(5766): p. 1471-4.
126. Kim, S., et al., *Polyglutamine protein aggregates are dynamic.* Nat Cell Biol, 2002. **4**(10): p. 826-31.
127. Csermely, P., *Chaperone overload is a possible contributor to 'civilization diseases'.* Trends Genet, 2001. **17**(12): p. 701-4.
128. Lu, T., et al., *Gene regulation and DNA damage in the ageing human brain.* Nature, 2004. **429**(6994): p. 883-91.
129. Heydari, A.R., et al., *Age-related alterations in the activation of heat shock transcription factor 1 in rat hepatocytes.* Exp Cell Res, 2000. **256**(1): p. 83-93.
130. Liu, A.Y., et al., *Attenuated induction of heat shock gene expression in aging diploid fibroblasts.* J Biol Chem, 1989. **264**(20): p. 12037-45.

131. Tonkiss, J. and S.K. Calderwood, *Regulation of heat shock gene transcription in neuronal cells.* Int J Hyperthermia, 2005. **21**(5): p. 433-44.
132. Cowan, K.J., M.I. Diamond, and W.J. Welch, *Polyglutamine protein aggregation and toxicity are linked to the cellular stress response.* Hum Mol Genet, 2003. **12**(12): p. 1377-91.
133. Yamanaka, T., et al., *Mutant Huntingtin reduces HSP70 expression through the sequestration of NF-Y transcription factor.* EMBO J, 2008. **27**(6): p. 827-39.
134. Hansen, J.J., et al., *Hereditary spastic paraplegia SPG13 is associated with a mutation in the gene encoding the mitochondrial chaperonin Hsp60.* Am J Hum Genet, 2002. **70**(5): p. 1328-32.
135. Magen, D., et al., *Mitochondrial hsp60 chaperonopathy causes an autosomal-recessive neurodegenerative disorder linked to brain hypomyelination and leukodystrophy.* Am J Hum Genet, 2008. **83**(1): p. 30-42.
136. Albanese, V., et al., *Systems analyses reveal two chaperone networks with distinct functions in eukaryotic cells.* Cell, 2006. **124**(1): p. 75-88.
137. Spiess, C., et al., *Mechanism of the eukaryotic chaperonin: protein folding in the chamber of secrets.* Trends Cell Biol, 2004. **14**(11): p. 598-604.
138. Kitamura, A., et al., *Cytosolic chaperonin prevents polyglutamine toxicity with altering the aggregation state.* Nat Cell Biol, 2006. **8**(10): p. 1163-70.
139. Kubota, S., H. Kubota, and K. Nagata, *Cytosolic chaperonin protects folding intermediates of Gbeta from aggregation by recognizing hydrophobic beta-strands.* Proc Natl Acad Sci U S A, 2006. **103**(22): p. 8360-5.
140. Rommelaere, H., et al., *The cytosolic class II chaperonin CCT recognizes delineated hydrophobic sequences in its target proteins.* Biochemistry, 1999. **38**(11): p. 3246-57.
141. Yam, A.Y., et al., *Defining the TRiC/CCT interactome links chaperonin function to stabilization of newly made proteins with complex topologies.* Nat Struct Mol Biol, 2008. **15**(12): p. 1255-62.
142. Behrends, C., et al., *Chaperonin TRiC promotes the assembly of polyQ expansion proteins into nontoxic oligomers.* Mol Cell, 2006. **23**(6): p. 887-97.
143. Coyle, J.E., et al., *GroEL accelerates the refolding of hen lysozyme without changing its folding mechanism.* Nat Struct Biol, 1999. **6**(7): p. 683-90.
144. Hillger, F., et al., *Probing protein-chaperone interactions with single-molecule fluorescence spectroscopy.* Angew Chem Int Ed Engl, 2008. **47**(33): p. 6184-8.
145. Shtilerman, M., G.H. Lorimer, and S.W. Englander, *Chaperonin function: folding by forced unfolding.* Science, 1999. **284**(5415): p. 822-5.
146. Diamant, S., et al., *Chemical chaperones regulate molecular chaperones in vitro and in cells under combined salt and heat stresses.* J Biol Chem, 2001. **276**(43): p. 39586-91.
147. Arakawa, T., et al., *Small molecule pharmacological chaperones: From thermodynamic stabilization to pharmaceutical drugs.* Biochim Biophys Acta, 2006. **1764**(11): p. 1677-87.
148. Kolter, T. and M. Wendeler, *Chemical chaperones--a new concept in drug research.* Chembiochem, 2003. **4**(4): p. 260-4.
149. Loo, T.W. and D.M. Clarke, *Chemical and pharmacological chaperones as new therapeutic agents.* Expert Rev Mol Med, 2007. **9**(16): p. 1-18.
150. Welch, W.J. and C.R. Brown, *Influence of molecular and chemical chaperones on protein folding.* Cell Stress Chaperones, 1996. **1**(2): p. 109-15.
151. Sawkar, A.R., et al., *Chemical chaperones increase the cellular activity of N370S beta -glucosidase: a therapeutic strategy for Gaucher disease.* Proc Natl Acad Sci U S A, 2002. **99**(24): p. 15428-33.
152. Sawkar, A.R., et al., *Chemical chaperones and permissive temperatures alter localization of Gaucher disease associated glucocerebrosidase variants.* ACS Chem Biol, 2006. **1**(4): p. 235-51.

153. Yancey, P.H., et al., *Living with water stress: evolution of osmolyte systems.* Science, 1982. **217**(4566): p. 1214-22.
154. Yancey, P.H., et al., *Trimethylamine oxide, betaine and other osmolytes in deep-sea animals: depth trends and effects on enzymes under hydrostatic pressure.* Cell Mol Biol (Noisy-le-grand), 2004. **50**(4): p. 371-6.
155. Bolen, D.W. and I.V. Baskakov, *The osmophobic effect: natural selection of a thermodynamic force in protein folding.* J Mol Biol, 2001. **310**(5): p. 955-63.
156. Yancey, P.H., *Organic osmolytes as compatible, metabolic and counteracting cytoprotectants in high osmolarity and other stresses.* J Exp Biol, 2005. **208**(Pt 15): p. 2819-30.
157. Yancey, P.H., et al., *Trimethylamine oxide counteracts effects of hydrostatic pressure on proteins of deep-sea teleosts.* J Exp Zool, 2001. **289**(3): p. 172-6.
158. Timasheff, S.N., *Protein hydration, thermodynamic binding, and preferential hydration.* Biochemistry, 2002. **41**(46): p. 13473-82.
159. Timasheff, S.N., *Protein-solvent preferential interactions, protein hydration, and the modulation of biochemical reactions by solvent components.* Proc Natl Acad Sci U S A, 2002. **99**(15): p. 9721-6.
160. Cayley, S. and M.T. Record, Jr., *Roles of cytoplasmic osmolytes, water, and crowding in the response of Escherichia coli to osmotic stress: biophysical basis of osmoprotection by glycine betaine.* Biochemistry, 2003. **42**(43): p. 12596-609.
161. Timasheff, S.N., *Control of protein stability and reactions by weakly interacting cosolvents: the simplicity of the complicated.* Adv Protein Chem, 1998. **51**: p. 355-432.
162. Auton, M. and D.W. Bolen, *Predicting the energetics of osmolyte-induced protein folding/unfolding.* Proc Natl Acad Sci U S A, 2005. **102**(42): p. 15065-8.
163. Bolen, D.W., *Effects of naturally occurring osmolytes on protein stability and solubility: issues important in protein crystallization.* Methods, 2004. **34**(3): p. 312-22.
164. Courtenay, E.S., et al., *Vapor pressure osmometry studies of osmolyte-protein interactions: implications for the action of osmoprotectants in vivo and for the interpretation of "osmotic stress" experiments in vitro.* Biochemistry, 2000. **39**(15): p. 4455-71.
165. Pradeep, L. and J.B. Udgaonkar, *Osmolytes induce structure in an early intermediate on the folding pathway of barstar.* J Biol Chem, 2004. **279**(39): p. 40303-13.
166. deCarvalho, A.C., et al., *A novel natural product compound enhances cAMP-regulated chloride conductance of cells expressing CFTR[delta]F508.* Mol Med, 2002. **8**(2): p. 75-87.
167. Sato, S., et al., *Glycerol reverses the misfolding phenotype of the most common cystic fibrosis mutation.* J Biol Chem, 1996. **271**(2): p. 635-8.
168. Hansen, P.A., A. Waheed, and J.A. Corbett, *Chemically chaperoning the actions of insulin.* Trends Endocrinol Metab, 2007. **18**(1): p. 1-3.
169. Tanaka, M., Y. Machida, and N. Nukina, *A novel therapeutic strategy for polyglutamine diseases by stabilizing aggregation-prone proteins with small molecules.* J Mol Med, 2005. **83**(5): p. 343-52.
170. Powers, E.T., et al., *Biological and chemical approaches to diseases of proteostasis deficiency.* Annu Rev Biochem, 2009. **78**: p. 959-91.
171. Kim, B.E., et al., *A conditional mutation affecting localization of the Menkes disease copper ATPase. Suppression by copper supplementation.* J Biol Chem, 2002. **277**(46): p. 44079-84.
172. McClellan, A.J., et al., *Protein quality control: chaperones culling corrupt conformations.* Nat Cell Biol, 2005. **7**(8): p. 736-41.
173. Wolf, D.H. and W. Hilt, *The proteasome: a proteolytic nanomachine of cell regulation and waste disposal.* Biochim Biophys Acta, 2004. **1695**(1-3): p. 19-31.

174. Langer, T. and W. Neupert, *Regulated protein degradation in mitochondria.* Experientia, 1996. **52**(12): p. 1069-76.
175. Eskelinen, E.L. and P. Saftig, *Autophagy: a lysosomal degradation pathway with a central role in health and disease.* Biochim Biophys Acta, 2009. **1793**(4): p. 664-73.
176. Hochstrasser, M., *Protein degradation or regulation: Ub the judge.* Cell, 1996. **84**(6): p. 813-5.
177. Hochstrasser, M., *Ubiquitin-dependent protein degradation.* Annu Rev Genet, 1996. **30**: p. 405-39.
178. Wickner, S., M.R. Maurizi, and S. Gottesman, *Posttranslational quality control: folding, refolding, and degrading proteins.* Science, 1999. **286**(5446): p. 1888-93.
179. Gottesman, S., S. Wickner, and M.R. Maurizi, *Protein quality control: triage by chaperones and proteases.* Genes Dev, 1997. **11**(7): p. 815-23.
180. Pak, M., et al., *Concurrent chaperone and protease activities of ClpAP and the requirement for the N-terminal ClpA ATP binding site for chaperone activity.* J Biol Chem, 1999. **274**(27): p. 19316-22.
181. Tatsuta, T. and T. Langer, *Quality control of mitochondria: protection against neurodegeneration and ageing.* EMBO J, 2008. **27**(2): p. 306-14.
182. Bota, D.A. and K.J. Davies, *Lon protease preferentially degrades oxidized mitochondrial aconitase by an ATP-stimulated mechanism.* Nat Cell Biol, 2002. **4**(9): p. 674-80.
183. Bota, D.A., H. Van Remmen, and K.J. Davies, *Modulation of Lon protease activity and aconitase turnover during aging and oxidative stress.* FEBS Lett, 2002. **532**(1-2): p. 103-6.
184. Koppen, M. and T. Langer, *Protein degradation within mitochondria: versatile activities of AAA proteases and other peptidases.* Crit Rev Biochem Mol Biol, 2007. **42**(3): p. 221-42.
185. Major, T., et al., *Proteomic analysis of mitochondrial protein turnover: identification of novel substrate proteins of the matrix protease pim1.* Mol Cell Biol, 2006. **26**(3): p. 762-76.
186. Leonhard, K., et al., *Membrane protein degradation by AAA proteases in mitochondria: extraction of substrates from either membrane surface.* Mol Cell, 2000. **5**(4): p. 629-38.
187. Van Melderen, L. and S. Gottesman, *Substrate sequestration by a proteolytically inactive Lon mutant.* Proc Natl Acad Sci U S A, 1999. **96**(11): p. 6064-71.
188. Bota, D.A., J.K. Ngo, and K.J. Davies, *Downregulation of the human Lon protease impairs mitochondrial structure and function and causes cell death.* Free Radic Biol Med, 2005. **38**(5): p. 665-77.
189. Stefani, M., *Protein misfolding and aggregation: new examples in medicine and biology of the dark side of the protein world.* Biochim Biophys Acta, 2004. **1739**(1): p. 5-25.
190. Caughey, B. and P.T. Lansbury, *Protofibrils, pores, fibrils, and neurodegeneration: separating the responsible protein aggregates from the innocent bystanders.* Annu Rev Neurosci, 2003. **26**: p. 267-98.
191. Bucciantini, M., et al., *Inherent toxicity of aggregates implies a common mechanism for protein misfolding diseases.* Nature, 2002. **416**(6880): p. 507-11.
192. Soto, C. and L.D. Estrada, *Protein misfolding and neurodegeneration.* Arch Neurol, 2008. **65**(2): p. 184-9.
193. McBride, H.M., M. Neuspiel, and S. Wasiak, *Mitochondria: more than just a powerhouse.* Curr Biol, 2006. **16**(14): p. R551-60.
194. Sas, K., et al., *Mitochondria, metabolic disturbances, oxidative stress and the kynurenine system, with focus on neurodegenerative disorders.* J Neurol Sci, 2007. **257**(1-2): p. 221-39.
195. Hoppins, S., L. Lackner, and J. Nunnari, *The machines that divide and fuse mitochondria.* Annu Rev Biochem, 2007. **76**: p. 751-80.

196. Danial, N.N. and S.J. Korsmeyer, *Cell death: critical control points.* Cell, 2004. **116**(2): p. 205-19.
197. Okamoto, K. and J.M. Shaw, *Mitochondrial morphology and dynamics in yeast and multicellular eukaryotes.* Annu Rev Genet, 2005. **39**: p. 503-36.
198. Kim, I., S. Rodriguez-Enriquez, and J.J. Lemasters, *Selective degradation of mitochondria by mitophagy.* Arch Biochem Biophys, 2007. **462**(2): p. 245-53.
199. Maiuri, M.C., et al., *Self-eating and self-killing: crosstalk between autophagy and apoptosis.* Nat Rev Mol Cell Biol, 2007. **8**(9): p. 741-52.
200. Lin, M.T. and M.F. Beal, *Mitochondrial dysfunction and oxidative stress in neurodegenerative diseases.* Nature, 2006. **443**(7113): p. 787-95.
201. Mancuso, M., et al., *Mitochondrial dysfunction, oxidative stress and neurodegeneration.* J Alzheimers Dis, 2006. **10**(1): p. 59-73.
202. Mancuso, M., et al., *Mitochondrial dysfunction and Alzheimer's disease: new developments.* J Alzheimers Dis, 2006. **9**(2): p. 111-7.
203. Petrozzi, L., et al., *Mitochondria and neurodegeneration.* Biosci Rep, 2007. **27**(1-3): p. 87-104.
204. Jazin, E.E., et al., *Human brain contains high levels of heteroplasmy in the noncoding regions of mitochondrial DNA.* Proc Natl Acad Sci U S A, 1996. **93**(22): p. 12382-7.
205. Lin, M.T., et al., *High aggregate burden of somatic mtDNA point mutations in aging and Alzheimer's disease brain.* Hum Mol Genet, 2002. **11**(2): p. 133-45.
206. Sun, J., et al., *Induced overexpression of mitochondrial Mn-superoxide dismutase extends the life span of adult Drosophila melanogaster.* Genetics, 2002. **161**(2): p. 661-72.
207. Gu, M., et al., *Mitochondrial defect in Huntington's disease caudate nucleus.* Ann Neurol, 1996. **39**(3): p. 385-9.
208. Choo, Y.S., et al., *Mutant huntingtin directly increases susceptibility of mitochondria to the calcium-induced permeability transition and cytochrome c release.* Hum Mol Genet, 2004. **13**(14): p. 1407-20.
209. Panov, A.V., et al., *Early mitochondrial calcium defects in Huntington's disease are a direct effect of polyglutamines.* Nat Neurosci, 2002. **5**(8): p. 731-6.
210. Sugars, K.L. and D.C. Rubinsztein, *Transcriptional abnormalities in Huntington disease.* Trends Genet, 2003. **19**(5): p. 233-8.
211. Bae, B.I., et al., *p53 mediates cellular dysfunction and behavioral abnormalities in Huntington's disease.* Neuron, 2005. **47**(1): p. 29-41.
212. Mandemakers, W., V.A. Morais, and B. De Strooper, *A cell biological perspective on mitochondrial dysfunction in Parkinson disease and other neurodegenerative diseases.* J Cell Sci, 2007. **120**(Pt 10): p. 1707-16.
213. Song, D.D., et al., *Enhanced substantia nigra mitochondrial pathology in human alpha-synuclein transgenic mice after treatment with MPTP.* Exp Neurol, 2004. **186**(2): p. 158-72.
214. Darios, F., et al., *Parkin prevents mitochondrial swelling and cytochrome c release in mitochondria-dependent cell death.* Hum Mol Genet, 2003. **12**(5): p. 517-26.
215. Kuroda, Y., et al., *Parkin enhances mitochondrial biogenesis in proliferating cells.* Hum Mol Genet, 2006. **15**(6): p. 883-95.
216. Canet-Aviles, R.M., et al., *The Parkinson's disease protein DJ-1 is neuroprotective due to cysteine-sulfinic acid-driven mitochondrial localization.* Proc Natl Acad Sci U S A, 2004. **101**(24): p. 9103-8.
217. Valente, E.M., et al., *PINK1 mutations are associated with sporadic early-onset parkinsonism.* Ann Neurol, 2004. **56**(3): p. 336-41.
218. Valente, E.M., et al., *Hereditary early-onset Parkinson's disease caused by mutations in PINK1.* Science, 2004. **304**(5674): p. 1158-60.

219. West, A.B., et al., *Parkinson's disease-associated mutations in leucine-rich repeat kinase 2 augment kinase activity.* Proc Natl Acad Sci U S A, 2005. **102**(46): p. 16842-7.
220. Plun-Favreau, H., et al., *The mitochondrial protease HtrA2 is regulated by Parkinson's disease-associated kinase PINK1.* Nat Cell Biol, 2007. **9**(11): p. 1243-52.
221. Strauss, K.M., et al., *Loss of function mutations in the gene encoding Omi/HtrA2 in Parkinson's disease.* Hum Mol Genet, 2005. **14**(15): p. 2099-111.

CHAPTER

2 FRATAXIN AND FRIEDREICH'S ATAXIA

2.1. Friedreich's Ataxia

Friedreich's ataxia (FRDA; OMIM: 229300) is the most common hereditary ataxia. This movement disorder was first described in 1863 by Prof. Nikolaus Friedreich, Professor of Medicine in Heidelberg, and his clinical observations already comprised the essential characteristics of the disease [1]. In his original report he described the disease as a "*degenerative atrophy of the posterior column of the spinal cord leading to progressive ataxia, particularly associated with clumsiness in walking, accompanied by sensory loss, lateral curvature of the spine, foot deformity and heart disease*".

Figure 2.1: The German pathologist and neurologist, Prof. Nikolaus Friedreich (1825-1882).

The cause of the disease remained unknown for over 130 years and even the rigorous diagnostic criteria and the autosomal recessive pattern of heritance were only established between 1976 and 1981 [2-3]. The authors of these studies, while trying to describe the unifying features of FRDA, came across a quite rare observation for a recessive disorder. The pathological manifestations of the disease are rather variable, especially concerning the age onset, rate of progression, severity and extent of disease. Also these studies have allowed for the collection of clinically homogeneous families that were subsequently used in biochemical studies and, after 1985, in genetic studies. In 1996, the gene associated with FRDA and its most common mutation, an intronic GAA triplet expansion, were finally identified [4], allowing for genotype-phenotype correlations, pathophysiological studies and new approaches to treatment.

In spite of being a rare disorder, FRDA is the most common inherited ataxia across Europe. Among the European Caucasian population, Friedreich's ataxia carrier frequency is estimated to be 1 in every 85 individuals, with a disease prevalence of 1-2 cases per 40,000 individuals [5]. The disease seems to be restricted to individuals of European, Middle Eastern, North African and Indian origin [6-7]. Located on chromosome 9q13, the FRDA gene codes a small protein: frataxin [4]. Although ubiquitously expressed, frataxin expression levels are higher in tissues with a high ATP demand such as heart, spinal cord and dorsal root ganglia. This differentiated expression correlates with FRDA clinical features: neuronal degeneration and cardiomyopathy [8].

The expansion of a GAA repeat within the first intron of FRDA gene was found to be the cause of over 90% of FRDA cases [4-5]. This is an autosomal recessive disease, meaning that FRDA only occurs when the GAA extension is present in both alleles coding for frataxin. A normal allele has between 6 and 12 repeats while disease associated alleles have between 40 and 1000 repeats (600 to 900 in most cases) [4, 9-10]. The number of non-pathogenic GAA repeats is also variable, and includes subgroups with up to 14 to 34 repeats. GAA expansions, just like other disease-related expansions, are unstable and prone to further expansion when transmitted from parent to child. Thus, non-pathogenic large expansions constitute a reservoir for disease-related expansions [4]. In FRDA, GAA expansions and contractions are equally likely after maternal transmission but more likely after paternal transmission contractions. This pattern is common to disorders resulting from triplet expansions in non-coding regions; in addition to FRDA, fragile X and myotonic dystrophy are also included in this group [11]. For disorders resulting from a triplet expansion in a coding region, such as Huntington’s disease, an opposite pattern after paternal transmission is observed, as triplet expansions are more likely [12].

The origin of the GAA expansion responsible for FRDA is now described by a two step-model. First, the duplication of the ancestral normal expansion (~9 GAA repeats) lead to the formation of large alleles with ~18 GAA repeats [9]. A second mutational event resulted in an unstable expansion with more than 34 repeats. According to this model, all large alleles originated from the same haplotype and the carriers of the expanded allele have passed through a population bottleneck, most likely the ice age refuges. The northern Spain refuge is a good candidate since the prevalence of FRDA in this region is the highest registered to date, explaining the prevalence observed in Western Europe.

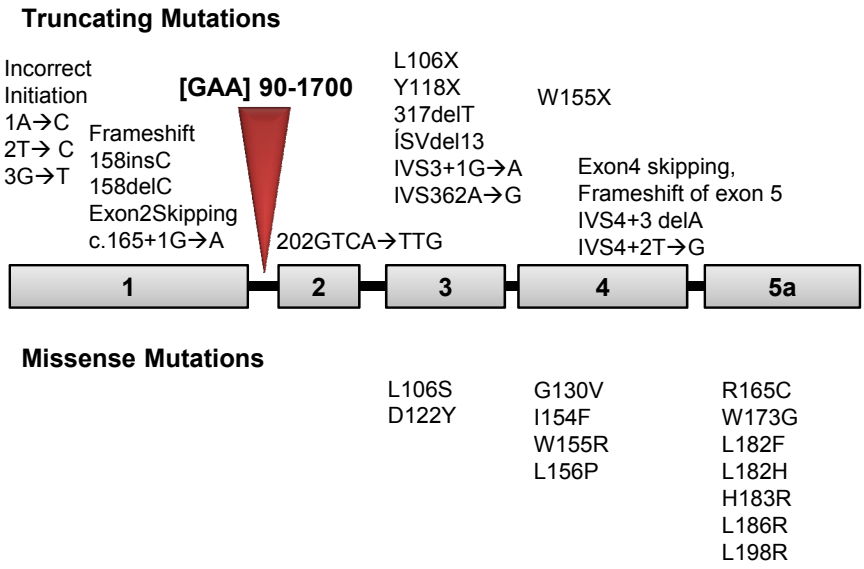

Figure 2.2: Schematic representation of frataxin gene highlighting the identified mutations. Boxes represent frataxin gene exons, while bars represent its introns. Above the gene representation, truncating mutations are described, X represents nonsense mutations. Below the gene representation, missense mutations are described; G130V and I154F are the most common and where identified in several families. The expansion mutation in intron 1, present in all FRDA patients, is also represented. Adapted from [9, 13].

It has been shown, *in vivo* and *in vitro,* that frataxin levels correlate inversely with the length of the expansion [13]. In peripheral blood leukocytes from FRDA patients, the levels of frataxin range between 5% and 30% of the normal levels [14-16]. The reduced amounts of mRNA depend on the length and orientation of the expansion and this reduction likely results from a disruption on transcription [17-18]. Sakamoto [19] has suggested that GAA repeats being “sticky” would self associate forming triple helix structures. These DNA triplexes could trap RNA polymerase suppressing frataxin gene expression. Normally, the formation of triplex structures is avoided by the presence GGA repeats within the GAA expansions.

Some patients (~4% [20]) are not homozygous for the triplet expansion but are compound heterozygous having the triplet expansion in one allele and a loss-of-function mutation on the other. Mutations identified so far are represented in **Fig. 2.1** and include missense, non-sense or splice mutations. Deletions involving large portions of the gene were only rarely detected [4, 21-22]. A patient with two point mutations, one in each allele, has not so far been identified, either because this would be lethal or just because carriers of point mutations are less common [4-5, 13, 17, 20, 23]. Identified FRDA-related missense mutations are summarised in **Table 2.1**; predicted constrains as well as the phenotype associated to each mutation are also described [13, 17, 20, 23-28]. While all homozygous patients present a typical and severe phenotype, some of the heterozygous patients show milder manifestations of the disease meaning that, in spite of the mutation, frataxin still retains some residual activity [21].

Table 2.1: Clinical point mutations described in heterozygous patients.

Point mutation			Yeast	*E. coli*	Effect	Phenotype	Ref
Leu106	→	Ser	Leu84	Ile17	Internal cavities with loss of packing energy	Severe	[23]
Asp122	→	Tyr	Ile99	Asp29	Change of a surface conserved negative charge (function)	Moderate	[13]
Gly130	→	Val	Gly107	Gly37	Steric strain by replacing a Gly that is in a conformation not allowed to other residues	Mild	[13]
Asn146	→	Lys	Asn122	Asn52	Disruption of an hydrogen bond on a β-hairpin	Severe	[25]
Ile154	→	Phe	Ile130	Val60	Steric strain by replacing a buried hydrophobic residues by a larger one	Severe	[13]
Trp155	→	Arg	Trp131	Trp61	Replacement of a bulky highly conserved aromatic chain by a positively charged residue	Severe	[7]
Leu156	→	Pro	Leu132	Leu62	Disruption in β-sheet hydrogen bonds	Severe	[13]
Agr165	→	Cys	Arg141	His70	Replacement of a conserved positively charge residue with an exposed Cys that might form intermolecular disulphide bridges	Mild	[20]
Trp173	→	Glyc	Trp149	Trp78	Internal cavities with loss of packing energy	Severe/ Mild	[13]
Leu182	→	His	Leu158	Phe87	Electrostatic strain by replacing a buried residue with a hydrophilic one	Moderate	[13]
Leu182	→	Phe	Leu158	Phe87	Steric strain by replacing a buried hydrophobic residues by a larger one	Moderate	[13, 20]
His183	→	Arg	Thr159	Trp88	Electrostatic strain by replacing a partially uncharged buried residues with a bulky charged one	Moderate	[13]
Leu186	→	Arg	Leu162	Leu91	Electrostatic strain by replacing a buried hydrophobic residues by a charged hydrophilic	Severe	[25]
Leu198	→	Arg	Gln174	Val103	Electrostatic strain by inserting a positive charge on the C-terminal tail likely will decrease protein stability.	Severe	[29]

Due to the limited number of patients with the same mutation, it is not possible to establish a firm genotype-phenotype correlation. Mutation G130V constitutes an exception; this mutation arose from a single ancestral mutation but is present in several families and correlates to a mild phenotype. Although associated to early onset of the disease the progression is very slow [13, 17, 20, 23].

2.1.1. Friedreich's Ataxia: a Mitochondrial Disease

Although FRDA is a neurodegenerative disease, extraneural organs are involved in its pathogenesis which suggests that mitochondria are involved in FRDA development. The co-localisation of frataxin with mitochondrial markers confirmed that frataxin is indeed a mitochondrial protein [30-32]. However, there have been reports of cytosolic frataxin, where it interacts with the cytosolic Aconitase/IRP1 switch controlling it [33-34].

The study of the molecular features associated to FRDA pathogenesis were first addressed using the yeast system as a model. Deleting yeast frataxin homologue resulted in the inhibition of growth, reduced mitochondrial respiration, iron accumulation and increased sensitivity towards oxidative stress [35-36]. Interestingly, human frataxin could complement yeast frataxin deletion, suggesting a high functional conservation throughout evolution. Studies on cardiac biopsy samples from FRDA patients revealed deficiencies on respiratory complexes I, II and III, and on aconitase [37]. These deficiencies correspond to deficits of iron-sulphur proteins and suggest a link between the lack of frataxin and iron-sulphur clusters biogenesis impairment. These results were further confirmed and supported by the analysis of autopsy samples and by *in vivo* quantification of the ATP production rate after exercise [38]. Whether iron deposits detected in FRDA patients [35, 39]

constitute a primordial cause of FRDA has been a matter of debate. Without excluding a direct role of frataxin on iron metabolism, murine models support the hypothesis that iron accumulation is a secondary effect of FRDA [40]. Homozygous deletion of the frataxin gene in this model leads to embryonic lethality, but this effect is not associated to iron accumulation. Furthermore, conditional mouse models of FRDA showed that cardiac hypertrophy and respiratory chain dysfunction were observed several weeks before mitochondrial iron accumulation was detected [41]. A recent report, using muscle creatine kinase conditional frataxin knockout mouse models, also supports this view of iron accumulation as a secondary effect of FRDA [42]. When analysing the gene expression in the conditional mutants, Richardson and co-workers observed that frataxin deficiency causes the down regulation of key enzymes involved in iron mitochondrial utilisation pathways, which contributes to mitochondrial iron loading and also alters the systemic iron metabolism [42]. In addition, frataxin knockout also causes the upregulation of transferrin receptor-1 and mitoferrin2 increasing respectively the iron cellular and mitochondrial uptake, which further contribute to the iron accumulation characteristic of FRDA-like cells [42].

Oxidative stress also plays a crucial role in FRDA pathogenesis. The first evidence of this relationship came from studies on yeast model and on cultured cells from FRDA patients, when it was demonstrated that both these cells have higher sensitivity towards hydrogen peroxide [35, 43]. Furthermore, cultured mouse cells expressing low levels of frataxin show increased production of free radicals. Accordingly, FRDA patients show markers of increased oxidative stress like urinary 8-hydroxy-2'-deoxyguanosine and increased levels of plasma glutathione–S-transferase activity and melondialdehyde [44]. The activation of stress pathways in frataxin deficient cells such as the c-Jun N-terminal kinase pathway further supports the pathogenic role of mitochondria

dysfunction and oxidative stress in FRDA [45]. A recent report shows that the increased oxidative stress associated to FRDA results from SOD's reduced, at least partially, the activity in FRDA-like cells [46]. Reduced levels of frataxin lead to the activation of AFT1 which, in time, results in a deprivation of cytosolic copper and reduced Cu,Zn-SOD activity [47]. In addition, frataxin depletion also induces a decrease in manganese uptake contributing to mitochondrial SOD inactivation (Mn-SOD) [48]. Experimental evidence suggests that supplementing FRDA-like cells with copper and manganese has a positive effect, restoring SOD's activities and preventing both oxidative damage and inactivation of magnesium-binding proteins [46]. Thus, the effect of frataxin deprivation on oxidative stress balance does not result entirely from its activity but also from side effects of its depletion.

2.1.2. Treatments Available

Treatment approaches that aim at reverting the mitochondrial pathogenesis associated to the disorder have been extensively explored [49]. These approaches have focused on improving mitochondrial function, reducing the amount of reactive species and of iron accumulation. A first approach involved the use of iron chelators such as desferrioxamine or phlebotomy, but, since iron chelators replaced iron instead of protecting against its toxic effect and studies on mouse models suggested that iron accumulation is a secondary event of FRDA and not the causative pathological mechanism [50], this approach was to some extent dropped. A second approach has focused on reducing the load of reactive species observed in FRDA patients. A combination of coenzyme Q10, a potent antioxidant and electron carrier, and vitamin E, an antioxidant, as well as the use of idebenone, a

short-chain benzoquinone structurally identical to coenzyme Q10, has been tested. A trial with ten FRDA patients has revealed that the treatment with coenzyme Q10 and vitamin E improves most FRDA symptoms but has no effect on either posture, gait or hand dexterity degeneration [51-52]. Treatment with idebenone has been quite promising and several clinical trials have already been performed [53-59]. Idebenone is well tolerated and 6 months of treatment with either intermediate (15mg/kg/d) or high-doses (45mg/kg/d) seems to completely prevent the disease progression and also improve the functional impairments by an amount equivalent to 1 year of disease progression [53-64]. In Canada, idebenone has received a conditional approval for the symptomatic treatment of FRDA while in Europe and the US additional clinical trials have been requested and two phase III trials are now being performed, one in Europe and one in the US [49]. In 2007, a promising trial combining idebenone treatment with and an iron chelator, hydroxypyridinone deferiprone (DFP), was published. This was a 6-month trial involving patients that had been treated with idebenone (30mg/kg/d) for at least 2 years. Patients continued the idebenone treatment and started to receive 20 or 30 mg/kg/d of DFP. Neuropathy and ataxic gait were reduced and no side effects were observed [65]. Although these results must still be regarded with caution they open a new and promising strategy.

In contrast to the above described approaches to FRDA treatment, gene-therapy strategies address the cause of the disease and aim to increase the cellular levels of frataxin; however, the discovery of treatments for FRDA following this approach are still in an early stage. Treatments combining drugs that facilitate chromatin opening, such as histones deacetylase (HDAC) inhibitors and DNA-demethylation agents, have shown positive results reverting fragile X syndrome defects [66], given the similarities and parallels between this pathology and FRDA is

likely that the same approach may also be useful for FRDA treatment. Different compounds have been tested and some are likely to reverse the heterochromatin induced by the GAA repeats, such as BLM-210 and HDAC ibhibitor that leads to an increase (approximately two-fold) in frataxin message level [67]; others are more likely to increase the proteins level due to specific transcription factor activation such as Cisplatin [68], 3-nitroproprionic acid [69], hemin [70] and erythropoietin [71]. Although the identification of these compounds that effectively enhance frataxin levels in the cell may represent a turning point on the way FRDA therapeutics are addressed, caution must be taken since we are still at the beginning of accessing this possible therapeutic approach. Many of the biochemical mechanisms involved have not yet been fully elucidated and, in addition, these molecules may also be harmful.

2.2. Frataxin: a Highly Conserved Mitochondrial Protein

Frataxin is highly conserved throughout evolution, having homologues in mammals, *Caenorhabditis elegans*, yeast and Gram-negative bacteria. The different homologues share a sequence identity of ~25% and a similarity of 40-70% (**Fig. 2.3**). Human C-terminal domain is similar to CyaY proteins of γ-purple bacteria suggesting that that FRDA gene evolved from a CyaY gene of the mitochondrial ancestor [72]. While bacteria only have the conserved C-terminal domain, Eukaryotes have an additional N-terminal tail that constitutes the mitochondrial import signal [32].

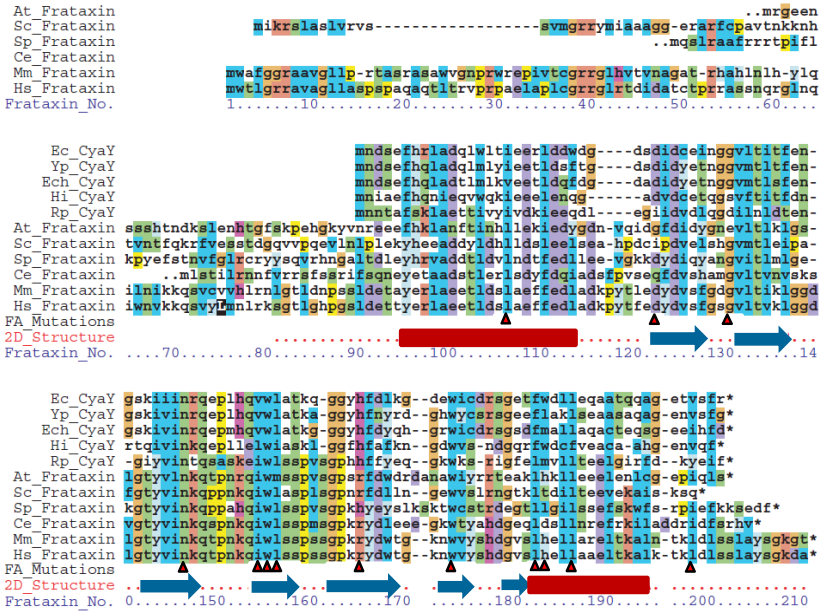

Figure 2.3: Alignment of eukaryote and bacterial frataxins sequences displayed with Clustal X colours to emphasise conserved sequence features [73]. On the 2D structure line, ▬ helices and ➡ β-sheets. The residues whose mutation leads to FRDA in heterozygous patients are marked with ▲ .

Eukaryotic frataxin homologues are nuclear encoded proteins and are thus synthesised in the cytosol as precursors with an N-terminal presequence that targets frataxin to the mitochondrial matrix. Once imported, the precursor frataxin is matured by the mitochondrial processing peptidase (MPP) through a two-step process [74-76] (**Fig. 2.4**). MPP is responsible for the maturation of most nuclear encoded protein, however, the maturation process usually involves only one step [77]. Studies on the maturation process using an *in vitro* hybrid system - maturation of human frataxin by rat MPP - suggested that the second cleavage constitutes the maturation limiting step, since this second reaction is ~12 times slower than the first [75]. Frataxin presequence is ~1.5-2 times the average length (20-40) [78-79] which might explain the need for two cleavages. *N. crassa* ATApase subunit 9, the other

described protein with a two step maturation process, also has a longer presequence [80].

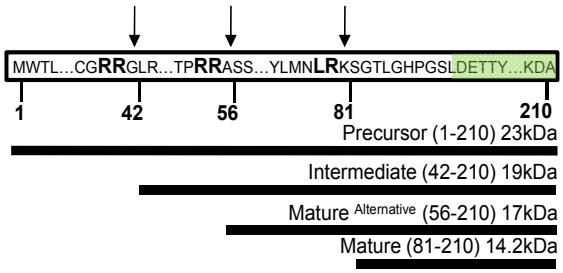

Figure 2.4: Schematic representation of human frataxin processing by MPP (Arrows point out MPP cleavage sites). Precursor protein ($^{1\text{-}210}$FXN) is targeted to the mitochondria and undergoes a two-step maturation process. The 1st step is slower leading to the formation of the intermediate $^{42\text{-}210}$FXN, the 2nd step leads to the formation of mature frataxin ($^{81\text{-}210}$FXN), however, if the normal cleavage site is blocked (between residues 80 and 81), alternative maturation can occur leading to the formation of $^{56\text{-}210}$FXN. Green corresponds to the highly conservative protein core [81].

There has been some controversy regarding frataxin cleavage sites during maturation, but a recent study *in vivo* using human cells has shown that $^{81\text{-}210}$FXN corresponds to frataxin mature form and $^{42\text{-}210}$FXN to the intermediate form [81]. Furthermore, this study has also revealed that human frataxin may have an alternative cleavage site when the cleavage between residues 80 and 81 is impaired (maybe due to a mutation or a posttranscriptional modification). This alternative cleavage site leads to the formation of $^{56\text{-}210}$FXN, which may suggest the existence of a proteolytic mechanism that can control the length of mature frataxin [81]. This idea is further supported by the fact that $^{56\text{-}210}$FXN is able to rescue frataxin deficient cells.

As shown by studies on the yeast homologue, the mitochondrial Hsp70's, Ssq1 and Ssc1, are involved in frataxin import and maturation. While Ssc1 is crucial for the import, Ssq1 is believed to be involved in frataxin maturation [82-83]. Nevertheless, Δ*ssq1* mitochondria show levels of mature frataxin that are approximately 75% of the observed in normal mitochondrial, suggesting that the absence of this chaperone does not completely impair maturation [83]. Maturation studies have also revealed that mutation on the C-terminal domain can affect MPP

processing efficiency but experimental data on this subject is controversial [75-76].

Extensive structural and biochemical studies have been performed in three of the frataxin's homologues: human (FXN), yeast (Yfh1) and bacteria (CyaY). These studies have focused on the evolutionary conserved domain (the C-terminal domain) and aimed at a better understanding of frataxin's cellular function and of the relation between reduced frataxin expression levels and FRDA development. Human frataxin (FXN) structure was the first to be solved (**Fig. 2.5**) [85-86], followed immediately by the CyaY [87-88]. Four years later the Yfh1 structure was solved [89] and now many structures, including the structure CyaY bound to metals as well as Yfh1 assemblies, have already been published [90-92].

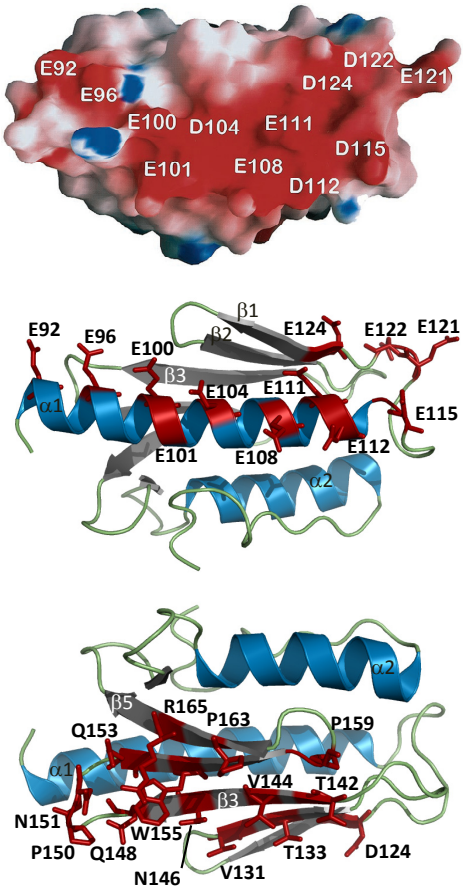

Figure 2.5: Top. Molecular surface representation of Human frataxin. The molecule is oriented as shown in the middle Fig. The molecular surface was calculated and was shaded according to the electrostatic potential (-10*kt/e*, red to +10 *kt/e,* blue). Individual residues within the acid ridge are labelled. **Middle.** Ribbon representation of human frataxin structure, α-helices are represented in blue, β-sheets in grey and loops in green. The residues comprising the acidic ridge at the α1/β1 surface are labelled (Putative iron binding region). **Bottom.** Side chains of highly conserved residues that project outward from the large, flat β sheet (β1–β5) create a 1008 $Å^2$ conserved surface on frataxin. Adapted from [84].

Initially FXN structure was solved considering only the residues comprising the protein core [84-86]; however, recently the FXN N-terminal tail was studied by NMR revealing that this region is intrinsically unfolded and does not alter the protein structure, iron binding properties or the monodispersity of the evolutionary conserved domain (the core) [84-86].

The orthologues sequence homology shown above (**Fig. 2.3**) is reflected on their identical folds. Five β-strands form a flat antiparallel β-sheet that is solvent exposed on one side and is tightly packed against the two helices on the other. N- and C-terminal helices have their axes nearly parallel with respect to the main antiparallel β-sheet. A second β-sheet intersects the helical and β-sheet planes and is formed by the C-terminus of the last β-strand (β5) of the antiparallel sheet and two additional strands (only one additional strand for Cyay and Yfh1); the loop between these two strands is less structured than the others. The main difference between these three orthologues is that the C-terminal extension that has variable lengths and hydrophobicities (**Fig. 2.6**). This extension is packed between the two helices filling the groove between them and its length correlates with the protein's stability [93]. Both sequence and fold are highly conserved between frataxin orthologues, but the thermodynamic stability diverges significantly. The human and bacterial frataxin's (FXN and CyaY) are thermally stable with melting temperatures (T_m) of ~58ºC and ~51ºC respectively. Whereas interestingly, Yfh1 is only marginally stable in its metal free form (T_m = ~35ºC even though the optimal growth temperature for yeast is 30ºC). The different thermo-stabilities show a correlation with the C-terminal tail length. Elongating Yfh1 C-terminal tail with 3 amino acid residues from the FXN sequence increases its thermal stability by 6ºC. The opposite strategy, removing 3 and 12 residues from the CyaY and FXN

tails respectively, results in constructs with different properties from the original proteins. FXN is no longer soluble and CyaY thermal stability is significantly impaired, showing a T_m identical to the Yfh1, T_m=36.8ºC corresponding to a ΔT_m=14ºC. In agreement with this hypothesis, no conserved function is associated to the C-terminal tail.

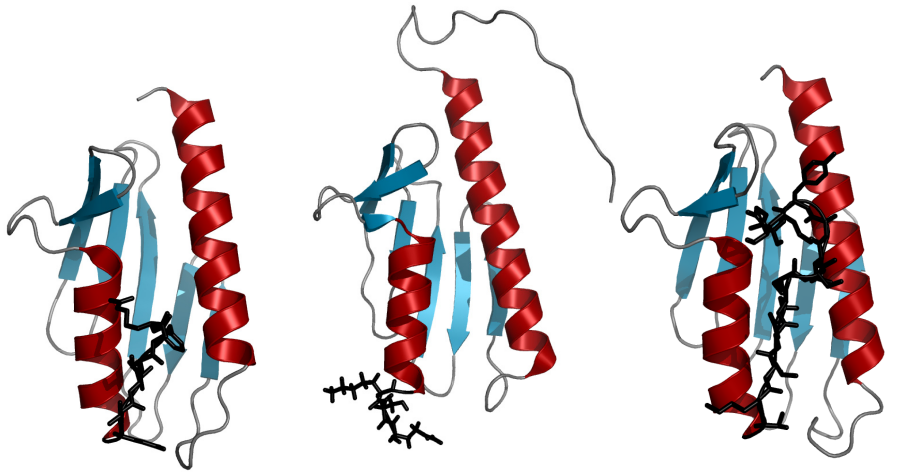

Figure 2.6: Ribbon representation of frataxin's orthologues structure. This structural comparison highlights the similarities between the orthologues. **Left**. E. coli frataxin - CyaY (PDB # 1ew4). **Middle.** S.cerevisiae frataxin - Yfh1 (PBD # 2ga5). **Right**. Human frataxin - FXN (PDB # 1ekg). The C-terminus residues are coloured in black and their side chains represented by sticks[93].

Frataxin fold is not common and only recently a similar fold was identified on a protein outside frataxin's family. The crystal structure of the hydrophilic domain of respiratory complex I from *Thermus thermophilus* revealed that its subunit Nqo15 has a fold similar to frataxin. The sequence homology is low (11-13%), but the structures superimpose with RMS values of 2.5 and 3.3 Å for CyaY and FXN respectively. [94]. Nqo15 interacts with complex I mainly through the

exposed β-sheet surface, the same region in that frataxin is proposed to be a protein-protein interaction site. Two putative roles are suggested for Nqo15 subunit; this subunit may function as an iron storage module, promoting the reconstitution of FeS clusters in the complex or/and it may stabilise the complex structure [94]. In addition to being structurally similar, the putative functions attributed to frataxin and this complex I domain are also related. The α–β sandwich motif structure is also recognised in the ferredoxin-like fold of some cytosolic copper chaperones (Human HAH1 [95], Yeast ATX1 [96] and BsCopZ [97]). These however, are smaller in size and their helices are tilted at 45º to each other.

Solving frataxin structure has allowed for the identification of residues, among the conserved ones, that are more likely to be associated to the protein's function. Conserved residues on the protein surface are likely to be involved in the protein function and while conserved buried residues are more likely to have a structural role [84, 86]. A large number of highly conserved acidic residues between the α1/β1 interface constitute a negatively charged surface that covers a quarter of the proteins surface (**Fig. 2.5 Top**). This region is likely to be functionally relevant and the presence of numerous Asp and Glu suggests that it might constitute a metal binding site (**Fig. 2.5 Middle**). Surface exposed residues in the β-sheet plane of frataxin are also quite conserved and are believed to be involved in the protein-protein interactions (**Fig. 2.5 Bottom**). On the other hand, highly conserved residues on the β-sheet that contribute to the protein core, as well as conserved residues in the helical plane, are likely to have a structural role in frataxin. Almost all mutations described in FRDA heterozygous patients involve conserved residues, which highlights either structural or functional roles [9, 13].

The high evolutionary conservation among frataxin orthologues has enabled the development and use of disease models of a wide range of organisms, from the unicellular eukaryote *Saccharomyces cerevisiae* to mice. The yeast model system has been extensively used and contributed significantly to what is now known about frataxin function and its implication in FRDA [28, 98]. Unicellular models are particularly relevant for the study of genetic and environment modifiers of a phenotype and for unbiased drug screenings. On the other hand, multi-cellular disease models contribute extensively to the understanding of the pathophysiology associated to FRDA. Different multicellular models have been developed using murine models, constitutive and conditional knockouts [41], GAA-based mouse models [99], *C. elegans* [100-102] and *Drosophila* models [103-105]. The last model allows investigators to use of conditional RNA interference technology to modulate frataxin expression [103].

2.3. Frataxin Function: What is Known so Far

Early studies on frataxin have suggested that this small mitochondrial protein is involved in iron homeostasis but its exact role is still not clear. Organisms with low levels of frataxin expression show metabolic disturbances associated to intramitochondrial iron accumulation, decreased activity of iron-sulfur (FeS), reduced oxidative phosphorylation and oxidative stress hipersensitivity.

2.3.1. An Iron Binding Protein

Considering the phenotype caused by reduced levels of frataxin expression it was not surprising to find that frataxin is an iron binding protein [106-112]. Frataxin does not have any cavities or hydrophilic

pockets to harbour bound iron, instead iron binding involves carboxylate oxygens, from Asp and Glu, and nitrogens on imidazole rings from His. In support of this notion, iron binding studies by NMR together with mutagenesis studies have shown that the conserved acidic residues on the $\alpha 1/\beta 1$ interface, rich in Asp and Glu, constitute the putative iron binding surface. **Table 2.2** enumerates the residues found to be involved in iron binding in three of frataxin's orthologues - CyaY, Yfh1 and FXN (**Fig. 2.6**). Ferrous iron to protein stoichiometries measured for these orthologues are 2, 2 and 7 Fe^{2+} per monomer respectively [108, 110-111]. While iron dissociation constants described for CyaY and Yfh1 are identical (~4 and 3μM) [108, 110], the K_d determined for the human orthologue is ~10 fold higher (55μM, **Table 2.3**).

Figure 2.7: Human frataxin putative iron binding sites identified by NMR spectroscopy. **Red.** At a stoichiometry of $1Fe^{2+}$:1FXN the amide resonances of the following residues disappear: Asp112, Leu113, Asp115 and Val125; **Pink.** Increasing the stoichiometry to $2Fe^{2+}$:1FXN further alters the amide resonance of the following residues: Asp104, Ala107, Glu108, Phe110, Ala114, Thr119, Phe120, Asp122 and Asp124; **Green.** Additionally at a stoichiometry of $6Fe^{2+}$:1FXN: Ser105, Phe109, Glu111, Lys116, Glu121 and Phe127. Increasing the iron concentration does not induce further changes in the amide resonances which is in agreement with the 6:1 iron stoichiometry determined for human frataxin [91].

Ferric iron binding has only been described for the bacterial and human orthologues [108, 111]. Human frataxin shows the same stoichiometry for iron III as for iron II, binding 6/7 irons per monomer but showing a higher affinity for ferric iron with a K_d of ~10μM [111]. Monomeric Cyay is also able to bind ferric iron with a stoichiometry of 6/7 irons per monomer. However, this orthologue presents additional,

but weaker, iron binding sites allowing CyaY to bind up to 25-26 iron atoms per monomer [108].

Table 2.2: Residues identified as being involved in iron binding by NMR spectroscopy and the sequence number conversion between different species for this functional residues [89, 91, 113-114].

Residue Number In				
CyaY[a]	**Yfh1[a]**	**Dfh[b]**	**mFXN[b]**	**FXN[a]**
-	Leu72	Gly70	Glu89	Glu92*
Ser4	Glu71	Ala71	Thr90	Thr93
Glu5	Lys72	Thr72	Ala91	Thr94
Phe6	Tyr 73	Tyr73	Tyr92	Tyr95
His7	His74	Glu74	Glu93	Glu96*
Arg8	Glu75	Arg75	Arg94	Arg97
Leu9	Glu76	Val76	Leu95	Leu98
Asp11	Asp78	Ser78	Glu97	Glu100*
Gln12	Asp79	Asp79	Glu98	Glu101*
Leu15	Asp82	Asp82	Asp101	Asp104
Thr16	His83	Ala83	Ser102	Ser105
Glu18	Leu85	Cys85	Ala104	Ala107
Glu19	Asp86	Asp86	Glu105	Glu108
Arg20	Ser87	Tyr87	Phe106	Phe109
Leu21	Leu88	Phe88	Phe107	Phe110
Asp22	Glu89	Glu89	Glu108	Glu111*
Asp23	Glu90	Glu90	Asp109	Asp112
Trp24	Leu91	Leu91	Leu110	Leu113
Asp25	Ser92	Thr92	Ala111	Ala114
Gly26	Glu93	Glu93	Asp112	Asp115
-	Pro96	Glu97	Thr116	Thr119
Asp27	Asp97	Leu98	Phe117	Phe120
Asp29	Ile99	Gly100	Asp119	Asp122
Asp31	Asp101	Asp102	Asp121	Asp124
Cys32	Val102	Val103	Val122	Val125
Glu33	Glu103	Ala104	Ser123	Ser126
Asn35	Ser105	Tyr106	Gly125	Gly128
Ile41	Leu111	Val112	Ile131	Val134
Thr42	Glu112	Asn113	Lys132	Lys135

[a] The putative iron binding sites for these three species, *E. coli, S. cereviseae* and *H. Sapiens*, were determined using NMR spectroscopy. In Black are the residues identified by NMR as involved in iron binding, in grey are the corresponding residues that in other species were identified as iron binding sites;

[b] Dfh – D. *melanogaster* (fruit fly) and mFXN – *M. musculus* (mouse). Sequence number conversion for the residues identified as binding sites on the other three species;

* Residues indentified in an additional study [114].

CyaY and Yfh1 oligomerise in an iron-dependent way [106, 108], but their oligomerisation process is different. Contrary to what is observed for the CyaY, Yfh1 oligomerisation process is well defined and ordered, leading to the formation of high molecular weight oligomers. Nonetheless, magnesium and calcium salts, at concentrations found within the mitochondria, stabilise the monomeric iron-bound Cyay and Yfh1 [106-107, 110], suggesting that oligomerisation may not be important for frataxin cellular function.

Table 2.3: Stoichiometry and dissociation constants determined, by both flurescence or ITC (isothermal titration calorimetry), for the interaction of frataxin with either ferrous or ferric iron.

	n	K_d (μM)	Ref.
Fe^{2+}			
CyaY	2	3.80	[108]
Yfh1	2[a]	2.50	[110]
Dfh	1	6.00	[115]
$^{46-210}$FXN	1	4.00	[116]
$^{78-210}$FXN	7	0.46	[114]
$^{78-210}$FXN (E100/E101/D104/E108/E111/D112A)	2	0.21	[114]
$^{78-210}$FXN (D115/E1221/D122/D124A)	4	0.32	[114]
$^{78-210}$FXN (E92/E96/E100/E101A)	5	0.18	[114]
$^{81-210}$FXN	6/7	55.0	[111]
Fe^{3+}			
CyaY	6[a]	n.d.	[108]
$^{81-210}$FXN	6/7	11.7/10.2[b]	[111]

[a] Additional irons can bind without protein precipitation, Yfh1 binds up to ~50FeII/monomer, while CyaY bind up to a stoichiometry of ~25-26Fe^{III}/monomer;
[b] As measured by fluorescence and ITC.

Human frataxin does not oligomerise *in vitro*, however it can assemble into holopolymers when expressed in *E. coli* or in Yeast [22, 109], but this oligomerisation depends on protein-protein interactions involving the non-conserved N-terminal region. Contrary to what is observed for other frataxin orthologues, human frataxin oligomerisation is not iron dependent but oligomers can bind up to 10 irons per monomer. Oligomers can be found in mouse and human heart mitochondria when $^{56\text{-}210}$FXN construct is expressed, suggesting that indeed oligomerisation can occur in native conditions [117]. The protein core does not oligomerise ($^{78\text{-}210}$FXN) [107, 109], but the identification of an alternative maturation site leading to the formation of $^{56\text{-}210}$FXN opens the possibility of oligomerisation *in vivo*. If this process does occur *in vivo* its biological relevance is still questionable since iron storage in human cells is much more efficiently accomplished by ferritin. Due to the lack of mitochondrial ferritin in yeast, yeast may alternatively use frataxin as an iron storage protein.

2.3.2. Iron-Chaperone

Frataxin acts as an iron chaperone for two fundamental processes: the FeS clusters and the heme biosynthesis. Frataxin involvement in FeS clusters formation was first suggested by the decreased activity of FeS clusters containing enzymes in FRDA patients, as well as in yeast and conditional knockout mice [35, 41, 118-120]. FeS proteins participate in several essential cellular processes such as electron transport (respiratory chain), gene regulation, iron uptake and catalysis [121]. FeS clusters assembly in eukaryotes is performed in the mitochondria by the ISC machinery (**Fig. 2.7**) [122-123]. Correct FeS assembly involves Nsf1 (a cystein desulfurase) [123-124], Arh1

(ferredoxin reductase) [125], Yah1 (ferredoxin), Isd11 [125-127] and Isu [123, 128-130]. Briefly, Isu provides a platform for the assembly of FeS clusters prior to the delivery to an apo protein. The scaffold protein Isu is dynamic as it forms dimers and binds Nsf1 forming an heterotetrameric complex that allows for the transfer of sulphide. While Nsf1 delivers sulphur, frataxin acts as an iron chaperone delivering iron to the scaffold protein Isu.

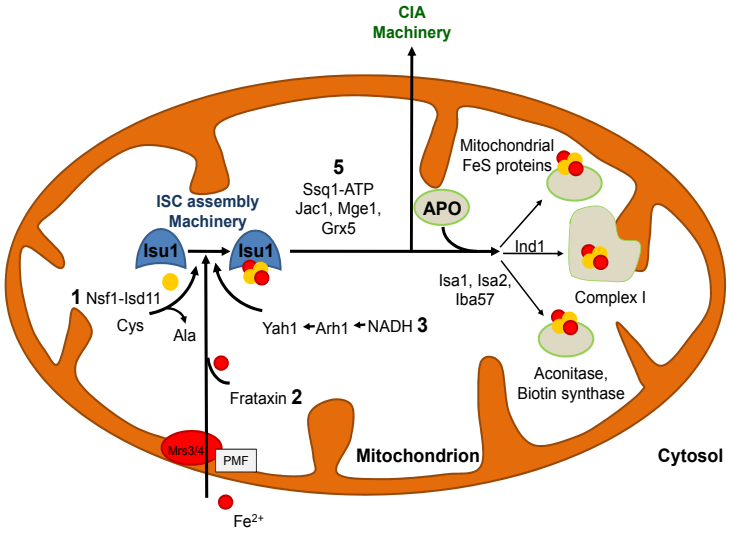

Figure 2.8: A model for FeS protein assembly in Eukaryotes. The assembly of FeS occurs inside the mitochondria, the ferrous iron is imported from the cytosol in a membrane potential-dependent manner (with proton-motive force (PMF) as a source of energy). Import is aided by the inner membrane carriers Mrs3 and Mrs4 (known as mitoferrin in mammals). FeS clusters assembly starts with sulphur liberation from cystein by the desulfurase complex Nsf1-Isd11 (1). The synthesis of transiently bound FeS clusters on the scaffold protein Isu1 (and Isu2 in yeast) further depends on the iron-binding protein frataxin as an iron donor, that undergoes an iron-stimulated interaction with Isu1-Nsf1(2) and electron-transport chain consisting of NADH, ferredoxin reductase (Arh1) and ferredoxin (Yah1), which possibly provides the electros for the reduction of sulphur to sulphide (3). The release of the FeS clusters from Isu and its transfer to apooriteins (APO) are facilitated by ATP-dependent Hsp70 chaperone Ssq1, DnaJ-like co-chaperone Jac1, the nucleotide exchange factor Mge1 and the monothiol glutaredoxin Grx5 (5). The nuclear and cytosolic FeS protein biogenesis require the mitochondrial ISC machinery assembly, export machinery and further involved the cytosolic FeS protein assembly machinery (CIA). Adapted from [123, 125, 131-134].

It was demonstrated that frataxin deficiency in human HeLa cells and Yeast compromises the maturation of both cytosolic and mitochondrial FeS cluster proteins [135-138]. This is the first defect to be detected once frataxin expression is impaired by iRNA [139], suggesting a specific role of frataxin on the biosynthesis FeS clusters.

Frataxin is involved in the early stages of FeS clusters biosynthesis and experimental evidence suggests that frataxin delivers iron to the scaffold protein Isu [111] [141]. *In vitro* frataxin-Isu interaction is iron dependent and **Table 2.4** presents the binding parameters assessed for this interaction.

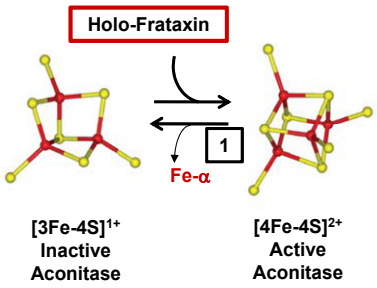

Figure 2.9: Frataxin can play a dynamic role in the regulation of aconitase during oxidative stress. It can protect the aconitase labile $[4Fe\text{-}4S]^{2+}$ from disassembly and facilitate Fe^{II} transfer to the $[3Fe4S]^{1+}$ cluster of aconitase reactivating its enzymatic activity [140].

Moreover, frataxin is also involved in FeS clusters' protection and repair. It interacts with aconitase in a citrate dependent fashion, delivering iron to aconitase ($[3Fe\text{-}4S]^{1+}$) and enabling the repair of its FeS cluster and its enzymatic reactivation [140].

Recently, a study using the *E. coli* orthologue, CyaY, has suggested an alternative and rather controversial role of frataxin on the FeS biosynthetic pathway [142]: Pastore and co-workers have suggested that frataxin may work as an inhibitor of FeS assembly and as an iron sensor. According to this new putative function, CyaY would, through a negative regulation mechanism, act as a gate-keeper of FeS clusters assembly, fine-tuning the assembly of the clusters to meet the concentration of apo-protein acceptors (**Fig. 2.10**).

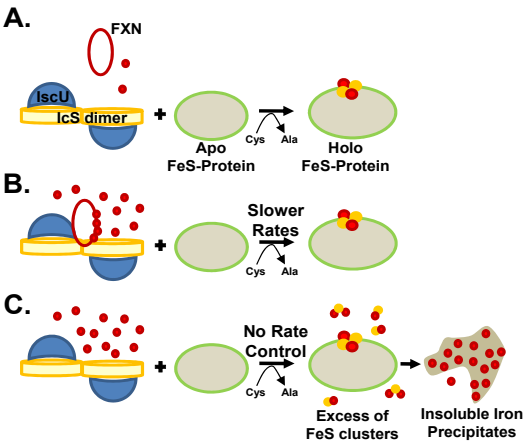

Figure 2.10: Schematic representation of the alternative molecular mechanism of frataxin in the cell proposed by Pastore and co-workers (proposed through the study on the bacterial mechanism). **(A)** Normal iron concentrations, FeS clusters are assembled by the IscS-IscU complex (corresponding to the Isu-Nsf1 complex). **(B).** Excess of iron in respect to the concentration of final accepters will be rebalance by slowing down the FeS clusters assembly and avoid unnecessary overproduction of these labile clusters**. (C).** When frataxin is down-regulated or produced in insufficient concentrations, as in FRDA, there is no regulation of the clusters assembly. FeS clusters will be produced in excess and iron excess will result in FeS clusters surplus which being very unstable will degraded generating Fenton reactions. Fe^{3+} will precipitate and form insoluble aggregates. Adapted from [142].

Frataxin also acts as an iron chaperone in another essential biosynthetic pathway - the Heme synthesis. Considering that prokaryotic frataxin in not part of a specific operon, frataxin involvement in more than one pathway is conceivable. Heme synthesis comprises several steps and the last involves ferrochelatase. Frataxin catalyses the insertion of ferrous iron into the porphyrin ring, leading to the formation of functional heme. In Eukaryotes, ferrochelatase is associated to the matrix side of the inner mitochondrial membrane and, in addition to iron, it can chelate other divalent ions being zinc the predominant alternative. Studies using the yeast model have shown that the absence of frataxin (Yfh1 deleted strain) leads to severe deficiency in cytochromes *b*, *c* and (*a*+*a3*). Interestingly, when using a system where the induction of Yfh1 could be controlled, it was observed that the

cytochrome *c* deficiency could be reversed once frataxin expression was reversed [143]. Later, it was shown that reduced levels of frataxin lead to a down regulation of mitochondrial transcripts and a kinetic inhibition of the heme biosynthetic pathway [144]. Altogether these results suggest an involvement of frataxin in heme assembly. Dancis and co-workers, through the use of Surface Plasmon Resonance (Biacore), have first reported a direct interaction between frataxin and ferrochelatase (K_d~40nM) [143].

Table 2.4: Stoichiometry and dissociation constants determined, by both flurescence, ITC or Biacore, for the interaction between frataxin and its protein partners Isu and ferrochelatase.

	n	K_d (μM)	Ref.
Isu1[a]			
$^{46\text{-}210}$FXN	1.0	5.40	[116]
$^{78\text{-}210}$FXN	1.0	0.03	[114]
$^{78\text{-}210}$FXN (E100/E101/D104/E108/E111/D112A)	0.9	0.05	[114]
$^{78\text{-}210}$FXN (D115/E1221/D122/D124A)	1.0	0.09	[114]
$^{78\text{-}210}$FXN (E92/E96/E100/E101A)	0.9	0.11	[114]
$^{81\text{-}210}$FXN	1	0.67[b] 0.45	[111]
Dfh	0.9	0.21	[115]
Ferrochelatase			
Yfh1	-	0.04	[143]
$^{81\text{-}210}$FXN	0.5[c]	0.17	[112]

[a] Measured Apo D37A Isu . Mutation D37A on Isu was found to stabilize The Isu-bound FeS clusters;
[b] Measured for Apo Isu;
[c] Frataxin monomer binds to ferrochalatase homodimer.

However, this study could not report any direct evidence of frataxin-mediated iron delivery to ferrochelatase, since interaction was detected in the absence of iron. Later, Cowan and co-workers characterised this interaction for the human system and have shown that holo-frataxin could be a potential iron donor to ferrochelatase for the insertion of iron into the protoporphyrin ring during heme synthesis (K_d=~17nM, Table 2.3) [112]. The interaction between frataxin and ferrochelatase could only be detected by ITC and fluorescence when iron was present, similarly to what it had been described for the Isu-frataxin interaction (**Table 2.4**) [112].

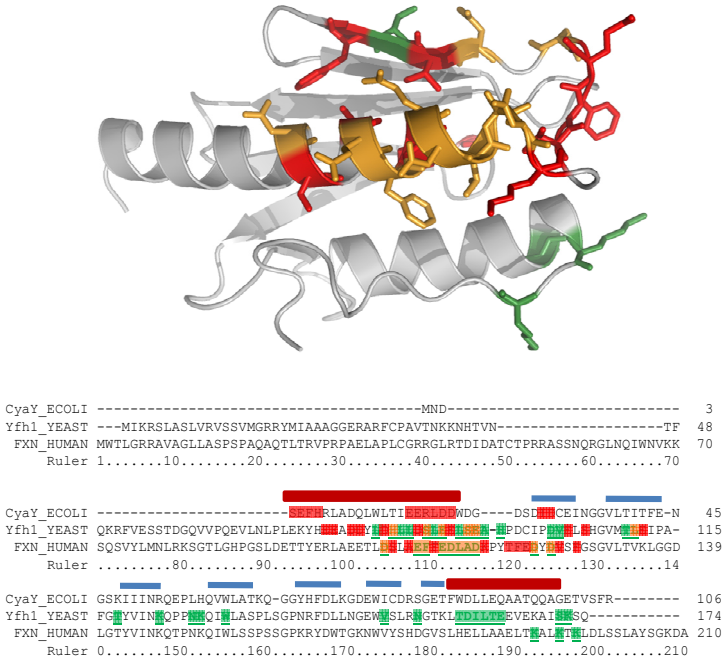

Figure 2.11: Top. Ribbon representation of the structure of human frataxin, putative iron and ferrochelatase binding sites are coloured and their side chains are presented by sticks. **red**: iron binding sites; **green**: ferrochelatase biding sites;**orange**: iron and ferrochelatase binding sites. **Bottom**: Alignment of the sequence of CyaY, Yeast and human frataxin; **red boxes** highlight the putative iron binding sites; **green boxes** with a green underline identify the putative ferrochelatase binding sites; o**range boxes** with a green underline identify the residues that constitute putative iron and ferrochelatase binding sites [91, 113-114].

Table 2.5: Residues identified as being involved in ferrochelatase binding by NMR spectroscopy and the sequence number conversion between different species for this functional residues [89, 113].

Residue Number In				
CyaY[b]	**Yfh1[a]**	**Dfh[b]**	**mFXN[b]**	**FXN[a]**
Trp14	Leu81	Leu81	Leu100	Leu103
Leu15	Asp82	Asp82	Asp101	Asp104
Thr16	His83	Ala83	Ser102	Ser105
Ile17	Leu84	Leu84	Leu103	Leu106
Glu18	Leu85	Cys85	Ala104	Ala107
Glu19	Asp86	Asp86	Glu105	Glu108
Arg20	Ser87	Tyr87	Phe106	Phe109
Leu21	Leu88	Phe88	Phe107	Phe110
Asp22	Glu89	Glu89	Glu108	Glu111
Asp23	Glu90	Glu90	Asp109	Asp112[§]
Trp24	Leu91	Leu91	Leu110	Leu113[§]
Asp25	Ser92	Thr92	Ala111	Ala114
Gly26	Glu93	Glu93	Asp112	Asp115[§]
-	Ala94	Asn94	Lys113	Lys116
-	His95	Ser96	Tyr115	Tyr118
Asp29	Ile99	Gly100	Asp119	Asp122
Asp31	Asp101	Asp102	Asp121	Asp124
Cys32	Val102	Val103	Val122	Val125
Glu33	Glu103	Ala104	Ser123	Ser126
Thr40	Thr110	Thr111	Thr130	Thr133
Ile41	Leu111	Val112	Ile131	Val134
Ser47	Thr118	Gly119	Thr138	Thr141
-	Lys123	Thr127	Thr146	Thr149
Leu57	Asn127	Asn129	Asn148	Asn151
His58	Lys128	Lys130	Lys149	Lys152
Trp61	Trp131	W133	Trp152	Trp155
Ile79	Val150	Ile156	Val171	Val174
Ser83	Asn154	Ser160	Asn175	Asn178
Trp88	Thr159	His165	His180	His183
Asp89	Asp160	Glu166	Glu181	Glu184
Leu90	Ile161	Leu167	Leu182	Leu185
Leu91	Leu162	Leu168	Leu183	Leu186
Glu92	Thr163	Gln169	Ala184	Ala187
Gln93	Glu164	Gln170	Arg185	Ala188
Gln97	Lys168	Gly174	Lys189	Lys192
Gly100	Ser171	Lys177	Asn192	Lys195
Glu101	Lys172	Ser178	Thr193	Thr196
Thr102	Ser173	Gln170	Lys194	Lys197

[a] The putative ferrochelatase binding sites for, *S. cereviseae* and *H. Sapiens*, were determined using NMR spectroscopy. In Black are the residues identified by NMR as involved in ferrochelatase binding, in grey are the corresponding residues that were identified as iron binding sites on the other specie; [b] CyaY - *E. coli,* Dfh – D. *melanogaster* (fruit fly) and mFXN – *M. musculus* (mouse). Sequence number conversion for the residues identified for the other two species;[§] Residues whose chemical shifts were already broadened beyond detection during the iron titration before ferrochelatase addition but that are believe to constitute the interface for ferrochelatase binding [113].

The identification of frataxin residues involved in the ferrochelatase-binding surface was performed by NMR spectroscopy for both yeast and human orthologues (**Table 2.5** and **Fig. 2.11**) [89, 113]. These studies suggested that frataxin's helical plane, primarily the conserved and exposed helical residues including the α1 iron binding residues, constitutes the interface for frataxin–ferrochelatase interaction. Furthermore, β6-loop-α2 residues are also involved in the interface for ferrochelatase binding. These residues on the β6-loop provide an hydrophobic patch on the interface surface which could suggest that this region maybe target the binding of frataxin the hydrophobic exterior of ferrochelatase.

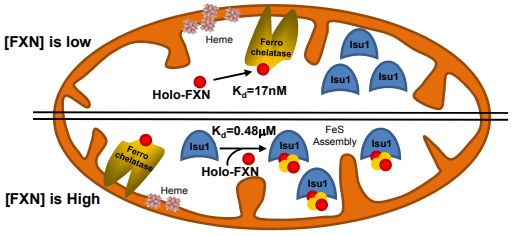

Figure 2.12: Model for the regulation of frataxin iron chaperon activity, FeS clusters biosynthesis vs Heme biosynthesis. Under normal growth conditions frataxin (FXN) concentration is sufficient to both biosynthetic pathways. However, when frataxin (FXN) expression levels are reduced the FeS suphur biosynthetic pathway should be more significantly affected due to the different affinities of holofrataxin to Isu1 and ferrochelatase. Adapted from [112].

Frataxin participates in two important and essential biosynthetic pathways thus there must be a control mechanism that determines which pathway holo-frataxin targets. After determining the frataxin affinity constant for Isu and ferrochelatase interactions, Yoon and Cowan have suggested a simple regulation mechanism (**Fig. 2.12**). When present in normal concentrations, holo-frataxin will primarily deliver iron to the more needed biosynthetic pathway. However, if frataxin levels are reduced, such as in FRDA patients, frataxin will first meet heme biosynthetic needs at the cost of the FeS clusters biosynthetic pathway leading to a drastic decrease in the amount of FeS clusters.

2.3.3. A Ferritin-Like Behaviour

In the absence of iron, Yfh1 is monomeric, but in the presence of oxygen and ferrous iron it undergoes iron-dependent oligomerisation. Anaerobic conditions fully inhibit oligomerisation [145] and other metals, such as calcium, cobalt, magnesium and manganese, as well as ferric iron are unable to promote Yfh1 assembly [106]. Oligomerisation follows according to the progression $\alpha \rightarrow \alpha_3 \rightarrow \alpha_6 \rightarrow \alpha_{12} \rightarrow \alpha_{24} \rightarrow \alpha_{48}$, where monomer to trimer transition constitute the rate limiting step [106, 145] (**Fig. 2.12**). Giving the similarities between this mechanism and the assembly process described for ferritin [146] it is suggested that frataxin may act as an iron storage protein. When ferrous iron to protein stoichiometries are high, Yfh1 forms a 48-multimeric homooligomers binding up to 50 iron atoms per monomer [145, 147-148]. This multimer is ~1.1MDa and keeps iron in a soluble, stable and available form [106]. However, anaerobic conditions, high concentrations of other divalent ions and physiological salt concentrations impair the assembly process [106-107, 110]. Yfh1 self-assembly is driven by two sequential iron oxidation reactions: first, the protein forms trimers containing ferroxidation sites (residues H74, D78, D79, D82 and H83) that catalyse iron II oxidation [148-149]; when all ferroxidase sites are occupied, the protein starts an autoxidation process that overcomes ferroxidation. The trimers then coalesce through a stepwise process yielding higher order multimers [90, 150]. It is suggested that at least part of the H_2O_2 produced by the ferroxidase reaction will react with the protein [148]. Structural studies on frataxin oligomers suggest a gating mechanism involving two conformations for Yfh1 trimer that enables frataxin to either deliver iron to its protein partners or transfer it to the oligomer core (iron detoxification role) [90]. These studies have also confirmed the remarkable similarities between the structural organisation of Yfh1

oligomers with those of the iron-storage protein ferritin. Although the biological significance of human frataxin oligomerisation capacity is debatable, if indeed this mechanism is relevant, FRDA-related mutations may cause its impairment. Analysis of the structure of Yfh1 trimer, the oligomerisation building block, suggests that four of the identified FRDA clinical mutations, G130V (Yfh1-G107), D122Y (Yfh1-I99), W155R (Yfh1-W131) and R165C (Yfh1-R141), are likely to impair its formation. [90].

Mutagenesis studies have allowed the identification of three residues critical for the oligomerisation capacity of Yfh1: the mutation of residues 86, 90 and 93 to alanines abolishes Yfh1 oligomerisation [151]. However, further studies have revealed that mutating only residue 93 is enough to almost completely abolish oligomerisation [152]. Under normal conditions mutations that compromise oligomerisation are asymptomatic which lead to the belief that this feature was dispensable *in vivo* [151]. However, Isaya group has shown that, under stress conditions, oligomerisation impairment becomes harmful, diminishing yeast lifespan, and lethal if SOD1 gene is deleted [152].

A recent study suggests that reversible Yfh1 iron dependent oligomerisation represents a mechanism that allows frataxin to promote mitochondrial FeS biosynthesis while limiting iron toxicity [153]. Similarly, as noted previously for CyaY, Fe^{III}-loaded oligomeric Yfh1 may deliver iron for the FeS cluster assembly. This study suggests that Yfh1 oligomeric form is the one interacting with Nfs1-Isd11 and Isu. However, low levels of oligomerisation are enough to guarantee FeS cluster assembly. The interaction between frataxin and Isd11 (a component of the Nsf1/Isu complex of mitochondrial FeS cluster biogenesis) had already been reported [129, 154]; Isd11 is thought to mediate the interaction of frataxin with the Nsf1/Isu complex as Isd11 deficiency results in many of the deficiencies described for frataxin

depletion. Interestingly, the frataxin-Isd11 interaction is inhibited by physiological concentrations of ferrous iron but this effect can be reversed by iron chelators. Other metals also inhibit the interaction with the exception of nickel that increases it [154].

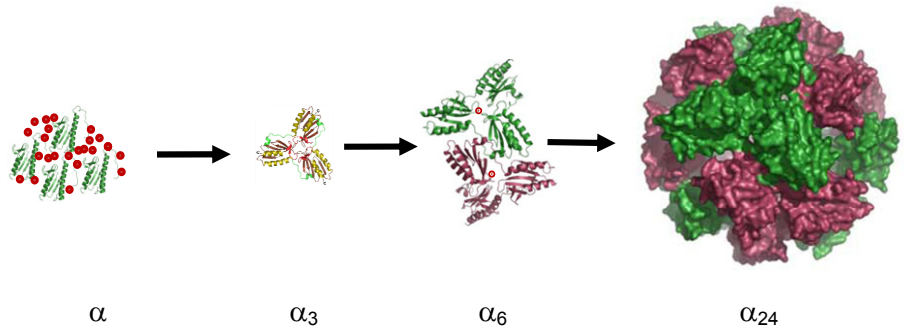

α α_3 α_6 α_{24}

Figure 2.13: Yfh1 iron induced oligomerisation. The excess of iron induces Yfh1 oligomerisation; the trimers constitute the building block of the supramolecular assembly and its formation is the rate limiting step of the process and involves two oxidation reactions: a ferroxidase reaction followed by an autoxidation. The trimer (α_3) is stabilised by the interactions between the loops marked in red, the N-terminal extension, in green, plays a crucial role in the stabilisation of the trimer and in addition is believed to be involved in the packing of the trimers within α_{24} . Iron binds to the channel at the 3-fold axis of the trimer, close to residues D143. Two putative conformations of the channel suggest a gate mechanism that controls whether iron stays in the channel to be delivered to frataxin partners or whether it is transferred to the detoxification sites (oxidation) at the exit of the channel. Adapted from [90].

2.3.4. Anti-Oxidant Activity

The relationship between oxidative stress and FRDA (and hence frataxin) function is rather controversial. The fact that, *in vivo*, reduced levels of frataxin lead to an increase of the oxidative stress is well accepted [100, 155-159], however, the mechanism that allows frataxin to maintain the oxidative balance is still a matter of debate [84,89,137,138]. In the yeast system, the dynamic oligomerisation

behaviour seems to explain how yeast frataxin holds the oxidative balance [117, 152, 160]. According to a mechanism proposed by Isaya's lab, the presence of ferrous iron and oxygen triggers Yfh1 oligomerisation, preventing the existence of free iron which would result in the formation of oxigen reactive species through Fenton reaction. *In vitro*, the presence of Yfh1, CyaY or Dfh1 (drosophila orthologue) inhibits the production of $OH^{\bullet}$ through Fenton chemistry [115, 149, 161] and this effect seems to result from the presence of ferroxidase sites. *In vivo,* it was shown that overexpressing frataxin increases cellular tolerance to stress conditions, such as increased iron concentrations, addition of Paraquat or H_2O_2, prolonging cells life span and preventing oxidative damage to proteins. [162]. This protective effect has been observed for human, drosophila and yeast frataxin [163-165]. The antioxidant protection resultant from overexpressing human frataxin has been linked to increased levels of glutathione and its peroxidase [166]. Interestingly, decreasing the levels of frataxin (yeast model) also leads to an enhanced activity of glutathione peroxidase, thus it seems that frataxin may also control cellular oxidative balance by regulating the cellular thiol content and the thiol-dependent response to oxidative stress [167].

Other studies suggest that frataxin may also act primarily as an activator of oxidative phosphorylation (OXPHOS) [168]. In human cell lines, overexpressing frataxin leads to an increase of Ca^{2+} uptake and respiration, which in turns results in an increased mitochondrial membrane potential ($\Delta\psi_m$ increased 2.5 fold) and elevated cellular ATP content (1.9 fold increase). This hypothesis is in agreement with the fact that FRDA patients have reduced ATP production in the skeletal muscle and with the cellular respiration defects described in Yfh1 deficient yeast. Considering this hypothesis, frataxin may act as an anti-oxidant directly but may also prevent oxidative stress by regulating oxidative

phosphorylation. Still regarding frataxin's putative role in OXPHOS, direct physical interactions between frataxin and succinate dehydrogenase and yeast ETF orthologue have been reported [169]. These suggest that frataxin may be involved in the entrance of electrons into the electronic transport chain and that its absence could lead to the incorrect use of electrons by complex II and the consequent accumulation of semiquinone. These results also suggest that the decreased succinate dehydrogenase activity associated to reduced levels of functional frataxin may not be a secondary effect but a direct effect.

Unravelling the mystery of frataxin function has been an intense and interesting quest that is still far from finished. Frataxin seems to have a wide and dynamic role on mitochondrial physiology and function and even the identification of the primary pathological consequences of its reduced expression is controversial.

2.4. References

1. Friedreich, N., *Uber degenerative Atrophie der spinalen Hinsterstrange.* Arch Pathol Anat, 1863. **26**: p. 391-419.
2. Harding, A.E., *Friedreich's ataxia: a clinical and genetic study of 90 families with an analysis of early diagnostic criteria and intrafamilial clustering of clinical features.* Brain, 1981. **104**(3): p. 589-620.
3. Geoffroy, G., et al., *Clinical description and roentgenologic evaluation of patients with Friedreich's ataxia.* Can J Neurol Sci, 1976. **3**(4): p. 279-86.
4. Campuzano, V., et al., *Friedreich's ataxia: autosomal recessive disease caused by an intronic GAA triplet repeat expansion.* Science, 1996. **271**(5254): p. 1423-7.
5. Delatycki, M.B., R. Williamson, and S.M. Forrest, *Friedreich ataxia: an overview.* J Med Genet, 2000. **37**(1): p. 1-8.
6. Juvonen, V., et al., *Dissecting the epidemiology of a trinucleotide repeat disease - example of FRDA in Finland.* Hum Genet, 2002. **110**(1): p. 36-40.
7. Labuda, M., et al., *Unique origin and specific ethnic distribution of the Friedreich ataxia GAA expansion.* Neurology, 2000. **54**(12): p. 2322-4.
8. Pandolfo, M., *Friedreich ataxia: the clinical picture.* J Neurol, 2009. **256 Suppl 1**: p. 3-8.
9. Durr, A., et al., *Clinical and genetic abnormalities in patients with Friedreich's ataxia.* N Engl J Med, 1996. **335**(16): p. 1169-75.
10. Epplen, C., et al., *Differential stability of the (GAA)n tract in the Friedreich ataxia (STM7) gene.* Hum Genet, 1997. **99**(6): p. 834-6.

11. Montermini, L., et al., *Somatic mosaicism for Friedreich's ataxia GAA triplet repeat expansions in the central nervous system.* Neurology, 1997. **49**(2): p. 606-10.
12. Tzagournissakis, M., et al., *Stability of the Huntington disease (CAG)n repeat in a late onset form occuring on the Island of Crete.* Hum Mol Genet, 1995. **4**(12): p. 2239-43.
13. Cossee, M., et al., *Friedreich's ataxia: point mutations and clinical presentation of compound heterozygotes.* Ann Neurol, 1999. **45**(2): p. 200-6.
14. Filla, A., et al., *The relationship between trinucleotide (GAA) repeat length and clinical features in Friedreich ataxia.* Am J Hum Genet, 1996. **59**(3): p. 554-60.
15. Giacchetti, M., et al., *Mitochondrial DNA haplogroups influence the Friedreich's ataxia phenotype.* J Med Genet, 2004. **41**(4): p. 293-5.
16. Montermini, L., et al., *Phenotypic variability in Friedreich ataxia: role of the associated GAA triplet repeat expansion.* Ann Neurol, 1997. **41**(5): p. 675-82.
17. Bidichandani, S.I., T. Ashizawa, and P.I. Patel, *Atypical Friedreich ataxia caused by compound heterozygosity for a novel missense mutation and the GAA triplet-repeat expansion.* Am J Hum Genet, 1997. **60**(5): p. 1251-6.
18. Ohshima, K., et al., *Inhibitory effects of expanded GAA.TTC triplet repeats from intron I of the Friedreich ataxia gene on transcription and replication in vivo.* J Biol Chem, 1998. **273**(23): p. 14588-95.
19. Sakamoto, N., et al., *Sticky DNA, a self-associated complex formed at long GAA*TTC repeats in intron 1 of the frataxin gene, inhibits transcription.* J Biol Chem, 2001. **276**(29): p. 27171-7.
20. Forrest, S.M., et al., *The correlation of clinical phenotype in Friedreich ataxia with the site of point mutations in the FRDA gene.* Neurogenetics, 1998. **1**(4): p. 253-7.
21. Beauchamp, M., et al., *Natural history of muscle weakness in Friedreich's Ataxia and its relation to loss of ambulation.* Clin Orthop Relat Res, 1995(311): p. 270-5.
22. Cavadini, P., et al., *Human frataxin maintains mitochondrial iron homeostasis in Saccharomyces cerevisiae.* Hum Mol Genet, 2000. **9**(17): p. 2523-30.
23. Bartolo, C., J.R. Mendell, and T.W. Prior, *Identification of a missense mutation in a Friedreich's ataxia patient: implications for diagnosis and carrier studies.* Am J Med Genet, 1998. **79**(5): p. 396-9.
24. Pook, M.A., et al., *Rescue of the Friedreich's ataxia knockout mouse by human YAC transgenesis.* Neurogenetics, 2001. **3**(4): p. 185-93.
25. Zuhlke, C.H., et al., *Extension of the mutation spectrum in Friedreich's ataxia: detection of an exon deletion and novel missense mutations.* Eur J Hum Genet, 2004. **12**(11): p. 979-82.
26. Gellera, C., et al., *Frataxin gene point mutations in Italian Friedreich ataxia patients.* Neurogenetics, 2007. **8**(4): p. 289-99.
27. McCormack, M.L., et al., *Frataxin point mutations in two patients with Friedreich's ataxia and unusual clinical features.* J Neurol Neurosurg Psychiatry, 2000. **68**(5): p. 661-4.
28. Pandolfo, M., *Friedreich ataxia: Detection of GAA repeat expansions and frataxin point mutations.* Methods Mol Med, 2006. **126**: p. 197-216.
29. Al-Mahdawi, S., M. Pook, and S. Chamberlain, *A novel missense mutation (L198R) in the Friedreich's ataxia gene.* Hum Mutat, 2000. **16**(1): p. 95.
30. Campuzano, V., et al., *Frataxin is reduced in Friedreich ataxia patients and is associated with mitochondrial membranes.* Hum Mol Genet, 1997. **6**(11): p. 1771-80.
31. Cossee, M., et al., *Frataxin fracas.* Nat Genet, 1997. **15**(4): p. 337-8.
32. Koutnikova, H., et al., *Studies of human, mouse and yeast homologues indicate a mitochondrial function for frataxin.* Nat Genet, 1997. **16**(4): p. 345-51.
33. Condo, I., et al., *Molecular control of the cytosolic aconitase/IRP1 switch by extramitochondrial frataxin.* Hum Mol Genet, 2010.

34. Acquaviva, F., et al., *Extra-mitochondrial localisation of frataxin and its association with IscU1 during enterocyte-like differentiation of the human colon adenocarcinoma cell line Caco-2.* J Cell Sci, 2005. **118**(Pt 17): p. 3917-24.
35. Babcock, M., et al., *Regulation of mitochondrial iron accumulation by Yfh1p, a putative homolog of frataxin.* Science, 1997. **276**(5319): p. 1709-12.
36. Wilson, R.B. and D.M. Roof, *Respiratory deficiency due to loss of mitochondrial DNA in yeast lacking the frataxin homologue.* Nat Genet, 1997. **16**(4): p. 352-7.
37. Martelli, A., et al., *Frataxin is essential for extramitochondrial Fe-S cluster proteins in mammalian tissues.* Hum Mol Genet, 2007. **16**(22): p. 2651-8.
38. Lodi, R., et al., *Deficit of in vivo mitochondrial ATP production in patients with Friedreich ataxia.* Proc Natl Acad Sci U S A, 1999. **96**(20): p. 11492-5.
39. Bradley, J.L., et al., *Clinical, biochemical and molecular genetic correlations in Friedreich's ataxia.* Hum Mol Genet, 2000. **9**(2): p. 275-82.
40. Cossee, M., et al., *Inactivation of the Friedreich ataxia mouse gene leads to early embryonic lethality without iron accumulation.* Hum Mol Genet, 2000. **9**(8): p. 1219-26.
41. Puccio, H., et al., *Mouse models for Friedreich ataxia exhibit cardiomyopathy, sensory nerve defect and Fe-S enzyme deficiency followed by intramitochondrial iron deposits.* Nat Genet, 2001. **27**(2): p. 181-6.
42. Huang, M.L., et al., *Elucidation of the mechanism of mitochondrial iron loading in Friedreich's ataxia by analysis of a mouse mutant.* Proc Natl Acad Sci U S A, 2009. **106**(38): p. 16381-6.
43. Wong, A., et al., *The Friedreich's ataxia mutation confers cellular sensitivity to oxidant stress which is rescued by chelators of iron and calcium and inhibitors of apoptosis.* Hum Mol Genet, 1999. **8**(3): p. 425-30.
44. Piemonte, F., et al., *Glutathione in blood of patients with Friedreich's ataxia.* Eur J Clin Invest, 2001. **31**(11): p. 1007-11.
45. Pianese, L., et al., *Up-regulation of c-Jun N-terminal kinase pathway in Friedreich's ataxia cells.* Hum Mol Genet, 2002. **11**(23): p. 2989-96.
46. Irazusta, V., et al., *Yeast frataxin mutants display decreased superoxide dismutase activity crucial to promote protein oxidative damage.* Free Radic Biol Med, 2009.
47. Philpott, C.C. and O. Protchenko, *Response to iron deprivation in Saccharomyces cerevisiae.* Eukaryot Cell, 2008. **7**(1): p. 20-7.
48. Irazusta, V., et al., *Manganese is the link between frataxin and iron-sulfur deficiency in the yeast model of Friedreich ataxia.* J Biol Chem, 2006. **281**(18): p. 12227-32.
49. Schulz, J.B., et al., *Diagnosis and treatment of Friedreich ataxia: a European perspective.* Nat Rev Neurol, 2009. **5**(4): p. 222-34.
50. Pandolfo, M., *Molecular basis of Friedreich ataxia.* Mov Disord, 2001. **16**(5): p. 815-21.
51. Hart, P.E., et al., *Antioxidant treatment of patients with Friedreich ataxia: four-year follow-up.* Arch Neurol, 2005. **62**(4): p. 621-6.
52. Lodi, R., et al., *Antioxidant treatment improves in vivo cardiac and skeletal muscle bioenergetics in patients with Friedreich's ataxia.* Ann Neurol, 2001. **49**(5): p. 590-6.
53. Rustin, P., et al., *Effect of idebenone on cardiomyopathy in Friedreich's ataxia: a preliminary study.* Lancet, 1999. **354**(9177): p. 477-9.
54. Hausse, A.O., et al., *Idebenone and reduced cardiac hypertrophy in Friedreich's ataxia.* Heart, 2002. **87**(4): p. 346-9.
55. Buyse, G., et al., *Idebenone treatment in Friedreich's ataxia: neurological, cardiac, and biochemical monitoring.* Neurology, 2003. **60**(10): p. 1679-81.
56. Mariotti, C., et al., *Idebenone treatment in Friedreich patients: one-year-long randomized placebo-controlled trial.* Neurology, 2003. **60**(10): p. 1676-9.

57. Ribai, P., et al., *Neurological, cardiological, and oculomotor progression in 104 patients with Friedreich ataxia during long-term follow-up.* Arch Neurol, 2007. **64**(4): p. 558-64.
58. Pineda, M., et al., *Idebenone treatment in paediatric and adult patients with Friedreich ataxia: long-term follow-up.* Eur J Paediatr Neurol, 2008. **12**(6): p. 470-5.
59. Schols, L., et al., *Idebenone in patients with Friedreich ataxia.* Neurosci Lett, 2001. **306**(3): p. 169-72.
60. Artuch, R., et al., *Monitoring of idebenone treatment in patients with Friedreich's ataxia by high-pressure liquid chromatography with electrochemical detection.* J Neurosci Methods, 2002. **115**(1): p. 63-6.
61. Di Prospero, N.A., et al., *Neurological effects of high-dose idebenone in patients with Friedreich's ataxia: a randomised, placebo-controlled trial.* Lancet Neurol, 2007. **6**(10): p. 878-86.
62. Di Prospero, N.A., et al., *Safety, tolerability, and pharmacokinetics of high-dose idebenone in patients with Friedreich ataxia.* Arch Neurol, 2007. **64**(6): p. 803-8.
63. Rustin, P., et al., *Heart hypertrophy and function are improved by idebenone in Friedreich's ataxia.* Free Radic Res, 2002. **36**(4): p. 467-9.
64. Schols, L., et al., *L-carnitine and creatine in Friedreich's ataxia. A randomized, placebo-controlled crossover trial.* J Neural Transm, 2005. **112**(6): p. 789-96.
65. Boddaert, N., et al., *Selective iron chelation in Friedreich ataxia: biologic and clinical implications.* Blood, 2007. **110**(1): p. 401-8.
66. Chiurazzi, P., et al., *In vitro reactivation of the FMR1 gene involved in fragile X syndrome.* Hum Mol Genet, 1998. **7**(1): p. 109-13.
67. Herman, D., et al., *Histone deacetylase inhibitors reverse gene silencing in Friedreich's ataxia.* Nat Chem Biol, 2006. **2**(10): p. 551-8.
68. Ghazizadeh, M., *Cisplatin may induce frataxin expression.* J Nippon Med Sch, 2003. **70**(4): p. 367-71.
69. Turano, M., et al., *3-Nitropropionic acid increases frataxin expression in human lymphoblasts and in transgenic rat PC12 cells.* Neurosci Lett, 2003. **350**(3): p. 184-6.
70. Sarsero, J.P., et al., *Upregulation of expression from the FRDA genomic locus for the therapy of Friedreich ataxia.* J Gene Med, 2003. **5**(1): p. 72-81.
71. Sturm, B., et al., *Recombinant human erythropoietin: effects on frataxin expression in vitro.* Eur J Clin Invest, 2005. **35**(11): p. 711-7.
72. Gibson, T.J., et al., *Friedreich's ataxia protein: phylogenetic evidence for mitochondrial dysfunction.* Trends Neurosci, 1996. **19**(11): p. 465-8.
73. Thompson, J.D., et al., *The CLUSTAL_X windows interface: flexible strategies for multiple sequence alignment aided by quality analysis tools.* Nucleic Acids Res, 1997. **25**(24): p. 4876-82.
74. Branda, S.S., et al., *Mitochondrial intermediate peptidase and the yeast frataxin homolog together maintain mitochondrial iron homeostasis in Saccharomyces cerevisiae.* Hum Mol Genet, 1999. **8**(6): p. 1099-110.
75. Cavadini, P., et al., *Two-step processing of human frataxin by mitochondrial processing peptidase. Precursor and intermediate forms are cleaved at different rates.* J Biol Chem, 2000. **275**(52): p. 41469-75.
76. Koutnikova, H., V. Campuzano, and M. Koenig, *Maturation of wild-type and mutated frataxin by the mitochondrial processing peptidase.* Hum Mol Genet, 1998. **7**(9): p. 1485-9.
77. Neupert, W., *Protein import into mitochondria.* Annu Rev Biochem, 1997. **66**: p. 863-917.
78. Hendrick, J.P., P.E. Hodges, and L.E. Rosenberg, *Survey of amino-terminal proteolytic cleavage sites in mitochondrial precursor proteins: leader peptides*

cleaved by two matrix proteases share a three-amino acid motif. Proc Natl Acad Sci U S A, 1989. **86**(11): p. 4056-60.
79. Branda, S.S. and G. Isaya, *Prediction and identification of new natural substrates of the yeast mitochondrial intermediate peptidase.* J Biol Chem, 1995. **270**(45): p. 27366-73.
80. Schmidt, B., et al., *Processing peptidase of Neurospora mitochondria. Two-step cleavage of imported ATPase subunit 9.* Eur J Biochem, 1984. **144**(3): p. 581-8.
81. Condo, I., et al., *In vivo maturation of human frataxin.* Hum Mol Genet, 2007. **16**(13): p. 1534-40.
82. Dutkiewicz, R., et al., *Ssq1, a mitochondrial Hsp70 involved in iron-sulfur (Fe/S) center biogenesis. Similarities to and differences from its bacterial counterpart.* J Biol Chem, 2003. **278**(32): p. 29719-27.
83. Voisine, C., et al., *Role of the mitochondrial Hsp70s, Ssc1 and Ssq1, in the maturation of Yfh1.* Mol Cell Biol, 2000. **20**(10): p. 3677-84.
84. Dhe-Paganon, S., et al., *Crystal structure of human frataxin.* J Biol Chem, 2000. **275**(40): p. 30753-6.
85. Musco, G., et al., *Assignment of the 1H, 15N, and 13C resonances of the C-terminal domain of frataxin, the protein responsible for Friedreich ataxia.* J Biomol NMR, 1999. **15**(1): p. 87-8.
86. Musco, G., et al., *Towards a structural understanding of Friedreich's ataxia: the solution structure of frataxin.* Structure, 2000. **8**(7): p. 695-707.
87. Cho, S.J., et al., *Crystal structure of Escherichia coli CyaY protein reveals a previously unidentified fold for the evolutionarily conserved frataxin family.* Proc Natl Acad Sci U S A, 2000. **97**(16): p. 8932-7.
88. Lee, M.G., et al., *Crystallization and preliminary X-ray crystallographic analysis of Escherichia coli CyaY, a structural homologue of human frataxin.* Acta Crystallogr D Biol Crystallogr, 2000. **56**(Pt 7): p. 920-1.
89. He, Y., et al., *Yeast frataxin solution structure, iron binding, and ferrochelatase interaction.* Biochemistry, 2004. **43**(51): p. 16254-62.
90. Karlberg, T., et al., *The structures of frataxin oligomers reveal the mechanism for the delivery and detoxification of iron.* Structure, 2006. **14**(10): p. 1535-46.
91. Nair, M., et al., *Solution structure of the bacterial frataxin ortholog, CyaY: mapping the iron binding sites.* Structure, 2004. **12**(11): p. 2037-48.
92. Pastore, C., et al., *Understanding the binding properties of an unusual metal-binding protein--a study of bacterial frataxin.* FEBS J, 2007. **274**(16): p. 4199-210.
93. Adinolfi, S., et al., *The factors governing the thermal stability of frataxin orthologues: how to increase a protein's stability.* Biochemistry, 2004. **43**(21): p. 6511-8.
94. Sazanov, L.A. and P. Hinchliffe, *Structure of the hydrophilic domain of respiratory complex I from Thermus thermophilus.* Science, 2006. **311**(5766): p. 1430-6.
95. Anastassopoulou, I., et al., *Solution structure of the apo and copper(I)-loaded human metallochaperone HAH1.* Biochemistry, 2004. **43**(41): p. 13046-53.
96. Arnesano, F., et al., *Solution structure of the Cu(I) and apo forms of the yeast metallochaperone, Atx1.* Biochemistry, 2001. **40**(6): p. 1528-39.
97. Banci, L., I. Bertini, and R. Del Conte, *Solution structure of apo CopZ from Bacillus subtilis: further analysis of the changes associated with the presence of copper.* Biochemistry, 2003. **42**(46): p. 13422-8.
98. Puccio, H. and M. Koenig, *Friedreich ataxia: a paradigm for mitochondrial diseases.* Curr Opin Genet Dev, 2002. **12**(3): p. 272-7.
99. Rai, M., et al., *HDAC inhibitors correct frataxin deficiency in a Friedreich ataxia mouse model.* PLoS One, 2008. **3**(4): p. e1958.
100. Vazquez-Manrique, R.P., et al., *Reduction of Caenorhabditis elegans frataxin increases sensitivity to oxidative stress, reduces lifespan, and causes lethality in a mitochondrial complex II mutant.* FASEB J, 2006. **20**(1): p. 172-4.

101. Ventura, N., et al., *Reduced expression of frataxin extends the lifespan of Caenorhabditis elegans.* Aging Cell, 2005. **4**(2): p. 109-12.
102. Zarse, K., et al., *Impaired respiration is positively correlated with decreased life span in Caenorhabditis elegans models of Friedreich Ataxia.* FASEB J, 2007. **21**(4): p. 1271-5.
103. Anderson, P.R., et al., *RNAi-mediated suppression of the mitochondrial iron chaperone, frataxin, in Drosophila.* Hum Mol Genet, 2005. **14**(22): p. 3397-405.
104. Anderson, P.R., et al., *Hydrogen peroxide scavenging rescues frataxin deficiency in a Drosophila model of Friedreich's ataxia.* Proc Natl Acad Sci U S A, 2008. **105**(2): p. 611-6.
105. Llorens, J.V., et al., *Causative role of oxidative stress in a Drosophila model of Friedreich ataxia.* FASEB J, 2007. **21**(2): p. 333-44.
106. Adamec, J., et al., *Iron-dependent self-assembly of recombinant yeast frataxin: implications for Friedreich ataxia.* Am J Hum Genet, 2000. **67**(3): p. 549-62.
107. Adinolfi, S., et al., *A structural approach to understanding the iron-binding properties of phylogenetically different frataxins.* Hum Mol Genet, 2002. **11**(16): p. 1865-77.
108. Bou-Abdallah, F., et al., *Iron binding and oxidation kinetics in frataxin CyaY of Escherichia coli.* J Mol Biol, 2004. **341**(2): p. 605-15.
109. Cavadini, P., et al., *Assembly and iron-binding properties of human frataxin, the protein deficient in Friedreich ataxia.* Hum Mol Genet, 2002. **11**(3): p. 217-27.
110. Cook, J.D., et al., *Monomeric yeast frataxin is an iron-binding protein.* Biochemistry, 2006. **45**(25): p. 7767-77.
111. Yoon, T. and J.A. Cowan, *Iron-sulfur cluster biosynthesis. Characterization of frataxin as an iron donor for assembly of [2Fe-2S] clusters in ISU-type proteins.* J Am Chem Soc, 2003. **125**(20): p. 6078-84.
112. Yoon, T. and J.A. Cowan, *Frataxin-mediated iron delivery to ferrochelatase in the final step of heme biosynthesis.* J Biol Chem, 2004. **279**(25): p. 25943-6.
113. Bencze, K.Z., et al., *Human frataxin: iron and ferrochelatase binding surface.* Chem Commun (Camb), 2007(18): p. 1798-800.
114. Huang, J., E. Dizin, and J.A. Cowan, *Mapping iron binding sites on human frataxin: implications for cluster assembly on the ISU Fe-S cluster scaffold protein.* J Biol Inorg Chem, 2008. **13**(5): p. 825-36.
115. Kondapalli, K.C., et al., *Drosophila frataxin: an iron chaperone during cellular Fe-S cluster bioassembly.* Biochemistry, 2008. **47**(26): p. 6917-27.
116. Yoon, T., E. Dizin, and J.A. Cowan, *N-terminal iron-mediated self-cleavage of human frataxin: regulation of iron binding and complex formation with target proteins.* J Biol Inorg Chem, 2007. **12**(4): p. 535-42.
117. O'Neill, H.A., O. Gakh, and G. Isaya, *Supramolecular assemblies of human frataxin are formed via subunit-subunit interactions mediated by a non-conserved amino-terminal region.* J Mol Biol, 2005. **345**(3): p. 433-9.
118. Foury, F., *Low iron concentration and aconitase deficiency in a yeast frataxin homologue deficient strain.* FEBS Lett, 1999. **456**(2): p. 281-4.
119. Foury, F. and O. Cazzalini, *Deletion of the yeast homologue of the human gene associated with Friedreich's ataxia elicits iron accumulation in mitochondria.* FEBS Lett, 1997. **411**(2-3): p. 373-7.
120. Rotig, A., et al., *Aconitase and mitochondrial iron-sulphur protein deficiency in Friedreich ataxia.* Nat Genet, 1997. **17**(2): p. 215-7.
121. Chen, O.S., et al., *Transcription of the yeast iron regulon does not respond directly to iron but rather to iron-sulfur cluster biosynthesis.* J Biol Chem, 2004. **279**(28): p. 29513-8.
122. Johnson, D.C., et al., *Structure, function, and formation of biological iron-sulfur clusters.* Annu Rev Biochem, 2005. **74**: p. 247-81.

123. Lill, R. and U. Muhlenhoff, *Iron-sulfur-protein biogenesis in eukaryotes.* Trends Biochem Sci, 2005. **30**(3): p. 133-41.
124. Kispal, G., et al., *The mitochondrial proteins Atm1p and Nfs1p are essential for biogenesis of cytosolic Fe/S proteins.* EMBO J, 1999. **18**(14): p. 3981-9.
125. Muhlenhoff, U., et al., *Components involved in assembly and dislocation of iron-sulfur clusters on the scaffold protein Isu1p.* EMBO J, 2003. **22**(18): p. 4815-25.
126. Adam, A.C., et al., *The Nfs1 interacting protein Isd11 has an essential role in Fe/S cluster biogenesis in mitochondria.* EMBO J, 2006. **25**(1): p. 174-83.
127. Wiedemann, N., et al., *Essential role of Isd11 in mitochondrial iron-sulfur cluster synthesis on Isu scaffold proteins.* EMBO J, 2006. **25**(1): p. 184-95.
128. Garland, S.A., et al., *Saccharomyces cerevisiae ISU1 and ISU2: members of a well-conserved gene family for iron-sulfur cluster assembly.* J Mol Biol, 1999. **294**(4): p. 897-907.
129. Gerber, J., U. Muhlenhoff, and R. Lill, *An interaction between frataxin and Isu1/Nfs1 that is crucial for Fe/S cluster synthesis on Isu1.* EMBO Rep, 2003. **4**(9): p. 906-11.
130. Schilke, B., et al., *Evidence for a conserved system for iron metabolism in the mitochondria of Saccharomyces cerevisiae.* Proc Natl Acad Sci U S A, 1999. **96**(18): p. 10206-11.
131. Bandyopadhyay, S., K. Chandramouli, and M.K. Johnson, *Iron-sulfur cluster biosynthesis.* Biochem Soc Trans, 2008. **36**(Pt 6): p. 1112-9.
132. Lill, R., *Function and biogenesis of iron-sulphur proteins.* Nature, 2009. **460**(7257): p. 831-8.
133. Lill, R. and U. Muhlenhoff, *Iron-sulfur protein biogenesis in eukaryotes: components and mechanisms.* Annu Rev Cell Dev Biol, 2006. **22**: p. 457-86.
134. Lill, R. and U. Muhlenhoff, *Maturation of iron-sulfur proteins in eukaryotes: mechanisms, connected processes, and diseases.* Annu Rev Biochem, 2008. **77**: p. 669-700.
135. Chen, O.S., S. Hemenway, and J. Kaplan, *Inhibition of Fe-S cluster biosynthesis decreases mitochondrial iron export: evidence that Yfh1p affects Fe-S cluster synthesis.* Proc Natl Acad Sci U S A, 2002. **99**(19): p. 12321-6.
136. Duby, G., et al., *A non-essential function for yeast frataxin in iron-sulfur cluster assembly.* Hum Mol Genet, 2002. **11**(21): p. 2635-43.
137. Muhlenhoff, U., et al., *Characterization of iron-sulfur protein assembly in isolated mitochondria. A requirement for ATP, NADH, and reduced iron.* J Biol Chem, 2002. **277**(33): p. 29810-6.
138. Muhlenhoff, U., et al., *The yeast frataxin homolog Yfh1p plays a specific role in the maturation of cellular Fe/S proteins.* Hum Mol Genet, 2002. **11**(17): p. 2025-36.
139. Zanella, I., et al., *The effects of frataxin silencing in HeLa cells are rescued by the expression of human mitochondrial ferritin.* Biochim Biophys Acta, 2008. **1782**(2): p. 90-8.
140. Bulteau, A.L., et al., *Frataxin acts as an iron chaperone protein to modulate mitochondrial aconitase activity.* Science, 2004. **305**(5681): p. 242-5.
141. Layer, G., et al., *Iron-sulfur cluster biosynthesis: characterization of Escherichia coli CYaY as an iron donor for the assembly of [2Fe-2S] clusters in the scaffold IscU.* J Biol Chem, 2006. **281**(24): p. 16256-63.
142. Adinolfi, S., et al., *Bacterial frataxin CyaY is the gatekeeper of iron-sulfur cluster formation catalyzed by IscS.* Nat Struct Mol Biol, 2009. **16**(4): p. 390-6.
143. Lesuisse, E., et al., *Iron use for haeme synthesis is under control of the yeast frataxin homologue (Yfh1).* Hum Mol Genet, 2003. **12**(8): p. 879-89.
144. Schoenfeld, R.A., et al., *Frataxin deficiency alters heme pathway transcripts and decreases mitochondrial heme metabolites in mammalian cells.* Hum Mol Genet, 2005. **14**(24): p. 3787-99.

145. Gakh, O., et al., *Physical evidence that yeast frataxin is an iron storage protein.* Biochemistry, 2002. **41**(21): p. 6798-804.
146. Levi, S. and P. Arosio, *Mitochondrial ferritin.* Int J Biochem Cell Biol, 2004. **36**(10): p. 1887-9.
147. Nichol, H., et al., *Structure of frataxin iron cores: an X-ray absorption spectroscopic study.* Biochemistry, 2003. **42**(20): p. 5971-6.
148. Park, S., et al., *Yeast frataxin sequentially chaperones and stores iron by coupling protein assembly with iron oxidation.* J Biol Chem, 2003. **278**(33): p. 31340-51.
149. Park, S., et al., *The ferroxidase activity of yeast frataxin.* J Biol Chem, 2002. **277**(41): p. 38589-95.
150. Schagerlof, U., et al., *Structural basis of the iron storage function of frataxin from single-particle reconstruction of the iron-loaded oligomer.* Biochemistry, 2008. **47**(17): p. 4948-54.
151. Aloria, K., et al., *Iron-induced oligomerization of yeast frataxin homologue Yfh1 is dispensable in vivo.* EMBO Rep, 2004. **5**(11): p. 1096-101.
152. Gakh, O., et al., *Mitochondrial iron detoxification is a primary function of frataxin that limits oxidative damage and preserves cell longevity.* Hum Mol Genet, 2006. **15**(3): p. 467-79.
153. Li, H., et al., *Oligomeric yeast frataxin drives assembly of core machinery for mitochondrial iron-sulfur cluster synthesis.* J Biol Chem, 2009. **284**(33): p. 21971-80.
154. Shan, Y., E. Napoli, and G. Cortopassi, *Mitochondrial frataxin interacts with ISD11 of the NFS1/ISCU complex and multiple mitochondrial chaperones.* Hum Mol Genet, 2007. **16**(8): p. 929-41.
155. Emond, M., et al., *Increased levels of plasma malondialdehyde in Friedreich ataxia.* Neurology, 2000. **55**(11): p. 1752-3.
156. Karthikeyan, G., et al., *Reduction in frataxin causes progressive accumulation of mitochondrial damage.* Hum Mol Genet, 2003. **12**(24): p. 3331-42.
157. Ristow, M., et al., *Frataxin deficiency in pancreatic islets causes diabetes due to loss of beta cell mass.* J Clin Invest, 2003. **112**(4): p. 527-34.
158. Schulz, J.B., et al., *Oxidative stress in patients with Friedreich ataxia.* Neurology, 2000. **55**(11): p. 1719-21.
159. Thierbach, R., et al., *Targeted disruption of hepatic frataxin expression causes impaired mitochondrial function, decreased life span and tumor growth in mice.* Hum Mol Genet, 2005. **14**(24): p. 3857-64.
160. O'Neill, H.A., et al., *Assembly of human frataxin is a mechanism for detoxifying redox-active iron.* Biochemistry, 2005. **44**(2): p. 537-45.
161. Ding, H., et al., *Distinct iron binding property of two putative iron donors for the iron-sulfur cluster assembly: IscA and the bacterial frataxin ortholog CyaY under physiological and oxidative stress conditions.* J Biol Chem, 2007. **282**(11): p. 7997-8004.
162. Runko, A.P., A.J. Griswold, and K.T. Min, *Overexpression of frataxin in the mitochondria increases resistance to oxidative stress and extends lifespan in Drosophila.* FEBS Lett, 2008. **582**(5): p. 715-9.
163. Shoichet, S.A., et al., *Frataxin promotes antioxidant defense in a thiol-dependent manner resulting in diminished malignant transformation in vitro.* Hum Mol Genet, 2002. **11**(7): p. 815-21.
164. Condo, I., et al., *A pool of extramitochondrial frataxin that promotes cell survival.* J Biol Chem, 2006. **281**(24): p. 16750-6.
165. Seguin, A., et al., *Overexpression of the yeast frataxin homolog (Yfh1): contrasting effects on iron-sulfur cluster assembly, heme synthesis and resistance to oxidative stress.* Mitochondrion, 2009. **9**(2): p. 130-8.
166. Tozzi, G., et al., *Antioxidant enzymes in blood of patients with Friedreich's ataxia.* Arch Dis Child, 2002. **86**(5): p. 376-9.

167. Auchere, F., et al., *Glutathione-dependent redox status of frataxin-deficient cells in a yeast model of Friedreich's ataxia.* Hum Mol Genet, 2008. **17**(18): p. 2790-802.
168. Ristow, M., et al., *Frataxin activates mitochondrial energy conversion and oxidative phosphorylation.* Proc Natl Acad Sci U S A, 2000. **97**(22): p. 12239-43.
169. Gonzalez-Cabo, P., et al., *Frataxin interacts functionally with mitochondrial electron transport chain proteins.* Hum Mol Genet, 2005. **14**(15): p. 2091-8.

CHAPTER 3

CONFORMATIONAL STABILITY OF HUMAN FRATAXIN AND EFFECT OF FRIEDREICH'S ATAXIA-RELATED MUTATIONS ON PROTEIN FOLDING

This Chapter was published in:

Ana R. Correia, Salvatore Adinolfi, Annalisa Pastore, Cláudio M. Gomes. "Conformational stability of human frataxin and effect of Friedreich's ataxia-related mutations on protein folding"

Biochem. J. **398**, 605-611 (2006).

3.1. Summary

To better understand the pathological mechanism associated to FRDA development in heterozygous patients, we have evaluated whether two particular FRDA mutants, FXN-I154F and FXN-W155R, retain frataxin fold. A detailed comparison of the conformational properties of the wild-type and mutant proteins combining biophysical and biochemical methodologies was undertaken. We show that FRDA mutants retain the native fold under physiological conditions but are differentially destabilised, as reflected both by their reduced thermodynamic stability and higher tendency towards proteolytic digestion. The I154F mutation has the strongest effect on the fold stability, as expected from the fact that the mutated residue contributes to the hydrophobic core formation. Functionally, the iron-binding properties of the mutant frataxins are found to be partly impaired. The apparently paradoxical situation of having clinically aggressive frataxin variants which are folded and are only slightly less stable than the wild-type form in a given adverse physiological stress condition is discussed and contextualised in terms of an hypothetical mechanism that could determine the pathology of heterozygous FRDA.

3.2. Introduction

At the present time, at least 15 missense frataxin point mutations have been described in FRDA patients [1]. Reports on these mutations indicate that they do not interfere with splicing and the fact that some compound heterozygous individuals have atypical milder phenotypic expressions of the disease is suggestive of the cellular presence of frataxin with a partly reduced function [1-2]. Although mapping these

mutations on to the available three-dimensional structures of frataxin [3-5] can provide a framework for predicting their effect on the protein structure, the exact impact of these clinically relevant missense mutations on the folding pathway of frataxin remains to be experimentally and quantitatively addressed.

In the present chapter, studies on the structural stability and folding properties of human frataxin and on two mutant variants comprising clinically relevant point mutations, I154F and W155R, are reported. These modifications involve highly conserved amino acids and previous studies have suggested that these two mutations represent two extreme possibilities, but both lead to an aggressive phenotypic development of FRDA [1]. The first one, I154F is one of the most common clinically occurring mutations and affects a residue which is part of the protein core. This mutation is therefore expected to directly affect the stability of the protein fold and should be structurally important. The second mutation involves the conserved Trp155, which is part of an invariant surface in the exposed region of the β-sheet. The aromatic ring of Trp155 is fully solvent-exposed, suggesting a role of this residue in the interaction with frataxin protein-partners. The mutation is expected to be functionally important since conservation of surface residues usually implies that they are involved directly in protein function; this putative functional role attributed to Trp155 has been recently confirmed [6]. Using the yeast homologue, Foury and co-workers have evaluated the putative contribution of 12 conserved residues in frataxin β-sheet for the interaction with Isu1. Their report shows that, in fact, frataxin (Yfh1) interaction with Isu1 is mediated by its β-sheet surface and Trp-131 (corresponding to FXN-Trp155) through its aromatic side chain is directly involved contributing to the Yfh1-Isu1 binding energy [6].

3.3. Materials and methods

Gene Expression and Protein purification

The constructs were expressed in *E. coli* (competent cells BL21 DE3 from Novagen) as fusion proteins with a His and a GST tag with cleavage site for tobacco etch virus (TEV) or PreScission protease as previously described [4-5, 7-8]. The constructs contained the gene coding for the truncated form of frataxin (91-210), hereon simply FXN. This form of frataxin has been compared with longer constructs (FXN_{61-210} and FXN_{75-210}) and the mature form (FXN_{81-210}); it has been shown that additional residues at the N-terminus are unstructured and flexible, which suggests that these residues are intrinsically unfolded and provide limited information about the protein fold [5, 9]. Both mutants were found to be stable in solution, although susceptible to precipitate upon slow freezing; however, thawed proteins that had been fast frozen retained their spectroscopic properties and melting temperatures.

Spectroscopic methods

UV/Vis Spectra were recorded at room temperature in a Shimadzu UVPC-1601 spectrometer equipped with cell stirring. Fluorescence spectroscopy was performed on a Cary Varian Eclipse instrument (λ_{ex} =280nm, λ_{em} =340nm, $slit_{ex}$: 5 nm, $slit_{em}$: 10 nm unless otherwise noted), equipped with cell stirring and peltier temperature control. Far-UV CD spectra were recorded typically at 0.2 nm resolution on a Jasco J-715 spectropolarimeter fitted with a cell holder thermostated with a Peltier.

Chemical denaturation

The chemical denaturation curves were measured using the dilutions method and two solutions with the same protein concentration were prepared: one with no denaturation agent and the other with a high concentration of denaturation agent. These were combined in different

proportions yielding different denaturant concentrations. After mixing, the solutions were equilibrated for two hours. Transitions curves were determined by plotting the average emission wavelength versus denaturant concentration, correcting for the pre- and post-transitions [10-12]. A non-linear least-square analysis was used to fit the data to a two state model [11]: the fits to the unfolding transitions were made using Origin (MicroCal).

Thermal denaturation

Thermal unfolding was followed by monitoring the intrinsic tryptophan fluorescence (λ_{exc}= 280 nm, λ_{em}=340 nm, $slit_{ex}$= 5 nm and $slit_{em}$=10 nm) and the ellipticity ($\Delta\varepsilon_{mrw}$ at 222 nm) variations. It has been previously demonstrated [13] that identical melting temperatures are obtained for frataxin by both CD and fluorescence spectroscopies, thus ruling out artefacts resulting from changes of fluorescence quantum yield with temperature. Further, DSC experiments confirmed melting temperatures (data not shown). In all experiments, a heating rate of 1ºC/min was used and the temperature was changed from 20 to 90ºC. Data was analysed according to a two-state model [11] and the fits to the unfolding transitions were made using Origin (MicroCal). For pH variations, the buffers used were 30mM acetate (pH 4.9), 40mM phosphate (pH 6.0, pH 7.9 and pH 11.6), 10mM HEPES (pH 7.0) and 40mM glycine (pH 8.9 and 9.7)**.** The reversibility of the reaction was investigated by downward temperature ramps, as well as repetition of the upward ramps after cooling down of the sample to 25°C.

Fluorescence quenching

Quenching experiments were performed using a neutral quencher – acrylamide (Bio-Rad) and an ionic quencher KI (Fluka). The samples were excited at 295nm in order to ensure that the light was absorbed almost entirely by tryptophanyl groups and the fluorescence intensity

decrease at 340nm was followed. Results were analysed according to the Stern-Volmer equation [14].

Trypsin limited proteolysis

Frataxins were incubated with trypsin (bovine pancreas trypsin, sequencing grade, Sigma) at 37°C in 0.1 M Tris-HCl pH 8.5, in a 100 fold excess over the protease. Aliquots (~0.5 nmol protein) were sampled at different incubation periods and the reaction stopped by the addition of 0.2% (v/v) of trifluoroacetic acid (TFA). The products of the proteolysis reaction were analysed by reverse-phase HPLC (Waters Alliance System 2695) using a C18 Column 150 x 3.9 mm (DeltaPak, Waters) run at a 0.5 $ml.min^{-1}$ flow rate, monitoring the absorbance at 214nm. The peptidic profiles were obtained running a three-step gradient from (A) 0.1% (v/v) TFA to (B) 80% (v/v) Acetonitrile + 0.1% (v/v) TFA: 0-37% (in 65 min), 37-75% (in 30 min) and 75-100% (in 20 min). The column was regenerated with 0.1% (v/v) TFA.

3.4. Results

3.4.1. Frataxin Chemical and Thermal Unfolding

To evaluate the effect of the introduced clinical mutations on the human frataxin fold, the chemical and thermal unfolding reactions of human frataxin were investigated in detail. Frataxin unfolding can be monitored either by fluorescence or by far-UVCD spectroscopy; in the present study, intrinsic tryptophan fluorescence changes were routinely used to monitor unfolding transitions (see Experimental section). Under most denaturation conditions tested, frataxin unfolding was found to be highly reversible. FXN exhibits considerable stability over the

physiological pH range: its thermal unfolding transition is reversible and essentially invariant between pH 6.0 and 9.0 (**Table 3.1**).

Table 3.1 – Parameters for FXN thermal denaturation as a function of pH**.**

pH	T_m (ºC)	ΔH_m (kcal.mol^{-1})	ΔT_m (ºC)	Refolding (%)
4.9	59.0 ± 0.1	65.7 ± 0.4	-7.3 ± 0.1	20
6.0	65.4 ± 0.2	88.8 ± 0.5	-0.9 ± 0.3	80
7.0	62.5 ± 0.2	59.8 ± 0.3	-3.8 ± 0.3	95
7.9	66.3 ± 0.1	89.2 ± 0.4	-	100
8.9	62.1 ± 0.2	86.5 ± 0.8	-4.2 ± 0.3	100
9.7	59.0 ± 0.1	67.4 ± 0.3	-7.3 ± 0.1	20

However, below pH 5.0, which is the isoelectric point of FXN as well as at higher pH values, an increasing extent of irreversibility was observed as a result of protein aggregation. At lower pH values, this is expected, considering the decreased solubility of the unfolded form of a protein near its isoelectric point [11, 15]. Chemical denaturation experiments were performed at pH 7.9 using urea, GdmCl and GuSCN as denaturants. The obtained curves were analysed assuming a two-state mechanism, and the unfolded fraction was plotted as a function of denaturant concentration; from the data in the transition region, and using the linear extrapolation model, the thermodynamic parameters ΔG_{H2O} and *m* were determined (**Fig. 3.1 and Table 3.2**). Frataxin conformational stability ranges from 5.7–8.5 kcal · mol^{-1}.

Table 3.2 - Parameters for the chemical denaturation of wild type FXN, pH 7.9

Denaturant	$[D]_{1/2}$ (M)	*m* (cal.mol^{-1}.M.$^{-1}$)	ΔG_{H2O} (cal.mol^{-1})
GuSCN	1.1	5354 ± 327	5675 ± 407
GdmCl	2.1	4009 ± 235	8539 ± 541
Urea	4.3	1353 ± 63	5833 ± 299

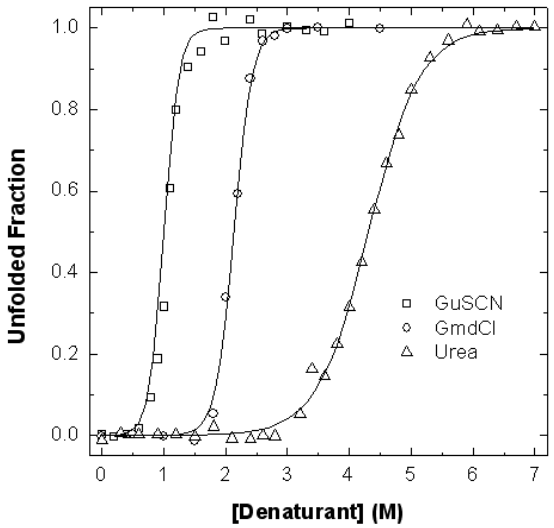

Figure 3.1: Chemical denaturation curve for FXN at pH 7.9. Fxn typical denaturation curves with (○) GdmCl, (□) GuSCN, (Δ) urea.

3.4.2. Conformational Dynamics

The impact of the clinical mutations on the frataxin fold and dynamics was evaluated from fluorescence quenching studies. Fluorescence quenching experiments were performed at 25ºC using acrylamide and iodide (**Fig. 3.2 and Table 3.3**). Acrylamide is a neutral quencher molecule, therefore it accesses the protein interior more easily and it quenches buried residues, whereas iodide is negatively charged and interacts with the protein's surface. The Stern–Volmer constant for the FXN-I154F mutant is comparable with that of the wild-type for both quenchers, which suggests that this structural core mutation does not result in protein misfolding.

With respect to the FXN-W155R variant, a lower Stern–Volmer constant was determined, which is in agreement with the fact that the two remaining tryptophan residues are not exposed, and the protein

matrix will strongly slow down the penetration of the quencher molecules.

For all frataxins studied, the accessibility of the tryptophan residues is increased in the presence of GmdCl, corresponding to a disrupted tertiary structure. Thus, quenching experiments show that, under physiological conditions, the mutant frataxins have a globally stable wild-type-like fold and breathing dynamics.

Table 3.3 – Effect of FRDA mutations on quencher accessibility, Stern-Volmer constants using different quenchers.

Protein	K_{sv} (M^{-1})	
	Acrylamide (close symbols)	**KI (open symbols)**
Wild Type	11.2 ± 0.2	5.0 ± 0.2
W155R	4.5 ± 0.1	3.2 ± 0.1
I154F	10.5 ± 0.2	5.9 ± 0.2

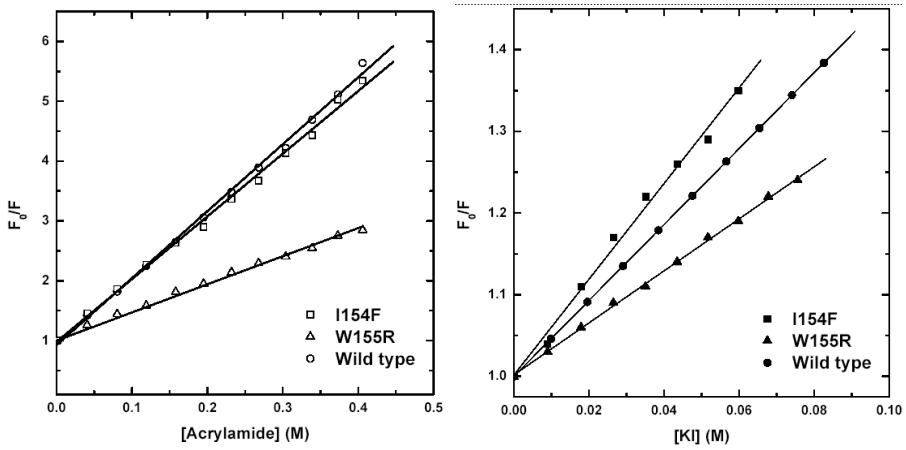

Figure 3.2: Stern–Volmer plots of acrylamide and iodide quenching of frataxin tryptophan fluorescence. Plots of F 0/F against concentration of acrylamide (A) and iodide (B) for the native wild type Fxn (○), FXN-W155R (Δ) and FXN-I154F (□). See **Table 3.3** for parameters.

3.4.3. Limited Proteolysis Experiments

The conformational differences between wild-type and the mutant frataxin forms were accessed by monitoring the progression of trypsin-mediated proteolysis. Trypsin was selected for this comparative mapping as it cleaves with high specificity at the C-terminal side of lysine and arginine, unless the following position is occupied by a proline residue [16]. Inspection of the protein sequence identifies 11 possible digestion sites for the wild-type and I154F proteins and an additional one for the W155R mutant, as a result of the inserted arginine residue. A comparison of these limited proteolysis experiments allows for the evaluation of the degree of destabilisation of the mutant forms with respect to the native protein. A destabilised fold will have more accessible cleavage sites due to increased flexibility and therefore undergo faster proteolysis. The obtained peptide maps show clearly that both mutant frataxins are destabilised with respect to the wild-type protein, as evidenced by the appearance of a substantially higher number of peptides during the same incubation period (**Fig. 3.3**). This observation indicates that the clinical mutant frataxins under study contain partly destabilised regions which make them more prone to degradation.

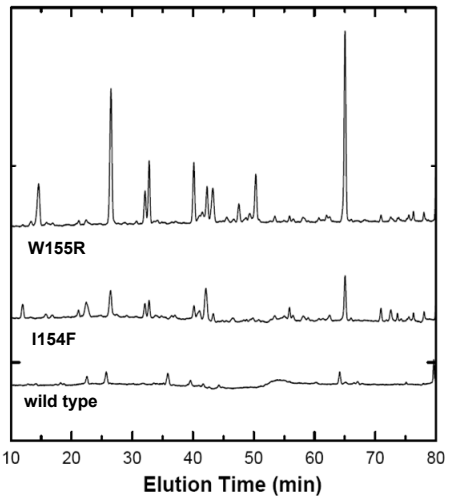

Figure 3.3: Peptide maps resulting from partial tryptic digestions. Wild-type and mutant variants (FXN-I154F and FXN-W155R) after being incubated with trypsin for 100 min at 37◦C.

3.4.4. Iron-Binding is Impaired by Protein Destabilisation

Iron binding was also investigated, as this may provide useful insights into the biological impact of the clinical variants. Frataxin is known to be able to bind six to seven irons per monomer, albeit with low affinity [17-18]. The FRDA-associated mutant frataxins were investigated with respect to their ability to bind iron, as well as the wild-type protein, which was used as a positive control. Iron binding monitored by fluorescence spectroscopy showed that progressive iron binding destabilises the mutants, resulting in protein precipitation. Although this occurs both with Fe(II) and Fe(III) and under pH-controlled conditions, the ferric ion seems to have a more destabilising effect and precipitation is observed above an iron/frataxin ratio of 2:1. Concerning ferrous ion binding, precipitation was only observed at iron/frataxin ratios ranging from 5:1 to 7:1. Thus, although none of these FRDA-associated mutations is directly involved in the proposed iron binding region [17, 19], its binding may have a negative functional impact as it probably induces structural modifications which destabilise the frataxin fold, leading to the formation of iron induces precipitates. In any case, iron-mediated colloidal precipitation of the mutant frataxins cannot be ruled out at this stage.

3.4.5. Frataxin Mutants Thermodynamic Stability

The conformational properties of the two FXN mutants were investigated spectroscopically using fluorescence and far-UV CD. The differences in conformational stability between the wild-type FXN and the two mutants were determined from the analysis of their chemical and thermal denaturation transitions, at pH 7.0 (**Table 3.4**).

For both mutants, cooperative unfolding transitions were observed and, under the experimental conditions used, the unfolding reactions

Table 3.4 - Parameters for urea denaturation of wild type and mutant forms (FXN-I154F and FXN-W155R). Comparing the differences in stability.

Protein	ΔG_{H2O} (kcal.mol^{-1})	*m* (kcal.mol^{-1}.M^{-1})	$[Urea]_{1/2}$ (M)	$\Delta[Urea]^{a}_{1/2}$	T_m (ºC)	ΔT_m (ºC)
Wild type	5.8 ± 0.3	1353 ± 63	4.3			66.3 ± 0.1
W155R	5.1 ± 0.2	1483 ± 78	3.4	-0.9	-1713	61.4 ± 0.4
I154F	5.9 ± 0.2	1836 ± 67	3.2	-1.1	-1401	50.7 ± 0.1

[a] difference between the $[urea]_{1/2}$ for the wild-type and the mutant forms.

were found to be reversible. Concerning chemical unfolding, the order of the midpoint unfolding urea concentrations was determined to be FXN wild-type>W155R>I154F (**Table 3.4**). The slightly higher *m* values determined for the two mutants also show that a larger fraction of buried residues is exposed upon unfolding. The midpoint denaturation concentrations determined for the mutants were about one unit below that observed for the wild-type and this corresponded to a destabilisation of 1.4–1.7 kcal as a result of the mutations. Thermal unfolding experiments also revealed that the mutant FXN-I154F is more destabilised than the FXN-W155R having a T_m approx. 16ºC lower than the wild-type protein, whereas the mutant W155R shows a decrease of only approx. 5ºC. Taken together, these data reveal that both mutations under study reduce the thermodynamic stability of frataxin and that the mutation FXN-I154F is more destabilising.

3.5. Discussion

Under chemically or thermally destabilising conditions, the two mutants, FXN-I154F and FXN-W155R, show distinct behaviours, but they are both folded at physiological temperature and pH. Mutant FXN-W155R, which from frataxin structure and sequence conservation analysis was suggested to have its functional properties impaired, shows

only some destabilisation when compared to the wild type protein. Inversely, a significant perturbation was detected for the FXN-I154F mutant whose fold is substantially destabilised. While this is reasonable since the mutation affects a buried residue which takes part of the hydrophobic core [5], the destabilisation effect only becomes evident under stressing conditions. Accordingly, I154F partly retains its iron-binding capability, as does W155R, which nevertheless depends strongly on the specific three-dimensional scaffold. These are curious observations since the severe effects of both mutations in FRDA patients were initially thought to exert a much stronger effect on the frataxin fold.

3.6. Acknowledgements

Stephen Martin (National Institute for Medical Research) is thanked for valuable assistance and comments during CD measurements.

Paula Chicau (Amino Acid Analysis Service, Instituto Tecnologia Química e Biológica) is gratefully acknowledged for skilled technical assistance on the HPLC separations of the limited proteolysis experiments.

3.7. References

1. Cossee, M., et al., *Friedreich's ataxia: point mutations and clinical presentation of compound heterozygotes.* Ann Neurol, 1999. **45**(2): p. 200-6.
2. Campuzano, V., et al., *Friedreich's ataxia: autosomal recessive disease caused by an intronic GAA triplet repeat expansion.* Science, 1996. **271**(5254): p. 1423-7.
3. Adinolfi, S., et al., *A structural approach to understanding the iron-binding properties of phylogenetically different frataxins.* Hum Mol Genet, 2002. **11**(16): p. 1865-77.
4. Dhe-Paganon, S., et al., *Crystal structure of human frataxin.* J Biol Chem, 2000. **275**(40): p. 30753-6.
5. Musco, G., et al., *Towards a structural understanding of Friedreich's ataxia: the solution structure of frataxin.* Structure, 2000. **8**(7): p. 695-707.
6. Leidgens, S., S. De Smet, and F. Foury, *Frataxin interacts with Isu1 through a conserved tryptophan in its {beta}-sheet.* Hum Mol Genet, 2009.

7. Adinolfi, S., et al., *The factors governing the thermal stability of frataxin orthologues: how to increase a protein's stability.* Biochemistry, 2004. **43**(21): p. 6511-8.
8. Musco, G., et al., *Assignment of the 1H, 15N, and 13C resonances of the C-terminal domain of frataxin, the protein responsible for Friedreich ataxia.* J Biomol NMR, 1999. **15**(1): p. 87-8.
9. Prischi, F., et al., *The N-terminus of mature human frataxin is intrinsically unfolded.* FEBS J, 2009.
10. Pace, C.N., Shirley, B. A. and Thomson, J., *Protein Structure: a Pratical Approach*. Measuring the conformational stability of proteins. , ed. T.E. Creighton. 1990, Oxford: IRL Press.
11. Pace, C.N., et al., *Conformational stability and thermodynamics of folding of ribonucleases Sa, Sa2 and Sa3.* J Mol Biol, 1998. **279**(1): p. 271-86.
12. Shirley, B.A., *Urea and guanidine hydrochloride denaturation curves.* Methods Mol Biol, 1995. **40**: p. 177-90.
13. Bolis, D., et al., *Protein stability in nanocages: a novel approach for influencing protein stability by molecular confinement.* J Mol Biol, 2004. **336**(1): p. 203-12.
14. Eftink, M.R. and C.A. Ghiron, *Fluorescence quenching studies with proteins.* Anal Biochem, 1981. **114**(2): p. 199-227.
15. Creighton, T.E., *Proteins: structure and molecular properties*. Proteins in solution and in membranes: aqueous solubility. 1996, New York: W. H. Freeman and Company.
16. Fontana, A., et al., *Probing protein structure by limited proteolysis.* Acta Biochim Pol, 2004. **51**(2): p. 299-321.
17. Nair, M., et al., *Solution structure of the bacterial frataxin ortholog, CyaY: mapping the iron binding sites.* Structure, 2004. **12**(11): p. 2037-48.
18. Yoon, T. and J.A. Cowan, *Iron-sulfur cluster biosynthesis. Characterization of frataxin as an iron donor for assembly of [2Fe-2S] clusters in ISU-type proteins.* J Am Chem Soc, 2003. **125**(20): p. 6078-84.
19. He, Y., et al., *Yeast frataxin solution structure, iron binding, and ferrochelatase interaction.* Biochemistry, 2004. **43**(51): p. 16254-62.

CHAPTER

4 DYNAMICS, STABILITY AND IRON BINDING ACTIVITY OF FRATAXIN CLINICAL MUTANTS

This Chapter was published in:

Ana R. Correia‡, Chiara Pastore‡, Salvatore Adinolfi, Annalisa Pastore, Cláudio M. Gomes. "Dynamics, stability and iron-binding activity of frataxin clinical mutants"

FEBS J. **275**, 3680-3690 (2008).

‡ These authors contributed equally to this work.

The NMR experiments here reported were carried at the National Institute for Medical Research (N.I.M.R.), Mill Hill-London, UK by Chiara Pastore.

4.1. Summary

In the present study, we analysed, *in vitro*, the consequences of disease-related mutations on the stability and dynamics of human frataxin. In addition to the FXN-I154F and FXN-W155R mutant variants, two other, FXN-G130V and FXN-D122Y, were investigated for the first time. CD spectroscopy analysis has demonstrated a substantial decrease in the thermodynamic stability of the variants during chemical and thermal unfolding (wild-type > W155R > I154F > D122Y > G130V), which was reversible in all cases. NMR showed that the clinical mutants retained a compact and relatively rigid globular core despite their decreased stabilities. Protein dynamics was studied in detail, revealing that the mutants have distinct propensities towards aggregation. Limited proteolysis assays coupled with LC-MS allowed the identification of particularly flexible regions in the mutants; interestingly, these regions included those involved in iron-binding. In agreement, the iron metallochaperone activity of the Friedreich's ataxia mutants was affected: some mutants precipitate upon iron binding (I154F and W155R) and others have a lower binding stoichiometry (G130V and D122Y). Our results suggest that, in heterozygous patients, the development of Friedreich's ataxia may result from a combination of reduced efficiency of protein folding and accelerated degradation *in vivo*, leading to lower than normal concentrations of frataxin.

4.2. Introduction

In preliminary studies, we addressed the question of whether prevalent mutations that result in classical FRDA phenotypes were correlated with complete impairment of the frataxin fold [9]. We showed that, although destabilised, the two tested mutations (W155R and I154F)

result in proteins that should be folded under physiological conditions. What physical property contributed to the pathogenic mechanism? Two possible working hypotheses are that, in the mutants, the efficiency of folding is reduced compared to that of the wild-type protein and that the mutants have an enhanced susceptibility towards degradation. Either scenario, or a combination of both, is likely to lead to frataxin concentrations lower than normal. To address this important question, which bears direct relevance for our understanding of FRDA, we performed a comparative study of the protein dynamics of frataxin variants carrying mutations of clinical interest. We focused on how the frataxin mutations I154F, W155R, D122Y and G130V encompass structural perturbations that may compromise protein‑protein interactions [1-3], impair functional activity (in terms of iron binding and metallochaperone activity) [4] and increase post-translational proteolytic susceptibility. We also addressed in detail how mutations affect the protein dynamics. This study is expected to contribute to a better molecular and structural understanding of the disease mechanism, especially when taken in combination with recent data obtained *in vivo* in human cells for some of these mutations [3].

4.3. Materials and Methods

Protein purification

All constructs were expressed in *Escherichia coli* competent cells (BL21 (DE3)) and the protein was purified as previously described [5-7]. As in previous studies, the protein used corresponded to the conserved C-terminal domain (amino acids 91–210). The mutants were stable in solution, although susceptible to precipitate upon slow freezing. Nevertheless, thawed proteins that had been fast frozen retained their spectroscopic properties and melting temperatures.

SDS/PAGE

After cell harvesting, 100 mg of cells from each bacterial growth were resuspended in 1.5 mL of lysis buffer (20 mM Tris–HCl, pH 8, 150 mM NaCl, 40 mm Imidazole, 1 mm phenylmethanesulfonyl fluoride, DNaseI and lysozyme) and lysed on the French press. After lyses, the samples were centrifuged at 168000 g for 45 min. The pellet fraction was resuspended in 1.5 mL of 6M GuHCl. The protein concentration of both the pellet and the soluble fraction was determine using Bradford reagent in order to prepare aliquots with the same protein concentration ($0.2 mg \cdot ml^{-1}$) to further apply on the gel. A 15% SDS/PAGE was performed at 200 V and 25 mA. Proteins were visualised by Coomassie blue staining.

Western blotting

Proteins separated using SDS/PAGE were transferred from the gel onto poly (vinylidene difluoride) membrane for 1 h at 45 mA using a ECL semi-dry blotter (GE Healthcare, Piscataway, NJ, USA). Immunochemical detection of the His-tagged GST frataxin fusion protein was achieved by incubation with anti-GST produced in rabbit (Sigma, St Louis, MO, USA). The antibody was diluted (1:1000) in NaCl/Pi-Tween containing nonfat milk. After washing with NaCl/Pi-Tween, the membrane was incubated with secondary anti-rabbit sera, conjugated with horseradish peroxidase (Sigma) and developed with ECL (GE Healthcare).

Spectroscopic methods

UV/visible spectra were recorded at room temperature in a Shimadzu UVPC-1601 spectrometer (Shimadzu, Kyoto, Japan) equipped with cell stirring. Fluorescence spectroscopy was performed on a Cary Varian Eclipse instrument (Varian NMR, Inc, Palo Alto, CA, USA) (λ_{ex} = 280 nm, λ_{em} = 340 nm, $slit_{ex}$: 5 nm, $slit_{em}$: 10 nm, unless otherwise noted)

equipped with cell stirring and Peltier temperature control (MJ Research, Watertown, MA, USA). Far-UV CD spectra were recorded typically at 0.2 nm resolution on a Jasco J-715 spectropolarimeter (Jasco Inc., Tokyo, Japan) fitted with a cell holder thermostated equipped with a Peltier.

Trypsin limited proteolysis and LC-MS analysis

Frataxins variants were incubated with trypsin (bovine pancreas trypsin, sequencing grade; Sigma) at 37 ºC in 0.1M Tris-HCl (pH 8.5), in a 100-fold excess over the protease. Aliquots (approximately 0.5 nmol of protein) were sampled at different incubation periods and the reaction stopped by the addition of 0.2% (v/v) of trifluoroacetic acid. The products of the proteolysis reaction were analysed by reverse-phase HPLC [6]. The column was regenerated with 0.1% (v/v) trifluoroacetic acid. MS analysis was carried out at the ITQB Mass Spectrometry Service Laboratory (Oeiras, Lisbon, Portugal).

Iron-binding assays

Iron binding stoichiometry was quantitated by iron dependent fluorescence measurements, essentially as described previously [6]. Briefly, tryptophan fluorescence was measured in 1 mL quartz cuvettes with continuous stirring. The excitation and monitoring wavelengths were 290 and 340 nm, respectively. The binding stoichiometry for ferrous and ferric ion are identical (six or seven irons per frataxin, [4]) and therefore binding of ferric iron was routinely monitored. For the measurements, a 10 μM solution of apo frataxin was titrated with ferric ion from a stock solution of $FeCl_3$, over the concentration range 0-120 μM. The quenching of tryptophan fluorescence induced by the binding of ferric ions was used to calculate the fraction of binding sites occupied. The stoichiometry, p, and apparent dissociation constant, K_d, were then obtained as previously described by Winzor and Sawyer [8]

NMR spectroscopic methods

^{15}N T_1, T_2 and NOE NMR relaxation measurements were performed at 600 MHz and 25 ºC on approximately 0.4 mm samples. Both T_1 data and T_2 data were acquired with ten relaxation delays (10, 100, 200, 300, 400, 500, 600, 700, 800, 100ms and 10, 20, 35, 50, 65, 80, 100, 125, 150, 250ms, respectively). Experimental steady-state NOE values were determined from the peak intensity ratios of amide signals obtained by recording interleaved 2D Watergate ^{1}H-^{15}N HSQC spectra with and without a proton saturation delay of 4 s and a repetition delay of 4.2 s. T_1 and T_2 relaxation times were obtained by fitting the data with atwo-parameter single exponential decay function. The T_1 and T_2 values of residues 115, 116, 127, 130, 171, 176, 177, 200, 207, 209 and 210 differ by more than one standard deviation from the mean value and therefore were not considered in the correlation time calculations.

The errors on the T_1 and T_2 measurements were estimated to have an average value of 3%, whereas the error on the NOE measurements is approximately 5%. The ^{15}N heteronuclear relaxation rates were interpreted using the program TENSOR2 [9]. The internuclear distance r_{NH} was assumed to be 1.02 Å. The dipolar and chemical shift anisotropy interactions were assumed to be collinear.

Frataxin degradation assay

Cells were transformed with vectors enabling the over expression of FXN (wild type or mutants) and a protease system. Double transformed cells were grown in LB medium at 37ºC to OD_{600}=0.6 and then plasmid-derived protein expression was induced by addition of IPTG (0.5mM). Following a 45min induction, general protein synthesis was inhibited by the addition of rifampicin (300μg/ml) and chloramphenicol (100μg/ml) at t=0 [10-11]. Samples were withdrawn at the mentioned intervals. Cells

were lysed and applied on a 15% SDS/PAGE; further, the intensity of the bands corresponding to frataxin were quantitated.

4.4. Results

4.4.1. Mapping Frataxin Mutations on the Structure

The four mutations D122Y, G130V, I154F and W155R were mapped onto the human frataxin structure (**Fig. 4.1**). Three of them are replacements of exposed residues. The mutation D122Y is located at the very beginning of the β1 strand and is an integral part of the turn connecting α1 to β1. The side chain of D122 could potentially form an H-bond with the amide group of the spatially contiguous G138. Being in a turn, the exact nature of this residue could influence the folding process. Furthermore, a stabilising surface ionic interaction of D122 with the nearby K135 residue is disrupted upon mutation. Similarly, G130 is in the tight turn formed by G128, S129 and G130 between strands β1 and β2 and both ϕ and ψ are positive. Its mutation into a valine must disturb the turn conformation, resulting in severe local strain. I154 is a buried residue that directly sits into the hydrophobic core; its replacement by another, albeit bulkier, but still hydrophobic residue does not disrupt the fold completely [6]. Finally, W155 is an exposed and extremely conserved residue that has been suggested to be relevant for protein-protein interactions. However, because W155 packs against a nearby arginine (R165), its mutation to an arginine results in a repulsive interaction arising from two spatially contiguous positively charged residues.

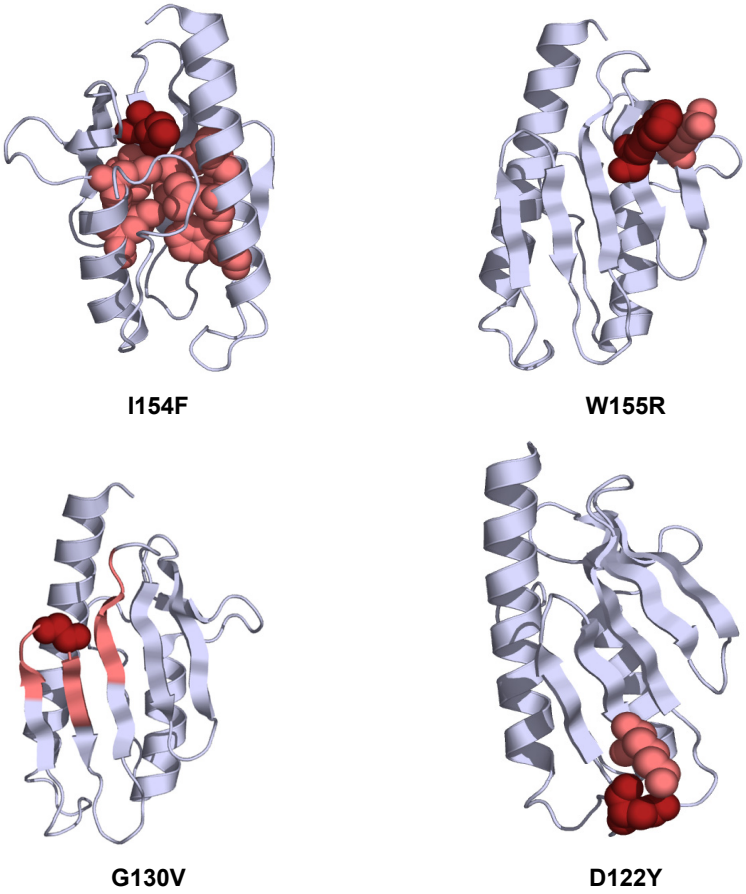

Figure 4.1: Mapping of frataxin clinical mutations onto the protein structure. The figures were drawn using the protein databank file 1EKG.

4.4.2. Protein Dynamics of Wild-type Human Frataxin

The dynamical properties of wild-type human frataxin were established by NMR ^{15}N relaxation experiments, looking specifically at regions around the mutated positions (**Fig. 4.2A**). This technique has proven to be very successful in providing information about molecular internal motions.

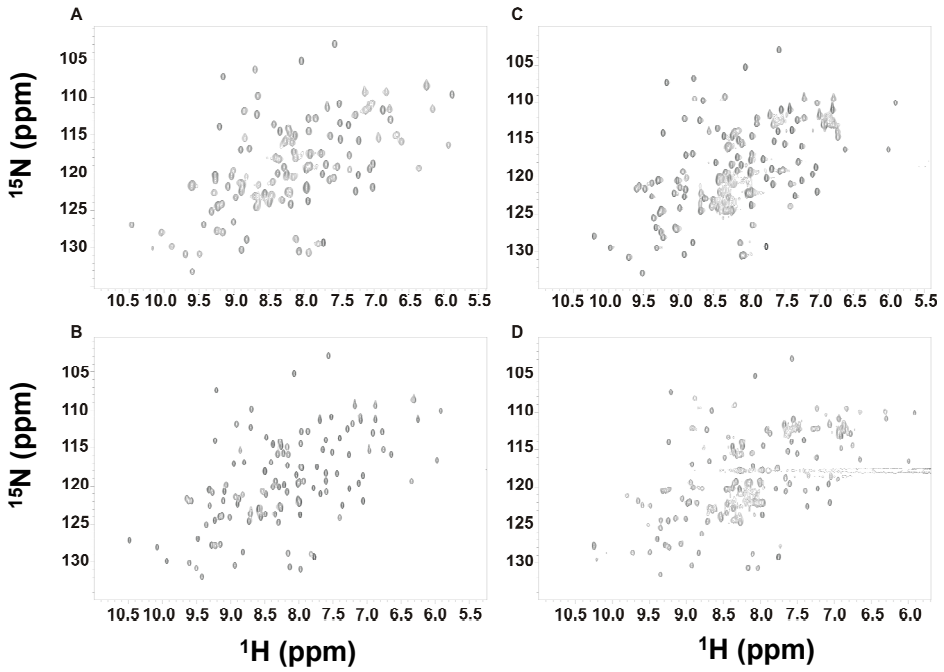

Figure 4.2: Comparison of the HSQC spectra for the four frataxin mutants. (A)D122Y; (B) G130V; (C) W155R; and (D) I154F. The spectra were recorded at 600 MHz and 25 ºC.

Overall, longitudinal (T_1) and transverse (T_2) relaxation rates and NOE values are rather uniform along the protein sequence, in agreement with what is expected for a compactly folded globular protein. Such a flat behaviour is consistent with the presence of only short and rather stiff turns between secondary structure elements. The Lipari-Szabo model-free formalism was used to analyse the data [12]. Smaller than average T_1/T_2 and small or negative NOE values, which suggest the presence of internal motions on the nano- and picosecond timescale, were observed at both termini and especially at the C-terminus. This suggests a higher mobility of these regions compared to the rest of the molecule, in agreement with the larger rmsd of the solution bundle in these regions [13]. Residues in the loop between strands β4 and β5 (Thr149, Asn151

and Lys152), and at the end of strand β6 (Val174), have larger than average T_1/T_2 ratios and shorter T_2. These features may indicate the presence of low-frequency motions, often associated with conformational exchange. The correlation time of the wild type at room temperature, as estimated from the T_1/T_2 ratio, is 7.9 ns. This value is in good agreement with the value expected for a monomeric globular domain of equivalent size [13].

4.4.3. Conformational Dynamics of Frataxin Mutants

The NMR spectra for the four frataxin mutants are all compatible with folded species, having appreciable peak dispersion (approximately 4 p.p.m. and 30 p.p.m. dispersion in the ^{1}H and ^{15}N dimensions, respectively) (**Fig. 4.2B-D**). This is confirmed by far-UV CD because the spectrum of the mutants is overall identical to that of the wild-type frataxin (not shown). The NMR spectra obtained for FXN-W155R and FXN-G130V are very similar to that of the wild-type [14] and the spectrum for FXN-D122Y shows some local rearrangement of several resonances. The spectrum for FXN-I154F is of lower quality, suggesting the presence of a small but appreciable population of either degraded or unfolded protein.

Table 4.1: Relaxation rate constants, NOE and correlation time. T_1 and T_2 as well, as steady-state ^{1}H-^{15}N NOE and τ_c, were measured or frataxin variants.

Protein	T_1 (ms)	T_2 (ms)	NOE	τc (ns)
WT	544.3	106.9	0.76	7.9
D122Y	578.2	115.5	0.76	7.7
G130V	634.5	98.4	0.77	7.5
I154F	712.1	97.7	0.75	8.5
W155R	746.6	90.6	0.71	9.2

Accordingly, it was relatively easy to assign the spectra for the FXN-W155R, G130V and D122Y mutants from that of the wild-type, whereas the spectrum for FXN-I154F could only be tentatively assigned. T_1 and T_2 as well as steady-state ^{1}H-^{15}N NOE and correlation times (τ_c) were determined and analysed for the wild-type and the mutant frataxins (**Table 4.1** and **Fig. 4.4**).

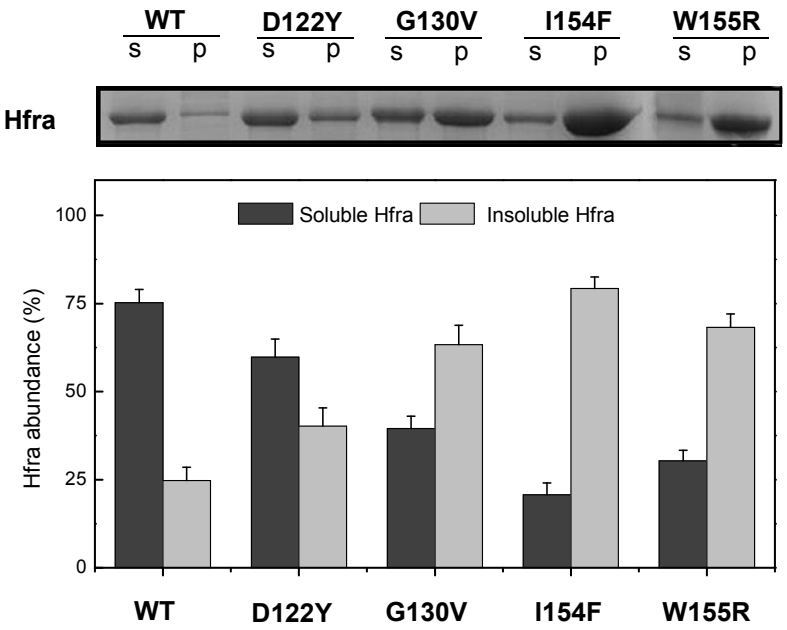

Figure 4.3: Effect of frataxin clinical mutations on the protein aggregation propensity. **Top:** SDS/PAGE gels obtained from *E. coli* lysates expressing GST-frataxin fusion proteins (Mr = 39.2 kDa). Frataxin identity was confirmed by Western blot analysis (not shown). For each protein variant, the electrophoretic separations of total protein in both the soluble (s) and insoluble (p) fractions are shown. **Bottom:** Semi-quantitive analysis of the relative proportion of frataxin present in the soluble and insoluble fractions, obtained from densitometric analysis of gel bands (n = 3).

Apart from I154, whose resonance is not observable because of overlap, the other mutation sites have average T_1 / T_2 and NOE values. We observed a progressive increase of the average T_1 values, with a concomitant decrease of the average T_2, which follows the order wild-type < D122Y < G130V < I154F < W155R. In agreement, the correlation times extend from 7.5 to 9.2 ns for FXN-W155R (**Table 4.1** and **Fig. 4.4**). This strongly suggests that the mutants have a different tendency towards aggregation. Such behaviour is fully consistent with what had been noticed at the protein purification level because expression of frataxin mutants always results in formation of aggregates and inclusion bodies.

This was further investigated by carrying out a semi-quantitative analysis of frataxin expression in cell extracts by SDS/PAGE (**Fig. 4.3**) and Western blot analysis (not shown). Expression systems have been used as a tool to study the foldability and conformational destabilisation of human proteins [15], including other mitochondrial proteins [10, 16]. The data obtained for the different frataxin variants showed that these have different tendencies to aggregate (**Fig. 4.3**). Although wild-type frataxin remains, to a considerable extent, mostly soluble after expression, the same is not observed for the mutant variants. For those, the percentage of frataxin that remains soluble after expression is considerably lower, and the FXN-I154F and FXN-W155R mutants are mostly expressed in an insoluble form (79% and 68%, respectively; **Fig. 4.3**). This analysis shows that, although all the variants are also found in the soluble fraction, their tendency to misfold in the confined cellular environment could result in an appreciable quantity of aggregated and/or destabilised protein. On the other hand, the average NOE values remain comparable among variants, indicating that the internal flexibility of the protein is essentially invariant.

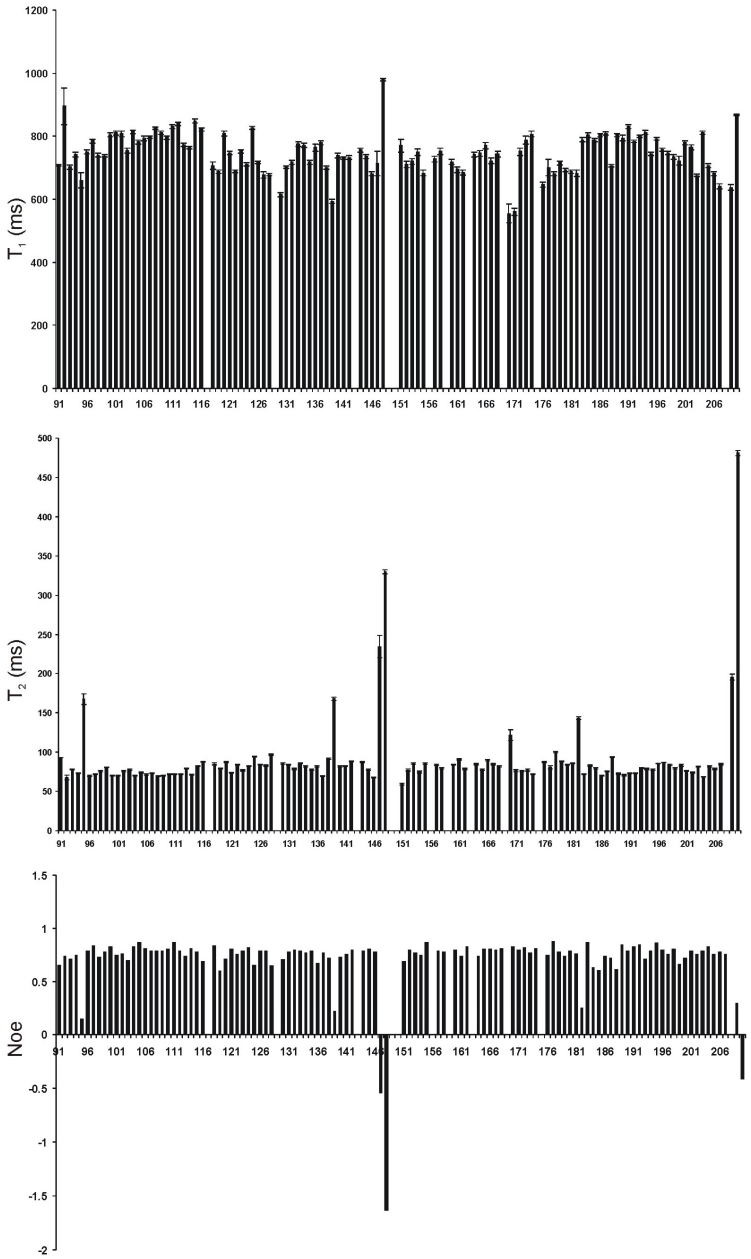

Figure 4.4: Representative relaxation parameters measured for the FXN-W155R mutant. The data were collected at 600 MHz and 25 ºC.

4.4.4. Structural Flexibility

Limited proteolysis experiments were used to further identify and characterise the sites of enhanced flexibility or of local unfolding in the frataxin mutants. The rationale for this approach is that chain flexibility is determinant in the proteolytic reaction because digestion of rigid secondary structure elements is extremely disadvantageous thermodynamically [17]. Frataxin nicking reactions were carried out at physiological temperature (37ºC), the reaction products were separated by reverse phase HPLC and the resulting peptides identified by MS. A comparison of the obtained tryptic maps clearly shows that mutant frataxins are destabilised relatively to the native protein (**Fig. 4.5**).

All frataxin mutants exhibit an increased proteolytic susceptibility compared to the wild-type, as shown by the higher number of obtained peptides during identical proteolysis periods (**Fig. 4.5**). Furthermore, the complexity of the tryptic maps is not identical between mutants: overall, FXN-I154F and FXN-W155R are more easily accessible to the protease having more degradation sites and peaks, whereas the FXN-G130V and FXN-D122Y mutants have simpler tryptic maps (**Fig. 4.5**).

Some additional differences are observed between the mutants, which are suggestive of the local impact that the different mutations have on the protein structure and dynamics. For example, the G130V and D122Y mutations are highly flexible in the loop between strands β3 and β4, as shown by the appearance of a peak corresponding to the Q153-K164 segment (approximately 36 min; **Fig. 4.5**), which is absent in the other mutants. On the other hand, the α1 helix in the FXN-I154F and FXN-W155R mutants has a decreased rigidity compared to the native protein and the remaining mutants. Proteolysis within a regular secondary structure element such as helices is very unfavourable and

does not occur unless some disorder or local breathing is present, as appears to be the case in the FXN-I145F and FXN-W155R mutants.

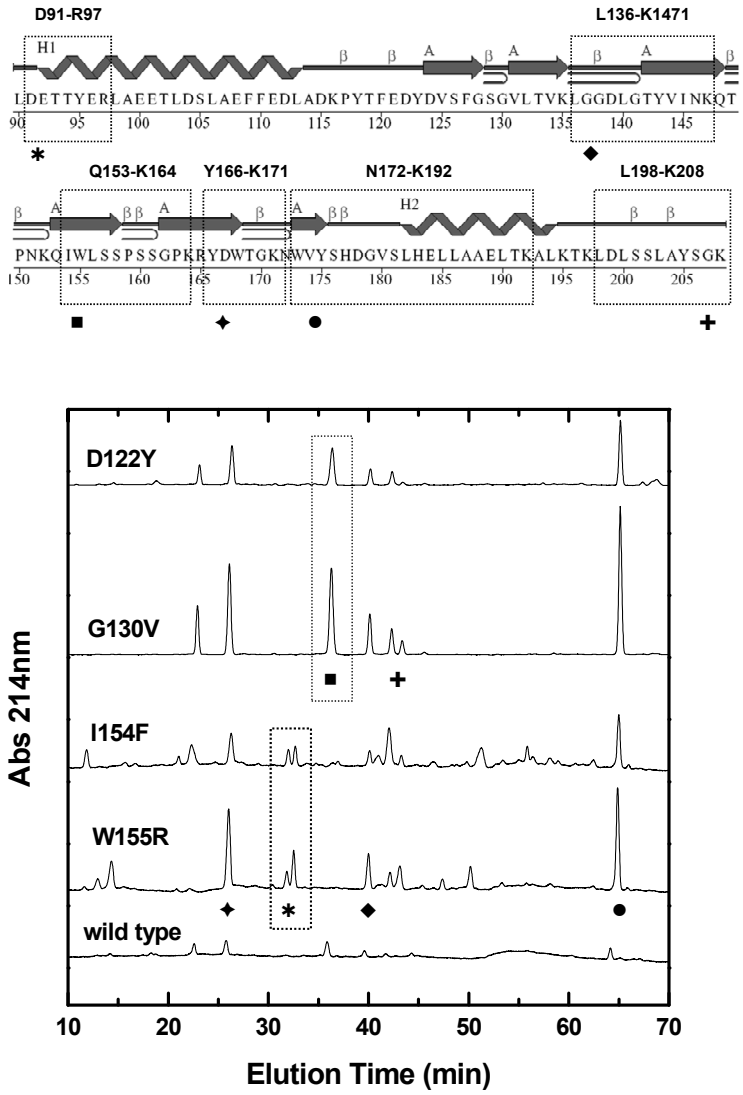

Figure 4.5: Trypsin limited proteolysis of frataxin at pH 8.5. **Top:** Secondary structure wiring diagram. The fragments resulting from thetryptic digestion are highlighted by boxes. **Bottom:** Peptide maps resulting from partial tryptic digestion: wild-type and mutant variants (FXN-D122Y, FXN-G130V, FXN-I154F and FXN-W155R) (data from the wild-type and the last two mutants are redrawn from the previous chapter [9]) after being incubated with trypsin for 90 min at 37ºC. Boxes highlight the peaks that are only present on the tryptic digestion of FXN-D122Y and FXN-G130V or FXN-I154F and FXN-W155R.

Table 4.2: Kinetic constants observed for all the identified peaks. Time course of trypsin limited proteolysis: appearance of the peaks with different elution times was monitored for all the proteins understudy and the data was fitted to a first order reaction.

	k_{obs} (x 10^{-3} min^{-1})				
Peak (min)	Wt	D122Y	G130V	I154F	W155R
32	D91-R97	-	-	28.1 ± 8.1	25.6 ± 11.2
40	L136-K147	25.0± 1.4	37.9 ±12.5		25.4 ± 11.0
23	L198-K208	22.7 ± 2.6	45.6 ± 5.1	-	-
36	Q153-K164	26.7 ± 2.0	48.1 ± 8.3	-	-
26	Y166-K171	26.7 ± 2.6	42.7 ± 8.1	14.5 ± 3.8	39.8± 9.8
66	N172-K192	24.5 ± 2.7	32.2 ± 2.9	26.4 ± 6.3	39.6 ± 21.1
42	L198-K208	26.9 ± 4.0	25.0 ± 5.1	-	18.5 ± 10.6

4.4.5. Proteolytic Degradation Kinetics

To investigate whether particular regions of frataxin have different degradation rates, we analysed the proteolysis kinetics of the different frataxin variants (**Fig. 4.6; Table 4.2**).

Under the tested conditions the FXN-G130V and FXN-D122Y variants are found to undergo proteolysis at higher rates. By contrast, for the FXN-I154F and FXN-W155R mutants, proteolysis is restricted to particular regions of the protein: fast degradation is observed at cleavage sites within helix α1 (R97), at strand β5 (R165) and on the loop between strands β5 and β6 (K171). The FXN-W155R mutant is also cleaved at a faster rate at the protein termini and at the loop between the β2 and β3 strands, probably as a result of the destabilisation of the β3/β4 inter-strand interactions, which likely increases the flexibility of the contiguous loop and its cleavability (K135). A comparison between these two mutants suggests that the conformational strain introduced by these mutations results in a more localised destabilisation, affecting the

stability of the first helix and eventually perturbing the ridge of negatively charged residues that cluster along the first helix and the first strand, which are known to be involved in iron binding [18].

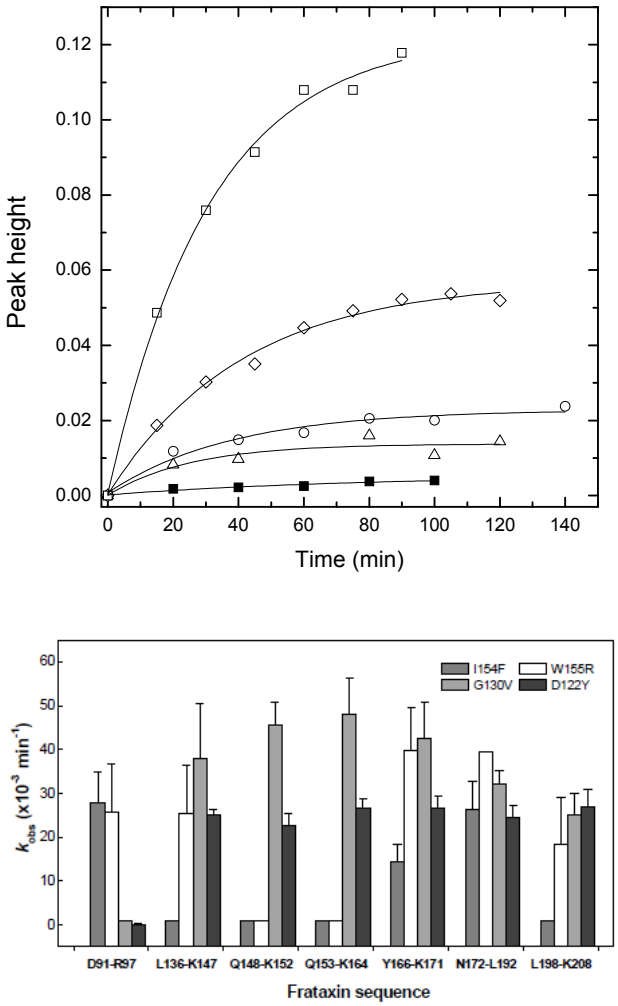

Figure 4.6: **Top.** Time course of trypsin limited proteolysis. The appearance of the peptide eluting at 66 min (**Fig. 4.5**) was monitored for wild type (■) and mutant variants: FXN-D122Y, (◊); FXN-G130V, (□); FXN-I154F, (○); FXN-W155R, (Δ) during incubation with trypsin at 37ºC. Solid traces are fits to first-order reaction rates. **Bottom.** Comparative plot of proteolysis rates per identified fragment. The observed proteolysis rates of the four frataxin mutant variants are compared for the different digested fragments. The rates determined for the native frataxin have been subtracted in each case.

4.4.6. Degradation by Lon and ClpXP

In order to evaluate whether frataxin variants are more prone to degradation by the mitochondrial proteases Lon and ClpXP, we have co-expressed frataxin together with either one of the protease systems. Frataxin concentration/amount was evaluated during a time period following the inhibition of protein synthesis (**Fig. 4.7**) [10-11].

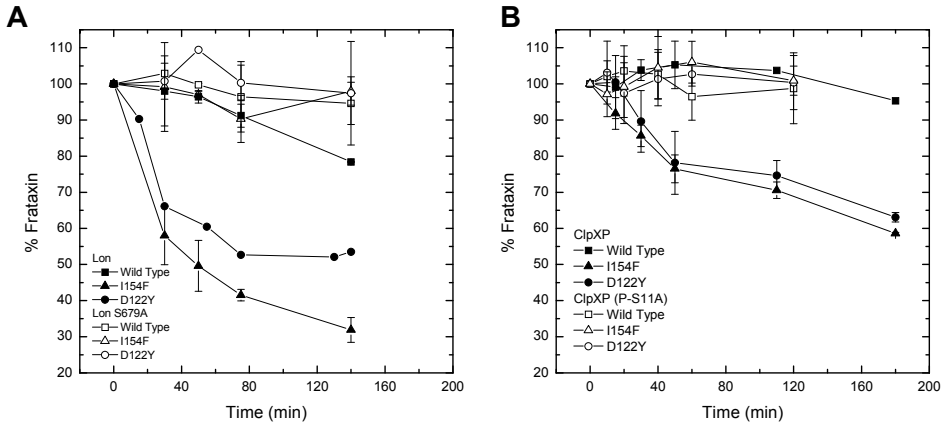

Figure 4.7: Degradation rate of wild type, FXN-D122Y and FXN-I154F proteins in cells co-overexpressing Lon **(A)** or ClpXP **(B)** proteases at 37ºC. The quantity of frataxin, either wild type or mutant variants, present in the cells was evaluated by SDS/PAGE.

We have evaluated the degradation rate of wild type and two of the mutant variants – FXN-D122Y and FXN-I154F. Lon co-expression leads to more efficient degradation rates and even the wild type protein is degraded. The decay of wild type protein is only observed 80min after the protein expression is blocked; by contrast, mutants' degradation is readily observed. After 140min the wild type registered a decay of ~20%, while D122Y and I154F showed a decay of ~50% and ~70% respectively.

Co-expression of ClpXP had no effect on the amount of wild type protein but lead to the degradation of the mutant variants and after 180min, both mutants showed a decay of ~30-40%. Controls co-

expressing frataxin proteins with proteolytically inactive proteases (Lon-S679A and ClpXP-S111A) showed that the decreased on the amount of frataxin proteins was a direct effect of a higher number of functional proteolytic units and not just a secondary effect of the co-overexpression *per se*. Overall, these results support what was suggested by the limited proteolysis experiments: frataxin FRDA variants are indeed more easily degraded by the mitochondrial proteolytic systems.

4.4.7. Clinical Mutations Impact on Stability and Iron Binding

To compare the effect of the mutations on the folding thermodynamics of frataxin, we studied their stabilities against chemical unfolding in the presence of urea as measured by far-UV CD and Trp fluorescence emission. As observed for the wild-type protein, the mutant variants show cooperative unfolding transitions (**Fig. 4.8**). The results obtained revealed that the two newly studied mutations (D122Y and G130V) are those leading to higher frataxin destabilisation, in agreement with what has been proposed for G130V [19]. The protein stability decreases according to the order: FXN-wild-type > FXN-W155R > FXN-I154F > FXN-D122Y > FXN-G130V and corresponds to a $\Delta(\Delta G)$ in the range −1.36 to −2.86 kcal· mol^{-1} (**Table 4.3**).

This behaviour was compared with thermal unfolding, as recorded by far-UV CD. We measured the melting curves for FXN-G130V and FXN-D122Y (**Fig. 4.8**) and compared the values with those previously obtained for FXN-I154F and FXN-W155R [6]. In agreement with the chemical unfolding data, the FXN-G130V and FXN-D122Y mutants showed the largest variations of melting transitions (ΔT_m of approximately 16 ºC and 23 ºC, respectively), while maintaining the reversibility of the unfolding reaction (> 95%).

Table 4.3 – Parameters for urea and thermal denaturation of wild type and mutant forms (FXN-W155R; FXN-I154F, FXN-D122Y and FXN-G130V). Comparing the differences in stability.

Protein	ΔG_{H2O} (kcal.mol^{-1})	*m* (cal.mol^{-1}.M^{-1})	$[Urea]_{1/2}$ (M)	$\Delta[Urea]_{1/2}$ [a]	$\Delta(\Delta G)$ [b] (cal.mol^{-1})	T_m (ºC)	ΔT_m (ºC)
Wild type[c]	5.6 ± 0.3	1407 ± 41	4.3			66.3±0.1	-
D122Y	4.3 ± 0.2	1498 ± 23	2.9	-1.4	-2110	50.4±0.1	-15.9
G130V	3.1 ± 0.3	1310 ± 60	2.4	-1.9	-2863	43.2±0.1	-23.1
I154F[c]	5.8 ± 0.3	1836 ± 67	3.2	-1.1	-1657	50.7±0.1	-15.6
W155R[c]	5.1 ± 0.2	1483 ± 78	3.4	-0.9	-1356	61.4±0.4	- 4.9

[a] Difference between the $[urea]_{1/2}$ for the wild type and the mutant forms.
[b] $\Delta(\Delta G)$ = From $\Delta[urea]_{1/2}$ x average of the three *m* values [20].
[c] Data from [6].

The impact of mutations in frataxin was also investigated with respect to its iron-binding properties. Independent experimental evidence suggests that frataxin acts as a cellular iron chaperone and human frataxin has been shown to bind six to seven irons, although with a low affinity [21].

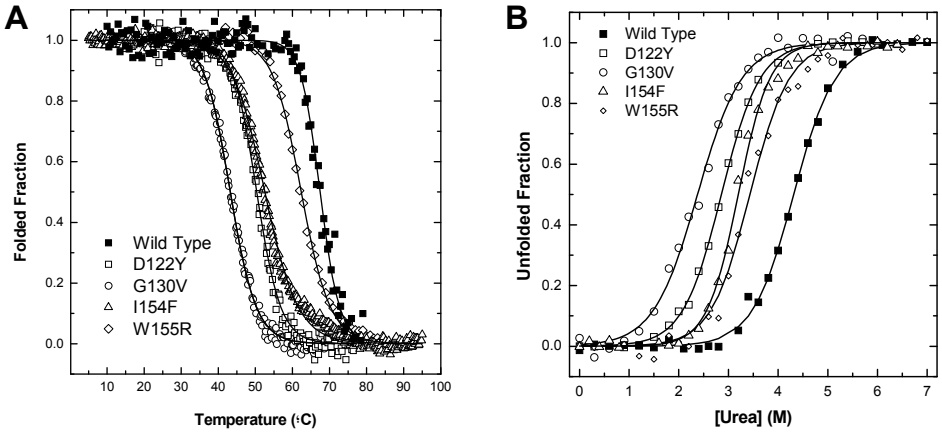

Figure 4.8: Thermal (**A**) and chemical (**B**) denaturation curves at pH 7.0. filled squares, FXN-Wild-type; unfilled diamonds, FXN-D122Y; unfilled squares, FXN-G130V; unfilled circles, FXN-I154F; unfilled triangles, FXN-W155R (data from the wild-type and the last two mutants are redrawn from [9]. Lines represent fits to the two-state model [22]; for parameters, see **Table 4.3**.

We monitored the iron binding capacity by fluorescence spectroscopy using wild-type frataxin as a control. Under controlled pH conditions and at 25 ºC, the ferric binding capacity of FXN-D122Y and FXN-G130V appears to be partially impaired: the mutants are only able to bind four irons per molecule (data not shown). As previously reported, the mutants, FXN-I154F and FXN-W155R, precipitate upon ferric binding above the two iron per frataxin threshold [6].

4.5. Discussion

In FRDA, the link between a point mutation in frataxin and the disease physiopathology remains unclear, and hypothetical scenarios for the impact of mutations include an effect on the folding efficiency, maturation, protein stability, proteolytic susceptibility or function. We have studied different point mutations found in compound heterozygotes FRDA patients. These mutations can be grouped according to FRDA symptoms: whereas the I154F and W155R mutations lead to severe FRDA, the mutations G130V and the D122Y account for milder clinical symptoms, although the latter has a very low prevalence [23]. From a structural point of view, our results demonstrate that none of the mutations significantly change the protein fold at room temperature. The heteronuclear single quantum coherence (HSQC) spectra obtained for the frataxin variants are typical of folded species and are very similar to those of wild-type protein. Furthermore, frataxin flexibility is not significantly altered by the insertion of the mutations. Despite retaining the fold, the four mutant variants present a reduced thermodynamic stability, which, *in vivo*, is likely to cause an increase in the molecular motions and enhance the susceptibility to aggregate and/or to be degraded by the cellular proteases. Limited proteolysis at 37ºC shows

that mutant frataxins have an increased susceptibility towards proteolytic degradation. In agreement co-expressing frataxin with Lon and ClpXP proteases at 37ºC shows that the FRDA-related variants are indeed more prone to degradation by the mitochondrial proteolytic systems.

The increased correlation times measured for the mutants (**Table 4.1**) reflect a higher tendency towards aggregation. Furthermore, expression assays revealed that, in mutant frataxins, the soluble/insoluble protein ratio is decreased and this may play a role in the molecular pathogenesis of FRDA.

The observed reduction in iron-binding could also be related to the increased molecular motions. The increased flexibility, combined with the enhanced propensity towards aggregation, could explain why some mutants precipitate upon iron binding (FXN-I154F and FXN-W155R) or have a lower binding stoichiometry (FXN-G130V and FXN-D122Y). Under adverse physiological conditions occurring *in vivo*, such as the oxidative stress observed in FRDA model cells [24-27], these effects could also lead to a perturbation of frataxin structure and dynamics, which could lead to its inactivation or misfolding, further reducing the cellular concentration of functional frataxin.

Altogether, the clinical effects in heterozygous FRDA patients are likely to result from a combination of effects, such as a reduced efficiency of protein folding (resulting in an increase of the aggregation rates), an accelerated degradation *in vivo* (leading to decreased frataxin levels); misfolding and conformational destabilisation contribute to a decrease in the levels of functional frataxin. In this scenario, FRDA in heterozygous patients carrying frataxin single point mutations could be considered to possess a type of protein misfolding disorder [28].

4.6. Acknoledgements

C. de Chiara, from N.I.M.R. (London, UK) is gratefully acknowledged for the help on relaxation data analysis.

P. Chicau, M. Regalla and A. Coelho from ITQB Analytical Services Facilities are gratefully the acknowledged for their technical contributions.

Peter Bross (University of Aarhus, Denmark) is gratefully acknowledged for sharing of Lon and ClpXP plasmids.

4.7. References

1. Gerber, J., U. Muhlenhoff, and R. Lill, *An interaction between frataxin and Isu1/Nfs1 that is crucial for Fe/S cluster synthesis on Isu1.* EMBO Rep, 2003. **4**(9): p. 906-11.
2. He, Y., et al., *Yeast frataxin solution structure, iron binding, and ferrochelatase interaction.* Biochemistry, 2004. **43**(51): p. 16254-62.
3. Shan, Y., E. Napoli, and G. Cortopassi, *Mitochondrial frataxin interacts with ISD11 of the NFS1/ISCU complex and multiple mitochondrial chaperones.* Hum Mol Genet, 2007. **16**(8): p. 929-41.
4. Yoon, T. and J.A. Cowan, *Iron-sulfur cluster biosynthesis. Characterization of frataxin as an iron donor for assembly of [2Fe-2S] clusters in ISU-type proteins.* J Am Chem Soc, 2003. **125**(20): p. 6078-84.
5. Adinolfi, S., et al., *The factors governing the thermal stability of frataxin orthologues: how to increase a protein's stability.* Biochemistry, 2004. **43**(21): p. 6511-8.
6. Correia, A.R., et al., *Conformational stability of human frataxin and effect of Friedreich's ataxia-related mutations on protein folding.* Biochem J, 2006. **398**(3): p. 605-11.
7. Musco, G., et al., *Towards a structural understanding of Friedreich's ataxia: the solution structure of frataxin.* Structure, 2000. **8**(7): p. 695-707.
8. Winsor, D.J.S., W.H., *Quantitative Characterisation of Ligand Binding*. 1995, New York: Wiley-Liss.
9. Dosset, P., et al., *Efficient analysis of macromolecular rotational diffusion from heteronuclear relaxation data.* J Biomol NMR, 2000. **16**(1): p. 23-8.
10. Hansen, J., N. Gregersen, and P. Bross, *Differential degradation of variant medium-chain acyl-CoA dehydrogenase by the protein quality control proteases Lon and ClpXP.* Biochem Biophys Res Commun, 2005. **333**(4): p. 1160-70.
11. Huang, H.C., et al., *The molecular chaperone DnaJ is required for the degradation of a soluble abnormal protein in Escherichia coli.* J Biol Chem, 2001. **276**(6): p. 3920-8.
12. Lipari, A., *Model-free approach to the interpretation of nuclear magnetic resonance relaxation in macromolecules. 1. Theory and range of validity.* J. Am. Chem. Soc., 1982. **104**: p. 1546-4559.
13. Maciejewski, M.W., et al., *Backbone dynamics and refined solution structure of the N-terminal domain of DNA polymerase beta. Correlation with DNA binding and dRP lyase activity.* J Mol Biol, 2000. **296**(1): p. 229-53.

14. Musco, G., et al., *Assignment of the 1H, 15N, and 13C resonances of the C-terminal domain of frataxin, the protein responsible for Friedreich ataxia.* J Biomol NMR, 1999. **15**(1): p. 87-8.
15. Santisteban, I., et al., *E. coli expression system for identifying folding mutations of human adenosine deaminase.* Methods Mol Biol, 2003. **232**: p. 175-82.
16. Bross, P., et al., *Effects of two mutations detected in medium chain acyl-CoA dehydrogenase (MCAD)-deficient patients on folding, oligomer assembly, and stability of MCAD enzyme.* J Biol Chem, 1995. **270**(17): p. 10284-90.
17. Fontana, A., et al., *Probing protein structure by limited proteolysis.* Acta Biochim Pol, 2004. **51**(2): p. 299-321.
18. Nair, M., et al., *Solution structure of the bacterial frataxin ortholog, CyaY: mapping the iron binding sites.* Structure, 2004. **12**(11): p. 2037-48.
19. Cavadini, P., et al., *Human frataxin maintains mitochondrial iron homeostasis in Saccharomyces cerevisiae.* Hum Mol Genet, 2000. **9**(17): p. 2523-30.
20. Pace, S., Thomson, *Protein Structure - a pratical approach*. 1990, Oxford: IRL Press.
21. Yoon, T. and J.A. Cowan, *Frataxin-mediated iron delivery to ferrochelatase in the final step of heme biosynthesis.* J Biol Chem, 2004. **279**(25): p. 25943-6.
22. Pace, C.N., et al., *Conformational stability and thermodynamics of folding of ribonucleases Sa, Sa2 and Sa3.* J Mol Biol, 1998. **279**(1): p. 271-86.
23. Cossee, M., et al., *Friedreich's ataxia: point mutations and clinical presentation of compound heterozygotes.* Ann Neurol, 1999. **45**(2): p. 200-6.
24. Bulteau, A.L., et al., *Oxidative stress and protease dysfunction in the yeast model of Friedreich ataxia.* Free Radic Biol Med, 2007. **42**(10): p. 1561-70.
25. Calabrese, V., et al., *Oxidative stress, mitochondrial dysfunction and cellular stress response in Friedreich's ataxia.* J Neurol Sci, 2005. **233**(1-2): p. 145-62.
26. Jauslin, M.L., et al., *Mitochondria-targeted antioxidants protect Friedreich Ataxia fibroblasts from endogenous oxidative stress more effectively than untargeted antioxidants.* FASEB J, 2003. **17**(13): p. 1972-4.
27. Seznec, H., et al., *Friedreich ataxia: the oxidative stress paradox.* Hum Mol Genet, 2005. **14**(4): p. 463-74.
28. Gregersen, N., et al., *Protein misfolding and human disease.* Annu Rev Genomics Hum Genet, 2006. **7**: p. 103-24.

CHAPTER

5 SMALL MOLECULES AS MODULATORS OF FRDA FRATAXIN VARIANTS

5.1. Summary

In vitro studies on frataxin clinical mutants suggested that, in heterozygous FRDA patients, the pathological process may arise from a combination of effects such as reduced efficiency of protein folding, accelerated degradation, misfolding and conformational destabilisation [3-4]. Here we have analysed the effect of different classes of chemical chaperones in two of the stages of the protein folding process: during early folding events and on the conformation and stability of the folded native-like frataxin. The experiments were performed using the wild type frataxin and two clinical variants – FXN-I154F and FXN-D122Y. The wild type was used as a control and 4-phenyl butyrate, trehalose (sugar), trimethylamine-N-oxide (methylamine) and glycerol (polyol), were tested for their potential chaperone-like function on frataxin clinical variants. Interestingly, the effect of the small compounds is mutant dependent. Considering the impact on early folding events, it is observed that, while FXN-D122Y folding efficiency is only modestly improved, FXN-I154F folding efficiency improves significantly with the amount of expressed soluble protein, increasing up to ~3fold in the presence of glycerol. Opposite, when analysing the effect on the protein native-like conformation and stability, the observed effects are more dramatic for the FXN-D122Y while only modest for the FXN-I154F. The presence of chemical chaperones stabilises FXN-D122Y considerably (ΔT_m up to ~7.8ºC) with trehalose and TMAO inducing thermal stability values identical to the ones observed for the wild type protein. In addition, FXN-D122Y conformational defects were also more successfully rescued. For Overall, our data shows that folding defects in FRDA frataxin variants may be partially rescued by the presence of chemical chaperones and that these compounds may become useful therapeutics.

5.2. Introduction

An increasing number of studies describe the use of low molecular weight compounds, called chemical chaperones, to overcome folding defects in proteins involved in conformational disorders [1-4]. This therapeutic strategy has been explored for many diseases such as cystic fibrosis [5-9], phenylketonuria [10-11], Huntington's [12] and Gaucher's disease [13]. The presence of chemical chaperones reverts, at least partially, the mistrafficking, misfolding and aggregation of the disease-protein ameliorating the pathological behaviour.

Chemical chaperones do not bind directly to proteins; their interaction with the peptide backbone is unfavourable, causing a preferential exclusion of the compound from water-protein interface and leading to a preferential hydration of the protein surface. Furthermore, the presence of these small molecules also results in an increased solvent density that restrains the proteins' free movements, increasing its compactness. In addition it is also described that, during protein synthesis, these compounds minimise the formation of intermediate states that could lead to folding dead-ends [14-17] and they may also induce the response of molecular chaperones [18].

Here, the possible use of chemical chaperones to rescue the folding defects and to modulate the misfolding and aggregation propensity of frataxin clinical mutants (FXN-D122Y and FXN-I154F) is addressed. Compounds from different classes were selected: 4-Phenylbutyrate (4PBA, a low molecular weight fatty acid), glycerol (a polyol), trehalose (a sugar) and Trimethylamine N-oxide (TMAO, a methylamine).

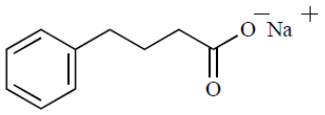

Sodium 4-Phenyl Butyrate (4PBA)

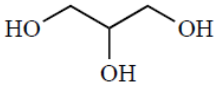

Glycerol

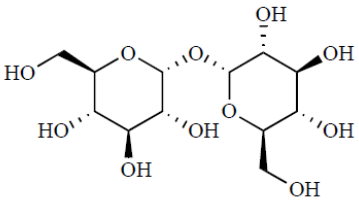

Trehalose

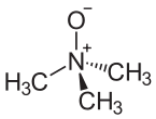

Trimethylamine N-oxide (TMAO)

Figure 5.1: Chemical structures of the small compounds here analysed for their potential chaperone-like action on frataxin clinical variants.

We have evaluated the effect of chemical chaperones on two different stages of the folding process: during the early folding events and on the conformation and stability of the folded protein. The effect on early folding events was accessed by comparing the protein folding efficiency in the presence and in the absence of the small compounds. The folding efficiency was quantified through the ratio of soluble versus insoluble protein during protein expression. Previously we have shown that frataxin clinical variants present smaller soluble/insoluble ratios [19] and here we aim to characterise impact chemical chaperones may have on this ratio. If a compound improves the mutants foldability (increases the soluble/insoluble ratio) this may lead to an increase of frataxin cellular levels, which may be sufficient to revert at least part of the pathological process associated to frataxin deficiency.

Furthermore, we will evaluate the impact of chemical chaperones on the protein conformational properties and also their potential stabilising

effect. Frataxin conformational variations will be evaluated thorough the chaperonin sink assay [20]. GroEL promiscuously binds a wide range of hydrophobic folding intermediates, partitioning them from solution and thus preventing or arresting off-pathway aggregation. Due to the mutants' increased propensity towards aggregation and their decreased stability and folding efficiency, these are likely to partition onto GroEL. Thus, we aim to evaluate whether the presence of chemical chaperones can modulate the conformational destabilisation observed for the mutants, reducing or preventing their partitioning onto GroEL. If the partitioning onto this molecular chaperone is modulated, it is likely that, *in vivo*, the proteins' recognition by proteases may also be modulated since the same features are recognised by GroEL and the protease systems. With this strategy, we aim to identify compounds that may extend the mutants cellular lifetime and like this increase the cellular levels of mutant frataxin.

Moreover, since the mutants' stabilisation may improve their functionality we have evaluated the potential stabilising effect of small compounds. In order to achieve this, differential scanning fluorimetry has been performed (DSF) [21-22]. Through this technique the protein unfolding is followed using a fluorescent dye (Sypro orange was used here). Upon unfolding, the protein exposes its hydrophobic region which corresponds to a lower dielectric environment to which Sypro orange is sensitive. The lower the dielectric medium, the higher the quantum yield of the dye which means that, as the protein unfolds, Sypro orange fluorescence increases. After reaching a *plateau,* the fluorescence intensity starts to decrease probably due to aggregation of the denatured protein-dye complex.

5.3. Materials and Methods

Accessing folding efficiency

Cells were transformed with vectors enabling FXN (wild type or mutants conserved C-terminal domain) overexpression and grown in LB medium at 37ºC up to an OD_{600}=0.6. Plasmid-derived protein expression was induced by addition of IPTG (0.5mM) and, at the same time, chemical compounds were added to the medium. Aliquots were withdrawn at the mentioned expression time (2 or 4H). Cells were lysed and soluble and insoluble fractions were separated through high speed centrifugation (45 min at 168 000 *g*). Both fractions were loaded on to a 15% SDS/PAGE and after staining with Roti-blue a semi-quantitive analysis of the relative proportion of frataxin present in the soluble and insoluble fractions was obtained from densitometric analysis of gel bands (n = 3).

Protein purification

All constructs were expressed in *Escherichia coli* competent cells (BL21 (DE3)) and the protein purified as previously described [23-25]. As in previous studies, the protein used corresponded to the conserved C-terminal domain (amino acids 91–210). The vector here used lead to the expression of recombinant proteins with only a poly-His tag. The mutants were stable in solution, although susceptible to precipitate upon slow freezing. Nevertheless, thawed proteins that had been fast frozen retained their spectroscopic properties and melting temperatures.

GroEL partitioning assay

GroEL immobilised onto Sepharose 4 fast flow beads (2mM) was resuspended in buffer A (50mM Tris pH7.5, 50mM KCl, 5mM $MgCl_2$, 0.5mM EDTA and 1mM DTT) with 1M urea. Protein sample was then added (1:1 to the GroEL) and the reaching mixture was incubated with constant shaking at 45ºC. Every 40 min the reaction mixture was spin

down and an aliquot of the non-partitioned mixture was withdrawn [26-27]. Aliquots were applied on a 15% SDS/PAGE and the amount of proteins quantified.

Differential scanning fluorimetry (DSF).

The effect of the chemical chaperones on the proteins thermal stability was evaluated through DSF [21-22]. The fluorescent dye Sypro orange (λ_{ex} 300nm and λ_{em} 470/570nm) was used as a probe to follow protein unfolding. In all experiments, the heating rate of 1.5ºC/min. Data were analysed according to a two-state model [28]. The fits to the unfolding transitions were made using Origin (MicroCal).

5.4. Results

5.4.1. Effect on Early Folding Events

Frataxin clinical mutations decrease the protein folding efficiency [19]. Here, we have analysed whether the small compounds understudy could rescue folding efficiency of frataxin clinical mutants (FXN-D122Y and FXN-I154F) if present during early folding events. In order to test this hypothesis, a bacterial system was used in which the foldability and conformational destabilisation of the frataxin proteins was monitored [19, 29-31]. Small molecular weight compounds (4PBA, Trehalose, TMAO and glycerol), at different concentrations, were added to the culture medium at the same time that protein expression was induced.

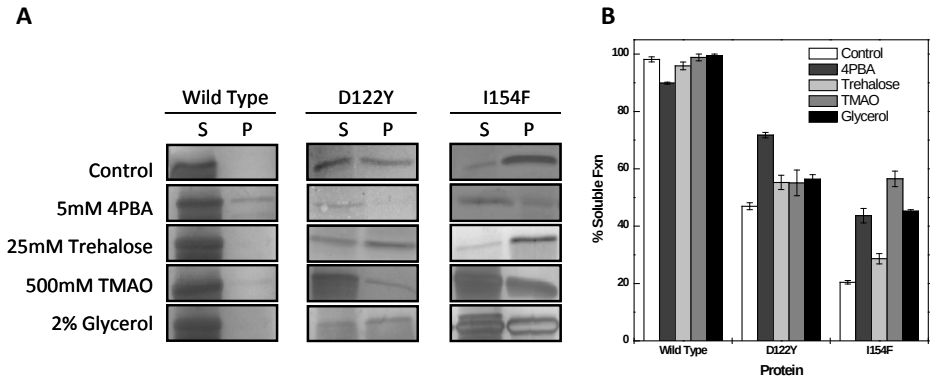

Figure 5.2: Effect of chemical chaperones on early folding events. **A**. SDS/PAGE gels obtained from *E. coli* lysates expressing frataxin. For each protein variant, the soluble (s) and insoluble (p) fractions are shown. **B.** Semi-quantitative analysis of the relative proportion of frataxin present in the soluble and insoluble fractions, obtained from densitometric analysis of gel bands (n = 3), allowed the determination of the protein expressed in the soluble form.

After inducing protein expression for 2h and 4h, aliquots were withdrawn and the soluble and insoluble fractions analysed. It was observed that some compounds can rescue mutants folding efficiency and that the extent of this rescue is concentration dependent (**Fig. 5.2** and **5.3**). Three of the tested compounds show different degrees of rescue depending on the mutant considered. Interestingly, while both TMAO and glycerol increase considerably the folding efficiency of the mutant FXN-I154F (over a two-fold increase), their impact on FXN-D122Y folding efficiency is very small. This suggests that the misfolding pathway observed for the two mutants should be different. 4PBA increases significantly the folding efficiency of both mutants and this increase is concentration dependent up to 7.5mM (**Fig. 5.3B**). However, 4PBA may not be acting as a chemical chaperone since different reports show that this compound can affect the expression

levels of chaperones and their mRNA's stability [32-33], as well as alter the expression levels of other proteins, since 4PBA inhibits histone deacetylases [34].

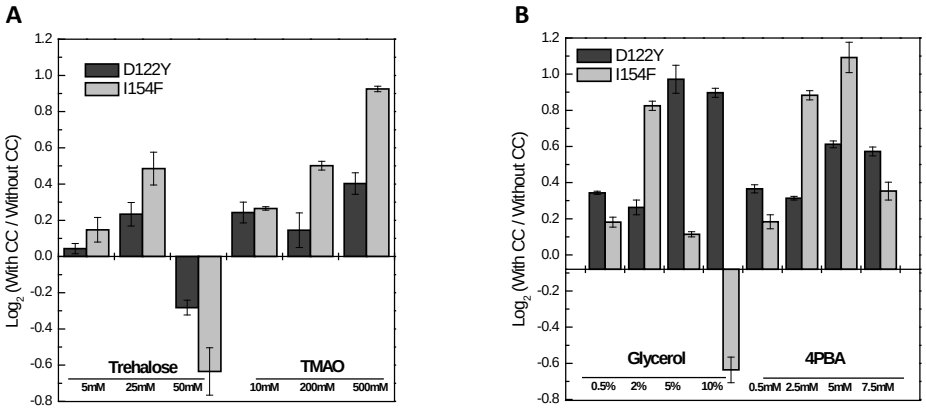

Figure 5.3: Variation of the folding efficiency induced by the presence of chemical chaperones. After the densitometric analysis of the gel bands the ration between the amount of soluble protein present in the presence and absence of the compounds were determined. The Log2 of this ration is here present to highlight the variation observed. A. Effect of increasing concentrations of Trehalose and TMAO. B. Effect of increasing concentrations of Glycerol and 4PBA. (n=2)

Comparative gel analysis of the control and osmolytes added cell lysates did not show any differences in terms of protein expression, meaning that the addition of osmolytes does not seem to have induced the expression of molecular chaperones, thus disfavouring the possibility that the effects observed are a result of an increased expression of the chaperone system and not a direct effect of the presence of the osmolytes during the early folding events.

5.4.2. Probing Conformational Variations: GroEL Sink Assay

Further, we have used the chaperonin sink assay to evaluate the efficiency of osmolytes in correcting folding defects. Nucleotide-free GroEL, has a high affinity towards hydrophobic intermediates and

promiscuously binds to them, allowing its efficient and stable capture. Here, GroEL is used as tool to probe frataxin conformational alterations, more specifically as a detection platform to examine the dynamic shift towards stable/well folded populations in the presence of various folding osmolytes. Previously, we have shown that frataxin mutants present a higher flexibility and higher tendency towards aggregation [19], thus it is likely that mutants will be more easily captured by GroEL. Immobilised and in solution, GroEL show an identical capacity to bind unfolded and partially folded substrate proteins [27, 35]. Here we have used GroEL covalently bound to Sepharose 4 fast flow beads, since this preparation allows an easy and immediate evaluation of the partitioning of any given substrate protein onto GroEL. The substrate protein and GroEL beads are put in buffered solution with a 1:1 stoichiometry; after a short spin down the solution is analysed (through an SDS-PAGE gel) and the protein in solution, correctly folded, is quantified. On the other hand if a protein is not correctly folded and has exposed hydrophobic regions, it will partition onto the GroEL beads and its concentration in solution will decrease.

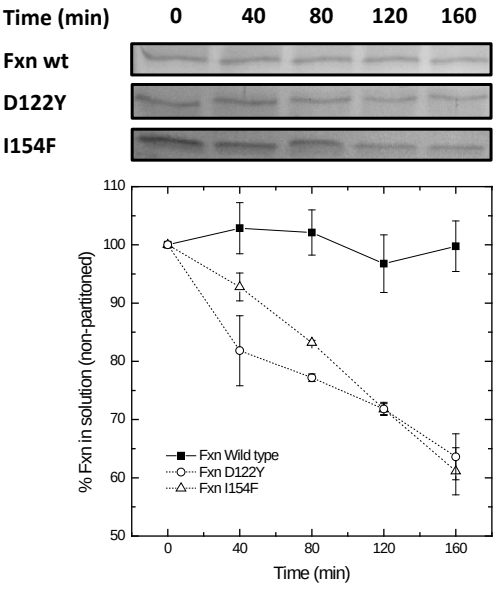

Figure 5.4: Partition of frataxin variants onto GroEL beads. **Top.** SDS/PAGE analysis of the reaction mixture aliquots withdrawn after spin down of the mixture. **Bottom.** Densitometric analysis of the gels bands, the initial point (before the proteins were incubated at 45ºC) corresponds to 100%.

The partition assays were performed for wild type frataxin and its clinical variants FXN-D122Y and FXN-I154F. In order to accelerate the partitioning reaction, the reaction mixtures were incubated at 45ºC in the presence of 1M urea. Under these conditions, even after an incubation of 160 min, the wild type frataxin remains in solution, thus FXN is well folded and stable. However, the mutants already start to partition onto GroEL after being at 45ºC for 40min and after 160min only ~60% of the initial protein remained in solution. These results confirm that the mutants show an increased destabilisation relative to the wild type (**Fig. 5.4**).

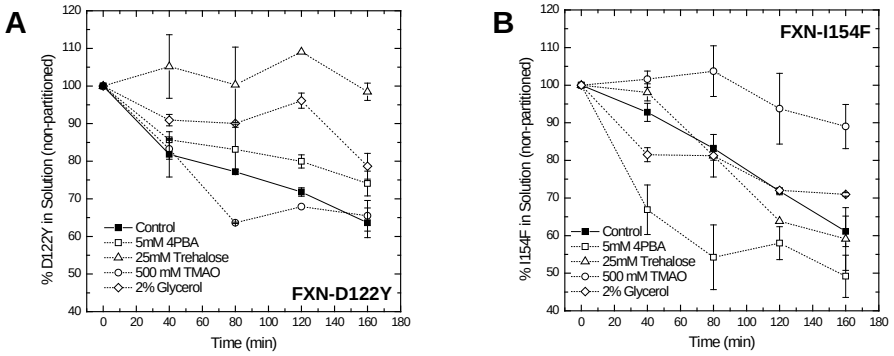

Figure 5.5: Modulating the partitioning GroEL partitioning of FRDA-related frataxin variants. (**A)** D122Y and (**B**) I154F. As is Figure 5.3, here we analysed the non-partitioned fraction along a 160min incubation time at 45ºC and in the presence of 1M urea.

Next, we have evaluated whether the presence of the different chemical chaperones under study could correct the mutants' conformational impairment, thus slowing down the partitioning or even preventing it (**Fig. 5.5**). In agreement to what had already been observed for the effect of chemical chaperones on early folding events, the same compound showed different efficiencies depending on the mutant variant considered. For instance, while the presence of 500mM TMAO significantly reduces the observed partitioning of the mutant

FXN-I154F, it has a negligible effect on the FXN-D122Y partitioning. The analysis of the partitioning profiles in the presence of the different compounds showed that FXN-D122Y partitioning can be prevented by trehalose (25mM) and also slowed down by both glycerol (2%) and 4PBA (5mM). However, FXN-I154F partitioning can only be rescued by TMAO (500mM); the other three chemical chaperones either have no effect (glycerol and trehalose) or even accelerate partitioning.

5.4.3. Stabilisation of Frataxin's Native State.

The analysis of the thermal denaturation curves in the presence of chemical chaperones has revealed that that all frataxin variants, including the wild type, can be stabilised by most small compounds under study (**Fig. 5.6** and **Table 5.1**). However, the extent of the stabilisation and the effect of each compound depends on the variant considered.

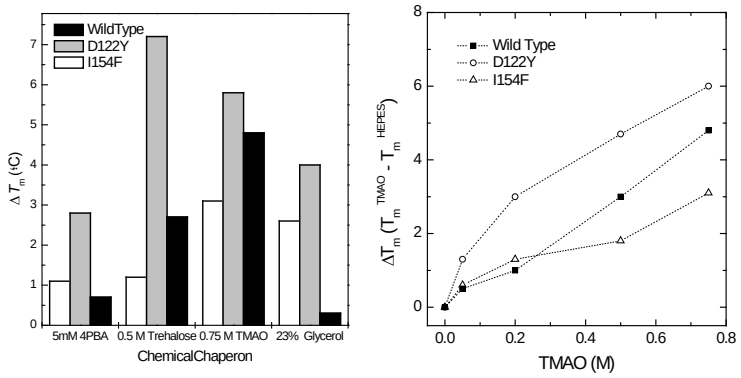

Figure 5.6: Stabilisation induced by the presence of chemical chaperones. **A.** Variations on the Tm values of FXN wild type (black), D122Y (Gray) and I154F (white) mutants by 5mM 4PBA, 500mM Trehalose, 750mM TMAO and 25% Glycerol. **B.** TMAO efficienctly increases the Tm values of all FXN variants in a concentration dependent way. (■) FXN wild type, (○) D122Y and (Δ) I154F.

The stabilising effects of the different compounds are more pronounced for the FXN-D122Y mutant and the addition of trehalose and TMAO to this mutant increases its thermal stability to T_m values close to the wild type intrinsic stability. By contrast, the stabilising effects on the FXN-I154F mutant are modest with TMAO and glycerol showing the most significant effects (maximum ΔTm = ~3.1 and 2.6ºC, respectively).

Table 5.1: Melting temperatures determined by the two state fits to the unfolding curved obtained by the DSF experiments.

		Wild Type[a]		D122Y[a]		I154F[a]	
		T_m (ºC)	ΔT_m	T_m (ºC)	ΔT_m	T_m (ºC)	ΔT_m
Control		55.1 ± 0.1	-	48.8 ± 0.1	-	39.1 ± 0.1	-
4PBA (mM)	**0.1**	54.5 ± 0.1	**-0.6**	49.5 ± 0.1	**3.3**	38.9 ± 0.1	**-0.2**
	0.5	54.8 ± 0.1	**-0.3**	49.3 ± 0.1	**3.1**	38.7 ± 0.1	**-0.4**
	1.0	54.8 ± 0.1	**-0.3**	49.4 ± 0.1	**3.2**	38.9 ± 0.1	**-0.2**
	2.5	55.3 ± 0.1	**0.2**	49.4 ± 0.1	**3.2**	38.9 ± 0.1	**-0.2**
	5.0	55.8 ± 0.1	**0.7**	49.0 ± 0.1	**2.8**	40.3 ± 0.1	**1.1**
	10.0	56.0 ± 0.1	**0.9**	48.3 ± 0.1	**2.1**	37.9 ± 0.1	**-1.2**
Trehalose (M)	**0.025**	54.6 ± 0.1	**-0.5**	50.1 ± 0.1	**3.9**	39.6 ± 0.1	**0.5**
	0.050	54.9 ± 0.1	**-0.2**	50.7 ± 0.1	**4.5**	39.5 ± 0.1	**0.4**
	0.125	55.3 ± 0.1	**0.2**	50.3 ± 0.1	**4.1**	38.3 ± 0.1	**-0.8**
	0.250	56.5 ± 0.1	**1.4**	50.3 ± 0.1	**4.1**	39.6 ± 0.1	**0.5**
	0.500	57.8 ± 0.1	**2.7**	53.4 ± 0.1	**7.2**	40.3 ± 0.1	**1.2**
	0.750	60.2 ± 0.1	**5.1**	54.1 ± 0.1	**7.9**	39.3 ± 0.2	**0.2**
TMAO (M)	**0.05**	50.1 ± 0.1	**0.5**	48.8 ± 0.1	**2.6**	39.7 ± 0.1	**0.6**
	0.2	51.3 ± 0.1	**1.0**	50.1 ± 0.1	**4.0**	38.4 ± 0.1	**1.3**
	0.5	52.0 ± 0.1	**3.0**	51.3 ± 0.1	**5.1**	40.9 ± 0.1	**1.8**
	0.75	54.0 ± 0.1	**4.8**	52.0 ± 0.1	**5.8**	42.2 ± 0.1	**3.1**
	1	48.8 ± 0.1	**5.8**	54.0 ± 0.1	**7.8**	41.6 ± 0.2	**2.5**
Glycerol (%)	**0.4**	55.1 ± 0.1	**0**	47.1 ± 0.1	**0.9**	39.2 ± 0.1	**0.1**
	4	54.6 ± 0.1	**-0.5**	44.5 ± 0.1	**-1.7**	37.8 ± 0.1	**-0.3**
	10	54.9 ± 0.1	**-0.2**	46.6 ± 0.1	**0.4**	-	**-**
	20	55.4 ± 0.1	**0.3**	50.2 ± 0.1	**4.0**	41.7 ± 0.1	**2.6**
	25	54.7 ± 0.1	**-0.4**	50.0 ± 0.1	**3.8**	-	**-**

[a] The control T_m are lower than the previously determined by CD or fluorescence spectroscopies, to evaluate whether the variations observed where not due to an artefact induced by the presence of the dye, the T_m variation caused by 250mM trehalose was confirmed by florescence spectroscopy.

5.5. Discussion

In spite of the basic mechanism responsible for the osmolyte effect, studies on the physical chemical origins of osmolyte action revealed that the mode of action of each osmolyte results from a combination of favorable or unfavorable interactions with backbone and side chains. This explains why some osmolytes are very effective in inducing structure while others are more likely to solubilise native proteins [14, 36-39]. Besides the different effects of the different compounds, it is also shown here that the effect of a given chemical chaperone is variable depending on the mutant variant considered. In fact, while the FXN-I154F folding efficiency is impressively altered by the presence of chemical chaperones, their effect on FXN-D122Y folding efficiency is for most conditions marginally impressive.

Although the mutations under study result in comparable decreased stabilities (ΔTm=~15ºC [19]), their impact on the protein conformation and structure are different and likely correlate to the different effect observed for each chemical chaperone. Residue I154 sits into the protein hydrophobic core and is completely buried, thus its mutation is likely to alter the protein compactness. However, mutating residue D122Y should have a less drastic effect on the overall conformation since this residue is at the protein surface on the $\alpha 1/\beta 1$ transition [25, 40]. Chemical chaperones disfavour backbone-water hydrogen bonds, favouring the scaffold hydrogen-bonds (structural); taking this into account and the fact that I154 is buried (the accessible surface of both backbone and side chains is for the native state zero), the presence of chemical chaperones during folding is likely to facilitate the insertion of a bulkier hydrophobic residue (phenylalanine) into the hydrophobic core of frataxin. However, the presence of chemical chaperones during the folding process of FXN-D122Y are likely to be small since the observed

reduced folding efficiency is likely to be caused by the impairment of two putative stabilising interactions (H-bond with G138 and a ionic interaction with K135) and not due to reduced compactness. On the other hand, the effect of chemical chaperones should stabilise the fold of the FXN-D122Y mutant fold since their presence will likely overcome the disruption of the stabilising bonds but, in contracts, their effects on stabilisation of the FXN-I154F should be very small.

The results here presented suggest that FXN-D122Y conformational variation might be overcome by the presence of chemical chaperones and that *in vivo* increased concentrations of different osmolytes may rescue the protein conformational properties. On the other hand, the FXN-I154F mutant should only be partially rescued and the presence of chemical chaperones may attenuate the phenotype observed. *In vivo* experiments using perhaps the well studied yeast model need to be performed but the approach here followed has revealed to be valuable for an initial screen of the potential rescuers of misfolding pathologies.

5.6. Acknowledgements

Mark Fisher (University of Kansas, Kansas City, USA) is gratefully acknowledged for support and for providing immobilised GroEL beads. Subhashchandra Naik (University of Kansas, Kansas City, USA) preformed the initial test to determine the optimal partitioning conditions.

Tiago Bandeiras (ITQB) is thanked for the knowledge and assistance on the DSF experiments.

5.7. References

1. Arakawa, T., et al., *Small molecule pharmacological chaperones: From thermodynamic stabilization to pharmaceutical drugs.* Biochim Biophys Acta, 2006. **1764**(11): p. 1677-87.
2. Kolter, T. and M. Wendeler, *Chemical chaperones--a new concept in drug research.* Chembiochem, 2003. **4**(4): p. 260-4.
3. Loo, T.W. and D.M. Clarke, *Chemical and pharmacological chaperones as new therapeutic agents.* Expert Rev Mol Med, 2007. **9**(16): p. 1-18.
4. Welch, W.J. and C.R. Brown, *Influence of molecular and chemical chaperones on protein folding.* Cell Stress Chaperones, 1996. **1**(2): p. 109-15.
5. Howard, M. and W.J. Welch, *Manipulating the folding pathway of delta F508 CFTR using chemical chaperones.* Methods Mol Med, 2002. **70**: p. 267-75.
6. Rubenstein, R.C. and P.L. Zeitlin, *A pilot clinical trial of oral sodium 4-phenylbutyrate (Buphenyl) in deltaF508-homozygous cystic fibrosis patients: partial restoration of nasal epithelial CFTR function.* Am J Respir Crit Care Med, 1998. **157**(2): p. 484-90.
7. deCarvalho, A.C., et al., *A novel natural product compound enhances cAMP-regulated chloride conductance of cells expressing CFTR[delta]F508.* Mol Med, 2002. **8**(2): p. 75-87.
8. Van Goor, F., et al., *Rescue of DeltaF508-CFTR trafficking and gating in human cystic fibrosis airway primary cultures by small molecules.* Am J Physiol Lung Cell Mol Physiol, 2006. **290**(6): p. L1117-30.
9. Wang, Y., et al., *Correctors promote maturation of cystic fibrosis transmembrane conductance regulator (CFTR)-processing mutants by binding to the protein.* J Biol Chem, 2007. **282**(46): p. 33247-51.
10. Pey, A.L., et al., *Mechanisms underlying responsiveness to tetrahydrobiopterin in mild phenylketonuria mutations.* Hum Mutat, 2004. **24**(5): p. 388-99.
11. Leandro, P., et al., *Glycerol increases the yield and activity of human phenylalanine hydroxylase mutant enzymes produced in a prokaryotic expression system.* Mol Genet Metab, 2001. **73**(2): p. 173-8.
12. Tanaka, M., Y. Machida, and N. Nukina, *A novel therapeutic strategy for polyglutamine diseases by stabilizing aggregation-prone proteins with small molecules.* J Mol Med, 2005. **83**(5): p. 343-52.
13. Sawkar, A.R., et al., *Chemical chaperones and permissive temperatures alter localization of Gaucher disease associated glucocerebrosidase variants.* ACS Chem Biol, 2006. **1**(4): p. 235-51.
14. Cayley, S. and M.T. Record, Jr., *Roles of cytoplasmic osmolytes, water, and crowding in the response of Escherichia coli to osmotic stress: biophysical basis of osmoprotection by glycine betaine.* Biochemistry, 2003. **42**(43): p. 12596-609.
15. Timasheff, S.N., *Control of protein stability and reactions by weakly interacting cosolvents: the simplicity of the complicated.* Adv Protein Chem, 1998. **51**: p. 355-432.
16. Timasheff, S.N., *Protein hydration, thermodynamic binding, and preferential hydration.* Biochemistry, 2002. **41**(46): p. 13473-82.
17. Timasheff, S.N., *Protein-solvent preferential interactions, protein hydration, and the modulation of biochemical reactions by solvent components.* Proc Natl Acad Sci U S A, 2002. **99**(15): p. 9721-6.
18. Diamant, S., et al., *Chemical chaperones regulate molecular chaperones in vitro and in cells under combined salt and heat stresses.* J Biol Chem, 2001. **276**(43): p. 39586-91.
19. Correia, A.R., et al., *Dynamics, stability and iron-binding activity of frataxin clinical mutants.* FEBS J, 2008. **275**(14): p. 3680-90.

20. Naik, S., et al., *Identifying protein stabilizing ligands using GroEL*. Biopolymers, 2009.
21. Lavinder, J.J., et al., *High-throughput thermal scanning: a general, rapid dye-binding thermal shift screen for protein engineering.* J Am Chem Soc, 2009. **131**(11): p. 3794-5.
22. Senisterra, G.A. and P.J. Finerty, Jr., *High throughput methods of assessing protein stability and aggregation.* Mol Biosyst, 2009. **5**(3): p. 217-23.
23. Adinolfi, S., et al., *The factors governing the thermal stability of frataxin orthologues: how to increase a protein's stability.* Biochemistry, 2004. **43**(21): p. 6511-8.
24. Correia, A.R., et al., *Conformational stability of human frataxin and effect of Friedreich's ataxia-related mutations on protein folding.* Biochem J, 2006. **398**(3): p. 605-11.
25. Musco, G., et al., *Towards a structural understanding of Friedreich's ataxia: the solution structure of frataxin.* Structure, 2000. **8**(7): p. 695-707.
26. Katayama, H., et al., *GroEL as a molecular scaffold for structural analysis of the anthrax toxin pore.* Nat Struct Mol Biol, 2008. **15**(7): p. 754-60.
27. Voziyan, P.A., et al., *Designing a high throughput refolding array using a combination of the GroEL chaperonin and osmolytes.* J Struct Funct Genomics, 2005. **6**(2-3): p. 183-8.
28. Pace, C.N., et al., *Conformational stability and thermodynamics of folding of ribonucleases Sa, Sa2 and Sa3.* J Mol Biol, 1998. **279**(1): p. 271-86.
29. Bross, P., et al., *Effects of two mutations detected in medium chain acyl-CoA dehydrogenase (MCAD)-deficient patients on folding, oligomer assembly, and stability of MCAD enzyme.* J Biol Chem, 1995. **270**(17): p. 10284-90.
30. Hansen, J., N. Gregersen, and P. Bross, *Differential degradation of variant medium-chain acyl-CoA dehydrogenase by the protein quality control proteases Lon and ClpXP.* Biochem Biophys Res Commun, 2005. **333**(4): p. 1160-70.
31. Santisteban, I., et al., *E. coli expression system for identifying folding mutations of human adenosine deaminase.* Methods Mol Biol, 2003. **232**: p. 175-82.
32. Rubenstein, R.C. and B.M. Lyons, *Sodium 4-phenylbutyrate downregulates HSC70 expression by facilitating mRNA degradation.* Am J Physiol Lung Cell Mol Physiol, 2001. **281**(1): p. L43-51.
33. Basseri, S., et al., *The chemical chaperone 4-phenylbutyrate inhibits adipogenesis by modulating the unfolded protein response.* J Lipid Res, 2009. **50**(12): p. 2486-501.
34. Iordache, C. and M. Duszyk, *Sodium 4-phenylbutyrate upregulates ENaC and sodium absorption in T84 cells.* Exp Cell Res, 2007. **313**(2): p. 305-11.
35. Naik, S., et al., *Identifying protein stabilizing ligands using GroEL*. Biopolymers, 2010. **93**(3): p. 237-51.
36. Auton, M. and D.W. Bolen, *Predicting the energetics of osmolyte-induced protein folding/unfolding.* Proc Natl Acad Sci U S A, 2005. **102**(42): p. 15065-8.
37. Bolen, D.W., *Effects of naturally occurring osmolytes on protein stability and solubility: issues important in protein crystallization.* Methods, 2004. **34**(3): p. 312-22.
38. Courtenay, E.S., et al., *Vapor pressure osmometry studies of osmolyte-protein interactions: implications for the action of osmoprotectants in vivo and for the interpretation of "osmotic stress" experiments in vitro.* Biochemistry, 2000. **39**(15): p. 4455-71.
39. Pradeep, L. and J.B. Udgaonkar, *Osmolytes induce structure in an early intermediate on the folding pathway of barstar.* J Biol Chem, 2004. **279**(39): p. 40303-13.
40. Dhe-Paganon, S., et al., *Crystal structure of human frataxin.* J Biol Chem, 2000. **275**(40): p. 30753-6.

CHAPTER 6

THE CONSERVED TRP-155 IN HUMAN FRATAXIN AS A HOTSPOT FOR OXIDATIVE RELATED CHEMICAL MODIFICATIONS

This Chapter was published in:

Ana R. Correia, Saw Y. Ow, Phillip C. Wright, Cláudio M. Gomes. "The conserved Trp-155 in human frataxin as a hotspot for oxidative stress related chemical modifications"

*BBRC,**390**(3):1007-11 (2009)*.

The MS analysis were carried out by Saw Y. Ow at ChELSI, University of Sheffield,UK.

6.1. Summary

Frataxin is a mitochondrial protein that is defective in Friedreich's ataxia (FRDA), resulting in iron accumulation and in an environment prone to Fenton reactions. Its cellular function, as well as its location, make frataxin a potential target for chemical oxidative modifications in the context of FRDA. Here, we analysed the impact of carbonylation and nitration on the structure and function of human frataxin. We found frataxin to be susceptible to carbonylation and nitration modifications in residues at the β-sheet surface (Tyr143, Tyr174, Tyr205 and Trp155). Frataxin functions are not significantly affected: frataxin-mediated protection against ROS is still observed as well as iron-binding necessary for the metallochaperone activity (5 $Fe^{3+}.mol^{-1}$, K_d=13-36 μM). However, the protein is up to 1.0 $kcal.mol^{-1}$ destabilised and the conformation opens. Interestingly, the strictly conserved Trp155, which is mutated in patients, may be a functional hotspot in frataxin.

6.2. Introduction

Frataxin function is not fully established but this essential protein was found to be involved in iron homeostasis, Fe-S cluster and heme biosynthesis, and metabolism of reactive oxygen species (ROS) [1-4]. The relationship between oxidative stress and FRDA is rather controversial. On the one hand, oxidative stress markers are used to monitor disease progression in patients [5-6], following the proposal that oxidative stress is involved in the pathogenic process [7-8]. On the other

hand, the fact that over-expression of antioxidant enzymes (SOD1, SOD2 and Cat) in fly and mouse models expressing low levels of frataxin fails to rescue the FRDA phenotype does not support the hypothesis that oxidative stress has a major role in FRDA pathogenesis [9-10]. Further, under aerobic conditions, the absence of frataxin in yeast results in aconitase degradation and accumulation of oxidatively modified proteins in both the cytosol and mitochondria, which lead to Pim1 expression and proteasome inhibition [11]. In any case, either directly or indirectly, frataxin seems to be important for maintaining the oxidative balance in the mitochondria. A question that remains to be answered is what happens to frataxin itself when iron accumulates in the mitochondria and oxidative stress arises. This is a pertinent point as frataxin is present in all FRDA patients, although at reduced levels. A priori, frataxin is a potential target for oxidative stress modifications, not only due to the fact that is localised in mitochondria, where oxygen and nitric oxide are available in a reducing environment, but also as a result of its iron-binding properties. Here we address whether human frataxin can be a target of oxidative stress related modifications, such as carbonylation and nitration, and if so, on which positions this occurs and what would be the structural and functional consequences of such modifications.

6.3. Materials and Methods

Protein production

Frataxin (91-210) was expressed in Escherichia. coli (competent cells BL21(DE3) from Novagen) as fusion proteins with a His-tag and purified as previously described [12-13]. The frataxin core construct

FXN (91-210), previously shown to keep the protein fold, stability and functional properties of the mature variant [14], was used in this study.

Metal-catalysed oxidation

Frataxin (50μM) was incubated at 37ºC in 10mM Tris buffer pH 7.0 supplemented with 0.2 mM $FeSO_4$ and 2mM hydrogen peroxide (H_2O_2). The concentration of H_2O_2 was determined spectrophotometrically at 240nm (ε^{240} = 0.0394 $mM^{-1}.cm^{-1}$). The reaction was stopped after 2h by addition of diethylene triamine pentaacetic acid (DTPA, final concentration 50mM) and catalase (final concentration 0.3 nM). Subsequently, the protein was applied on a desalting column to remove excess iron and H_2O_2 for further analysis.

$$Fe^{2+} + H_2O_2 \rightarrow Fe^{3+} + {}^{\bullet}OH + OH^-$$

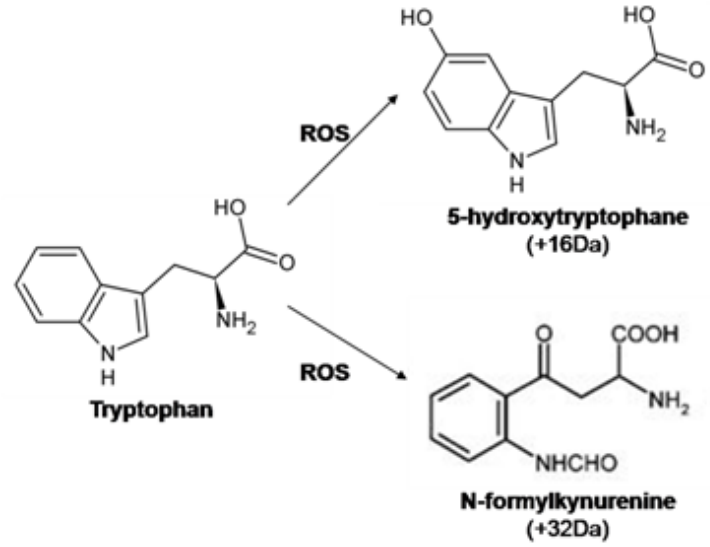

Figure 6.1: Top. Iron Fenton reaction. **Bottom.** Tryptophan carbonylation.

Nitration reactions

Frataxin (50μM) was incubated in 200 mM potassium phosphate pH 7.0, 25μM DTPA and 500μM peroxynitrite (ONOO-) for 2h. Peroxynitrite was synthesised and stored at -80ºC as described in [15], just before each nitration reaction ONOO- was thawed and the concentration measured spectrophotometrically at 302 nm (ε^{302} = 1,670 $M^{-1} \cdot cm^{-1}$). After the nitration reaction the excess of ONOO- was removed by passing the protein solution through a desalting column.

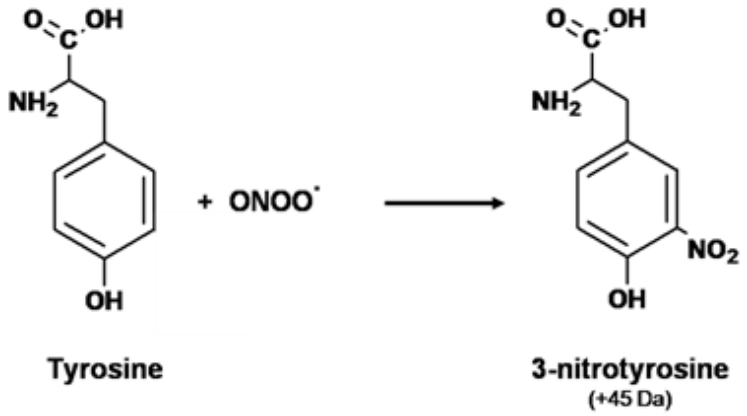

Figure 6.2: Nitration reaction of Tyrosine by peroxynitrite. Modified peptides will present a characteristic mass shift of +(n×45) Da due to the addition of n×NO_2 as a consequence of the nitration reaction.

Analysis of protein modifications by mass spectrometry

Modified and unmodified frataxin were resuspended in 0.5M triethylammonium bicarbonate pH 7.5 and digested using sequencing grade trypsin (Promega; 1:50 trypsin to sample ratio). Digested aliquots containing 200fmol of FXN were eluted independently on a 300μm x 150mm Atlantis dC18 reverse phase (3μm, Waters Corporation,

Lancashire UK) capillary LC column via an Ultimate 3000 (Dionex, Surrey UK) capLC-MS. The LC-CapESI interface (typical voltage of 4kV) was interfaced to both the maXis ESI-Q-UHR-TOF and HCT Ultra ESI-Q-Ion Trap (Bruker Daltonics, Coventry UK). Maintenance for ultra high resolution scans on the maXis (42k resolving power) and focus mass for the Ion Trap were achieved using Tunemix reference standard 922 m/z (Agilent, Cheshire UK). All ion trap accumulations were dynamically controlled to either achieve 200000 ions or no less than 5 Hz. Confirmatory SRM-MS/MS analysis of all identified modification sites were performed using CapLC MRM-MS/MS scans at a 250000 charge limit. Data interrogation of site modifications and unmodified peptides were provided via manual spectra sequencing, and automated in-house Phenyx server v2.5 (Genebio, Geneva, Switzerland) database searching. Additional parameters and criteria for peptide matching are available as supplementary materials.

Thermal stability

Thermal denaturation experiments were performed as previously described, using 8 μM frataxin in 10mM HEPES pH 7.0 [12-13] and using circular dichroism and fluorescence spectroscopy to monitor conformational changes during heating.

Limited proteolysis

Frataxin (modified and control) was incubated with trypsin (bovine pancreas trypsin, sequencing grade, Sigma) at 37°C in 0.1 M Tris-HCl pH 8.5 in a 100 fold excess over the protease, during 90 min. Aliquots (~0.5 nmol protein) were subsequently analysed by reverse-phase HPLC as described in [12-13]. For comparing the extension of proteolysis among different preparations, the sum of the integrated peak

areas was determined for each tryptic map. The variations in the relative proteolytic susceptibility were determined from modified/unmodified ratios.

Frataxin functional assays

Iron binding to FXN was determined by monitoring quenching of tryptophan fluorescence (λ_{exc}=290 nm and λ_{em}=340 nm) during a titration of frataxin (10 μM) with Fe(III), which has allowed to calculate the fraction of binding sites occupied, as described in [4, 12-13]. The attenuation of Fenton chemistry by frataxin was assessed following the oxidative degradation assay described elsewhere [16-17].

6.4. Results

6.4.1. Frataxin Carbonylation and Nitration

We have investigated whether human frataxin can be a target for oxidative stress related modifications, such as carbonylation and nitration, by exposing frataxin to conditions mimicking oxidative stress. We have analysed the effects of the hydroxyl radical (OH•) and peroxynitrite (ONOO-) on human frataxin (FXN). While OH• attack to proteins leads to the formation of carbonyls (e.g. [18]), the reaction with ONOO- results in the nitration of amino acid side chains [18-20]. The differences between the exposed and unmodified FXN species were evaluated for nitration and carbonylation using tandem MS. Seven different unmodified tryptic peptides of FXN were identified, corresponding to 85% of the total protein sequence (**Fig. 6.3**). After

carbonylation and nitration reactions no peptide fragmentation was detected. MS/MS and SRM-MS/MS analysis identified four potentially modified peptides with a +45 Da mass shift after peroxynitrite treatment. The +(n×45) Da mass shift is characteristic of the n×NO2 addition in nitrated peptides. Subsequent stepwise fragmentation (SPS SmartFrag) of these ions provided site-specific confirmation of four +45 Da amino acid positions.

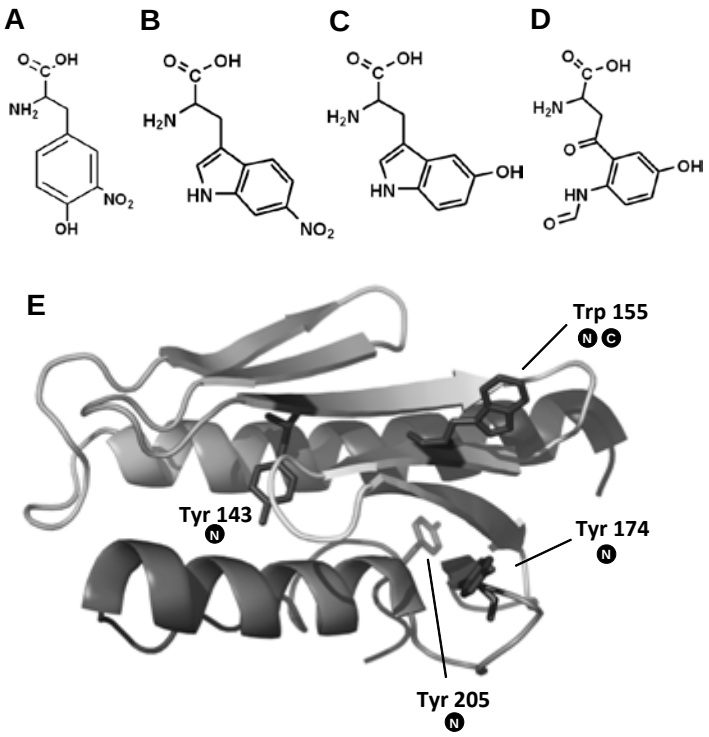

Figure 6.3: (A-D) Structure of the modified Trp and Tyr identified in frataxin subsequently to carbonylation and nitration. (A) 3-nitroyrosine; (B) 6-nitrotryptophane; (C) 5-hidroxytryptophane; (D) N-formylkynurenin; (E) Ribbon representation of human frataxin structure (PDB ID: 1EKG). Modified residues are labeled and represented sticks.

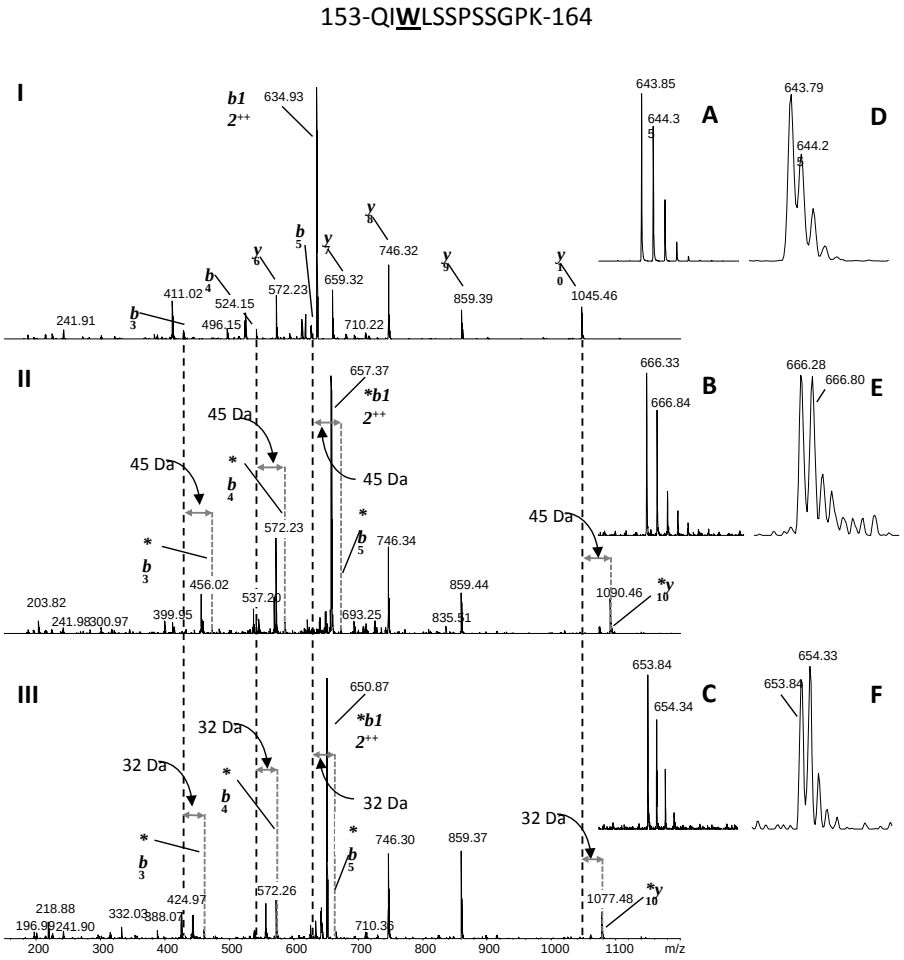

Figure 6.4: Mass spectra of Human frataxin peptide 153-QIWLSSPSSGPK-164. LC-MS/MS peptide sequencing and site-specific determination for nitration and carbonylation in doubly charged FXN peptide QIWLSSPSSGPK. Intact peptide mass MS scans; UHR-TOF scans (**A: unmodified, B: nitrated, C: carbonylated**); Ion Trap scans (D: unmodified, E: nitrated, F: carbonylated). Fragment spectra (MS/MS) of QIWLSSPSSGPK in unmodified (I), Trp nitrated (II) and Trp carbonylated (III) form. The peptide nitration site and its associated ions exhibit a characteristic +45 Da mass shift on singly charged species, and +22.5 Da on doubly charged species. Carbonylated Trp (W) and associated ions show two distinct stages of modification resulting in a +16 Da (not shown) or +32 Da shift. Subfigure III shows the latter with the characteristic +32 and +16 Da shifts on singly and doubly charged species. Remark: asterisks (*) denote ions carrying site of modification, y^n and b^n denotes the y and b collision induced fragment ion series. ++ denotes doubly charges ion series species.

Nitration was identified on three tyrosines (**Fig.6.2**, 3-nitrotyrosine; Tyr143, Tyr174, Tyr205) and on one tryptophan (6-nitrotryptophane, Trp155). We observed that the treatment with $OH^{\bullet}$ resulted in less extensive modifications: only a single tryptophan residue (Trp155) was found to be carbonylated (**Fig. 6.1 and 6.4**). The carbonylation of Trp155 leads to the formation of 5-hydroxytryptophan and N-formylkynurenine, two common modifications [20-22] which result in mass shifts of +16Da and +32Da, respectively. Interestingly, it was observed that Trp-155 is a target for both carbonylation and nitration. Considering that Trp-155 is strictly conserved among frataxin homologues, this observation suggests that this position could be a hot spot for oxidative stress modifications.

6.4.2. Effect on Frataxin Functions

Functionally, frataxin has been suggested to play a role in preventing the iron-mediated production of hydroxyl free radicals [16-17, 23], therefore we have analysed whether this role as an oxidative stress protector was impaired by oxidative stress related modifications. For the purpose, we have followed the production of $OH^{\bullet}$ by the Fenton reaction using the deoxyribose assay as described [24]. In agreement with previous observations, we have noted that unmodified frataxin is able to reduce $OH^{\bullet}$ production to nearly half of the values observed in its absence. This function is not affected by frataxin carbonylation nor by its nitration, as the modified frataxins retained the ability to prevent Fenton reactions at the same level as the unmodified frataxin (**Fig. 6.5**).

One of the other proposed roles of frataxin is that of an iron-chaperone. Human FXN binds 6-7 $Fe^{3+}.mol^{-1}$ at a K_d of 17 μM [4] and is involved in pathways leading to the biosynthesis of Fe-S clusters [4]. We have investigated if this function would be perturbed by the modifications and we have found that neither carbonylation nor nitration abolish iron binding, although the stoichiometry is slightly decreased to 5.5 ± 0.4 $Fe^{3+}.mol^{-1}$ (n=5) for both cases and the binding affinities remain either unaltered in nitrated frataxin (K_d=14.0 ± 1.1 μM, n=2) or slightly decreased in the carbonylated protein (K_d=34.0 ± 2.0 μM, n=3).

6.4.3. Impact on Frataxin Conformation and Stability

The effect of the chemical modifications on the protein structure and stability was also investigated. The protein fold did not change upon the modifications but, on the other hand, there was an effect on protein stability: nitration has a rather significant effect (ΔT_m=-5°C), whereas carbonylation reactions are less perturbing (ΔT_m=-1.6°C) (**Fig. 6.6** and **Table 6.1**). The modifications also decrease the refolding efficiency upon thermal denaturation, as the reactions are still reversible, but at lower yields.

Table 6.1: Thermodynamic stability from thermal denaturation of modified frataxins.

Frataxin variants	**T_m** (ºC)	**ΔH_m** (kcal.mol^{-1})	**ΔT_m (ºC)**	**ΔG^a** (cal/mol)	**$\Delta(\Delta G)^b$** (cal/mol)	**Refolding** %
Unmodified	60.0 ± 0.1	68.6 ± 1.8	-	4462	-	95
Nitrated	55.0 ± 0.2	60.1 ± 2.8	-5.0 ± 0.3	3457	-916	70
Carbonylated	58.4 ± 0.2	64.9 ± 3.5	-1.6 ± 0.3	4030	-313	40

[a] ΔG at 25ºC for ΔC_p= 12 cal/mol/K; [b] $\Delta(\Delta G) = [\Delta(T_m)] \times \Delta S_m = [\Delta(T_m)] \times (\Delta H_m/T_m)$, where ΔS_m and ΔH_m are values for the wild type.

We have investigated if the modifications would promote frataxin oligomerisation and aggregation that could affect the refolding reaction. However, we could not detect the formation of oligomers when nitrated and carbonylated apo frataxin (50μM) were analysed using gel filtration. To probe for the effect of chemical modifications on frataxin flexibility, we have carried out limited proteolysis experiments using trypsin. The susceptibility to degradation was evaluated comparing the HPLC tryptic peptide maps after a 90 minute digestion at 37°C (**Fig. 6.6B**). The data shows that, whereas carbonylation does not enhance proteolysis in comparison with unmodified frataxin, nitration does increase the flexibility and induces opening of the conformation, making more sites available for cleavage and yielding a higher number of peptides.

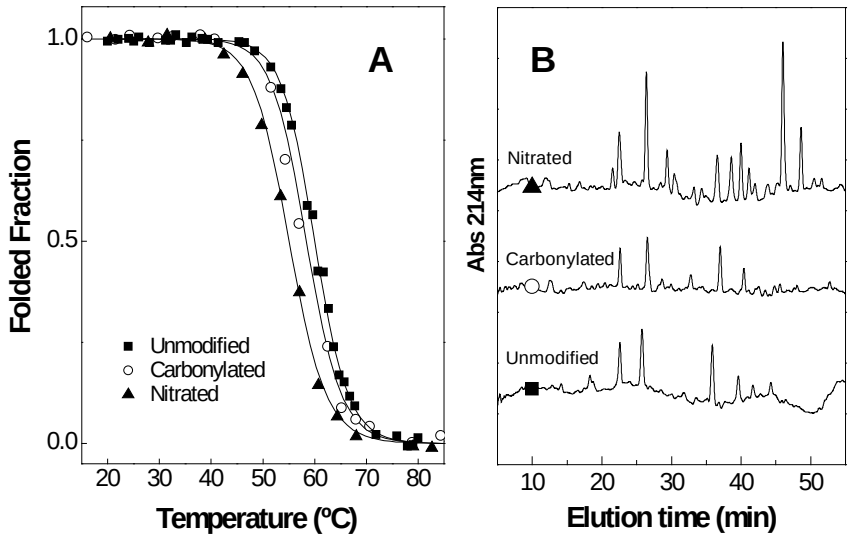

Figure 6.6: Effect of oxidative related modification on frataxin thermal stability (A) and proteolytic susceptibility of (B) unmodified frataxin (■) carbonylated (○) and nitrated (▲) variants. (A) Thermal denaturation curves. Lines represent fits to a two state model [25], see Table 1 for parameters; (B) Peptide maps resulting from

HPLC analysis of partial tryptic digestions. The yy-axis represents absorbance at 214nm and chromatograms are normalized for digested frataxin concentrations, which was always the same for comparison purposes.

6.5. Discussion

All Friedreich's ataxia patients express frataxin, although at much reduced levels. Within their mitochondria, iron accumulation and the presence of oxygen and nitric oxide in a reducing environment make frataxin a likely target for oxidative damage. We have addressed this hypothesis and here we have shown that, under oxidative stress conditions, frataxin is indeed modified with some compromise of the conformational properties but without a functional impairment. Structural mapping of the modified residues showed that most of the modifications occur on the β-sheet, a region of the protein believed to be involved in protein-protein interactions (**Fig. 6.3E**). We have identified four targets of oxidative modifications: Tyr143, Tyr175, Tyr205 and Trp155. All are targets for nitration but Trp155 is the only carbonylated amino acid. In fact, it is interesting to notice that Trp155 is particularly susceptible to modifications since it is both carbonylated and nitrated. There are two factors that may account for this increased susceptibility of Trp155 towards modifications. One could be that Trp is highly susceptible to oxidative stress modifications; however, the specific analysis of other residues (Trp168 and Trp173) showed that they are not modified, excluding a bias for Trp oxidation. The other more plausible aspect is that the location of this amino acid and its orientation specifically facilitate modification. Indeed, Trp155 is strictly conserved across frataxin homologues and is located at the protein surface with the aromatic ring turned to the outside. Further, one other interesting aspect

is that the Trp155Arg mutation is found among FRDA compound heterozygotes [26]. Previously, we have characterised the impact of this mutation at the protein level and we have noticed that it does not disrupt the frataxin fold, but does increase the susceptibility towards proteolytic degradation, and partly compromises iron binding [12-13]. So, it might be relevant in the FRDA context, that a residue whose mutations result in FRDA is also a hot spot for carbonylation and nitration modifications. Future work made possible by the observations here reported will hopefully allow for the establishment of the effect of oxidative modifications on the frataxin interactome.

6.6. Acknowledgements

Annalisa Pastore (NIMR, UK) is gratefully acknowledged for support and sharing of plasmids. This work was partly supported by a collaborative grant from the Conselho Reitores das Universidades Portuguesas (CRUP, Portugal to C.M.G.) and National Ataxia Foundation Grant (to CMG).

Paula Chicau (Amino Acid Analysis Service, ITQB) is gratefully acknowledged for technical assistance on the HPLC separations of the limited proteolysis experiments.

The British Council Portugal (Treaty of Windsor Programme) and the UK's EPSRC are acknowledged for funding (GR/S84347/01 and EP/E036252/1).

6.7. References

1. Delatycki, M.B., R. Williamson, and S.M. Forrest, *Friedreich ataxia: an overview.* J Med Genet, 2000. **37**(1): p. 1-8.
2. Huynen, M.A., et al., *The phylogenetic distribution of frataxin indicates a role in iron-sulfur cluster protein assembly.* Hum Mol Genet, 2001. **10**(21): p. 2463-8.
3. Muhlenhoff, U., et al., *The yeast frataxin homolog Yfh1p plays a specific role in the maturation of cellular Fe/S proteins.* Hum Mol Genet, 2002. **11**(17): p. 2025-36.
4. Yoon, T. and J.A. Cowan, *Iron-sulfur cluster biosynthesis. Characterization of frataxin as an iron donor for assembly of [2Fe-2S] clusters in ISU-type proteins.* J Am Chem Soc, 2003. **125**(20): p. 6078-84.
5. Piemonte, F., et al., *Glutathione in blood of patients with Friedreich's ataxia.* Eur J Clin Invest, 2001. **31**(11): p. 1007-11.
6. Schulz, J.B., et al., *Oxidative stress in patients with Friedreich ataxia.* Neurology, 2000. **55**(11): p. 1719-21.
7. Emond, M., et al., *Increased levels of plasma malondialdehyde in Friedreich ataxia.* Neurology, 2000. **55**(11): p. 1752-3.
8. Puccio, H. and M. Koenig, *Friedreich ataxia: a paradigm for mitochondrial diseases.* Curr Opin Genet Dev, 2002. **12**(3): p. 272-7.
9. Anderson, P.R., et al., *RNAi-mediated suppression of the mitochondrial iron chaperone, frataxin, in Drosophila.* Hum Mol Genet, 2005. **14**(22): p. 3397-405.
10. Seznec, H., et al., *Friedreich ataxia: the oxidative stress paradox.* Hum Mol Genet, 2005. **14**(4): p. 463-74.
11. Bradley, J.L., et al., *Role of oxidative damage in Friedreich's ataxia.* Neurochem Res, 2004. **29**(3): p. 561-7.
12. Correia, A.R., et al., *Dynamics, stability and iron-binding activity of frataxin clinical mutants.* Febs J, 2008. **275**(14): p. 3680-90.
13. Correia, A.R., et al., *Conformational stability of human frataxin and effect of Friedreich's ataxia-related mutations on protein folding.* Biochem J, 2006. **398**(3): p. 605-11.
14. Musco, G., et al., *Towards a structural understanding of Friedreich's ataxia: the solution structure of frataxin.* Structure Fold Des, 2000. **8**(7): p. 695-707.
15. Radi, R., et al., *Peroxynitrite oxidation of sulfhydryls. The cytotoxic potential of superoxide and nitric oxide.* J Biol Chem, 1991. **266**(7): p. 4244-50.
16. Park, S., et al., *The ferroxidase activity of yeast frataxin.* J Biol Chem, 2002. **277**(41): p. 38589-95.
17. Kondapalli, K.C., et al., *Drosophila frataxin: an iron chaperone during cellular Fe-S cluster bioassembly.* Biochemistry, 2008. **47**(26): p. 6917-27.
18. Radi, R., *Nitric oxide, oxidants, and protein tyrosine nitration.* Proc Natl Acad Sci U S A, 2004. **101**(12): p. 4003-8.
19. Alvarez, B. and R. Radi, *Peroxynitrite reactivity with amino acids and proteins.* Amino Acids, 2003. **25**(3-4): p. 295-311.
20. Dean, R.T., et al., *Biochemistry and pathology of radical-mediated protein oxidation.* Biochem J, 1997. **324 (Pt 1)**: p. 1-18.
21. Finley, E.L., et al., *Identification of tryptophan oxidation products in bovine alpha-crystallin.* Protein Sci, 1998. **7**(11): p. 2391-7.
22. Guptasarma, P., et al., *Hydroxyl radical mediated damage to proteins, with special reference to the crystallins.* Biochemistry, 1992. **31**(17): p. 4296-303.
23. Ding, H., et al., *Distinct iron binding property of two putative iron donors for the iron-sulfur cluster assembly: IscA and the bacterial frataxin ortholog CyaY under*

physiological and oxidative stress conditions. J Biol Chem, 2007. **282**(11): p. 7997-8004.
24. Halliwell, B. and J.M. Gutteridge, *Formation of thiobarbituric-acid-reactive substance from deoxyribose in the presence of iron salts: the role of superoxide and hydroxyl radicals.* FEBS Lett, 1981. **128**(2): p. 347-52.
25. Pace, C.N., et al., *Conformational stability and thermodynamics of folding of ribonucleases Sa, Sa2 and Sa3.* J Mol Biol, 1998. **279**(1): p. 271-86.
26. Cossee, M., et al., *Friedreich's ataxia: point mutations and clinical presentation of compound heterozygotes.* Ann Neurol, 1999. **45**(2): p. 200-6.

CHAPTER 7 IRON BINDING ACTIVITY IN YEAST FRATAXIN ENTAILS A TRADE OFF WITH STABILITY IN THE α1/β1 ACIDIC RIDGE REGION

This chapter was published in:

Ana R. Correia, Tao Wang, Elizabeth A. Craig and Cláudio M. Gomes. "Iron binding activity in yeast frataxin entails a trade off with stability in the a1/b1 acidic ridge region"

Biochemical J., **426**(2):197-203 (2010).

The yeast growth experiments as well as the quantification of the aconitase activity were performed by Tao Wang from University of Wisconsin, USA.

7.1. Summary

To better understand the functional characterisation of frataxin structure, we have here characterised eight frataxin variants involving mutations on two putative functional regions – the $\alpha 1/\beta 1$ acidic ridge and the conserved β-sheet surface. It is shown that frataxin iron binding capacity is quite robust: even when five of the most conserved residues from the putative iron binding region are mutated, the protein still binds iron (~2 iron atoms per monomer), although with decreased affinity. Furthermore, the data suggest that the acidic ridge is designed to favour function over stability. The negative charges have a functional role but, at the same time, also significantly impair frataxin's stability. Removing five of those charges results in a thermal stabilisation of ~24ºC and reduces the inherent conformational plasticity. Mutations on the conserved β-sheet residues have only a modest impact on the protein stability, highlighting the functional importance of residues 122-124.

7.2. Introduction

The human and yeast frataxin orthologs have a high degree of amino acid (65%) and structural identity. The phenotype observed as a consequence of frataxin's deficiency is very similar in human and yeast cells [1-2]. Hence, the yeast model system has been frequently used to study frataxin's function, as well as the pathological events associated with FRDA. Yeast frataxin, Yfh1, is not absolutely essential, but its absence causes severe growth defects and a reduction in the activity of Fe-S cluster–containing enzymes, such as aconitase [1-4]. Iron binding by frataxins, a requirement for a role as a metallochaperone, has been well documented by several laboratories [5-7]. Frataxins bind iron at

micromolar binding affinities with different stoichiometries: while monomeric human frataxin binds 6/7 iron ions (K_d ~ 12-55μM [7]), monomeric frataxin from *Drosphila* binds 1 ferrous iron (K_d ~6μM, [6]) and yeast frataxin binds 2 ferrous irons (K_d ~2.5μM, [5]). This variability suggests a certain plasticity of the frataxin fold in respect to binding iron. In fact, an NMR based investigation of the iron binding to Yfh1 at low stoichiometry (up to 2Fe:Yfh1) denoted changes in 10 distinct residues [8], which could indicate long range effects upon iron binding or lower affinity sites. More complex effects arise at higher Fe:Yfh1 stoichiometries. Like human frataxin, Yfh1 undergoes iron-dependent oligomerisation, above a threshold of 2 irons per monomer, according to the progression $\alpha \rightarrow \alpha_3 \rightarrow \alpha_6 \rightarrow \alpha_{12} \rightarrow \alpha_{24} \rightarrow \alpha_{48}$ [9-10]. This property has been established as important for iron-induced oxidative stress protection, but not for Fe-S cluster biogenesis [3, 11].

The first helix (α1) and the edge of the first β-strand (β1) form a semi-conserved acidic ridge that constitutes the putative iron binding region of the protein [5, 8, 12]. A set of conserved residues in the β-sheet surface constitutes the other putative functional region of the protein, believed to be involved in the binding of frataxin to its protein partners [8, 13]. Recently it has been shown that mutations at the conserved β-sheet residues 122-124 affect neither iron binding capacity nor the oligomerisation properties of frataxin, these mutations, however, do compromise the interaction with Isu [14]. To complement previous functional characterisation of *YFH1* mutants, here we address the structural and conformational effects of eight functional mutants in yeast frataxin that alter either the acid ridge or conserved residues on the β-sheet surface. We found that the negatively charged residues in the acid ridge that are important for iron binding reduce Yfh1's stability,

indicating a trade-off between functionality and stability. In addition, alterations in the conserved residues of the portion of the acid ridge found in the β-sheet affected interaction with the scaffold protein Isu but did not affect overall protein stability.

7.3. Materials and Methods

Yeast strains, plasmids and media.

Saccharomyces cerevisiae strains carrying *YFH1* mutant or wild type genes on plasmids were created by sporulation and dissection of *YFH1/yfh1Δ* (W303 background) transformed with the plasmids. *YFH1* mutants were generated by site-directed mutagenesis using pCM189-YFH1 as a template, having *YFH1* under the control of the tetO promoter [15]. Constructs containing the following mutations were prepared: yfh1-D86A/E90A/E93A, yfh1-D101A/E103A, yfh1-D86A/E90A/E93A/D101A/E103A, yfh1-N122A, yfh1-N122K (corresponding to the human clinical mutation N146K), yfh1-K123T, yfh1-Q124A and yfh1-N122A/K123T/Q124A. Doxycycline was used at 1 μg/ml to reduce expression. Cells were grown in minimal synthetic media with –ura DO at 30ºC for 2 days.

Aconitase activity in isolated mitochondria.

Mitochondria were isolated, according to the method described in [16], from cells grown in synthetic minimal media (-ura) in the absence of doxycycline. Aconitase activity was measured in isolated mitochondria by monitoring the decrease in the absorbance of the substrate isocitrate at 240 nm as described in [17].

Gene Expression and Protein purification.

The mature form of Yfh1 (amino acids 52-174) with an N-terminal His tag and a thrombin cleaving site in between were cloned into pET-3a vector (Novagen, Madison, WI, USA) [3]. Protein expression was induced over 3h at 37ºC in BL21(DE3) *E. coli* by adding IPTG (isopropyl-b-galactopyranoside) at a final concentration of 0.5mM. With the exception of Yfh1-K123T, which was expressed at much lower levels (approximately 30%), all other mutant variants had expression levels identical to those of the wild type Yfh1. The reduced expression levels of Yfh1-K123T had already been described when expressing this mutant in yeast [14]. Under the tested conditions, wild type Yfh1 was exclusively expressed as a soluble protein, as was most of the mutants. The only exceptions are Yfh1-86/90/93A, Yfh1-N122A and Yfh1-N122A/K123/Q124A, in which ~15% of the expressed protein was found in the insoluble fraction. After harvesting the cells, they were lysed on a French press. Cell lysate was subjected to His-binding resin (Amersham) chromatography and the protein was eluted with a gradient to 500mM Imidazole in the binding buffer (50mM Tris-HCl Ph8.0, 200mM NaCl, 10mM Imidazole). The His tag was cleaved using biotinylated thrombin and thrombin was removed by streptavidin agarose (Amersham). When necessary (purity less than 90%) the protein was further purified by applying the sample on a Superdex 75. At the end, the buffer was changed to 10mM HEPES, 50mM NaCl pH 7.0 using Centricons (Millipore). Protein concentration was determined using the extinction coefficient ε^{280nm} = 15470 $M^{-1}.cm^{-1}$. The mature form of Isu1 (amino acids 35-165) with an His tag and a TEV cleaving site in between was cloned into pKLD37 vector. Protein expression was induced over 4h at 30ºC in C41 *E. coli* by adding IPTG (isopropyl-β-galactopyranoside) at a final concentration of 1mM. The purification was

performed as described above for the Yfh1 variants. Protein concentration was determined using the extinction coefficient ε^{280nm} = 14161.4 $M^{-1}.cm^{-1}$

Spectroscopic methods.

UV/Vis Spectra were recorded at room temperature in a Shimadzu UVPC-1601 spectrometer. Fluorescence spectroscopy was performed on a Cary Varian Eclipse instrument (λ_{ex} =280nm, λ_{em} =340nm, $slit_{ex}$: 5 nm, $slit_{em}$: 10 nm unless otherwise noted) equipped with cell stirring and Peltier temperature control. Far-UV CD spectra were recorded typically at 0.2 nm resolution on a Jasco J-715 spectropolarimeter fitted with a cell holder thermostated with a Peltier thermal cell.

Thermal denaturation. Thermal unfolding was followed by ellipticity ($\Delta\varepsilon_{mrw}$ at 222nm) variations and by Trp fluorescence spectroscopy. In all experiments, a heating rate of 1ºC/min was used, and the temperature was changed from 10 to 90ºC. All reactions were found to be reversible under the tested conditions, as inferred from obtaining identical far-UV CD spectra of the proteins before the thermal ramping and after cooling down the heated sample; a second temperature ramp of the same sample also yielded identical melting transitions. Protein aggregation was not observed during thermal unfolding. Data was analysed according to a two-state model and the thermodynamic data parameters were determined as in [18].

Trypsin limited proteolysis and LC-MS analysis. Frataxins were incubated with trypsin (bovine pancreas trypsin, sequencing grade, Sigma) at 37°C in 0.1 M Tris-HCl pH 8.5, in a 150 fold excess over the protease. Aliquots (300 μmol of protein) were sampled at different

incubation periods and the reaction was stopped by adding loading buffer with 5μM BSA followed by a 10min incubation at 100ºC. The products of the proteolysis reaction were analysed by SDS-PAGE [19].

Iron-binding assays. Yeast frataxin oligomerises in an iron-concentration dependent fashion but, at up to a stoichiometry of 2 irons per protein the protein, remains in the monomer form [8-10, 20]. To avoid side effects from different oligomerisation behaviours we have measured iron binding before oligomerisation takes place, i.e. up to a iron:protein ratio of 2. Trp fluorescence emission spectroscopy was used to monitor iron binding, which quenches Trp emission as the iron-frataxin complex is being formed. As previously shown, these methods yield results identical to those obtained by isothermal titration calorimetry [7, 21]. For the purpose, the quenching of the Trp fluorescence (λ_{exc}=290nm; λ_{em}=340 nm) of a 50μM solution of apo frataxin in 100mM HEPES pH 7.0, 50mM NaCl was measured upon stepwise addition of an iron citrate solution in 1 ml quartz cuvettes under continuous stirring. This data was used to calculate the fraction of binding sites occupied. The stoichiometry, p, and apparent dissociation constant, K_d, were then determined as described by Winzor and Sawyer [22].

Isu:Yfh1 interaction assay. Holo-Yfh1 was prepared using a stoichiometry of 2 irons per frataxin to avoid interference from oligomer formation. The formation of a Isu:holo-frataxin complex was followed monitoring frataxin Trp fluorescence, since yeast Isu does not contain any Trp residue. Thus, when Isu binds to holo-Yfh1, the Trp fluorescence emission (λ_{exc}=290nm; λ_{em}=340 nm) of the latter is quenched and this can be used to monitor binding. Holo-Yfh1 were

prepared in 100mM HEPES pH 7.0, 50mM NaCl. Aliquots of Isu were added to 2.5 mM holo frataxins under constant stirring. The stoichiometry, p, and apparent dissociation constant, K_d, were then obtained as described by Winzor and Sawyer [22].

7.4. Results

7.4.1. Frataxin's Cellular Function

To gain a better understanding of the relationship between the structure and function of frataxin, we compared four Yfh1 variants. Three variants (Yfh1-D101/E103A, Yfh1-D86/E90/E93A and a combination of these two, Yfh1-86/90/93/101/103A) alter the putative iron binding region at the α1/ β1 acidic ridge and oligomerisation region **(Fig. 7.1)**.

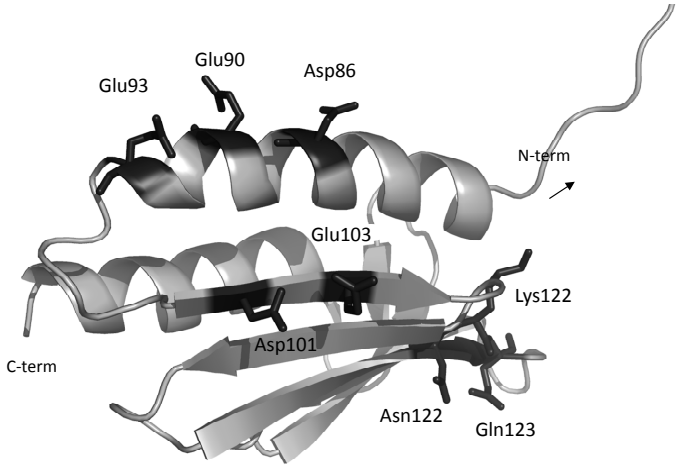

Figure 7.1: Yfh1 ribbon structure generated using PyMOL (PDB accession #2ga5). Mutated residues are represented by sticks, labelled and highlighted in black. The present study has focused on the structural and conformational characterisation of the following variants: Yfh1-D86A/E90A/E93A, Yfh1-D101A/E103A, Yfh1-D86A/E90A/E93A/D101A/E103A, Yfh1-N122A, Yfh1-N122K (corresponding to the human clinical mutation N146K), Yfh1-K123T, Yfh1-Q124A and Yfh1-N122A/K123T/Q124A.

The fourth, Yfh1-N122A/K123T/Q124A (hereafter referred to as Yfh1-122-4), alters the conserved β-sheet in the putative binding surface for interaction with Isu, the scaffold on which Fe-S clusters are built [14]. Since Yfh1 cellular levels can be significantly reduced before any growth defects are detected [23], wild type and mutant *YFH1* genes were placed under the control of the *tetO* promoter in order to be able to modulate protein expression using doxycycline. In this way, *in vivo* function could be tested under both normal and reduced levels of expression. At normal Yfh1 expression levels (*minus* doxycycline) all mutant genes were able to support the same growth as observed for the wild type **(Fig. 7.2)**.

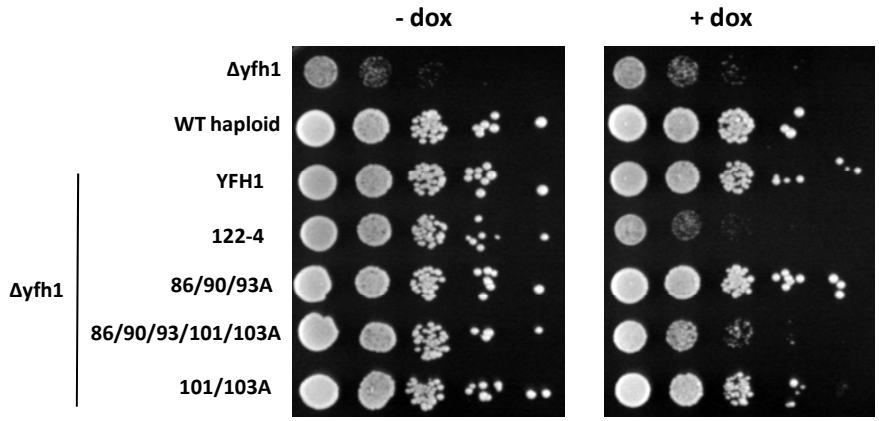

Figure 7.2: Growth of YFH1 mutants. 10-fold serial dilutions of cell suspension of wild type, Δ*yfh1* and Δyfh1 transformed with plasmids harbouring the indicated YFH1 mutant genes under the control of the tetO-regulatable wild type or mutant yfh1 were plated on minimal synthetic medium –ura DO containing (+) or lacking (-) doxycycline (dox). Plates were incubated at 30ºC for 2 days.

In addition, as we previously reported [3, 14], Yfh1-122-4 cells grew poorly when the variant was expressed at reduced levels (*plus* doxycycline), while cells expressing low levels of Yfh1-86/90/93A grew as well as wild type cells. Yfh1-101/103A cells growth was only slightly affected but, when these mutations were combined with those of Yfh1-86/90/93A, altering five of the charged residues in the acidic ridge, growth was severely compromised. Consistent with this growth impairment phenotype, mitochondria isolated fromYfh1-101/103A had lower levels of activity of the Fe-S enzyme, aconitase even when the mutant protein was expressed at normal levels **(Fig. 7.3)**. This effect was more extreme in Yfh1- 86/90/93/101/103A mitochondria, which had only 40% the aconitase activity of wild type mitochondria. Consistent with the effects on growth, Yfh1-122-4 mitochondria had only 20% the aconitase activity as wild type mitochondria.

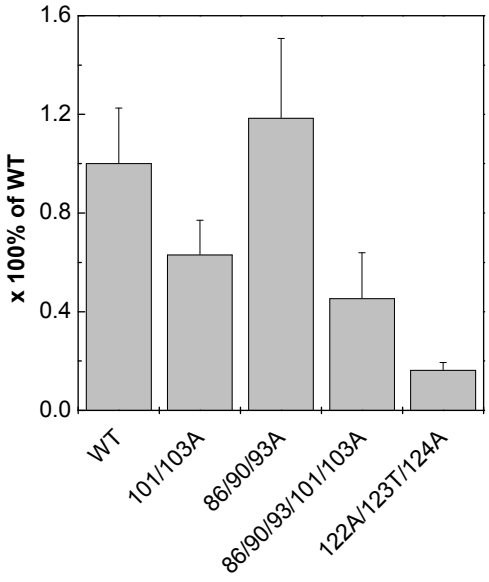

Figure 7.3: Aconitase activity. Measured for mutant mitochondria represented as a percentage of wild type aconitase activity.

7.4.2. Iron Binding

Since iron binding is an essential functional feature of frataxin, we asked if iron-binding properties of the Yfh1 variants were affected. In order to exclude iron-induced frataxin oligomerisation effects, we have investigated iron-binding at low stoichiometry (up to 2 Fe(II)/Yfh1), i.e. under conditions in which oligomerisation does not take place. We have used Trp-fluorescence to monitor iron binding to Yfh1 variants, as Trp emission is a specific reporter for iron-binding to frataxin. Our measurements indicated that mutations altering the iron binding region, D86A, E93A, D101A and E103A, had no effect on the iron binding capacity at low stoichiometry, the variants showed decreased binding affinity **(Table 7.1)**. Conversely, iron must be able to bind to frataxin through other residues, as even the quintuple mutant Yfh1-86/90/93/101/103A retained the ability to bind ~2 Fe(II)/Yfh1. We hypothesise that iron is binding to secondary sites with a lower affinity, as evidenced by the higher affinity constants (~20 μM). In fact, a previous NMR study[8] has shown that under identical conditions at low iron stoichiometry, iron binding to Yfh1 affected multiple sites: mainly interactions with carboxylate and nitrogen from acidic residues within the α1/β1 ridge (His83, Asp86, Glu93,

Table 7.1: Iron binding affinity determined by Trp fluorescence for Yfh1 and its functional mutants.

Protein	K_d (μM)[a]
Wild Type	10.4 ± 2.1
N122K	11.0 ± 3.8
N122A	14.0 ± 1.0
K123T	18.8 ± 2.4
Q124A	13.2 ± 3.8
N122A/K123T/Q124A	27.1 ± 1.0
101/103A	20.9 ± 0.6
86/90/93A	21.3 ± 1.0
86/90/93/101/103A	22.8 ± 0.9

[a](n=2)

His95, Asp101, Glu103), but other residues (Ala94, Leu104, Ser105 and Asn140) were also found to change their resonance positions upon binding of up to 2 irons per frataxin [8].

The lower binding affinity that we have determined in the Yfh1 variants (nevertheless still in the micromolar range comparable to that of human frataxins) could possibly indicate the recruitment of secondary positions, rather than unspecific binding. However, iron-binding remains functional, as shown by the fact that yeast expressing these variants still have some aconitase activity (**Fig. 7.3**), an activity that depends on frataxin-mediated iron transfer [24]. In addition, a previous study confirms our observations: single point mutations to alanine on residues 86, 90, 93, 101 and 103 reduce Yfh1 affinity to iron but do not abolish iron binding [11]. Single point mutations in the Asn122-Gln124 segment seem to have an intermediate effect in respect to the binding affinity (~14-18 μM). Presumably, alterations in the protein-protein interaction region of Yfh1 result in long-range effects on the iron-binding acid ridge leading to decrease of the iron binding affinity.

7.4.3. Isu Binding

Since low stoichiometry iron binding was not impaired in the mutants, we next evaluated whether the interaction between Yfh1 and Isu was compromised. This interaction is mediated by iron, as only holo-Yfh1 interacts with Isu [7]. Yfh1-86/90/93A was found to bind to Isu with a wild type like affinity (K_d ~5μM), while no interaction with Yfh1-122-4 was detected, which is consistent with previously published results [3] and [14], respectively. The fact that the alteration of residues 122, 123 and 124 individually (N122K, N122A, K123T or Q124A) severely affects the Isu interaction supports the hypothesis that all three residues are

important for this interaction. No interaction between Isu and Yfh1-101/103A (or Yfh1-96/90/93/101/103A) was detected in our *in vitro* assay. This reduced interaction is somewhat surprising considering that Yfh1-101/103A could significantly rescue the growth defect of *yfh1*Δ cells, even when expressed at low levels **(Fig. 7.2).** Mutating these two residues have only been found to cause a growth defect when the alterations are to lysines and the medium is supplemented with high levels of iron [4]. *In vivo,* other cellular factors may promote the interaction between Yfh1-101/103A and Isu, explaining the difference between the *in vivo* and *in vitro* results. Indeed frataxin was found to interact with Isd11 of the Nfs1/Isu complex and multiple mitochondrial chaperones [25]. It appears that significantly reduced affinity may be tolerated *in vivo*.

7.4.4. Activity-Stability Trade-off

In order to evaluate if functional impairments may result from decreased protein stability, the effect of the alterations on Yfh1 folding thermodynamics was analysed by comparing the thermal stability of mutant variants to that of wild type. According to the analysis of the far-UV CD spectra at 20ºC, before and after thermal denaturation, thermal unfolding was reversible for all protein variants studied and no aggregation was observed after thermal unfolding. The results showed that charge-to-neutral alterations in the acidic ridge result in an impressive stabilisation of the protein fold: an increase of up to ~24ºC was noted for the Yfh1-86/90/93/101/103A variant while alterations in the β–sheet surface had almost no effect on protein thermal stability (**Fig. 7.4, Table 7.2**).

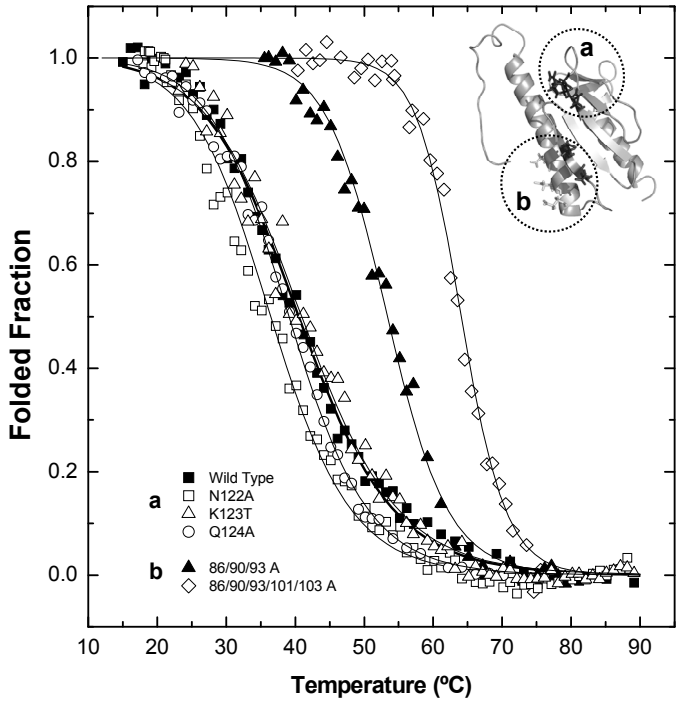

Figure 7.4: Thermal denaturation curves at pH 7.0 following Trp emission. Impact of mutations on Yfh1 thermal stability. (■) Wild Type **, (a)** single point mutations of β-sheet surface residues (122-123). (□) N122A, (Δ) K123T, (○)Q124A, **(b)** Mutations on putative iron binding sites: (▲) D86A E90A E93A, (◊) 86/90/93/101/103 A. Lines represent fits to the two-state model [18]; for parameters see Table 7.2.

The protein stability decreased in the order: Yfh1-86/90/93/101/103 A > Yfh1-86/90/93 A > Yfh1-101/103 A > Yfh1-N122K > Yfh1-K123T > Wild Type > Yfh1-N122A/K123T/Q124A > Yfh1-Q124A > Yfh1-N122A. The exception for the effect on the β–sheet surface are the mutations in residue Asn-122: changing to an alanine (ΔT_m = -4.5 ºC) or to a lysine (ΔT_m = +4.3 ºC) had opposite effects, probably due to the impact that would be expected by these alterations on the β–hairpin between strands β3 and β4. This β–hairpin involves two hydrogen bonds (Asn122-Trp131 and Val120-A133); while the insertion of an Ala at

position 122 likely disrupts the hydrogen bond with Trp131, the positively charged Lys might strengthen it, thus stabilising the protein. The 101/103A alterations stabilise the protein in spite of compromising 2 of the 3 hydrogen bonds involved in the β–hairpin connecting strands β1 and β2. This suggests that minimising repulsive interactions overcomes the stabilisation obtained by the two hydrogen bonds.

Table 7.2: Thermodynamic parameters for thermal denaturation of yeast frataxin variants**.** Effect of functional mutations on the protein thermal stability.

Protein	ΔH (kcal.mol^{-1})	ΔG[a] (cal.mol^{-1})	T_m (ºC)	ΔT_m (ºC)	Δ(ΔG)[b] (cal.mol^{-1})
Wild Type	28.2 ± 0.3	1421.3	40.4 ± 0.1	-	-
N122K	34.8 ± 0.5	1857.6	44.7 ± 0.1	+ 4.3 ± 0.2	546.5
N122A	30.1 ± 0.4	981.4	35.9 ± 0.1	- 4.5 ± 0.2	-588.3
K123T	28.7 ± 0.4	1481.3	41.0 ± 0.1	+ 0.6 ± 0.2	77.2
Q124A	34.3 ± 0.3	1282.5	39.0 ± 0.1	- 1.4 ± 0.2	181.2
N122A/K123T/Q124A	21.7 ± 0.3	1401.4	40.2 ± 0.1	- 0.2 ± 0.2	25.8
101/103A	55.1 ± 0.8	2629.4	52.0 ± 0.1	+ 11.6 ± 0.2	1441.3
86/90/93A	51.3 ± 0.9	2759.6	53.2 ± 0.1	+ 12.8 ± 0.2	1584.6
86/90/93/101/103A	77.1 ± 1.5	3988.5	64.2 ± 0.1	+ 23.8 ± 0.2	2850.2

[a] ΔG at 25ºC, considering an estimate for ΔC_p of 12 cal/mol/K.

[b] $\Delta(\Delta G) = [\Delta(T_m)] \times \Delta S_m = [\Delta(T_m)] \times (\Delta H_m/T_m)$, where ΔS_m and ΔH_m are values for the wild type.

Since protein conformational plasticity affects both protein function and degradation rates, we next analysed whether the functional mutations were also affecting frataxin flexibility, by performing limited proteolysis experiments using trypsin. Our underlying rationale was that mutations resulting in an increased structural flexibility would increase trypsin access to cleavage sites and consequently increase the degradation rate. The results show two distinct patterns, depending on the region in which the alteration is located (**Fig. 7.5**). Alterations on the acidic ridge had a pronounced effect on frataxin dynamics, making the protein more rigid and substantially less susceptible to proteolysis. In fact, the Yfh1-86/89/93/101/103A variant remains essentially intact

under conditions in which wild type frataxin is essentially completely digested (80% versus 10% integrity after 100 min digestion). On the other hand, alterations on the β-sheet surface (Yfh1-N122K/K123T/Q124A) behave almost identically to the wild type, suggesting that modifications in this region have either a very small or no effect on the protein conformational plasticity.

Overall, alterations in the acidic ridge that prevent iron binding at the primary sites increased substantially the protein stability, presumably due to decreased flexibility. It is possible that decreases in the structural flexibility may prevent conformational changes necessary to allow the interaction with protein partners. This increase in both thermal stability and resistance to proteolytic degradation suggests that the iron binding region is particularly susceptible to an activity-stability trade off.

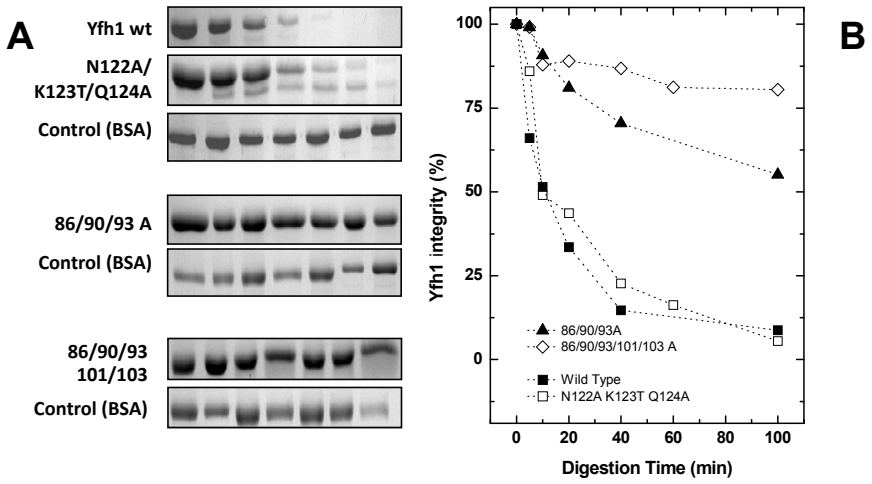

Figure 7.5: Time course of trypsin limited proteolysis**.** Comparison between wild type and functional mutants **(A)** SDS-PAGE analysis of the time course trypsin limited proteolysis experiments. **(B)** Evaluation/quantification of frataxin degradation during incubation with trypsin. Gels (A) densitometric analysis allowed the quantification frataxin for the different incubation times with trypsin. (■) Wild Type, (□) N122A K123T Q124A, (▲) D86A E90A E93A, (◊) 86/90/93/101/103 A.

7.5. Discussion

Here we present a detailed characterisation of eight yeast frataxin functional variants, that either alter the acidic ridge between α-helix 1 and β-sheet 1 or the conserved β-sheet surface between strands 3 and 4. Changing the conserved β-sheet residues Asn122-Lys-123-Gln124 had almost no effect on Yfh1 stability and plasticity, indicating that changes in this region did not disrupt overall conformation but are relevant for the Yfh1-Isu interaction. Alteration of up to five residues in the acidic ridge region, four of which had been identified as iron binding sites [8], significantly increase frataxin stability. This illustrates a rather interesting trade off between activity and stability in this region. In addition, our study suggests that residues Asp101 and Glu103 are involved in the iron-mediated interaction between Isu and Yfh1 but their alteration does not abrogate the interaction, as evidenced by the rescue of the *Δyfh1* phenotype.

7.6. Acknowledgements

Tao Wang preformed the yeast growth experiments as well as the quantification of the aconitase activity at University of Wisconsin, USA.

This work is partly financed by grants from the Fundação para a Ciência e Tecnologia (PTDC/QUI/70101) and National Ataxia Foundation (to CMG) and grants from the National Institutes of Health Grant (GM27870) and Muscular Dystrophy Association (to EAC.). A.R.C and T.W were recipients of FCT PhD Fellowship (SFRHBD/24949/2005) and an American Heart Association Postdoctoral Fellowship 0525728Z, respectively.

7.7. References

1. Babcock, M., et al., *Regulation of mitochondrial iron accumulation by Yfh1p, a putative homolog of frataxin.* Science, 1997. **276**(5319): p. 1709-12.
2. Rotig, A., et al., *Aconitase and mitochondrial iron-sulphur protein deficiency in Friedreich ataxia.* Nat Genet, 1997. **17**(2): p. 215-7.
3. Aloria, K., et al., *Iron-induced oligomerization of yeast frataxin homologue Yfh1 is dispensable in vivo.* EMBO Rep, 2004. **5**(11): p. 1096-101.
4. Foury, F., A. Pastore, and M. Trincal, *Acidic residues of yeast frataxin have an essential role in Fe-S cluster assembly.* EMBO Rep, 2007. **8**(2): p. 194-9.
5. Cook, J.D., et al., *Monomeric yeast frataxin is an iron-binding protein.* Biochemistry, 2006. **45**(25): p. 7767-77.
6. Kondapalli, K.C., et al., *Drosophila frataxin: an iron chaperone during cellular Fe-S cluster bioassembly.* Biochemistry, 2008. **47**(26): p. 6917-27.
7. Yoon, T. and J.A. Cowan, *Iron-sulfur cluster biosynthesis. Characterization of frataxin as an iron donor for assembly of [2Fe-2S] clusters in ISU-type proteins.* J Am Chem Soc, 2003. **125**(20): p. 6078-84.
8. He, Y., et al., *Yeast frataxin solution structure, iron binding, and ferrochelatase interaction.* Biochemistry, 2004. **43**(51): p. 16254-62.
9. Adamec, J., et al., *Iron-dependent self-assembly of recombinant yeast frataxin: implications for Friedreich ataxia.* Am J Hum Genet, 2000. **67**(3): p. 549-62.
10. Gakh, O., et al., *Physical evidence that yeast frataxin is an iron storage protein.* Biochemistry, 2002. **41**(21): p. 6798-804.
11. Gakh, O., et al., *Mitochondrial iron detoxification is a primary function of frataxin that limits oxidative damage and preserves cell longevity.* Hum Mol Genet, 2006. **15**(3): p. 467-79.
12. Nair, M., et al., *Solution structure of the bacterial frataxin ortholog, CyaY: mapping the iron binding sites.* Structure (Camb), 2004. **12**(11): p. 2037-48.
13. Musco, G., et al., *Towards a structural understanding of Friedreich's ataxia: the solution structure of frataxin.* Structure Fold Des, 2000. **8**(7): p. 695-707.
14. Wang, T. and E.A. Craig, *Binding of yeast frataxin to the scaffold for Fe-S cluster biogenesis, Isu.* J Biol Chem, 2008. **283**(18): p. 12674-9.
15. Gari, E., et al., *A set of vectors with a tetracycline-regulatable promoter system for modulated gene expression in Saccharomyces cerevisiae.* Yeast, 1997. **13**(9): p. 837-48.
16. Li, J., et al., *Yeast mitochondrial protein, Nfs1p, coordinately regulates iron-sulfur cluster proteins, cellular iron uptake, and iron distribution.* J Biol Chem, 1999. **274**(46): p. 33025-34.
17. Murakami, H., D. Pain, and G. Blobel, *70-kD heat shock-related protein is one of at least two distinct cytosolic factors stimulating protein import into mitochondria.* J Cell Biol, 1988. **107**(6 Pt 1): p. 2051-7.
18. Pace, C.N., et al., *Conformational stability and thermodynamics of folding of ribonucleases Sa, Sa2 and Sa3.* J Mol Biol, 1998. **279**(1): p. 271-86.
19. Correia, A.R., et al., *Dynamics, stability and iron-binding activity of frataxin clinical mutants.* Febs J, 2008. **275**(14): p. 3680-90.
20. Bencze, K.Z., et al., *The structure and function of frataxin.* Crit Rev Biochem Mol Biol, 2006. **41**(5): p. 269-91.
21. Correia, A.R., et al., *Conformational stability of human frataxin and effect of Friedreich's ataxia-related mutations on protein folding.* Biochem J, 2006. **398**(3): p. 605-11.
22. Winzor, D.J. and W.H. Sawyer, *Quantitative characterisation of ligand binding*. 1995, New York: Wiley-Liss.

23. Karthikeyan, G., et al., *Reduction in frataxin causes progressive accumulation of mitochondrial damage.* Hum Mol Genet, 2003. **12**(24): p. 3331-42.
24. Bulteau, A.L., et al., *Frataxin acts as an iron chaperone protein to modulate mitochondrial aconitase activity.* Science, 2004. **305**(5681): p. 242-5.
25. Shan, Y., E. Napoli, and G. Cortopassi, *Mitochondrial frataxin interacts with ISD11 of the Nfs1/ISCU complex and multiple mitochondrial chaperones.* Hum Mol Genet, 2007.

CHAPTER

8 FRATAXIN AND ITS PUTATIVE ROLE ON COPPER METABOLISM

8.1. Summary

Frataxin has been shown to be stabilised by different metal ions, in addition to iron. In this section we explore the potential binding properties of this mitochondrial protein. We have evaluated the potential binding of other common metals present within the mitochondria, namely manganese, zinc and copper and others like magnesium, sodium, calcium and nickel. Most of the metals were tested due to their effect on the protein stability [1] but nickel was included due to its ability to rescue, at least partially, FRDA-mutants cellular deficiencies [2]. Studies performed by Trp fluorescence emission revealed that, apart from iron, frataxin only binds copper and also that this feature (Cu(II) binding) was further confirmed by EPR. Frataxin was able to bind both copper oxidation states and the stoichiometries observed were nearly identical (the protein was shown to bind 3 Cu(I) or alternatively 4 Cu(II)). However, the protein affinity towards Cu(I) was higher. In contrast to what was observed during iron binding, DLS measurements have shown that copper is not able to induce Yfh1 oligomerisation. Thus, if Yfh1 has an antioxidant effect regarding copper toxicity, this is not associated to the protein oligomerisation capacity as in iron detoxification. Copper titrations of the functional Yfh1 mutants, described in the previous chapter, suggest that the copper binding region may also be located on the acidic ridge. Furthermore, Yfh1 was tested for a potential role as a copper-chaperone. In spite of exhibiting a dissociation constant in the micromolar range, Yfh1 was shown to be able to act as a copper-chaperone promoting apo-SOD1 metallation.

8.2. Copper in the mitochondria

Iron, zinc, copper and manganese are found in the in the mitochondria (**Table 8.1** for metal mitochondrial concentration in yeast cells) [3]. The mitochondrial steady stated concentration of copper is nearly one order of magnitude above the predicted to be required for the activation of the mitochondrial Cu-dependent cytochrome c oxidase (CcO), the most abundant cupro-protein within the mitochondria [3]. The excess of copper is located within the mitochondrial matrix on a non proteinaceous pool of copper; in yeast, this corresponds to 85% of the total mitochondrial copper, while in the mouse liver extracts it corresponds to 70% [3-4]. This pool constitutes the copper source for the maturation (metallation) of the two described mitochondrial copper-dependent enzymes: CcO and superoxide dismutase (Cu,ZnSOD or SOD1) [5-7]. In the matrix, copper (Cu(I)) forms a low molecular complex (CuL) with an unidentified non-proteinaceous ligand whose structure remains known. The targeted expression of two heterologous Cu(I) binding proteins, human SOD1 and yeast Cr5 metallothionein, depletes the complex as copper is directed to the maturation of those proteins [8]. Thus, CuL complex seems to work as a Cu(I) storage but, once needed, copper is transfered to the appropriated copper-chaperones to further take part on the metallation reactions within the mitochondrial inner membrane. The copper-free ligand is also present in the cytosol, but how this ligand is transferred to mitochondrial matrix is still not clear. Once free copper binds to the ligand, it forms an anionic

Table 8.1: Metal concentrations within the mitochondria.

Metal	Mitochondrial concentration (nmol/mg of protein)
Iron	2.3 ± 0.1
Copper	1.3 ± 0.2
Zinc	0.7 ± 0[a]
Manganese	0.13 ± 0[a]

[a]S.D.≤ 0.5

complex and it is postulated that this copper-ligand complex is further targeted to the matrix.

Within the inner mitochondrial space (IMS), several proteins (Cox17, Cox19, Sco1 and Cox11) transiently bind copper and contribute to the metallation/activation of CcO. SOD1, the other mitochondrial copper-binding protein, is also localised within the IMS. Although most SOD1 is cytosolic, 1-5% of total cellular SOD1 is within the IMS where its metallation takes place. The metallochaperone Ccs1 activates SOD1 by inserting Cu(I) into the apo-protein and by catalysing the formation of an essential disulfide bond. Moreover, this metallochaperone is also responsible for the accumulation of SOD1 within the mitochondrion.

There might be another copper chaperone involved in SOD1 maturation. It was observed that human, mouse and *C. elegans* SOD1 activity is retained in ΔCcs cells [3, 9-13], meaning that these organisms should have a SOD1 activation pathway that is Ccs-independent. The existence of an alternative copper chaperone promoting Ccs-independent SOD1 metallation may be suggested, however, Ccs-independent metallation has some constrains, as it strictly depends on reduced glutathione or on low redox potentials of the cells and is sensitive to certain structural perturbations in SOD1 structure [8,11].

Like iron, copper also catalyses the generation of ROS, thus its intracellular transport requires strict regulation and copper chaperones (**Table 8.2**), such as Ccs and Cox17 among others, which sequester and deliver copper imported via Ctr1 or/and DMT1. This last protein is a key protein in intestinal iron uptake, however its broad substrate range includes copper making it a potential alternative for the cellular copper import [14].

Table 8.2: Examples of Copper-binding and copper homeostasis proteins. Their known functions and binding parameters.

Protein	Function	N*	Kd (μM)	Technique, Ref.
Amyloid precursor (APP)‡	Protein involved in neuronal development and potentially Cu metabolism; cleavage leads to generation of αβ peptide that aggregates in senile plaque associated with Alzheimer's disease	2	10×10^{-3}	SPR,[15]
Atox1†	Metallochaporine that delivers Cu to ATP7A and ATP7B Cu(I) transporters	0.5	3.5×10^{-4}	ITC, [16]
CCS†	Metallochaperone that delivers Cu to Cu,Zn SOD	2†	$< \sim 10^{-14}$	[17], [18]
Cox17†	Metallochaperone that transfers Cu to Sco1 and Cox11 ft cyt oxidase C loading in the mitochondria	4	13×10^{-9}	UV absorption and Trp fluor, [19]
CopZ†	Archaeoglobus fulgidus [2Fe-2S] and Zn^{2+}-containing Cu chaperone	0.5	10^{-11}-10^{-12}	BCS competition assay, [20]
SOD1†	Antioxidant enzyme, catalyses the disproportionation of superoxide to hydrogen peroxide and dioxygen	1	6×10^{-9}	[17]
PrP‡	Protein whose function is unclear but binds Cu via the N-terminal octapeptide repeats	Up to 6	$13\text{-}66 \times 10^{-3}$	Trp Fluor and CD, [21]
S100A13‡	Is involved in the nonclassical export of signal peptide less proteins such as fibroblast growth factor (FGF-1) and interleukin 1α	2	12 and 55	ITC, [22]

* Binding sites per monomer
† Cu(I)
‡ Cu(II)

The coordination chemistry of Cu(I) and Cu(II) is often distinct, with Cu(I) preferring sulphur donors such as cysteine and methionine, whereas Cu(II) prefers nitrogen donors such as histidine or oxygen donors such as glutamate or aspartate [23]. The metal-binding motif, MXCXXC, is common not only among copper chaperones (ATPases ATP7A and ATP7B) but also in chaperone-like proteins, such as

cadmium and mercury binding proteins [23]. Cox17 presents a different motif, CXXC [24], as well as the high affinity copper importer Ctr1, MX_3M [23]. Other copper binding proteins show abnormal copper binding motifs such as RNAse A that binds copper through two histidines and a glutamic acid [25]. Histidine (His) has a very efficient nitrogen donor in its side chain imidazole. This residue provides 2 nitrogen donors and 6-memberate chelate rings for coordination. Its coordination properties will however depend enormously on the residue position on the polypeptide chain.

Here, we extend the characterisation of frataxin metal binding properties, to examine its ability to bind copper in both oxidation states and its possible implications at the cellular level.

8.3. Materials and Methods

Protein purification

The mature form of Yfh1 (amino acids 52-174), in both wild type and mutant variants, with an N-terminal His tag and a thrombin cleaving site in between was cloned into pET-3a vector (Novagen, Madison, WI, USA) [26-27]. Protein expression was induced over 3h at 37ºC in BL21(DE3) *E. coli* by adding IPTG (isopropyl-b-galactopyranoside) at a final concentration of 0.5mM. Cells were harvested and lysed on a French press. Cell lysate was subjected to His-binding resin (Amersham) chromatography and the protein was eluted with 500mM Imidazole in the binding buffer (50mM Tris-HCl Ph8.0, 200mM NaCl, 10mM Imidazole). The His tag was cleaved using biotinylated thrombin and thrombin was removed by streptavidin agarose (Amersham). When necessary (purity less than 90%) the protein was further purified applying the sample on a Superdex 75. At the end, the buffer was

changed to 10mM HEPES, 50mM NaCl pH 7.0 using Centricons (Millipore). Protein concentration was determined using the extinction coefficient ε^{280nm} = 15470 $M^{-1}.cm^{-1}$.

Fluorescence binding assay

Binding was followed by fluorescence spectroscopy, essentially as described previously for iron binding [28]. Briefly, tryptophan fluorescence was measured in 1 mL quartz cuvettes with continuous stirring. The excitation and monitoring wavelengths were 290 and 340 nm, respectively. For the measurements, a 15 μM solution of apo frataxin was titrated with stock solution of different metals. The quenching of tryptophan fluorescence induced by the binding was used to calculate the fraction of binding sites occupied. The stoichiometry, p, and apparent dissociation constant, K_d, were then obtained as previously described by Winzor and Sawyer [29].

DLS measurements

DLS measurements were performed at a protein concentration of 0.5 mg/ml at pH 7.0. Protein samples were passed through a 0.22 μm filter before DLS measurements. All experiments were performed at a 90° scattering angle on a Malvern Instruments Zetasizer Nano-ZS. Measurements were carried out at 25°C using a built-in temperature controller. The experimentally measured hydrodynamic radius (Rh) of the protein was determined by the Zetasizer software 6.01 software (Malvern instruments Lda). The radius is represented as a function of volume and not intensity, to avoid errors resultant from the increased intensity associated to larger particles.

SOD1 reconstitution[30]

The reconstitution of SOD1 was performed under anaerobic atmosphere in a VAC Atmospheres glove box. The copper source as either Cu(I) -glutathione complex (10μM) or Cu-bound Yfh1(10μM) was combined with ZnSO4 (10μM) and reduced GSH (1mM) in one eppendorf; the apo-SOD1 (2μM) and BCS chelate competitor (200μM) in another. Both solutions were prepared anaerobically in deoxygenated and Chelex-treated, 50 mM potassium phosphate buffer, pH 7.8, and the total copper concentration was normalised for all reaction samples. The two solutions were then combined and incubated in a heating block at 34 °C for 2 h. Reconstitution was also performed with copper II. An aliquot of each reaction mixture was extracted from the anaerobic chamber and diluted into an aerobic 50 mM potassium phosphate buffer, pH 7.8, for assay of SOD activity by standard cytochrome *c* assay [31].
Because SOD1 can incorporate copper ions from solution, control assay were performed and consisted in adding equal amounts of copper (but not bond to Yfh1); the copper insertion evaluation was performed in respect to these controls. The activity of the apo-SOD1, without any metal additions, was also measured as a control.

8.4. Results

8.4.1. Yfh1 Copper Binding Properties

Fluorescence spectroscopy was used to monitor binding of different metals to frataxin (Yfh1). We have seen that among calcium, copper, sodium, magnesium, nickel, manganese and zinc, only copper binding can be detected by Trp fluorescence quenching (data not shown). Cu(II)

binding analysis revealed a stoichiometry of 4.2 ± 0.1 and a K_d = 26.0 ± 4.3 μM (n=4) (**Fig. 8.1A**). Further, the binding of Cu(I) was also evaluated but, since Cu(I) is not soluble under our assay conditions, we have complexed it with GSH [30]. When comparing the binding of Cu(I) and Cu(II) to Yfh1, we observed that, although the protein has a lower stoichiometry for Cu(I) (3CuI:1Yfh, n=4), its affinity is higher (steeper slope observed for copper I titration, **Fig. 8.1 A**) [29].

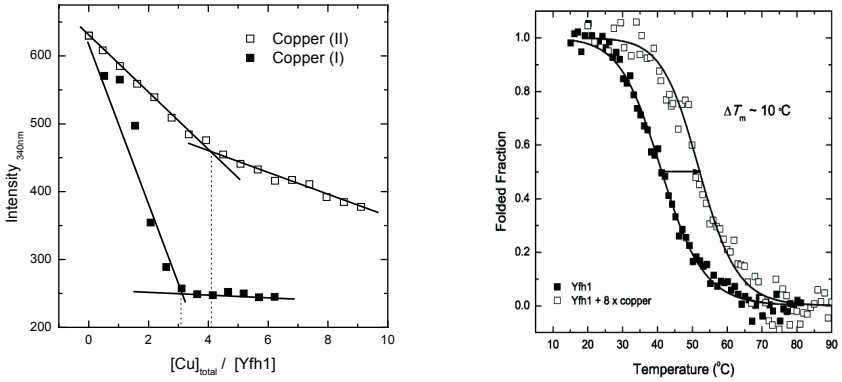

Figure 8.1: Copper binding and its stabilising effect. **Left.** Binding curve for copper I and copper II. **Right.** Yfh1 thermal denaturation curves in the presence and absence of copper II.

Furthermore, we have studied Cu(II) binding to Yfh1 by electron paramagnetic resonance (EPR). We have performed steady state measurements (**Fig.8.2A**) and we have titrated both the protein and the buffer solution with increasing amounts of copper (**Fig.8.2B**). This study allowed us to confirm that copper is binding directly to the protein using different binding sites. Yfh1 has 3 histidine, 2 methionines and 1 cysteine, which constitute Yfh1 potential copper binding sites. In addition, frataxin glutamates and aspartates may also be involved in Cu(II) coordination. The fact that all Glu and Asp residues cluster around

the iron binding region, suggests that iron and copper binding regions are likely to overlap.

Next, we evaluated whether copper binding stabilised Yfh1. As shown by the analysis of the thermal denaturation curves in the presence and in the absence of copper, this metal induces a stabilisation of up to ~10ºC (**Fig. 8.1B**). The same stoichiometry of iron:Yfh1 (8Fe(II):Yfh1) shows a more modest effect in terms of protein stabilisation, leading to a ΔT_m ~4ºC [1].

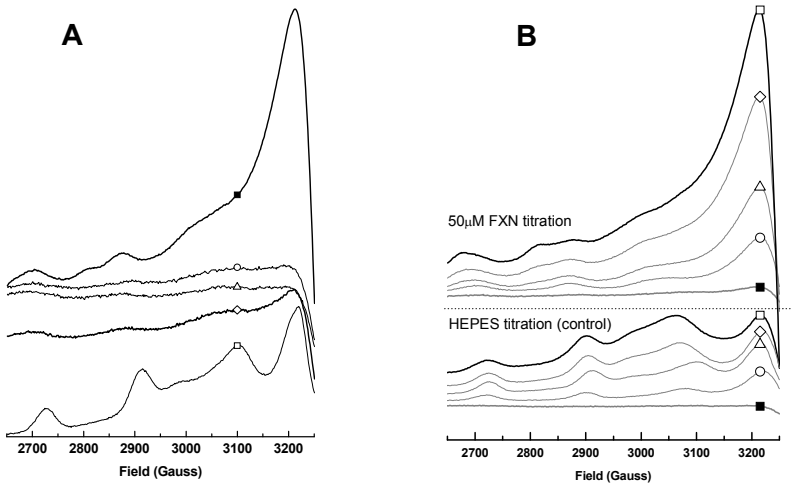

Figure 8.2: Cu(II) binding evaluated through EPR. **A:** EPR spectra of (■) FXN 50μM + 200μM Cu(II), (○) FXN after desalting to remove Cu(II), (Δ) concentrated (○), (◊) 50μM FXN in HEPES buffer and (□) 200μM in HEPES buffer. **B:** EPR spectra as a function of Copper concentration ((■) no copper, (○) 54μM (1eq.), (Δ) 97μM (2eq.), (◊) 165 μM (3.6eq.) and (□) 265μM (6eq.)**. Top:** FXN (50mM) titration and bottom HEPES titration (control).

Furthermore, we have explored the protein metal-induced oligomerisation properties. Previously it has been demonstrated that Yfh1 undergoes iron induced oligomerisation and this feature seems to be related to the protein's antioxidant function. Copper, as well as iron, may produce reactive oxygen species through the Fenton reaction. Thus, if this protein also oligomerises in the presence of excess copper,

preventing its oxidation and the consequent formation of reactive oxygen species, these would represent a direct role of Yfh1 on copper metabolism. Dynamic light scattering (DLS) measurements for the Yfh1 monomer are in agreement with Yfh1 overall molecular dimensions determined by NMR, 47Å x 29Å x 23Å (corresponding to radius of 2.4nm x 1.5nm x 1.2nm). Thus, we have further used this technique to follow Yfh1 oligomerisation.

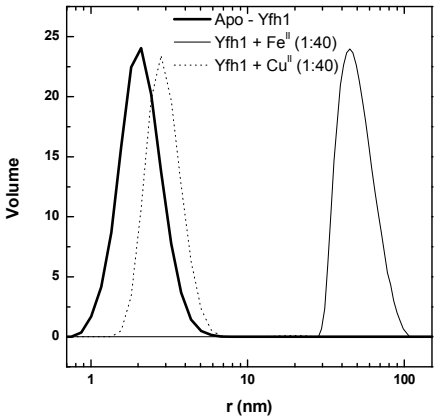

Figure 8.3: Dynamic light scattering (DLS) measurements, in the presence of excess of copper or iron.

Substantially increasing the copper concentration (up to 40 times the concentration of protein) does not induce copper-induced Yfh1 oligomerisation. This increase in copper concentration results in a modest variation of the particles radius ~0.8nm **(Fig. 8.3).** The same Fe(II) to protein ratio induces Yfh1 oligomerisation and the particles radius increase from ~2 nm to ~45 nm (diameter of ~900Å) (in agreement with previously published data [32]), which corresponds to a 20-fold increase compared with the radius measured in the presence of copper.

8.4.2. Putative Copper Binding Sites

Considering the yfh1 mutants described on the previous chapter, we have evaluated if any of those showed reduced copper stoichiometries relative to the wild type protein **(Table 8.3).** Since three of the variants contain mutations of extremely conserved residues associated to iron

binding, if these residues are also involved in copper binding their mutation may partially compromise Yfh1 copper binding properties.

Analysis of the binding curves shows that residues D86, E90 and E93 constitute putative copper binding sites. These residues mutation leads to a reduction in the binding stoichiometry of 4 to 1 copper ion per monomer, along with the concomitant increase in the K_d. Mutations on the conserved β-sheet that have a reduced impact on the protein copper binding properties (**Table 8.3**). Since copper binding sites seem to overlap with iron binding, at least partially, we hypothesised that the presence of copper may modulate frataxin iron chaperone function, displacing iron from the surface of Yfh1. To test this hypothesis we titrated iron bound holo-Yfh1 with Isu1 in the presence of increasing amounts of copper **(Fig. 8.4)**. The addition of copper to holo-Fe(II)-Yfh1 solution appears to partially displace iron, since copper

Table 8.3: Copper binding parameters obtained according to the methods described in [29] .

Protein	Cu(II)	
	p	K_d (μM)
Wild Type	4.2	26.0
N122A	2.8	44.3
K123T	3.2	34.7
Q124A	3.0	30.6
N122A/K123T/Q124A	3.3	54.0
101/103A	3.5	38.5
86/90/93A	1.3	46.2
86/90/93/101/103 A	1.3	59.9

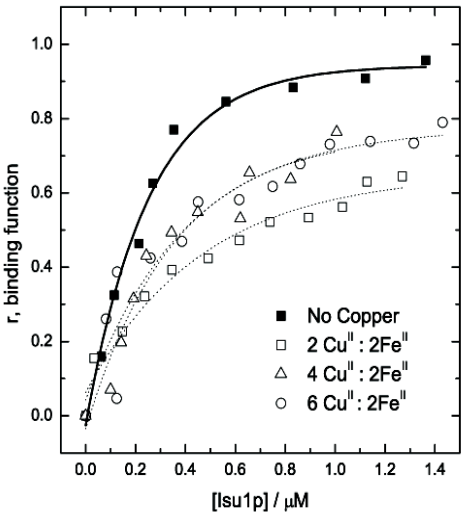

Figure 8.4: Binding of Isu1 to Yfh1. Possible displacement of iron by the presence of copper. The iron stoichiometry was retained for all titration ($2Fe^{II}$ per Yfh1) but increased amounts of copper (Cu^{II}) where added to the titrated solution.

addition results in reduce binding of holo-Yfh1 to Isu. However, excess of copper fails to abolish the Yfh1-Isu interaction, which suggests that copper is unable to cause a complete displacement of iron from Yfh1 surface.

8.4.3. Frataxin Can Also Be a Copper Chaperone

Frataxin binds iron and acts as an iron chaperone, thus we have further looked into a potential role of frataxin as a copper chaperone. We have followed SOD1 reconstitution without a copper-chaperone by adding free copper directly to the SOD1 solution, and by using copper-loaded Yfh1 as a putative copper chaperone. Frataxin was shown to be able to facilitate copper insertion onto apo-SOD1 as the presence of copper-loaded Yfh1 approximately doubles the reconstitution efficiency obtained by the addition of free copper to the reconstitution mixture **(Fig. 8.5)**; hCcs chaperone activity is however higher. In the presence of hCcs, the copper-chaperone responsible for the SOD1, metallation efficiency is twice the quantified for the copper-loaded Yfh1 [30]. As a control, the

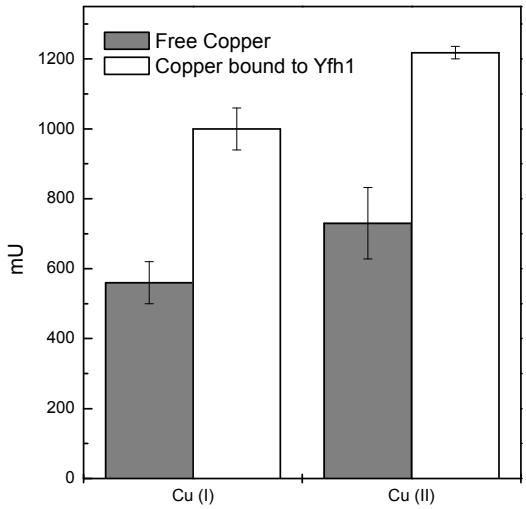

Figure 8.5: SOD1 activity after anaerobic reconstitution with free copper (grey bars) and or alternatively with copper bound to yeast frataxin (white bars). The SOD1 concentration was the same in all the assay (n=3).

activity of Apo-SOD1 prior to the reconstitution experiment was evaluated and was shown to be identical to the observed for the control reconstitutions.

8.5. Discussion

Our results suggest that frataxin may also play a role in copper homeostasis. The protein binds copper with an affinity identical to the observed for iron and it may also act as a copper-chaperone as evidenced by the SOD1 reconstitution experiment. By binding copper, frataxin prevents copper Fenton reactions (and in fact the protein has a higher affinity towards Cu(I)) and, in addition, its reduced copper binding affinity allows it to "direct" the copper within the mitochondrial matrix to the appropriate metallochaperones and indirectly promote copper metallation. Thus, we hypothesised that frataxin may be contributing to the homeostasis of the non-proteinaceous mitochondrial copper pool. In order to test this hypothesis, and to test whether Yfh1 binds copper *in vivo* and if it may in fact be involved in metallation reactions, *in vivo* experiments must be performed. Using the yeast model system, we can obtain yeast cells with different controlled Yfh1 expression levels. ∆yfh1 cells must be transformed with a plasmid coding for Yfh1 with a tight control expression and Yfh1 copper binding must be evaluated *in vivo*. As previously described, the matrix Cu(I) can be mobilised by the expression of copper containing enzymes [8], thus, if increased Yfh1 expression leads to a depletion of matrix Cu(I), this will strongly indicate that Yfh1 binds Cu(I) *in vivo*.

Frataxin does not contain a typical copper binding motif which could explain its reduced binding affinity. Other proteins such as S100 are also known to bind copper with affinities lower than the observed for the identified copper chaperones (some with affinities identical to the

observed for frataxin). Their ability to bind copper is associated to a wide range of biological functions which also include a protective mechanism against copper toxicity [33].

Frataxin binding sites must be further explored and the use of chemical compounds such as DEPC, that chemically modifies histidines, [34] or methanethiosulfonates [35], that modifies cysteines, may be useful for the identification of the residues involved in copper binding.

Current results cannot yet clarify what is the biological meaning of the frataxin's ability to bind copper, thus further studies must be performed in order to clarify this intriguing yet interesting new feature of frataxin cellular function.

8.6. Acknowledgments

Joan Valentine, from UCLA, is gratefully acknowledged for sharing SOD1 and Apo-SOD1 proteins.

Isabel Pacheco is gratefully acknowledged for the knowledge and assistance on the use of the anaerobic chamber.

8.7. References

1. Adinolfi, S., et al., *The factors governing the thermal stability of frataxin orthologues: how to increase a protein's stability.* Biochemistry, 2004. **43**(21): p. 6511-8.
2. Shan, Y., E. Napoli, and G. Cortopassi, *Mitochondrial frataxin interacts with ISD11 of the NFS1/ISCU complex and multiple mitochondrial chaperones.* Hum Mol Genet, 2007. **16**(8): p. 929-41.
3. Cobine, P.A., et al., *Yeast contain a non-proteinaceous pool of copper in the mitochondrial matrix.* J Biol Chem, 2004. **279**(14): p. 14447-55.
4. Cobine, P.A., et al., *Mitochondrial matrix copper complex used in metallation of cytochrome oxidase and superoxide dismutase.* J Biol Chem, 2006. **281**(48): p. 36552-9.
5. Sturtz, L.A., et al., *A fraction of yeast Cu,Zn-superoxide dismutase and its metallochaperone, CCS, localize to the intermembrane space of mitochondria. A physiological role for SOD1 in guarding against mitochondrial oxidative damage.* J Biol Chem, 2001. **276**(41): p. 38084-9.
6. Tsukihara, T., et al., *Structures of metal sites of oxidized bovine heart cytochrome c oxidase at 2.8 A.* Science, 1995. **269**(5227): p. 1069-74.

7. Culotta, V.C., M. Yang, and T.V. O'Halloran, *Activation of superoxide dismutases: putting the metal to the pedal.* Biochim Biophys Acta, 2006. **1763**(7): p. 747-58.
8. Leary, S.C., D.R. Winge, and P.A. Cobine, *"Pulling the plug" on cellular copper: the role of mitochondria in copper export.* Biochim Biophys Acta, 2009. **1793**(1): p. 146-53.
9. Beckman, J.S., et al., *CCS knockout mice establish an alternative source of copper for SOD in ALS.* Free Radic Biol Med, 2002. **33**(10): p. 1433-5.
10. Carroll, M.C., et al., *Mechanisms for activating Cu- and Zn-containing superoxide dismutase in the absence of the CCS Cu chaperone.* Proc Natl Acad Sci U S A, 2004. **101**(16): p. 5964-9.
11. Subramaniam, J.R., et al., *Mutant SOD1 causes motor neuron disease independent of copper chaperone-mediated copper loading.* Nat Neurosci, 2002. **5**(4): p. 301-7.
12. Wong, P.C., et al., *Copper chaperone for superoxide dismutase is essential to activate mammalian Cu/Zn superoxide dismutase.* Proc Natl Acad Sci U S A, 2000. **97**(6): p. 2886-91.
13. Jensen, L.T. and V.C. Culotta, *Activation of CuZn superoxide dismutases from Caenorhabditis elegans does not require the copper chaperone CCS.* J Biol Chem, 2005. **280**(50): p. 41373-9.
14. Arredondo, M., et al., *DMT1, a physiologically relevant apical Cu1+ transporter of intestinal cells.* Am J Physiol Cell Physiol, 2003. **284**(6): p. C1525-30.
15. Hesse, L., et al., *The beta A4 amyloid precursor protein binding to copper.* FEBS Lett, 1994. **349**(1): p. 109-16.
16. Yatsunyk, L.A. and A.C. Rosenzweig, *Cu(I) binding and transfer by the N terminus of the Wilson disease protein.* J Biol Chem, 2007. **282**(12): p. 8622-31.
17. Rae, T.D., et al., *Undetectable intracellular free copper: the requirement of a copper chaperone for superoxide dismutase.* Science, 1999. **284**(5415): p. 805-8.
18. Eisses, J.F., et al., *Domains I and III of the human copper chaperone for superoxide dismutase interact via a cysteine-bridged Dicopper(I) cluster.* Biochemistry, 2000. **39**(25): p. 7337-42.
19. Palumaa, P., et al., *Metal-binding mechanism of Cox17, a copper chaperone for cytochrome c oxidase.* Biochem J, 2004. **382**(Pt 1): p. 307-14.
20. Zhou, L., C. Singleton, and N.E. Le Brun, *High Cu(I) and low proton affinities of the CXXC motif of Bacillus subtilis CopZ.* Biochem J, 2008. **413**(3): p. 459-65.
21. Nadal, R.C., et al., *Evaluation of copper2+ affinities for the prion protein.* Biochemistry, 2009. **48**(38): p. 8929-31.
22. Sivaraja, V., et al., *Copper binding affinity of S100A13, a key component of the FGF-1 nonclassical copper-dependent release complex.* Biophys J, 2006. **91**(5): p. 1832-43.
23. Kim, B.E., T. Nevitt, and D.J. Thiele, *Mechanisms for copper acquisition, distribution and regulation.* Nat Chem Biol, 2008. **4**(3): p. 176-85.
24. Banci, L., et al., *Mitochondrial copper(I) transfer from Cox17 to Sco1 is coupled to electron transfer.* Proc Natl Acad Sci U S A, 2008. **105**(19): p. 6803-8.
25. Balakrishnan, R., et al., *Crystal structures of the copper and nickel complexes of RNase A: metal-induced interprotein interactions and identification of a novel copper binding motif.* Proc Natl Acad Sci U S A, 1997. **94**(18): p. 9620-5.
26. Aloria, K., et al., *Iron-induced oligomerization of yeast frataxin homologue Yfh1 is dispensable in vivo.* EMBO Rep, 2004. **5**(11): p. 1096-101.
27. Wang, T. and E.A. Craig, *Binding of yeast frataxin to the scaffold for Fe-S cluster biogenesis, Isu.* J Biol Chem, 2008. **283**(18): p. 12674-9.
28. Correia, A.R., et al., *Conformational stability of human frataxin and effect of Friedreich's ataxia-related mutations on protein folding.* Biochem J, 2006. **398**(3): p. 605-11.
29. Winsor, D.J.S., W.H., *Quantitative Characterisation of Ligand Binding*. 1995, New York: Wiley-Liss.

30. Rae, T.D., et al., *Mechanism of Cu,Zn-superoxide dismutase activation by the human metallochaperone hCCS.* J Biol Chem, 2001. **276**(7): p. 5166-76.
31. Fridovich, I., *CRC Handbook of Methods for Oxygen Radical Reasearch*, ed. R.A. Greenwald. 1985, Boca Raton: CRC press, Fl.
32. Gakh, O., et al., *Physical evidence that yeast frataxin is an iron storage protein.* Biochemistry, 2002. **41**(21): p. 6798-804.
33. Nishikawa, T., et al., *Identification of S100b protein as copper-binding protein and its suppression of copper-induced cell damage.* J Biol Chem, 1997. **272**(37): p. 23037-41.
34. Potter, S.Z., et al., *Binding of a single zinc ion to one subunit of copper-zinc superoxide dismutase apoprotein substantially influences the structure and stability of the entire homodimeric protein.* J Am Chem Soc, 2007. **129**(15): p. 4575-83.
35. Jiang, L.H., et al., *Identification of amino acid residues contributing to the ATP-binding site of a purinergic P2X receptor.* J Biol Chem, 2000. **275**(44): p. 34190-6.

CHAPTER

9 DISCUSSION

9.1. Frataxin and FRDA

9.1.1. FRDA in Heterozygous Patients

Genetic diseases resulting from missense mutations can involve many different and distinct pathological mechanisms. A single amino acid chain can trigger a disease by causing loss of function, accumulation of toxic species, such as aggregates or amyloid fibers, or through dominant negative effects inhibiting the normal function of the protein [1]. Single nucleotide polymorphisms are rather common in the human genome: about 10 million [2] have been identified, which corresponds to over 1% of nucleotides, but only an estimate of 67,000-200,000 of these polymorphisms are nonsynonymous. This type of polymorphism is a missense variation of a single base in a coding region that results in an amino acid change in the corresponding protein. Missense mutations have been associated to several diseases such as cystic fibrosis, phenylketonuria, amylotrophic lateral sclerosis (ALS) or Parkinson's disease.

In FRDA, the link between frataxin point mutations, described in compound heterozygous patients, and the disease physiopathology remain unclear. Hypothetical scenarios for the impact of mutations include an effect on the folding efficiency, maturation, protein stability and proteolytic susceptibility or function. In addition to these direct effects on the expressed protein, missense mutations may also alter the splicing of pre-mRNA, resulting in aberrant spliced mRNA that could be rapidly digested and leading to decreased levels of synthesised protein [3]. Here we have studied different FRDA-related point mutations found in compound heterozygous patients. These mutations can be grouped according to FRDA symptoms: whereas the I154F and W155R

mutations lead to severe FRDA phenotype, the mutations G130V and the D122Y account for milder clinical symptoms [3]. Reports on these mutations and also the recently developed cellular models based on frataxin missense mutations (G130V and I154F) indicate that the studied mutations do not interfere with mRNA splicing [3-5]. In addition, the mild phenotypes are suggestive of the cellular presence of frataxin with partially reduced function [3]. Focusing on the impact the different clinical point mutations have on the protein conformation, flexibility and function and framing our results with recent data on *in vivo* systems we have aimed at contributing to a better molecular and structural understanding of FRDA mechanism.

From a structural point of view, our results demonstrate that none of the mutations change significantly the protein fold at room temperature. Furthermore, frataxin flexibility is not significantly altered by the insertion of the mutations. Nevertheless, the four mutant variants present a reduced thermodynamic stability, which, *in vivo*, is likely to cause an increase of the molecular motions and enhance the protein susceptibility to aggregate and/or to be degraded by the cellular proteases. At 37ºC, the mutant frataxin's have an increased susceptibility towards proteolytic degradation as shown by the limited proteolysis experiments. This suggests that increasing the temperature from 25ºC to physiological conditions increases the molecular motions enough to allow proteolysis. In addition to a higher tendency towards degradation, the mutants have also reflected a higher tendency towards aggregation and a lower folding efficiency, which may suggest that the mutations affect the protein folding kinetics. Accordingly, it has been found that there is an inverse correlation between the level of protein expression and the aggregation rate [6], so that proteins are only marginally soluble to function and aggregation can result from small changes such as chemical modifications (e.g. as a consequence of

oxidative stress) or genetic mutations (e.g. as in the case of FRDA heterozygous patients).

Isaya and co-workers have demonstrated that human frataxin expression can rescue Yfh1-deficient cells (Δyfh1) phenotype and have further used this hybrid system to explore the biogenesis and functional impairment of two clinical variants: FXN-G130V and FXN-W173G. In contrast to the phenotype associated to the G130V mutation, W173G mutation results in a severe phenotype similar to the one observed for homozygous and heterozygous patients expressing the mutants FXN-W155R or FXN-I154F. While the expression of FXN-G130V mutant complemented Δyfh1 cells, FXN-W173G expression lead to typical Δyfh1 phenotype. However, both mutants showed decreased stability, resulting in decreased levels of mature frataxin. The protein maturation process is also reduced by the W173G mutation, decreasing even further the levels of mature FXN-W173G protein [7]. In addition, the expression of mutants FXN-G130V, FXN-I154F, FXN-W155R, FXN-W173G and FXN-L156P in HEK293T cells suggests that, with exception of mutations I154F and W155R, the other three mutations, including G130V, are likely to affect frataxin expression, maturation or degradation, since these are poorly expressed in the mature form [8]. These *in vivo* observations are in agreement with our data on the decreased stability and increased flexibility, described for the clinical mutants *in vitro*, and sustain the hypothesis that FRDA pathology in compound heterozygous may be associated to either a decreased folding ability or/and increased degradation.

Further, we have evaluated the mutants' function in terms of their iron binding ability. Iron titrations have shown that all the clinical mutants under study have their iron binding abilities partially impaired. While mutants FXN-D122Y and FXN-G130V have a lower binding stoichiometry, FXN-I154F and FXN-W155R mutants precipitate upon

exciding a threshold of $2Fe^{III}$/monomer. This observed reduction in iron-binding capacity could also be related to increased molecular motions. *In vivo*, cellular models based on frataxin missense mutations show a pattern of iron deposits that is compatible with the iron binding deficiencies we have detected *in vitro*. While only 10% of fibroblasts expressing the FXN-G130V mutant show small iron deposits, these are present in over 50% of fibroblasts expressing the FXN-I154F mutant [5]. Direct measurement of mitochondrial iron content showed a 2-fold increased in the FXN-I154F expressing cells in respect to wild type expressing cells (from 5 to 10 mmol/mg of protein) [5]. In addition, expression of the mutants FXN-G130V and FXN-W173G in Yfh1-defficient cells also leads to an identical observation [7]. Mitochondrial iron level in ∆yfh1 [FXN-G130V] cells is identical to the observed for ∆yfh1 [FXN-wt] cells, however, expressing the mutant associated to a severe phenotype leads to a 4-fold increase of the mitochondrial iron levels [7]. In addition, the biochemical pattern concerning the activity of FeS clusters containing enzymes is identical for these two model systems, as in both systems mutations associated to severe phenotypes lead to more significant impairments of the FeS clusters containing enzymes activities [5, 7].

The functional impairment cannot be fully explained by the partial impairment of frataxin iron binding properties, suggesting that adverse physiological conditions occurring *in vivo*, such as oxidative stress [9-12] and iron accumulation, can potentiate mutants' defects, leading to further perturbation of frataxin structure and dynamics; these could also lead to frataxin inactivation or misfolding, further reducing the cellular concentration of functional frataxin.

Altogether, the clinical effects in heterozygous FRDA patients are likely to result from a combination of effects, as observed in other

human diseases. For example, in amyotrophic lateral sclerosis the mutations identified in SOD1 are very different in character and it has been suggested that the pathology emerges as a result of different reasons, or a combination of reasons, from apo-protein destabilisation to local unfolding [13]. Also, missense mutations leading to lysosomal storage diseases are associated to different pathological mechanisms like active-site impairment, pH-dependent protein instability, protein degradation, improper protein trafficking or disruption of protein-protein interaction crucial for cellular function. In Gaucher's disease, the most prevalent lysosomal disorder, the phenotypic diversity is very large and cannot be solely explained by the effect of mutations on enzyme activity, suggesting that increased degradation may also be associated.

In the case of FRDA, the results obtained in the present study suggest that factors such as a reduced efficiency of protein folding (resulting in an increase of the aggregation rates), an accelerated degradation *in vivo* (leading to decreased frataxin levels) and misfolding and conformational destabilisation contribute to a decrease in the levels of functional frataxin. In this scenario, FRDA in heterozygous patients carrying frataxin single point mutations could be considered a type of protein misfolding disorder leading to a "loss of function" phenotype [14]. In addition, the existence of frataxin clinical mutants whose mutations cause severe functional impairment and whose phenotype does not result from increased conformational instability cannot be excluded. Our studies on the yeast model system have allowed for the identification of one of those mutations: Yfh1-N122K (in human frataxin, FXN-N146K). This mutation involves a well conserved residue on the protein exposed β-sheet surface and severely compromises the interaction between frataxin and its protein partner Isu without compromising the protein stability or its plasticity. However, the FXN-N146K mutation is associated to a severe phenotype and

biochemical analysis of the Δ(yfh1) cells expressing Yfh1-N122K (corresponding to human FXN-N146K) show iron accumulation and severe aconitase activity deficiency [15-16].

9.1.2. Modulators of FRDA variants

Defects in protein folding constitute the basis for many human diseases which can be associated to trafficking impairment (α1-antitrypsin deficiency and cystic fibrosis), misfolding (cancer and ALS) or increased aggregation propensity (familial amyloidosis, Scrapie or Alzheimer's) [17-20]. Although some misfolding diseases are directly associated to mutations, these are not an absolute requirement for misfolding to occur [21]. Protein stabilisers, small molecules now described as chemical chaperones, have been shown to be able to correct numerous folding defects [21-24]. Thus, we have analysed whether the presence of chemical chaperones could revert the FXN-D122Y and FXN-I154F mutants' decreased folding efficiency and stability. In spite of the basic mechanism responsible for the osmolyte effect [21, 25-27] some are very effective in inducing structure while others are more likely to solubilise native proteins. Studies on the physical and chemical origins of the osmolyte action have revealed that their overall effect results from a combination of favourable and unfavourable interactions with backbone and side chains which explains the apparent discrepancy in their mode of action [25-26, 28-30]. Three complementary approaches were followed and the effect of four small molecular weight compounds (glycerol, trimethylamine-N-oxide (TMAO), trehalose and 4-phenylbutirate (4PBA)) during early folding events and on the native state was here explored.

The small compounds presence during early folding events can have a strong positive effect on the FXN-I154F folding efficiency, their impact on FXN-D122Y folding efficiency is however modest. An opposite effect is observed when looking at the folded protein. The chemical chaperones were efficient in reverting the decreased stability observed for FXN-D122Y but their impact on FXN-I154F stability was marginal. The effect of the small compounds on the fold quality/conformation was also mutant dependent. The fold quality was assessed through GroEL partitioning experiments; GroEL has a high affinity to non-native exposed hydrophobic regions, thus partitioning will depend on the protein conformation. Control experiments have shown that, under the conditions used, FXN wild type does not partition onto GroEL. In contrast, both mutant variants show an identical partition onto GroEL which is indicative of their fold defects. FXN-D122Y conformation was more easily corrected by the presence of the tested small compounds. Trehalose completely abrogates FXN-D122Y partitioning onto GroEL whereas 4PBA and TMAO partially impair it. On the other hand, FXN-I154F partitioning is only decreased by the presence of TMAO, all the other compounds either have no effect or even lead to an increase partitioning, meaning that their presence causes an exposure of hydrophobic regions that are recognised by GroEL.

The fact that small molecules have different effects depending on the mutation considered can be rationalised in terms of the impact each mutation has on the protein plasticity and conformation [31-33]. It also suggests that the pathological process resulting from each mutation is likely to be different. The data here presented suggests that chemical chaperones may rescue FXN-D122Y phenotype since their presence increases the protein's stability and fold quality and, most likely, also decreases the protein’s propensity towards degradation. Thus, therapy with ‘protector’ molecules may increase the amount of functional FXN-

D122Y, rescuing the mild phenotype observed. On the other hand, the mutant FXN-I154F is not significantly stabilised by the presence of chemical chaperones nor does their presence reverts the partitioning onto GroEL. They do however increase the mutant's folding efficiency, which may result in an increased amount of soluble protein and consequently may lead to a reduction of the phenotype severity. These *in vitro* experiments allowed us to evaluate the potential use of chemical chaperones supplementation in FRDA and, according to the results, some of the clinical mutant's conformational deficiencies may be partially rescued by the presence of chemical chaperones. The optimal conditions to improve both mutants' stability and folding efficiency have been selected and *in vivo* studies must now be performed. The recently cellular models expressing frataxin containing FRDA-related missense mutations would be ideal for these studies [5].

In addition to the direct study of the impact of chemical chaperones on two clinical mutants, this study has also allowed to establish a valuable method to study the effect of chemical chaperones on proteins. The GroEL sink assay, differential scanning fluorometry and the effect on folding efficiency give complementary information on the impact of chemical chaperones and have proven to be valuable approaches for the initial screen of potential rescuers of proteins associated to misfolding diseases.

9.1.3. Oxidative Stress Related Modification and FRDA

The exact role of oxidative stress in FRDA and the understanding of how frataxin promotes an antioxidant function have not so far been fully understood. However, increased ROS production is undoubtedly associated to FRDA development. Oxidative stress markers are used to monitor disease progression [34-36]; overexpressing frataxin leads to

decreased amounts of carbonylated proteins and cells increase their ability to sustain exogenous oxidative stress. Furthermore, the most promising FRDA treatment involves the administration of Idebenone [37-38]. This compound can interact with the mitochondrial respiratory chain as an electron carrier, supporting mitochondrial function and ATP production and it also acts as an antioxidant. However, other experimental evidences dismiss a role of oxidative stress in FRDA pathogenesis: overexpression of antioxidant enzymes in fly and mouse models fails to rescue the FRDA phenotype if frataxin gene is deleted [12, 39]. Further, in yeast, mouse and cellular mouse models, the absence of frataxin in aerobic conditions is associated to aconitase degradation and accumulation of oxidatively modified proteins in both the cytosol and mitochondria, which in yeast has been shown to lead to Pim1 expression and proteasome inhibition [9]. Murine fibroblasts expressing frataxin clinical mutants (FXN-G130V and FXN-I154F) show an increased sensitivity towards exogenous oxidative stress but, while the levels of catalase are reduced to at least half the values observed for the wild type, the SOD expression remains unaltered [5]. In agreement, when using the FRDA *Drosophila* model it was shown that the FRDA phenotype could be rescued by catalase overexpression but overexpressing SOD's had no effect [40]. However, the effect of overexpressing SOD's should have been performed with concomitant overexpression of catalase since overexpression of SOD's may result in an accumulation of H_2O_2 and the FRDA *Drosophila* model shows a great sensitivity towards H_2O_2. Recently, Tamarit and co-workers have shown that Δyfh1 cells show reduced SOD1 and SOD2 activities but, if the medium is supplemented with copper or manganese, these activities are restored and cellular oxidative damage prevented [41]. Thus, either directly or indirectly, frataxin seems to be important for maintaining the oxidative balance.

A question that remained to be answered was what happens to frataxin itself, which is present at reduced levels in all FRDA patients, if this balance is disturbed. *A priori*, frataxin is a potential target for oxidative stress modifications, not only due to its location in the mitochondria, where oxygen and nitric oxide are available in a reducing environment, but also as a result of its iron-binding properties, which may prompt the formation of ROS via Fenton chemistry reactions. Oxidative damage on proteins is extremely relevant *in vivo* since this modulates the protein function (both positively and negatively), its fragmentation, oligomerisation and turnover [42]. Residues at the protein surface are primary targets as these are more susceptible to oxidation reactions. The latter can alter the protein hydrophilicity and, consequently, its conformation and function [43-44]. Thus, it is not surprising that these modifications are involved both in ageing and diseases such as Alzheimer's and Parkinson's disease and amyotrophic lateral sclerosis, where an increase in protein carbonyls and 3-nitrotyrosin is observed [42, 45]. Here, we have explored the consequences of subjecting the human orthologue to conditions mimicking increased oxidative stress. The human frataxin core is susceptible to oxidative stress related modifications; four nitration sites (Tyr143, Tyr175, Tyr205 and Trp155) and one carbonylation site (Trp155) were identified by MS analysis. Interestingly the only residue identified as carbonylated (W155) was also found to be susceptible to nitration. There are two factors that may account for this residue's increased susceptibility towards modifications: its nature and its localisation/orientation. Tryptophans are highly susceptible to oxidative stress related modifications, however, there are two other relatively solvent accessible tryptophans, Trp168 and Trp173, which were analysed, and were not modified, suggesting that a bias for Trp is not occurring. Trp155 is strictly conserved across frataxin orthologues and

its location at the protein surface with the aromatic ring turned to the outside facilitates the access of reactive species to this residue. Thus, the second factor location/orientation seems to significantly contribute to Trp155 increased susceptibility towards oxidative stress related modifications.

The oxidative related modifications did not alter the wild type frataxin ability to bind iron nor its ability to avoid Fenton chemistry. However, they do result in destabilising conformational changes ranging from 0.3 to 1.0 kcal.mol^{-1}, and induce an 'open' conformation. This decreased stability may not be relevant in the context of the wild type protein, however, in compound heterozygous patients, this small reduction in stability, associated to the mutants' intrinsic decreased stability, may trigger the development of FRDA. Preliminary data on thermal stability of mutant frataxin suggests that treatment with metals plus hydrogen peroxide or with peroxynitrite may induce different variations on the thermal stability of mutant proteins. While peroxynitrite seems to induce a considerable stabilisation of the FXN-G130V, the opposite effect is observed for FXN-W155R mutant. However, the impact of oxidative related modifications on the FRDA-related mutants has to be further explored. First, the extent of the modifications has to be evaluated followed by its impact.

At this point no pathological meaning can be attributed to oxidative modifications in frataxin but a possible role should not be completely excluded. Interestingly, one of the known clinical point mutations associated to a severe phenotype also involves the tryptophan highly susceptible to modifications, Trp 155; its mutation to an arginine is described in FRDA compound heterozygote patients [3]. The characterisation of the impact of this mutations at the protein level, has shown that modifying this residue does not disrupt frataxin fold but does increase the susceptibility towards proteolytic degradation and partially

compromised iron binding [33, 46]. So it might be relevant, in the FRDA context, that a residue whose mutations result in FRDA is also a hot spot for carbonylation and nitration modifications. Furthermore the characterisation of the effect of oxidative modifications on the frataxin interactome may rule out the hypothesis that modification on frataxin protein may trigger FRDA development or in the other hand it may exclude that possibility.

9.2. Frataxin Function

9.2.1. Characterisation of Functional Mutants

The human and yeast frataxin orthologs have a high degree of amino acid (65%) and structural identity. In addition, the phenotype observed as a consequence of frataxin's deficiency is very similar in human and yeast cells [47-48] and thus the yeast model system has been frequently used to study frataxin's function, as well as the pathological events associated with FRDA. Here, yeast frataxin orthologue was used on the studies focused on frataxin functional properties. Yeast frataxin functional mutants allowed for the exploration of the conformational and functional relevance of the two putative functional regions in frataxin structure: the acidic ridge between α-helix 1 and β-strand 1 and residues in the conserved β-sheet surface between strands 3 and 4.

Mutations on the acidic ridge have shown that frataxin iron binding capacity is quite robust and that the acidic ridge is particular sensitive to an activity-stability trade off. Mutating up to five acidic residues, four of each identified as iron binding sites [49], significantly increases the protein's stability without compromising its iron binding stoichiometry. However, these mutations diminish frataxin's affinity to iron (~2-fold),

suggesting that the mutated residues (D86, E90, E93, D101 and E103) constitute primary iron binding sites. The existence of primary iron binding sites had already been suggested for the *E. coli* orthologue [50]. The quintuple mutant shows a significant increase in terms of both protein stability (ΔT_m~23ºC) and protein rigidity (lower propensity towards proteolytic digestions), thus the acidic ridge, in addition to its direct functional implications, also determines frataxin conformational properties. Evaluating the functional impairment caused by the replacement of negative charges in the acidic ridge must then be done cautiously, as charge-to-neutral mutations also alter the protein flexibility, which may impair the conformational fluctuations that are crucial for protein-protein interactions and interfere with complementary protein-protein interactions dependent on electrostatic interactions.

In addition, the studies here presented suggest that the variant Yfh1 -101/103A could be a valuable model to study frataxin cellular role and ultimately FRDA development. Under normal growth conditions, if only one of the residues, Asp 101 or Glu103, is mutated, no phenotype is observed [51-52]. However, the double mutant, D101/E103A, even when Yfh1 expression levels are normal, results in a reduction of aconitase activity (<80% of the wild type). No *in vitro* interaction is detected between this mutant and Isu. Nevertheless, growth impairment is only observed when these two residues are changed to lysines and the medium supplemented with iron [51]. The decreased interaction between variant Yfh1-101/103 A and Isu cannot be explained by the reduced conformational plasticity observed for this mutant as Yfh1-86/90/93A shows an identical reduction in flexibility and its interaction with Isu is still detected *in vitro*. Hence, residues Asp101 and Glu103 should be involved in the interaction with Isu but its alteration is not enough to completely abolish the interaction *in vivo*. Mutation of the corresponding residues in the human orthologue have not been

identified in FRDA patients but this double mutant seems to confer partial functional impairment and thus more detailed *in vivo* functional studies; using this variant may shed some light onto the controversial FRDA pathway.

The characterisation of the mutants involving the conserved β-sheet residues 122-123, excludes any structural relevance that might be attributed to them as their alteration has only a modest impact on Yfh1 stability and plasticity. As previously reported, the mutation Yfh1-N122K has been identified in an heterozygous patient (corresponds to FXN-N146K); our study suggests that the phenotype observed results from a direct functional impairment, the mutation comprises Yfh1 interaction with Isu. The rescue by chemical chaperones or small molecules protectors should not be efficient for these strictly functional mutants.

9.2.2. Copper Binding: A New Functional Feature of Frataxin?

Frataxin has been shown to be stabilised by different cations and metals [53]. In addition, CyaY weakly interacts with calcium and manganese with a K_d in the mM range, while zinc promotes its aggregation at higher ion/protein ratios [54]. Furthermore, *in vivo* studies have shown that nickel supplementation can improve frataxin-Isd11 interaction and partially rescue the interaction between FRDA-related mutants and Isd11 [8]. Thus, we have explored whether yeast frataxin could bind other metal ions. Apart from iron, only copper was able to bind frataxin. The addition of calcium, manganese or zinc, that were shown to interact with CyaY, had no effect on the protein fluorescence spectra. Either Yfh1 does not interact with these ions or the interaction is too weak to be detected and if so its biological

meaning is also questionable. Nickel had no effect on the protein spectra nor on its thermal stability.

The interaction of frataxin with copper has not yet been reported, but iron and copper homeostasis are tightly linked in Eukaryotes (as shown by studies on the yeast and human systems) [55]. Iron uptake depends on cytosolic copper availability since it depends on the activity of Fet3p. This enzyme catalyses the oxidation of Fe(II) to Fe(III) and Fet3p-Fe(III) is the substrate for the permeation facilitated by Ftrp1, resulting in iron uptake [56-57]. However, Fet3p activity depends on the post-translational insertion of 4 copper ions [58-59]; thus, the disruption of any of the genes involved in copper homeostasis leads to a deficiency in Fet3p activity and in other high affinity iron transporters [60-61]. The first evidence of a direct connection between iron and copper homeostasis was only recently disclosed. Yfh1 deletion activates the iron regulon AFT1, which in turn promotes Ftr1 and Fet3p expression and iron acquisition [62-63]. These alterations lead to cytosolic copper depletion that ultimately compromise SOD1 activity, promoting the inactivation of FeS clusters containing enzymes and triggering the formation of chelatable iron [41]. Supplementation of Δyfh1 cells with small concentrations of Cu(II) (5μM) enables the recovery of SOD1 activity and prevents protein oxidation by superoxide [41], however, if the cells are exposed to higher Cu(II) concentrations, this will lead to cell growth arrest (0.5mM) [64].

The toxicity exerted by copper supplementation (0.5mM) has been associated to the copper ability to generate oxygen radicals via Fenton reaction [64] but, since frataxin can also bind copper, this explanation may have to be reviewed. Frataxin can bind Cu(I) and Cu(II), but its affinity for Cu(I) is higher. Frataxin antioxidant capacity may then also involve its ability to bind copper, preventing the formation of reactive species and, at same time, contribute to the mitochondrial copper

homeostasis. Nonetheless, the presence of excess of copper does not induce oligomerisation, thus frataxin ability to prevent copper oxidation via Fenton chemistry is limited to its stoichiometry: 3/4 copper ions per frataxin. Considering this hypothesis, the toxicity exerted by copper supplementation may result from mitochondrial copper homeostasis imbalance caused by frataxin deletion.

Copper binding sites overlap at least partially with frataxin iron binding sites, however, excess of copper does not abolish frataxin interaction with Isu. Thus, in spite of a new putative function involving copper, frataxin role in FeS clusters biogenesis as a iron donor should still constitute its prime cellular function.

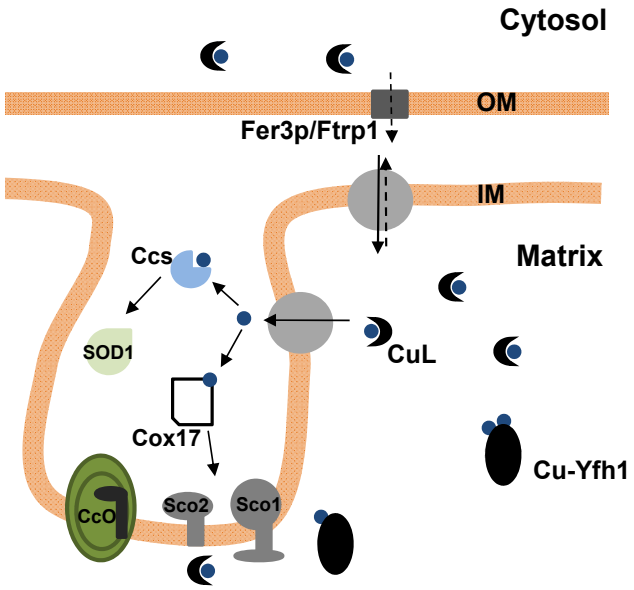

Figure 9.1: Schematic representation of mitochondrial copper trafficking pathways including the putative role of frataxin in copper metabolism. Copper in the matrix may also be bound to frataxin in addition to forming the anionic complex previously described. Adapted from [65].

The results here presented also suggest that frataxin may act as a copper chaperone. Frataxin is able to bind copper and further deliver it to apo-SOD1 promoting SOD's reconstitution. *In vivo*, it has been

shown that the copper levels in the mitochondria are significantly higher than expected, considering the mitochondrial copper needs for the activation of mitochondrial copper-dependent proteins [66]. Further, it was demonstrated that the excess of copper is, as frataxin, localised in the mitochondrial matrix. This copper within the matrix corresponds to 70-85% of the total mitochondrial copper and it has been associated to a non proteinaceous pool [66-67]. While many mitochondrial proteins have been associated to the metallation of cytochrome C oxidase [65, 67-70], only one metallochaperone, Ccs1, has been identified as responsible for the metallation of SOD1 [71]. SOD1 activity is retained in ΔCcs cells, although with some constrains, which suggests that an alternative copper chaperone may exist.

In view of the mitochondrial copper localisation, as well as its quantity, our results may suggest that frataxin could contribute to the copper homeostasis in the mitochondrial matrix. Frataxin may have a dual role on mitochondrial copper regulation: it may prevent Fenton chemistry and, at the same time, promote the trafficking of copper from the non-proteinaceous pool to the metallochaperones known to be directly involved in copper insertion/metallation. However, further experiments on the role of frataxin in copper homeostasis *in vivo* must be performed.

Throughout the work developed we have aimed at contributing to a better understanding of FRDA pathology as well as to a better molecular understanding of frataxin conformational and functional properties. Since the frataxin gene was first described in 1996, the studies on frataxin and on the pathological pathway leading to FRDA have been extremely intense but still many uncertainties and challenges remain.

9.3. References

1. Chiti, F. and C.M. Dobson, *Protein misfolding, functional amyloid, and human disease.* Annu Rev Biochem, 2006. **75**: p. 333-66.
2. Sherry, S.T., et al., *dbSNP: the NCBI database of genetic variation.* Nucleic Acids Res, 2001. **29**(1): p. 308-11.
3. Cossee, M., et al., *Friedreich's ataxia: point mutations and clinical presentation of compound heterozygotes.* Ann Neurol, 1999. **45**(2): p. 200-6.
4. Bidichandani, S.I., T. Ashizawa, and P.I. Patel, *Atypical Friedreich ataxia caused by compound heterozygosity for a novel missense mutation and the GAA triplet-repeat expansion.* Am J Hum Genet, 1997. **60**(5): p. 1251-6.
5. Calmels, N., et al., *The first cellular models based on frataxin missense mutations that reproduce spontaneously the defects associated with Friedreich ataxia.* PLoS One, 2009. **4**(7): p. e6379.
6. Tartaglia, G.G., et al., *Life on the edge: a link between gene expression levels and aggregation rates of human proteins.* Trends Biochem Sci, 2007. **32**(5): p. 204-6.
7. Cavadini, P., et al., *Human frataxin maintains mitochondrial iron homeostasis in Saccharomyces cerevisiae.* Hum Mol Genet, 2000. **9**(17): p. 2523-30.
8. Shan, Y., E. Napoli, and G. Cortopassi, *Mitochondrial frataxin interacts with ISD11 of the NFS1/ISCU complex and multiple mitochondrial chaperones.* Hum Mol Genet, 2007. **16**(8): p. 929-41.
9. Bulteau, A.L., et al., *Oxidative stress and protease dysfunction in the yeast model of Friedreich ataxia.* Free Radic Biol Med, 2007. **42**(10): p. 1561-70.
10. Calabrese, V., et al., *Oxidative stress, mitochondrial dysfunction and cellular stress response in Friedreich's ataxia.* J Neurol Sci, 2005. **233**(1-2): p. 145-62.
11. Jauslin, M.L., et al., *Mitochondria-targeted antioxidants protect Friedreich Ataxia fibroblasts from endogenous oxidative stress more effectively than untargeted antioxidants.* FASEB J, 2003. **17**(13): p. 1972-4.
12. Seznec, H., et al., *Friedreich ataxia: the oxidative stress paradox.* Hum Mol Genet, 2005. **14**(4): p. 463-74.
13. Shaw, B.F. and J.S. Valentine, *How do ALS-associated mutations in superoxide dismutase 1 promote aggregation of the protein?* Trends Biochem Sci, 2007. **32**(2): p. 78-85.
14. Gregersen, N., et al., *Protein misfolding and human disease.* Annu Rev Genomics Hum Genet, 2006. **7**: p. 103-24.
15. Wang, T. and E.A. Craig, *Binding of yeast frataxin to the scaffold for Fe-S cluster biogenesis, Isu.* J Biol Chem, 2008. **283**(18): p. 12674-9.
16. Correia, A.R., et al., *Iron binding activity in yeast frataxin entails a trade off with stability in the alpha1/beta1 acidic ridge region.* Biochem J, 2009.
17. Kelly, J.W., *The alternative conformations of amyloidogenic proteins and their multi-step assembly pathways.* Curr Opin Struct Biol, 1998. **8**(1): p. 101-6.
18. Lomas, D.A. and R.W. Carrell, *Serpinopathies and the conformational dementias.* Nat Rev Genet, 2002. **3**(10): p. 759-68.
19. Stefani, M., *Protein misfolding and aggregation: new examples in medicine and biology of the dark side of the protein world.* Biochim Biophys Acta, 2004. **1739**(1): p. 5-25.
20. Stefani, M. and C.M. Dobson, *Protein aggregation and aggregate toxicity: new insights into protein folding, misfolding diseases and biological evolution.* J Mol Med, 2003. **81**(11): p. 678-99.
21. Arakawa, T., et al., *Small molecule pharmacological chaperones: From thermodynamic stabilization to pharmaceutical drugs.* Biochim Biophys Acta, 2006. **1764**(11): p. 1677-87.

22. Diamant, S., et al., *Chemical chaperones regulate molecular chaperones in vitro and in cells under combined salt and heat stresses.* J Biol Chem, 2001. **276**(43): p. 39586-91.
23. Welch, W.J. and C.R. Brown, *Influence of molecular and chemical chaperones on protein folding.* Cell Stress Chaperones, 1996. **1**(2): p. 109-15.
24. Leandro, P. and C.M. Gomes, *Protein misfolding in conformational disorders: rescue of folding defects and chemical chaperoning.* Mini Rev Med Chem, 2008. **8**(9): p. 901-11.
25. Bolen, D.W., *Effects of naturally occurring osmolytes on protein stability and solubility: issues important in protein crystallization.* Methods, 2004. **34**(3): p. 312-22.
26. Cayley, S. and M.T. Record, Jr., *Roles of cytoplasmic osmolytes, water, and crowding in the response of Escherichia coli to osmotic stress: biophysical basis of osmoprotection by glycine betaine.* Biochemistry, 2003. **42**(43): p. 12596-609.
27. Timasheff, S.N., *Control of protein stability and reactions by weakly interacting cosolvents: the simplicity of the complicated.* Adv Protein Chem, 1998. **51**: p. 355-432.
28. Auton, M. and D.W. Bolen, *Predicting the energetics of osmolyte-induced protein folding/unfolding.* Proc Natl Acad Sci U S A, 2005. **102**(42): p. 15065-8.
29. Courtenay, E.S., et al., *Vapor pressure osmometry studies of osmolyte-protein interactions: implications for the action of osmoprotectants in vivo and for the interpretation of "osmotic stress" experiments in vitro.* Biochemistry, 2000. **39**(15): p. 4455-71.
30. Pradeep, L. and J.B. Udgaonkar, *Osmolytes induce structure in an early intermediate on the folding pathway of barstar.* J Biol Chem, 2004. **279**(39): p. 40303-13.
31. Dhe-Paganon, S., et al., *Crystal structure of human frataxin.* J Biol Chem, 2000. **275**(40): p. 30753-6.
32. Musco, G., et al., *Towards a structural understanding of Friedreich's ataxia: the solution structure of frataxin.* Structure, 2000. **8**(7): p. 695-707.
33. Correia, A.R., et al., *Dynamics, stability and iron-binding activity of frataxin clinical mutants.* Febs J, 2008. **275**(14): p. 3680-90.
34. Piemonte, F., et al., *Glutathione in blood of patients with Friedreich's ataxia.* Eur J Clin Invest, 2001. **31**(11): p. 1007-11.
35. Schulz, J.B., et al., *Oxidative stress in patients with Friedreich ataxia.* Neurology, 2000. **55**(11): p. 1719-21.
36. Emond, M., et al., *Increased levels of plasma malondialdehyde in Friedreich ataxia.* Neurology, 2000. **55**(11): p. 1752-3.
37. Meier, T. and G. Buyse, *Idebenone: an emerging therapy for Friedreich ataxia.* J Neurol, 2009. **256 Suppl 1**: p. 25-30.
38. Schulz, J.B., et al., *Diagnosis and treatment of Friedreich ataxia: a European perspective.* Nat Rev Neurol, 2009. **5**(4): p. 222-34.
39. Anderson, P.R., et al., *RNAi-mediated suppression of the mitochondrial iron chaperone, frataxin, in Drosophila.* Hum Mol Genet, 2005. **14**(22): p. 3397-405.
40. Anderson, P.R., et al., *Hydrogen peroxide scavenging rescues frataxin deficiency in a Drosophila model of Friedreich's ataxia.* Proc Natl Acad Sci U S A, 2008. **105**(2): p. 611-6.
41. Irazusta, V., et al., *Yeast frataxin mutants display decreased superoxide dismutase activity crucial to promote protein oxidative damage.* Free Radic Biol Med, 2009.
42. Davies, M.J., *The oxidative environment and protein damage.* Biochim Biophys Acta, 2005. **1703**(2): p. 93-109.
43. Dean, R.T., et al., *Biochemistry and pathology of radical-mediated protein oxidation.* Biochem J, 1997. **324 (Pt 1)**: p. 1-18.

44. Chao, C.C., Y.S. Ma, and E.R. Stadtman, *Modification of protein surface hydrophobicity and methionine oxidation by oxidative systems.* Proc Natl Acad Sci U S A, 1997. **94**(7): p. 2969-74.
45. Beal, M.F., *Oxidatively modified proteins in aging and disease.* Free Radic Biol Med, 2002. **32**(9): p. 797-803.
46. Correia, A.R., et al., *Conformational stability of human frataxin and effect of Friedreich's ataxia-related mutations on protein folding.* Biochem J, 2006. **398**(3): p. 605-11.
47. Babcock, M., et al., *Regulation of mitochondrial iron accumulation by Yfh1p, a putative homolog of frataxin.* Science, 1997. **276**(5319): p. 1709-12.
48. Rotig, A., et al., *Aconitase and mitochondrial iron-sulphur protein deficiency in Friedreich ataxia.* Nat Genet, 1997. **17**(2): p. 215-7.
49. He, Y., et al., *Yeast frataxin solution structure, iron binding, and ferrochelatase interaction.* Biochemistry, 2004. **43**(51): p. 16254-62.
50. Nair, M., et al., *Solution structure of the bacterial frataxin ortholog, CyaY: mapping the iron binding sites.* Structure, 2004. **12**(11): p. 2037-48.
51. Foury, F., A. Pastore, and M. Trincal, *Acidic residues of yeast frataxin have an essential role in Fe-S cluster assembly.* EMBO Rep, 2007. **8**(2): p. 194-9.
52. Gakh, O., et al., *Mitochondrial iron detoxification is a primary function of frataxin that limits oxidative damage and preserves cell longevity.* Hum Mol Genet, 2006. **15**(3): p. 467-79.
53. Adinolfi, S., et al., *The factors governing the thermal stability of frataxin orthologues: how to increase a protein's stability.* Biochemistry, 2004. **43**(21): p. 6511-8.
54. Pastore, C., et al., *Understanding the binding properties of an unusual metal-binding protein--a study of bacterial frataxin.* FEBS J, 2007. **274**(16): p. 4199-210.
55. Taylor, A.B., et al., *The copper-iron connection in biology: structure of the metallo-oxidase Fet3p.* Proc Natl Acad Sci U S A, 2005. **102**(43): p. 15459-64.
56. Stoj, C. and D.J. Kosman, *Cuprous oxidase activity of yeast Fet3p and human ceruloplasmin: implication for function.* FEBS Lett, 2003. **554**(3): p. 422-6.
57. Kosman, D.J., *Molecular mechanisms of iron uptake in fungi.* Mol Microbiol, 2003. **47**(5): p. 1185-97.
58. Osaki, S., D.A. Johnson, and E. Frieden, *The possible significance of the ferrous oxidase activity of ceruloplasmin in normal human serum.* J Biol Chem, 1966. **241**(12): p. 2746-51.
59. Frieden, E. and H.S. Hsieh, *The biological role of ceruloplasmin and its oxidase activity.* Adv Exp Med Biol, 1976. **74**: p. 505-29.
60. Dancis, A., et al., *Molecular characterization of a copper transport protein in S. cerevisiae: an unexpected role for copper in iron transport.* Cell, 1994. **76**(2): p. 393-402.
61. Askwith, C. and J. Kaplan, *Iron and copper transport in yeast and its relevance to human disease.* Trends Biochem Sci, 1998. **23**(4): p. 135-8.
62. Foury, F. and D. Talibi, *Mitochondrial control of iron homeostasis. A genome wide analysis of gene expression in a yeast frataxin-deficient strain.* J Biol Chem, 2001. **276**(11): p. 7762-8.
63. Philpott, C.C. and O. Protchenko, *Response to iron deprivation in Saccharomyces cerevisiae.* Eukaryot Cell, 2008. **7**(1): p. 20-7.
64. Foury, F. and O. Cazzalini, *Deletion of the yeast homologue of the human gene associated with Friedreich's ataxia elicits iron accumulation in mitochondria.* FEBS Lett, 1997. **411**(2-3): p. 373-7.
65. Leary, S.C., D.R. Winge, and P.A. Cobine, *"Pulling the plug" on cellular copper: the role of mitochondria in copper export.* Biochim Biophys Acta, 2009. **1793**(1): p. 146-53.
66. Cobine, P.A., et al., *Yeast contain a non-proteinaceous pool of copper in the mitochondrial matrix.* J Biol Chem, 2004. **279**(14): p. 14447-55.

67. Cobine, P.A., et al., *Mitochondrial matrix copper complex used in metallation of cytochrome oxidase and superoxide dismutase.* J Biol Chem, 2006. **281**(48): p. 36552-9.
68. Cobine, P.A., F. Pierrel, and D.R. Winge, *Copper trafficking to the mitochondrion and assembly of copper metalloenzymes.* Biochim Biophys Acta, 2006. **1763**(7): p. 759-72.
69. Horng, Y.C., et al., *Specific copper transfer from the Cox17 metallochaperone to both Sco1 and Cox11 in the assembly of yeast cytochrome C oxidase.* J Biol Chem, 2004. **279**(34): p. 35334-40.
70. Rigby, K., et al., *characterization of the cytochrome c oxidase assembly factor Cox19 of Saccharomyces cerevisiae.* J Biol Chem, 2007. **282**(14): p. 10233-42.
71. Rae, T.D., et al., *Mechanism of Cu,Zn-superoxide dismutase activation by the human metallochaperone hCCS.* J Biol Chem, 2001. **276**(7): p. 5166-76.

Most proteins need to fold to a specific three-dimensional structure in order to be functional. Usually this process is extremely efficient but not perfect: stress conditions such as changes in the cellular environment and genetic mutations are known to compromise its efficiency. The cells' protein quality control system, comprising chaperones and proteases, deals with the burden of misfolded proteins. Its capacity, however, is limited and protein misfolding and aggregation are now recognised as the cause of a large and diverse group of diseases called protein conformational/misfolding diseases.

This dissertation focuses on the study of frataxin, a small mitochondrial protein whose deficiency is associated with the neurodegenerative disease Friedreich's ataxia (FRDA). Aiming at a better understanding of the frataxin's conformational and functional properties, two lines of research were followed: first, the effect of FRDA-related mutations in human frataxin (FXN) were studied and the role of oxidative stress related modification addressed; second, yeast frataxin (Yfh1) orthologue was used to explore the conformational and functional properties of the protein.

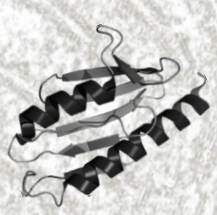

FCT Fundação para a Ciência e a Tecnologia
MINISTÉRIO DA CIÊNCIA, TECNOLOGIA E ENSINO SUPERIOR